A Systems Architecture Approach to the Design of Autonomous Underwater Vehicles and their Servicing Platforms

By

Brendan K. Horton

B.A. Geology
Amherst College, 2008

M.S. Geology and Geophysics
University of Utah, 2012

SUBMITTED TO THE SYSTEM DESIGN AND MANAGEMENT PROGRAM IN PARTIAL FULFILMENT OF THE REQUIREMENTS FOR THE DEGREE OF
MASTER OF SCIENCE IN ENGINEERING AND MANGEMENT

AT THE

MASSACHUSETTS INSTITUTE OF TECHNOLOGY

SEPTEMBER 2020

Signature of Author:_____
Brendan K. Horton
System Design and Management Program, August 7, 2020

Certified by:_____
Thesis Advisor: Dr. Bryan Moser
Academic Director, SDM Program

Certified by:_____
Thesis Co-Advisor: Dr. Maha Haji
Postdoctoral Research Associate, AeroAstro

Accepted by:_____
Joan S. Rubin
Executive Director, SDM Program

A Systems Architecture Approach to the Design of Autonomous Underwater Vehicles and their Servicing Platforms

By

Brendan Horton

Submitted to the System Design and Management Program on August 7th, 2020 in Partial Fulfilment of the Requirements for the Degree of Master of Science in Engineering and Management

Abstract

Autonomous underwater vehicles hold great potential in the realms of industry, military, scientific, and personal usage. The applications of intelligently applied autonomous functionality could improve work performed on subsea infrastructure, commercial shipping lane maintenance, canal and channel observation, search and rescue, military applications, as well as general scientific research. Given such potential, and supposing that existing technological barriers to progress could be overcome, what could a potential system architecture of future autonomous underwater vehicles look like?

Fundamentally this thesis asks: "could novel architectures of AUV systems – specifically pairing AUVs to remote service platforms – lead to significant performance increases?" In approaching this subject, a specific case study is leveraged where autonomous underwater vehicles were extensively used: the search for Malaysian Air flight 370. This specific mission profile has been extensively documented by others laying a comprehensive framework. It represents the single largest search and rescue operation ever performed. Within this thesis, whole-system performance metrics of this search and rescue operation are compared against calculated performance metrics of systematically

generated possible architectures. In decomposing the system into its functional elements, a deterministic evaluation is executed followed by a probabilistic examination of the system as modeled. The results of the probabilistic model are also interpreted via a Pareto ranking methodology where Pareto surfaces are identified in multidimensional tradespaces. These component cases which comprise the Pareto surface are subsequently removed from the dataset, and the process is run again. This iterative approach demonstrated that the top ten performing architectures were comprised entirely out of architectures with either one or four AUVs. The outputs of these models are subsequently compared against the baseline system used in the search for MH370.

Following the analysis, a major fault was identified in the foundations of all of the models surrounding a figure of merit wherein the time to the seafloor was calculated for all architectures. All of the top ten performing design vectors – systems which contained one or four AUVs – were unchanged due to this error. Architectures which were affected by this error – systems with more than four AUVs – were impacted negatively. Several methods of re-imagining the error are presented herein as complexities that are inherent in the system, which are not handled by these models. These new emergent complexities were present in the system prior to the model construction, but unaccounted for. Discovery of this faulty assumption laid bare several architectural decisions which are unexplored in this thesis, but could provide the foundation for future work in this space.

The outcome of these modeling efforts suggests that pairing an autonomous underwater vehicle with an autonomous service platform can result in increases in all performance metrics. Specific metrics which are improved include daily search area rate, calendar mission completion time, and total project cost. This improvement is specifically calibrated to the case study of MH370, but the performance metrics themselves are not exclusively applicable to search and rescue operations. This model indicates that such a system could accomplish the same mission in less time for half the cost. This thesis presents a vision of future autonomous underwater vehicle systems in which daily operational time, search area rates, calendar mission completion times, and total system costs can all be improved relative to the existing standards. Such improvements are equally applicable to commercial, industrial, military, civilian, and scientific endeavors in which autonomous underwater vehicles could be a potential tool.

Thesis Advisor: Dr. Bryan Moser

Thesis Co-Advisor: Dr. Maha Haji

Table of Contents

Acknowledgements

I would like to thank my thesis supervisors, Dr. Maha Haji and Dr. Bryan Moser for their continued patience, support, encouragement and guidance as I have worked through this thesis. They have been phenomenal guides when I felt particularly lost. Their care has been exemplary and nothing short of the embodiment of role-model behavior. They were always willing to make sacrifices to meet with me when I needed their help, and I am grateful for their commitment to me as a student, scholar, and scientist. Additional thanks to Prakash Mandahar and T. C. Flemming Goolsby for their help.

Thank you for the unwavering support I have received from all of my sponsors - especially my previous business unit who always encouraged me to try new things and exist outside of my comfort zone. I am immensely grateful for the trust they have placed in me while I spent a year outside of their business unit. Joe, Lianne, Ken, Dharmen, Chris, Helen, and Alexei were all especially inspirational. They helped motivate me when I wasn't sure I had what it takes, and pushed me to explore areas that I hadn't previously experienced.

To my all of my colleagues – especially those who joined me in our niche journey – meeting you and experiencing MIT over the past year will turn out to be one of the most formative experiences of my life. I never dreamed I would get the distinction to attend such a prestigious institution, much less with such excellent and admirable people. While the program is unquestionably amazing, it is you who have made the lifelong impact on my life. The socio-technical system in which we participate has been immensely rewarding because of you. I can't sufficiently express how wonderful working and existing with you for the past year has been.

The SDM faculty and staff, and the MIT faculty and staff as a whole deserve immense credit for supplying an environment and atmosphere in which we can all learn and grow. Thank you all for your commitment to excellence in academic and personal pursuits.

I also must extend my thanks to Dr. Tekla Harms, Mark Norville, Dr. Lee Billingsley, and Dr. Lauren Birgenheier. They instilled an inquisitive and dedicated ethic that I have tried to live up to. Thank you to John Green for inspiring me for so many years. Thanks to my family far and farther.

My life is not complete without my co-pilot Tiffany. She is now and will forever be a font of wisdom, source of inspiration, and talented editor. I am the luckiest person alive to have her unyielding support. Finally, thank you to Amy and Sarah for letting me work late nights and miss a bedtime or two. I dedicate this work to you three. I love you all.

1 Introduction

In this chapter, a broad exposition to the project at hand is discussed. The broader context in which this work sits is explored from a holistic vantage point, and then more detail is elucidated from the autonomous underwater vehicle (AUV) industry as a whole. The history of AUVs is outlined and a case is built claiming that as a technology, AUVs are lagging behind other industries which employ similar foundational elements. Following this historical context, key research questions and objectives are stated. Finally, the structure of the research is outlined.

1.1 Motivation

The development of technology has been one of the hallmarks of human civilization. The past 30 years have not only seen immense improvements in many fields of technology, but the pace of technology development has in fact been accelerating (Berman, 2016). Today's technological landscape is one of rapid improvement, digitalization, and autonomy. There are countless examples of technology development that have seen exponential growth in the past decades. Classic examples include computing power – illustrated in Figure 1-1 – (Kurzweil, 2006), data transmission, luminosity, and battery storage capacity – illustrated in Figure 1-2 (Magee, 2014). A consistent theme in charting technological progress through time is to identify figures of merit upon which a particular technology or system can be judged. Figures of merit are defined as a numerical value which represents an aspect of performance of a system. In these classic examples, figures of merit include number of calculations per second per $1000, lumens per $, watt hours per kilogram and so forth. Selecting an appropriate figure of merit is an important building block to construct a comprehensive and defensible evaluation of any technology or system. Indeed, some products that were merely manifestations of an active imagination (or closely guarded military technology) are now commonplace household items.

This progress is manifest in analyzing the specific figures of merit that are selected for any given technology. For instance, aerial drones with 4k video capability and multiple kilometer ranges, for instance, can be purchased at nearly any big-box electronics retailer at any given time. While there are many figures of merit that could be used to evaluate how this technology has evolved over the past decades, a simple approach could be to identify the cost a consumer would pay per unit time they could film 4k resolution imagery from these given drones. If that figure of merit were selected, then any time prior to 2016 would have a value of infinity – there were no such drones available to the

public for purchase (Dà-Jiāng Innovations, 2016). Today, this price is approximately $50 (Banggood, 2020). This exemplifies how dramatically a single figure of merit can change through a very short period of time – even in the consumer product market.

Different disciplines and fields have witnessed growth in their capacities over the last decade, which have made notions previously thought to be science fiction, real and commonplace. In the field of robotics specifically, significant advancements have been made in which robots have reduced in size while becoming more capable. In addition, new emergent properties of robotic systems have been uncovered when an individual agent is paired with another. These swarms of robots have shown promise in commercial and military applications. Robotic swarm research has been advancing on land, in the air, and in space, but there has been a proportionately slow advancement in autonomous underwater vehicles. Even ocean-going vessels have seen substantial technological growth with the expanded use of autonomous drone ships (e.g., SpaceX landing barges) and vessels which navigate completely without the input of human operators to a very high degree of precision (e.g., seismic acquisition vessels).

However, one area of technology in which there has been continuous – but less rapid – technological progress has been in the realm of autonomous underwater vehicles (AUVs). To prove that a specific area of technology is developing "slowly" is a very difficult task. Various figures of merit (e.g., economic return, sensor acuity, autonomous navigation, etc. (Blidberg, 2001; Wang, 2009)) have indeed seen improvements over time. Is it really possible to claim with a reasonable basis that these improvements are "slow?" Is it not possible that they are developing at precisely the rate that they can? When compared to autonomous vehicles that operate in other media, the state of the art in underwater vehicles is significantly farther behind in terms of technological development. Consider again the example of unmanned autonomous vehicles – specifically aerial drones. The first proof of concept of swarm behavior in drones (where swarm is defined as a set of robots which distribute a single task amongst the collection of agents) was demonstrated in 2011 by project Perdix (Massachusets Institute of Technology - Lincoln Laboratory, 2011). Since then, elaborate displays (Figure 1-3) where over 1000 drones have behaved as a swarm have become commonplace (Jeffery Lin, 2018). On the ground, major automobile manufacturers are investing in technology which will improve traffic flow by converting traffic into a swarm through information sharing (Honda, 2017).

Even in space, swarms of satellites (e.g., Starlink, OneWeb, and SWARM) have become more common through recent years.

Yet in the oceans and waterways, as AUV adoption advances, swarming technology remains stagnant. By this comparison, it is clear that there is a lack of progress in this technology relative to other applications. There are two possible explanations for this lag: there is a technological limitation that has yet to be hurdled, and/or architectures which would enable this swarming concept have not been adequately characterized or explored. Assuming that any specific technological limitations can eventually be overcome – what then would the architectures look like when examining AUV swarms and completely autonomous AUV systems? Is there an architectural concept which has to date remained unexplored through which the system could drastically improve performance? These are questions that will be at the heart of this paper.

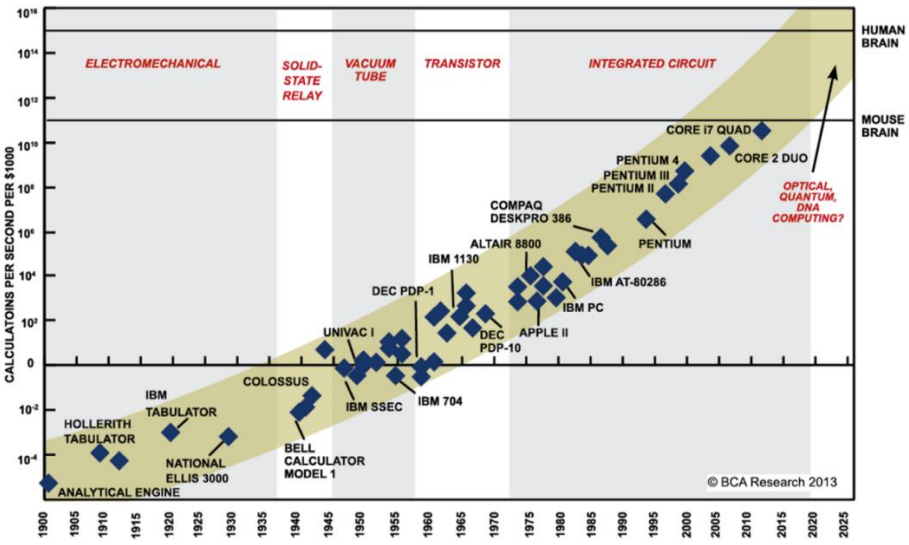

Figure 1-1: Technological development through time of computing power. Figure from (Kurzweil, 2006).

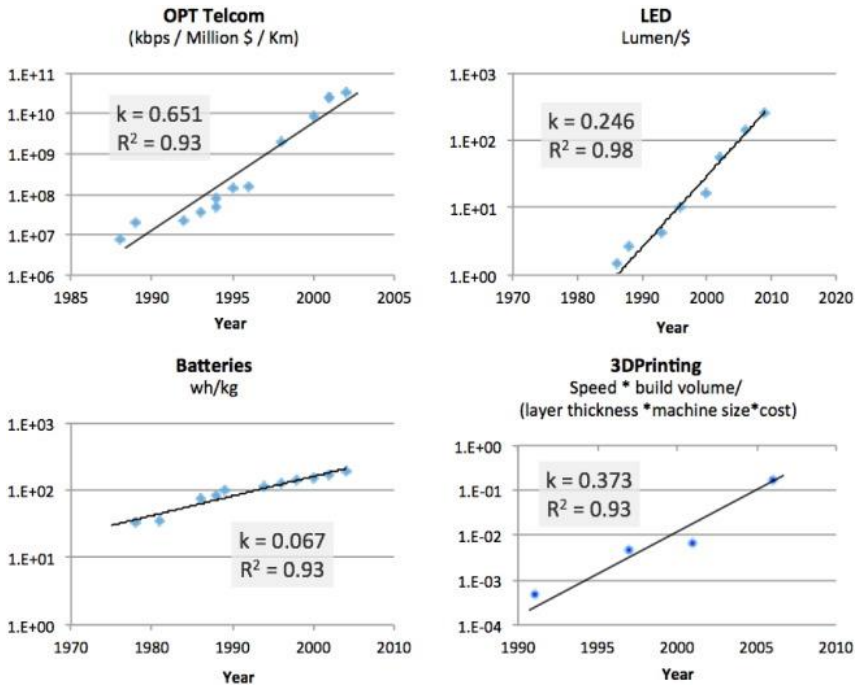

Figure 1-2: Technological development through time of telecom, LED, battery, and 3D printing technologies. Figure from (Magee, 2014).

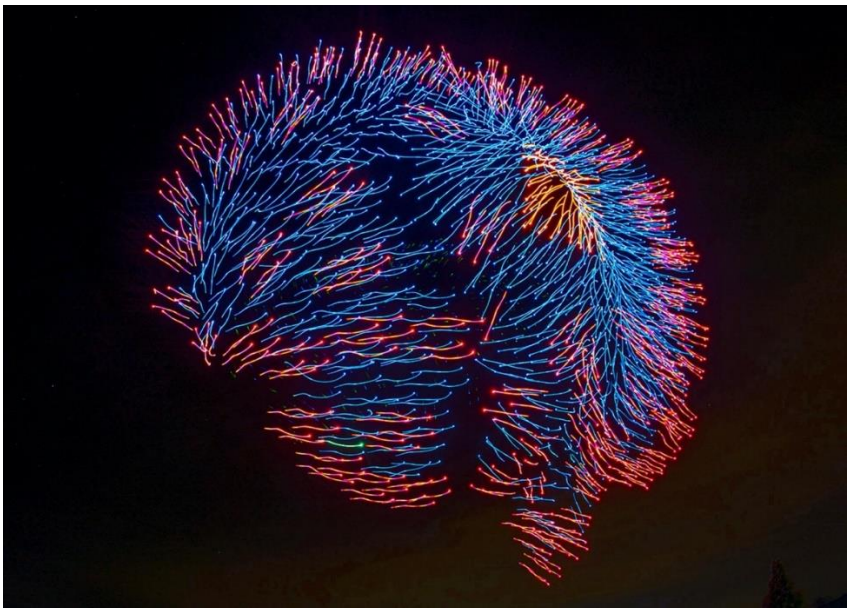

Figure 1-3: 2,018 UAVs perform in unison setting a world record for most unmanned aerial vehicles airborne simultaneously (Divis, 2019).

To define terms which will be utilized throughout the thesis, systems are comprised of both forms and functions (Edward Crawley, 2016). In decomposing systems, their component entities are identified. Each entity has both form and function. A single form or function that composes an entity is itself comprised of a set of elements which can be either formal or functional in nature. Individual forms accomplish their functions to varying degrees of efficacy. This performance can be measured in a number of different ways, and each measurement of performance is referred to as a figure of merit. Emergent functionality of a system is the property that couldn't exist if the system were not appropriately configured. This emergent functionality is a function of all the functional and formal elements in the system and its performance is measured by a calculated performance metric.

AUVs are classically defined as "underwater systems that contain its own power and is controlled by an onboard computer" (Wang, 2009). More expansive definitions include "while accomplishing a pre-defined task…[and] requires no communication during its missions" (Blidberg, 2001). AUVs as systems have been in operation for over 100 years and they have had relatively consistent architectures across platforms. A schematic representation of a typical AUV is shown in Figure 1-4. AUVs as systems can be decomposed into the following functional elements: communicating outside of the system, energizing the system, navigating, propelling the system, and sensing the surrounding environment. What has changed significantly in the recent decades is the capacity for each of these functions to be performed completely autonomously with greater degrees of complexity. For instance, the first AUVs were only capable of propelling themselves along a single designated course (Museum, 1980). Today, however, there are platforms (e.g., the Bluefin AUV platform) which can perform sophisticated deep-water operations over 24-hour operational cycles launching and returning completely autonomously (Bluefin Robotics Corporation, 2015).

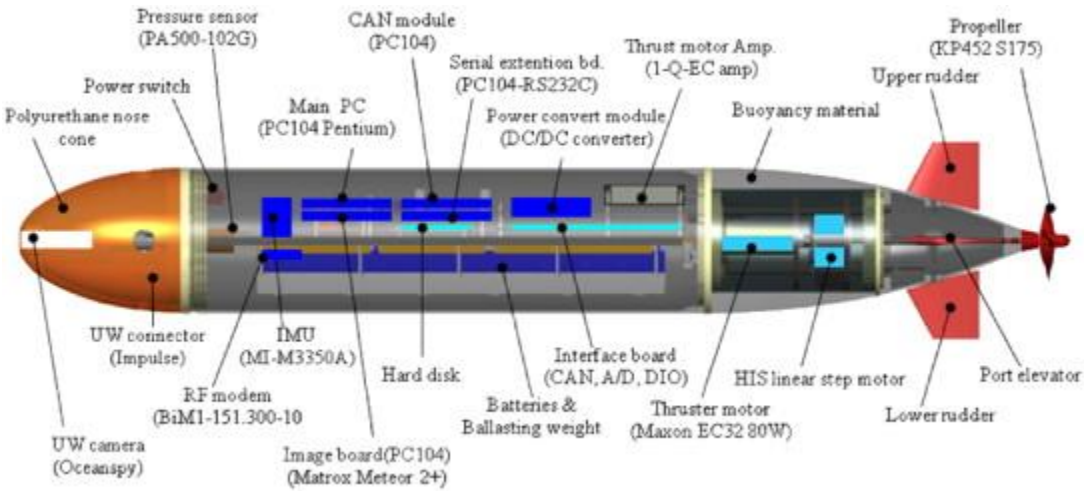

Figure 1-4: Schematic view of a small AUV built by KORDI. This represents a typical arrangement of formal elements within the AUV. Figure6 from (Bong-Huan Jun, 2009)

With the advancement of the underlying technologies, there are a vast number of operating environments in which AUVs can successfully be deployed. These environments include, but are not limited to scientific surveys, remote search and rescue operations, underwater infrastructure inspection, and canal and waterway monitoring. A chief reason why AUVs may not be favored in these environments, however, is that as a system they are still tied to non-autonomous operations immediately preceding and proceeding autonomous operations. In other words, while the AUV itself has seen significant growth and advancement, the launching and landing procedures of AUVs are largely the same as they were at inception: AUVs still require people on boats or people on the land to fish the AUVs out and manually process data that have been collected (Figure 1-5). For this reason, remotely operated vehicles (ROVs) are favored in many common demanding operating environments such as subsea maintenance of infrastructure. ROVs differ from AUVs in that they are tethered via hard connections which stream power and data to a base station. These base stations can exist either below or above the surface of the water. ROVs are not autonomous – they have human operators who are in charge of maintaining operational control for any given mission. This is an area where AUVs stand to gain a technological edge: if AUVs can eliminate the need for non-autonomous elements (e.g., launching and landing an AUV), then their possible mission parameters could dramatically change the subsea monitoring environment.

In this sense, the perspective of what constitutes the AUV system must shift. Previous work has focused primarily on the internal formal elements of an AUV (Blidberg, 2001; Griffiths; Wang, 2009) and not the interfaces between the AUV and the operational support elements. In other words, the full AUV system is not just the vehicle, but also the method with which the vehicle transfers information offboard, how the vehicle charges, how the vehicle receives instructions for its next mission, and other operational considerations (Figure 2-2). It is these operational considerations that have remained stagnant over the past 100 years, and these elements require architectural evaluation to see if a novel approach could improve full system performance of AUVs.

The current standard system architecture of AUV missions includes pairing one or more AUVs with a deployment vessel. Commonly, these deployment vessels scale with the number of AUVs that are going to operate. In the case of search and rescue operations, deployment vessels are on the order of 100 meters long with a beam of 20 meters or more (Australia Department of Infrastructure, Transport, Regional Development, and Communications, 2018). It is not uncommon for these large vehicles to require to port in order to resupply and change crew on semi-regular basis. It should be noted, however, that it is common for these vessels to support other operations simultaneously. Operation of these systems frequently limits the number of active assets to one or two AUVs simultaneously. A single AUV will be programmed for a specific mission, and deployed. Following deployment, the AUV will perform its specific mission, and upon return it will be retrieved from the water where it will be serviced on the boat. During this servicing period, the data are commonly transmitted via hard link and the batteries are either charged on site, or swapped out with full batteries. This standard CONOPS outline is illustrated in Figure 1-5.

Challenging this established construction requires that each component of the system be decomposed into its own functional and formal elements. For instance, the paired vessel serves as a platform upon which the AUV recharges. Any number of forms can fulfil that function, but by both convention, and ease of repurposing existing architectures that form is commonly a large support vessel (i.e., ship). Furthermore, we see in the AUV industry a distinct aversion from a product platform approach. Rather, in 2001, there were over 140 distinct AUVs that were all tailored to specific mission profiles (Blidberg, 2001). Today, there are an estimated 400+ distinct AUV designs for specific mission profiles (Yuh, 2000).

This leaves the system as a whole ripe for re-imagining. Within this paper the relationship that exists between AUVs and the service platform is explored. Specifically, AUV swarms and autonomous

and mobile servicing platforms will be examined. A schematic CONOPS for such a pairing between an AUV and a service platform is illustrated in Figure 1-6.

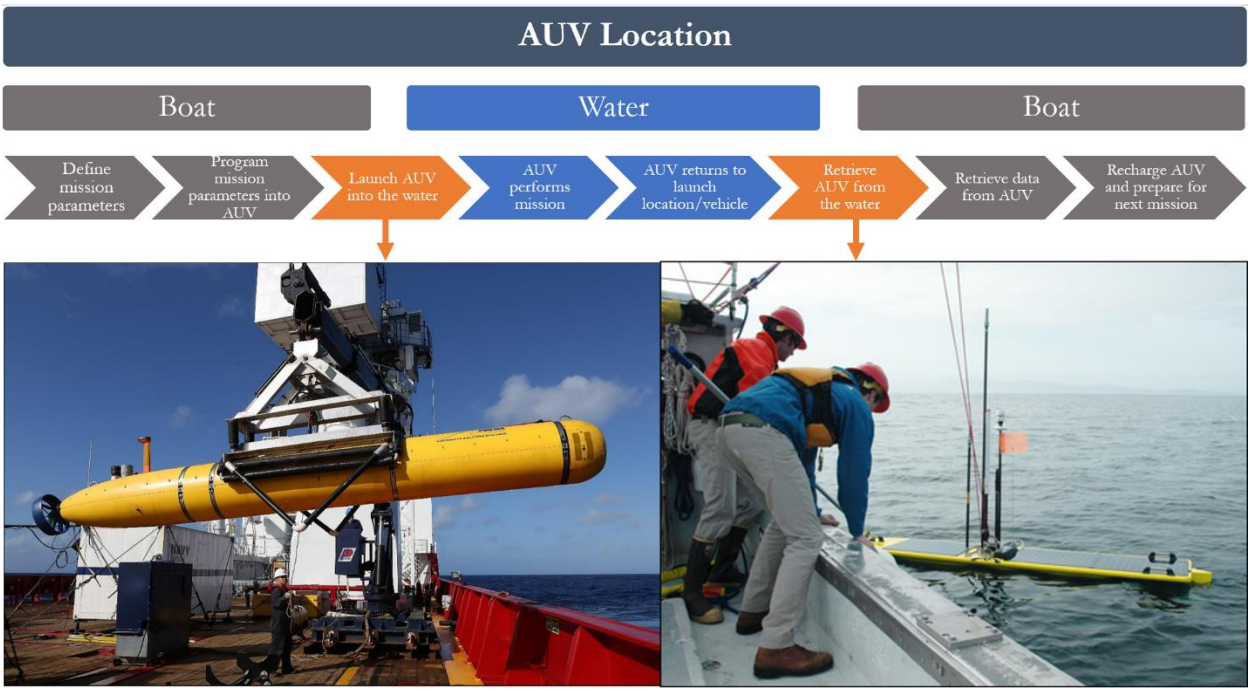

Figure 1-5: Standard CONOPS for operating AUVs. Image of launching an AUV is Figure 24 from (Australian Transport Safety Bureau, 2017). Image of AUV retrieval courtesy of (Monterey Bay Aquarium Research Institute, 2014).

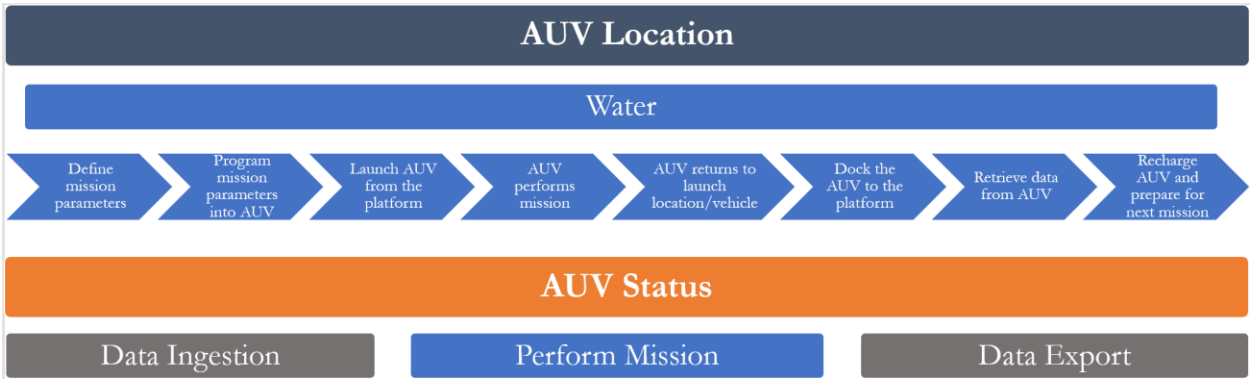

Figure 1-6: CONOPS for expanded system. The AUV remains in the water for the duration of the mission. The status of the AUV changes depending on its relationship to the service platform.

1.2 Literature Review and Historical Context

While the concept of remote operation of naval systems has existed for hundreds of years, the first completely autonomous underwater vehicles were torpedoes that were built by the Austro-Hungarian Navy in the late 1880's (Stein, 2007). The so-called "Whitehead torpedo" was a device that was a locomotive torpedo which contained an explosive warhead as a payload, a three-cylinder compressed-air engine, gearbox, propellers, rudder, and a pendulum-and-hydrostat control. By the late 1890s, the design was modified to include gyroscopic gears. The torpedo itself was constructed out of steel and bronze and had a maximum range of 800 yards (Museum, 1980). This first AUV was without a doubt a harbinger of the field that would emerge (Figure 1-7).

Even in the earliest AUVs, then, there were precisely the same architectural elements present as in modern counterparts. Propelling the Whitehead torpedo was achieved through the gearbox, the compressed-air engine, and the propellers. Modern AUVs accomplish this same function with different formal elements. Instead of compressed-air engines, they use lithium-ion batteries. Gearboxes have been lightened with different materials, and propellers have been optimized for specific operating environments (Bluefin Robotics Corporation, 2015).

The first major technological advancement that shifted AUVs from the realm of torpedoes to robotics that are more recognizable today occurred in the 1970's with the advent of increased internal computing capacity (Blidberg, 2001). However, these early AUVs were still largely testbeds for emerging technologies. The main users of these AUV systems were largely academic entities that were seeking to increase research efforts in difficult to reach environments – such as the Arctic. Military applications of course, continued throughout the decades, although their true capabilities are not well documented. There are several instances in which autonomous underwater vehicles have been the focus of military contracts (e.g., for detecting mines (General Dynamics, 2011; General Dynamics, 2019; Whitman, 2002)), but little in the public domain pertaining to persistent subsea monitoring or data collection. It was because of these successful testbed and proof of concept efforts that the subsequent growth in the industry was enabled. The 1980's saw a major growth in the private AUV industry with major projects funded through Draper labs for U.S. Navy projects (Blidberg, 2001). Truly the enabling technology that was allowing for this continued growth was the increased miniaturization of, and increased capacity of computing elements in the system. It was here that the

current state of AUV architecture was also seemingly cast – there were very few prototype vehicles that were operated without a paired ship that acted as a mobile servicing platform.

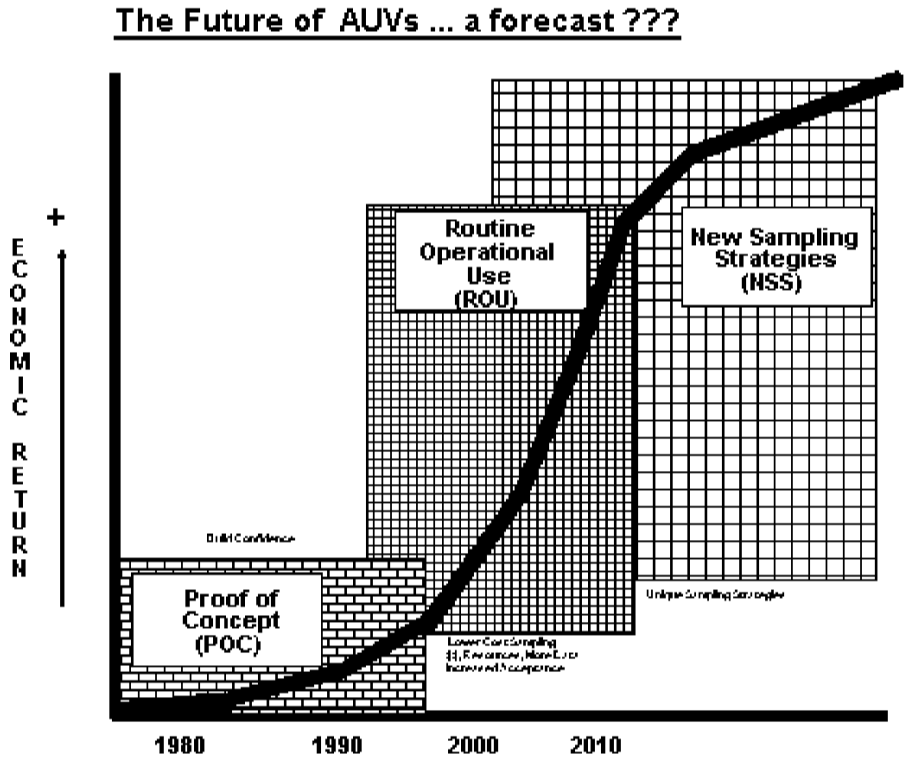

Figure 1-7: Qualitative evolution of AUVs through time. Figure 3, (Blidberg, 2001)

Why was this architecture selected? It could certainly be that it was the simplest solution at the time, but a more nuanced claim would be to examine how the forms of the enabling technology influenced the functions. The main functional elements of an AUV are communicating outside of the system, energizing the system, navigating, propelling the system, and sensing the surrounding environment. Increased computing power allowed the system to improve functionality in some of these elements, but it did not improve in others. Specifically, increased miniaturization and complexity of computer systems allowed for more specialized sensors to develop, and more advanced navigation. However, improved computing power came with increased power requirements. Battery technology was not improving at the same rate as computing during the 80's and 90's and thus AUVs would soon become limited in operational time (Blidberg, 2001). To stretch their active operation, other systems would get further de-prioritized. Saving power by limiting communication outside of the environment would be one such function that would be de-prioritized. Thus, the pairing with surface vessels was

cemented. Surface vessels would serve as recharging platforms and also data transfer stations. Interestingly, this also created new mission risk parameters – if a surface vessel had to leave the mission area, or if communications were severed with the AUV then all of the data would potentially be lost. This risk, of course, led to increased mission costs as mitigation strategies had to be put in place (Blidberg, 2001).

The 1990's saw the very first emergence of operational and commercial systems (Blidberg, 2001). It was required of these systems that very specific mission parameters be set because of the aforementioned limitations on some functional elements of the system. When an AUV was developed, it would be highly specialized and fit for purpose. 34 different vehicles were developed by nearly as many manufacturers for different users (Yuh, 2000). However, the purpose of each of these vehicles was limited to ten different missions: bottom survey, testbed, search and mapping, cable inspection, water column, mine countermeasures, science missions, pipeline inspection, undersea shuttle, and unspecified military applications (Yuh, 2000). It was in this environment that another key pain point of the modern AUV landscape was crystallized: instead of building platforms that standardized AUVs based on their mission profiles, each project was treated as a one-off and designed from more or less square one. Again, this leads to increased costs of operating a program with an AUV because design and build costs must be factored in to the overall program costs.

In the early 2000's, AUVs became much more commonplace. New use cases had started to emerge beyond research and military. Those applications included industry specific monitoring systems (e.g., oil and gas subsea infrastructure), climatology, and meteorology among others. It is because of the previously mentioned concept anchors, however, that profitability is still highly challenged for manufacturers and users. Some of the architectural choices that were made in the 1800's are still the dominant architectures during this time such as the shape of AUVs – specifically cylindrical shapes (Wang, 2009) – while others naturally evolved – such as sensors and instrumentation (Wang, 2009). One major area that had started to see improvement was in the discipline of battery power management. New battery technologies started to allow for more than several dozen recharge cycles for each battery, which greatly extended the life of a single powerplant. However, there was still insufficient advancement in autonomy for these AUVs to dock without assistance to their support vessels. Launching and retrieving AUVs was a laborious process during which care had to be taken so as not to damage the AUVs to the point where failures post retrieval may occur. By the end of the 2000's the community was once again hopeful that the coming decade would bring the technological

advancements that would allow for AUVs to finally take a greater role in commercial, industrial, and military use.

In recent years, advancements in AUV technology have been seen in areas of sensors, computing power (Figure 1-1), and autonomy. Historically, the sensors onboard an AUV were limited to those which would measure water pressure, temperature, orientation about three axes, and imagery (e.g., camera or webcam) (Wang, 2009). Modern advanced AUVs can be equipped with advanced sensors such as high-resolution side scan sonar (Bluefin Robotics Corporation, 2015), and detectors for trace chemical or biological data (Randolph, 2016). Side scan sonar is a technology that is particularly relevant for this thesis. It is a technology where acoustic beams are emitted normal to the direction of the AUV on both the port and starboard sides of the craft. As an AUV flies at an arbitrary elevation above the seafloor, the width of investigation (swath) can either increase or decrease. Side scanning sonar systems have a "blind spot" (called a nadir) beneath the AUV (Figure 1-8). To compensate, many AUVs install multibeam echo sounders to cover this area. The advances experienced in sensor technology can be attributed to such factors as improved power management systems, miniaturizations of existing technologies, and economic drivers. Regardless of the reason for increased functionality of sensor suites on modern AUVs, it is unquestionable that increased functionality is a result of more capable and broader functioning instrumentation. This increased functionality is sometimes colloquially referred to as increased autonomy, but that is not precisely accurate. Strictly speaking, autonomy is the "capacity for a machine to perform tasks in the world by themselves, without explicit human control" (Bekey, 2005). By this definition, autonomy is a binary feature – a robot either is or is not autonomous with respect to a task. As such, it would be accurate to say that since the range of tasks that AUVs can accomplish has broadened in recent years, and since AUVs can perform those specific tasks without explicit human control, then AUVs are still autonomous. In other words, AUVs have not become more autonomous, so much as they have become more capable at performing a broader set of tasks autonomously.

"Potential" is a word that is frequently used throughout the literature to describe the development of AUVs. "AUVs have a lot of potential in the scientific and military use" (Wang, 2009). "The potential for AUV systems is clearly recognized by most researchers" (Blidberg, 2001). "AUVs have various potential applications and great advantages over ROVs in terms of operational cost and safety" (Yuh, 2000). Despite this, their potential has perhaps been limited over their development lifecycle. Throughout the years, the advancements that have come to AUVs have been due to

technological advancements associated with the formal elements that comprise the detailed functionality of the system. Developments in battery capacity in the 2010s, sensors that were far more capable than their predecessors in the 2000's, computerization and miniaturization in the 1990's, and bold prototyping of new mechanical systems in the 1980's all contributed to AUVs that are without question more capable than their earlier generations. However, the higher-level architectures have remained the same since the very first Whitehead torpedo. AUVs are still tied to surface vessels that are manned. When the AUVs mission is complete, it returns to the surface vessel where it is manually fished out of the water, and recharged on the deck as its data is downloaded. This is where the emergent opportunity may lie. What can be gained from a system when its high-level architectural choices are challenged? Moreover, are technologies ripe for such an overhaul? Is now the right time to make this jump in AUV technology?

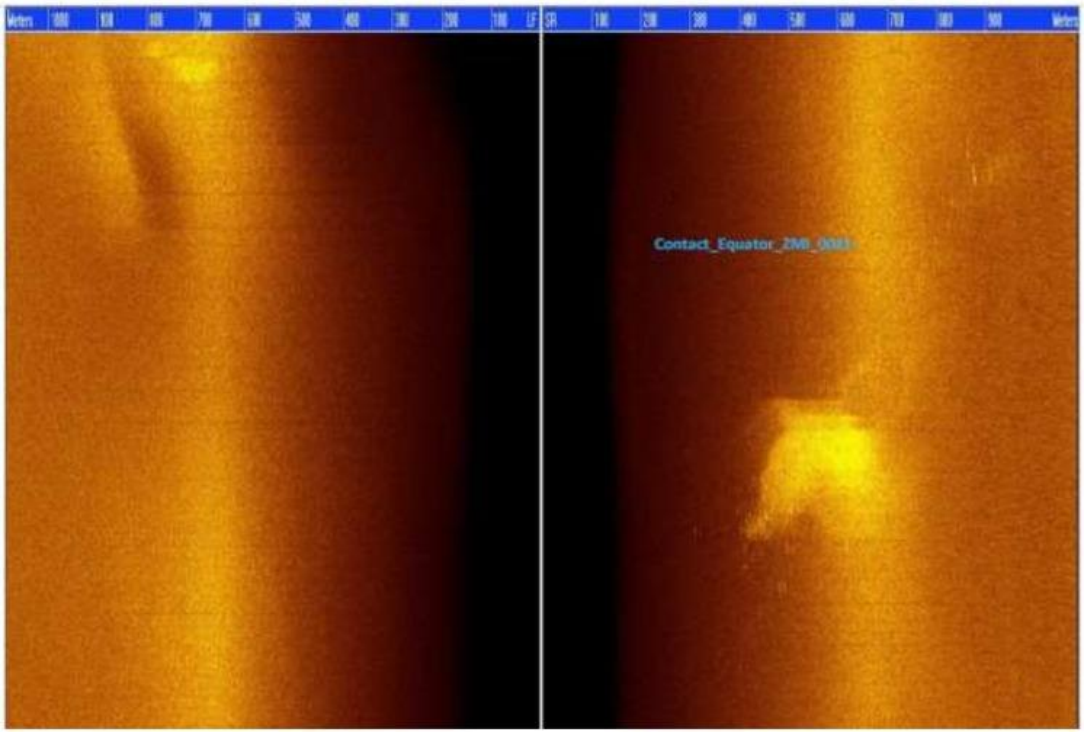

Figure 1-8: Image of side scan sonar data from the wreckage of MH370 (Australian Transport Safety Bureau, 2017). Note the blind spot in the middle of the image. In this case, the swath of investigation is ~1,000m in either direction from the AUV.

1.3 General Research Objectives

The primary research goal of this thesis is to explore which figures of merit can be improved by using swarms of AUVs and mobile service platforms over conventional methods. To answer this question, there are six implicit sub-objectives which will be touched upon throughout the text.

1) What figures of merit can be used to effectively evaluate system elements and which performance metrics can evaluate whole systems such that existing non-autonomous systems can be compared against hypothetical designed systems?
2) To what degree can a specific case study guide the evaluation of a full AUV system?
3) What specific performance metrics can be improved by pairing an AUV with an autonomous service station compared to existing implementations?
4) What performance metrics are in tension when evaluating the full system of AUV operations?
5) Can specific architectural combinations of functional elements be recommended and defended by using statistical evaluations of classical systems architectural analyses?
6) What – if any – are the emergent outcomes that are enabled with the novel pairing of AUVs and mobile service platforms?

These questions will all be focused through the lens of a case study where we have historical data that benchmarks recent AUV operations against estimated projections of future AUV performance metrics. The case study that will be tested is the AUV search and rescue efforts to find the crashed flight of Malaysian Air 370 (MH370) in 2014. This is an appropriate analogy because of its recent occurrence, high budget, and long-term operation. However, it is important to note that this report will not limit the findings to only search and rescue operations. Instead, the neutral function of continuous AUV operation to acquire subsurface data is a much broader application that sees use in many industries – including oil and gas, sub-sea data management, oceanography, climatology, meteorology, and other industry and academic circles.

1.4 Thesis Structure

In order to achieve these research objectives, this thesis is organized to first approach AUV systems and their service platforms from a neutral perspective. The initial analyses are equally applicable to any AUV system, although the specific forms which are investigated in detail are intentionally selected for the case study at hand. Following this neutral approach, the system is

evaluated on its performance metrics without any applied utility functions. Through the analyses all reported values are directly related to the underlying figures of merit. This allows for transparency and repeatability.

Within this thesis, the architecture of autonomous underwater vehicles and their proposed service platforms will be analyzed. In Chapter 2, the functions of AUV systems will be decomposed into their constituent elements. There are multiple options presented as formal solutions to the functional requirements. These formal options are associated with a collection of figures of merit. The relationships between the functions are also analyzed. In Chapter 3, an operational environment is defined, and performance metrics are derived based off of the figures of merit described in Chapter 2. The system is then evaluated deterministically across these performance metrics. Several key architectures are then identified through this deterministic approach which are in turn modelled probabilistically in Chapter 4. Chapter 5 focuses on synthesizing the results and interpreting the outcomes of the models. Specific recommendations are then made for the best overall performing architectures. Following this rigorous process, a serious underlying fault was found in the figures of merit. In Chapter 6, the impacts of this error are analyzed and recommendations are updated. Finally, this thesis closes with a discussion on opportunities for future research.

2 Architecture of AUVs and Their Service Platforms

In this chapter, the underlying architecture of AUV technology is evaluated. A brief introduction of terminology is followed by listing the critical functions of an AUV system. There are critical differentiations between conventional AUV system boundaries and the system proposed herein and those differentiations are explored. Next, since this thesis focuses not only on the architecture of single AUVs and their proposed service platforms, the scaling relationships which exist between multiple entities in the system are also discussed.

2.1 Introduction

When evaluating systems as complete entities, it is important to maintain perspective surrounding the formal and functional elements that combine to create the emergent functionality. Functional decompositions of systems allow for careful examination of the purpose of each contributing element of the system. Figure 2-1 provides an example of a functional decomposition of a sailboat as an example for functional decomposition. In this example, there are two levels of functions that are listed – note that this is not a comprehensive evaluation of all functions that are required for a sailboat system, but merely a few for demonstrational purposes. Level one functions are colloquially referred to as "high level" functions, and these can be further decomposed into their component functional elements. This "lower level" of function is an example of a set of level-two functions.

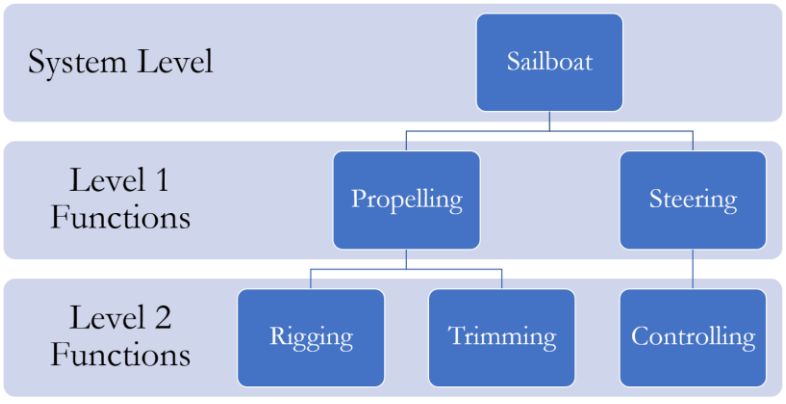

Figure 2-1: Schematic example of the functional decomposition of a sailboat as a system.

Formal decompositions of a system are structurally identical to functional decompositions. They are comprised of elements which can be broken into component elements in subsequent decompositions. On the other hand, however, formal decompositions allow for evaluation of the physical components of a system. Put simply, functional decompositions are focused on the purpose of parts of a system, whereas a formal decomposition looks at the individual items that comprise a system. In an effort to maintain neutrality surrounding the study of AUVs as a whole, a functional decomposition is a more appropriate analysis. The following chapter examines the specific required functions of an AUV and identifies possible formal solutions to achieve specific functionality.

2.2 Functional Architecture Background

For this thesis, the AUV system boundary is defined in Figure 2-2. Previously, an AUV system was centered about the AUV, but in this work the system has expanded. It is comprised of the AUV, its service platform, and the operating environment. These three elements interact with each other, and where that interaction occurs there is – by definition – an interface. Outside the system boundary exists the land-, sea-, or space-based crews or machines, data transmission mechanisms, and raw data conversion mechanisms. These elements all interact with each other through a different set of interfaces.

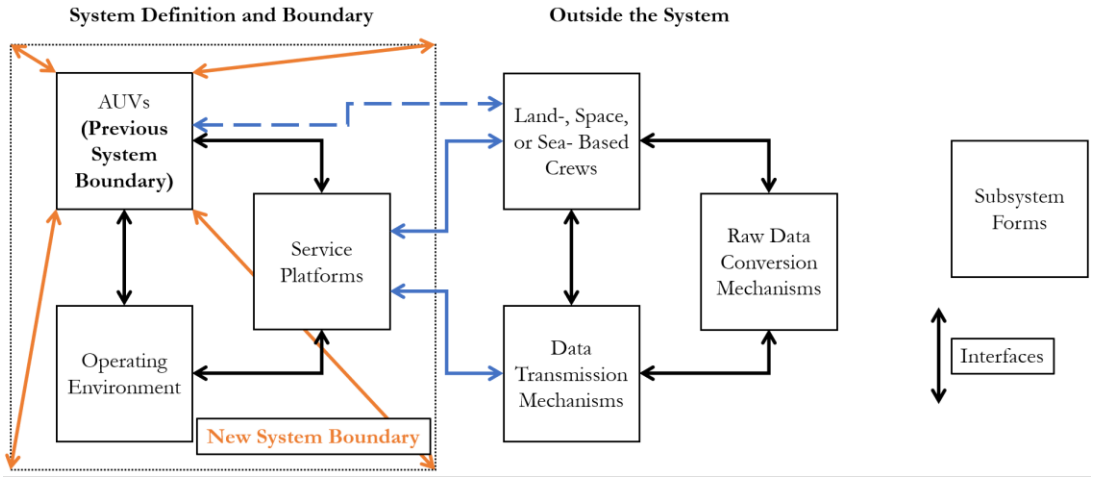

Figure 2-2: AUV system boundary definitions. Previous system boundaries existed around the AUV itself. In this thesis, the system boundary has expanded to include service platforms and the operating environment. Blue lines indicate interfaces between the system and elements outside the system. A dashed blue line represents previous interfaces that may or may not exist in previous AUV analyses, but will not exist in this analysis.

In an AUV, there are two high level and five distinct level-two functions that must be achieved in the system to meet any mission requirements. High level functions are the functions that must be performed for the system to perform. In the case of AUVs, the high-level functions are automation and navigation. Automation is an emergent property of the system, and navigation decomposes into five level-two functions. The lack of any of these functions will result in an architecture that does not meet the emergent capability of being an AUV. The level-two functions are instruments which are employed to accomplish the higher-level functionality. They include:

1) Communicating outside the system boundary
2) Energizing/powering the system
3) Propelling the system
4) Orienting the AUV
5) Sensing the surrounding environment

All of these functions were present in the Whitehead torpedo to some degree – although the evolution of these functions has significantly improved over the last 100 years. In the Whitehead torpedo, for instance, there was a pressure sensor mounted on the tip of the cylinder (United States Naval Undersea Museum, 1980) which would sense when the contact was made with the target, thus fulfilling the function of sensing the surrounding environment. Modern AUVs, by contrast, employ cutting edge acoustic mechanisms to map their surroundings in three dimensions and high resolution. The core functionality, however, remains unchanged.

The highest level of operation requires two functions to be carried out: autonomy and navigating the surrounding environment. Both of these functions are emergent through the interaction of lower-level forms and functions. Navigating is an emergent outcome when powering the system, propelling, sensing the surrounding environment, and orienting the AUV are all successfully integrated. The outcome of navigation is the ability of the AUV to locate where it is now, identify where it needs to go, reorient itself, and get to the target location.

Colloquially, autonomy is used to refer to an overall advancement in the capabilities of a system as a whole. In the realm of AUV operation, this usually refers to either the task complexity (specifically, the more complex a task an AUV can accomplish, the higher the level of autonomy) or task magnitude (specifically, the ability to accomplish more tasks simultaneously or throughout a single mission). This definition is insufficient for a technical analysis of the functionality of an AUV because

they both belie the critical fact that AUVs are by definition completely autonomous. Rather, they are each a different measure of the value that is delivered by AUVs in specific operating environments, or under different mission parameters. The ability to execute more complex tasks (measured in resolution, data acquisition, or other figures) and increased task magnitude (measured in different instrumentation used for instance) are nothing more than figures of merit that clarify that, in fact, an AUV is performing autonomously. Autonomy itself is an emergent function of all of the low-level functions previously listed. Without achieving any of these second-level functions, autonomy, as a high-level function, is lost. Detailed analysis of the underlying functional capability as it stands now will allow for a detailed tradespace analysis of the AUV industry as it currently stands as well as where it could exist in the near future with new architectures.

2.2.1 Communicating outside the system boundary

Modern AUVs utilize several different mechanisms for communication outside of the system boundary. There are two main categories of communication that are of concern in this analysis: communication directly to a control station (or service platform) and communication with other AUVs during operation. When communicating directly with a control station, communications can be required to either transfer data or to transfer operational requirements. For instance, an AUV could need to update its mission parameters (e.g., go to a different location and collect new types of data) or transfer (or stream) the collected data from a mission to a service platform. Communications between AUVs in operation are required if fleet operations need to be synchronized, or if there are different vehicles that specialize in different data collection operations.

Fundamentally, communication in an underwater environment is fraught with challenges because of the physical limitations on signal speed and attenuation in water. Both of these challenges, of course, are circumvented if a direct line is attached to the vehicle. However, by definition, if there is a direct connection between an AUV and a surface vehicle which provides either power or data transmission capability to the AUV, then the AUV is classified as an ROV – remote operated vehicle (Blidberg, 2001). When evaluating the communication options, the specific figures of merit include transfer range, data transfer rate, power consumption, and cost. By using these figures of merit, the different forms that achieve communication are comparable across the tradespace.

Communicating with a control station or service platform is a major hurdle for the AUV industry to overcome. Most existing systems transmit data to service platforms via direct communication following the mission. Generally, this is accomplished either through direct ethernet connection (or similar standards wired data transmission) or wireless networks once the AUV has been retrieved (Bluefin Robotics Corporation, 2015). Direct communication via dedicated network protocol (either through ethernet connection or via wireless transmission) is a very effective solution when the AUV is communicating with a surface vehicle, but the distance between the AUV and the surface vehicle must be very small. If the connection is wired, to achieve system autonomy (meaning no direct connection to the service platform), then the connection process at the service platform must also be automated. Wireless data connections have very low losses and very small delays when operating in air, but because of the physical properties of water, typical wireless signals are absorbed in fractions of a meter in a sea-water environment (Umair Mujtaba Qureshi, 2016; Anonymous, 2016).

Radio waves suffer this same difficulty with very low frequency waves. Thus, even standard radio frequencies (~20,000Hz) can only penetrate tens of feet of seawater (The United States Navy, 2001). The largest radio antennae in the world have around 30 miles of overhead signal transmission line, and even then, operating at 76Hz, radio frequency penetration into ocean waters is limited to hundreds of feet (The United States Navy, 2001).

One final electromagnetic solution currently being explored in academia and in industry is using laser communication (lasercom). Lasercom requires a direct linkage between the source and the receiver. In water, laser beams are limited in their capacity because of electromagnetic absorption of water. However, if a link is established very high data transfer rates (megabits per second) are within the range of possibility. To date, there are only experimental proofs of concept that work in controlled test environments and over short distances (tens of meters) (Parde, 2018).

Unlike light-based communications, acoustic-based communications in the subsea environment are far more effective than in air. However, there are physical challenges that face acoustic communications. Multi-path propagation and low bandwidth are the two most important hurdles to address. When a single source of sound waves is emitted, it can travel many different paths to arrive at a hydrophone receiver. The main issue with this limitation is that the time at which the signal will arrive is different depending on the length of the path that the wave traveled. Concerning the second physical limitation, bandwidth available in acoustic signals is generally very low. In 2017, NATO announced JANUS, the first standardized protocol with the intention to transmit digital

information using acoustic waves underwater (North Atlantic Trade Organization, 2017), and in 2019 the first publicly available modem that communicates in this frequency was made available. The Popoto Modem uses a 11.52kHz carrier frequency to transmit data acoustically at a rate of 80 bps (DellaMorte, 2019).

The five viable options for communication outside of the system boundary are direct connection, wireless protocol, radio frequency, lasercom, and acoustic. Each of these options have distinct advantages and disadvantages. Table 2-1 summarizes existing technologies and compares the figures of merit for each of these methods. While each of the figures of merit are estimated, the critical limitations are laid bare – the tension exists between communication range and data transfer rate. As range increases, the data transfer rate decreases with different options for the architecture.

Method	Transfer Range (m)	Data Transfer Rate (bps)	Power Consumption (W)	Cost ($)	Source
Ethernet	1	10,000,000,000	5	50	(1)
WiFi	0.1	300,000,000	20	100	(2)
Radio Waves	10	20,000	5	150	(3)
Lasercom	100	1,000,000,000	5(?)	1000(?)	(4)
Acoustic	1000	80	?	?	(5)

Table 2-1: Options for forms that achieve the function of communication outside of the system for AUVs. All cost values are estimates. Sources: 1 - (IEEE 802.3 Ethernet Working Group, 2020), 2 - (IEEE 802.11 Working Group, 2018), 3 - (Kinkade, 2016), 4 - (Whited, 1979), 5 - (DellaMorte, 2019).

2.2.2 Energizing and powering the system

While the earliest AUVs were powered via a range of methods and mechanisms, modern AUVs are exclusively powered electrically. The electricity in the system is what provides the AUV with the power to run sensors, internal computers, control surfaces, propellers, and all other system functionality. Because everything runs on electrical power, the only existing architecture for providing the electricity used by the system are battery packs. The battery packs themselves vary in their chemistry (e.g., lithium-ion, lithium-polymer, nickel-metal hydride, and lead-acid options for instance) but they are all limited in their abilities as their recharging capacity is located outside of the AUV itself. In this examination, the service platform would act as a recharging station. While some architectures

may exist where onboard generators convert fuel to electricity in the AUV itself, such options would only shift the burden of requiring electricity transfer to fuel transfer. Finally, the question of generating the electricity which will charge the AUV must be considered. For remote service stations, there are options that include renewable assets (e.g., solar panels, or wind turbines) as well as conventional methods (e.g., diesel electric generator). While there is ongoing work in the field of AUVs capable of self-charging (D. Richard Blidberg, 2004), they are considered outside of the scope of this research. Thus, for energizing the system, three distinct sub-categories must be considered:

1) Internal AUV battery – size and chemistry
2) Energy transfer method between service platform and AUV
3) Method to harvest electricity on the service platform

When evaluating battery options, it is important to recognize that there may be multiple uses in the system for batteries. Specifically, the remote servicing platform may require a significant power bank in which energy will be stored for some number of operational vehicles. This battery architecture may be different than that which is present in the AUV itself. As such, the figures of merit and metrics bear special consideration. For the AUV, classic operational metrics are of critical importance – specific energy (Wh/Kg), energy density (Wh/L), and power density (W/Kg) being of utmost importance. However, for the service platform battery bank, those metrics may matter considerably less than the cost of the batteries, number of cycles delivered from the power bank, and maintenance requirements. The maintenance costs associated with battery operation on the service platform are expected to be minimal compared to the maintenance costs associated with energy generation, but they will certainly scale with location to the service platform – the more remote the platform, the higher the associate maintenance costs. As such, it is prudent to prioritize system redundancy and longevity in the platform over other figures of merit.

2.2.2.1 Internal AUV Battery

There are two main factors to consider for placing batteries inside AUVs: the battery size and the battery chemistry. There exist four proven battery chemistry technologies that are currently used in industrial capacities: iron acid, nickel metal hydride, lithium-ion, and lithium-polymer. There are also emerging technologies in batteries that could improve upon existing chemistry. For instance, solid state batteries could improve battery performance by factors of 2.5 or greater. (Nancy J Dudney, 2015).

There are five figures of merit across which batteries will be compared: specific energy (Wh/Kg), energy density (Wh/L), power density (W/Kg), cycles to 80% (number), and cost ($). Cycles to 80% represents how robust a battery architecture is to frequent recharging. If there is a high number of cycles before a battery degrades to 80% of its initial energy capacity, then it is more robust to recharging. Costs that are provided are based on similarly sized 7-9V examples (Battery University, 2017). These 7-9V costs will likely not be identical to 12V or 24V systems that could be emplaced on an AUV, but power conversion systems tend to "decrease as system voltage increases" (United States Department of Energy, July 2019). Thus, the cost estimates for these batteries represent a realistic, current, medium to high-end estimate. Low and high estimates for all architectures are provided to demonstrate that by subtle variations in the physical construction of the battery, different performance can be met. These ranges represent the possible outcomes for specific architecture forms, as there is no single correct or standard value for any battery architecture across these figures of merit.

Lithium-based batteries are frequently used in electronic devices and large consumer electronics worldwide. Lithium-ion and lithium-polymer batteries are very common. Lithium-ion batteries have slightly improved energy density, and are considerably cheaper than their lithium-polymer counterparts, but lithium-polymer batteries have greatly improved battery degradation characteristics (Sabatini, 2011). Existing architectures tend to favor lithium-polymer solutions because of their flexible design and improved long-term performance (Bluefin Robotics Corporation, 2015).

Lead-acid batteries were the first rechargeable batteries that were ever invented (Battery Association of Japan, 2015). They have low specific energy, energy density, power density, and poor cycle degradation characteristics compared to lithium-based batteries. However, where they excel is their cost. Lead-acid battery configurations can cost up to five times less than lithium batteries (Wholesale Solar, 2018). For systems that rely on increasing the number of functions that can be completed autonomously, lead-acid batteries are not the ideal solution. They have shorter lifespans, require regular maintenance, and perform more poorly.

Finally, nickel-metal hydride batteries have been used in industry since the 1970s. One of the driving reasons that they are no longer used in the modern autonomous vehicle industry is the poor battery degradation characteristics compared to other architectures – specifically lithium-ion architectures (Paul Gerin Fahlstrom, 2012). Other performance limiting features include high operating temperatures and frequent full discharge cycles to prevent further performance degradation. A summary of existing battery metrics is summarized in Table 2-2.

Chemistry	Specific Energy (Wh/Kg)	Energy Density (Wh/L)	Power Density (W/Kg)	cycles to 80% (approximate)	Cost ($) (~7-9V example)	Source
Lithium-Polymer Low	100	185	245	500	100	(1, 2, 3)
Lithium-Polymer High	130	220	430	1000	100	(1, 2, 3)
Lithium-Ion Low	110	250	250	300	100	(1, 2, 4, 5)
Lithium-Ion High	160	693	340	500	100	(1, 2, 4, 5)
Lead-Acid Low	30	80	180	200	25	(2, 6, 7, 8)
Lead-Acid High	50	90	180	300	25	(2, 6, 7, 8)
Nickel Metal Hydride Low	60	140	250	300	60	(2, 9)
Nickel Metal Hydride High	120	300	1000	500	60	(2, 9)

Table 2-2: Summary of existing battery technologies and their associated metrics. Sources: 1 - (Sabatini, 2011) 2 - (Battery University, 2017), 3 - (Bluefin Robotics Corporation, 2015), 4 - (Panasonic, 2020), 5 - (Harding Energy, 2020), 6 - (PowerTHRU, 2016), 7 - (Battery Association of Japan, 2015), 8 - (Wholesale Solar, 2018), 9 - (Paul Gerin Fahlstrom, 2012).

2.2.2.2 Energy Transfer Method Between Service Platform and AUV

Beyond storing energy for the AUV in the form of a battery, there must exist a system in place to recharge the energy expended through nominal and off-nominal operations. From an architectural perspective, there are two viable methods for recharging the energy storage system – either a direct contact method or an indirect method. Indirect methods of energy transfer include electromagnetic induction, magnetic resonance, electric field coupling, and radio reception. Direct contact methods are numerous, but share many architectural elements (e.g., cables that connect directly to the electronics system of the target device, and the energy storage device). In exploring energy transfer architectures, the critical figures of merit for each recharging technology are recharging rate current (amperes), power delivery (watts), efficiency (a percentage of energy provided to the target relative to the energy drained from the source), and transmission distance (meters). It is critical to note that the transmission distance is reported in air as a medium instead of water. If wireless transmissions were performed in air, then attenuation would be much lower, and thus the possible communication range would increase.

Concerning indirect methods of energy transfer from energy storage sources to targets, the most commonly used method today is electromagnetic induction. Electromagnetic induction transfers power between the source and the target via magnetic field. This technology is used in small appliances such as toothbrushes, electric shavers, prosthetic devices in the medical field, and has recently experienced a surge of usage in small electronic devices such as cell phones. Modern standards for electromagnetic induction are evolving. A common standard for small products is the Qi open interface standard which specifies low power transfer constraints up to 30W (Wireless Power Consortium, 2017). Higher power standards have yet to be established. Using Qi standards – which are optimized for small electronics – the rate of current transfer is 1.67A (at 15W and 9V). The efficiency of electromagnetic induction charging changes as a function of distance between the source and the target, as well as alignment between the two, but efficiencies of up to 88% have been recorded (A. Berger, 2016). Using this method, transmission distance is highly limited using existing architectures – on the order of centimeters between the source and the target.

A complementary technology called magnetic resonant power transfer can extend the distance between the source and the target to up to two meters with an associated drop in transfer efficiency to 40% (Aristeidis Karalis, 2007). There are two differences between electromagnetic induction and magnetic resonant power transfer. First, as the distance between a source and receiver coil increases, their coupling decreases. This leads to lower power transfer efficiency (Wireless Power Consortium, 2018). Second, in order to increase transfer efficiency, the transmitting and receiving coils oscillate at matching frequencies (André Kurs, 2007). Figure 2-3 demonstrates a schematic of these differences. This technology is still developing, but there are large commercial offerings (such as WiTricity) where this technology is actively developed. Power delivery on the order of 1 to 10kW with efficiencies increasing to 90% as transmission distance decreases have been documented across multiple demonstrations (Takehiro Imura, 2009; Taylor M. Fisher, 2014).

Technology that is still under early exploration is the concept of electric field coupling wherein instead of matching magnetic resonance between the transmission source and the receiver, the impedance is matched. This architecture is a simpler design than magnetic resonance, can match power delivery and transfer efficiency, but can be limited by coupling distance and geometrical constraints (Bien, 2013). Experimental technology exploration has yielded results of power delivery up to 2kW at ~7.5A, transmission distances of up to .15m, and efficiency of 80% (H. Zhang, 2016).

Power transmission via radio, micro, or light waves utilize fundamentally different architectures than other indirect methods of energy transfer. Energy is emitted from an antenna regardless of whether a receiver is in place to receive the energy or not. This method of power transfer is traced back to attempts by Nikola Tesla and Heinrich Hertz at the turn of the 20th century. While early wireless power transmission efforts were highly inefficient, the development of antennas that can focus beams (instead of radiating in all directions) and a greater command over frequency control and advanced rectennas has led to the ability to advance this technology significantly. Despite decades of research, however, major limitations exist concerning transmission efficiency with the highest recorded efficiency of 84% (Matsumoto, 2002). Additionally, the power delivery is proportionate to the area of the receiver. It is very difficult to bound the precise figures of merit for this method of energy transfer given the prolific history, but a classic cited example delivered 100W of power at approximately 1A and an efficiency of 13% at a distance of approximately ten meters (Brown, 1984).

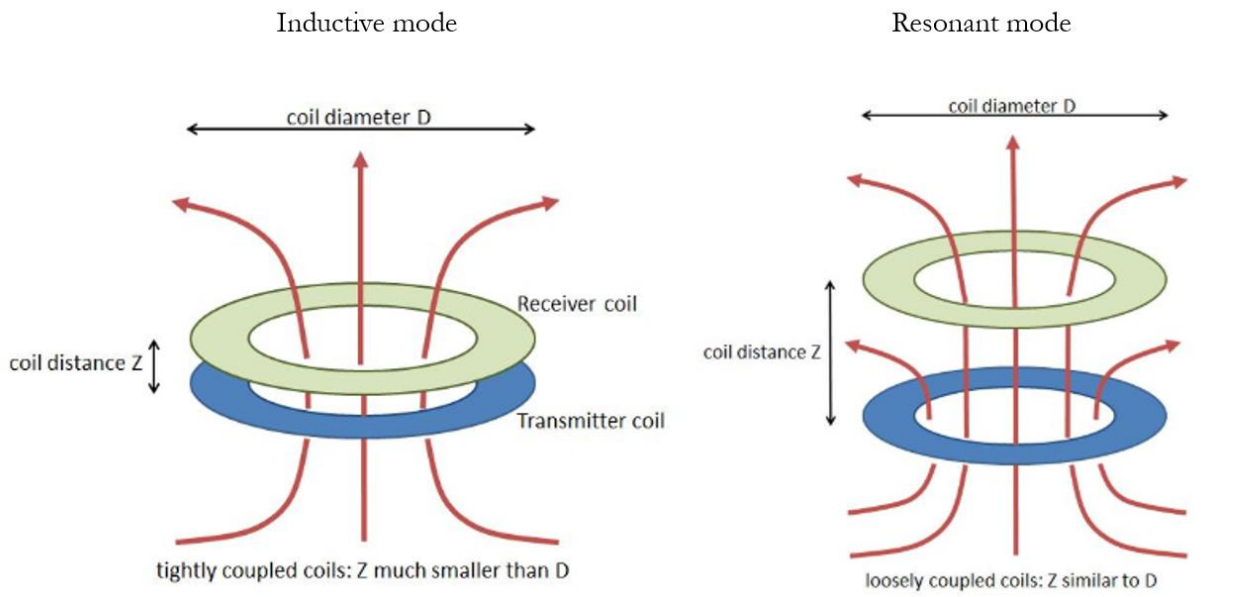

Figure 2-3: Schematic diagram illustrating the differences between two modes of wireless charging. Modified from (Wireless Power Consortium, 2018). In resonant mode, the two coils oscillate at constructively interfering or identical frequencies. There is no requirement for the coils to have the same dimensions.

It is critical to note that with all of these methods of wireless energy transfer between a source and a target, the medium in which the transmission occurs must be considered. In this instance, it is

highly likely that any AUV and their paired service platform would commence energy transfer operations in at least partially wet – if not entirely underwater – environments. The result is that any method of energy transfer via electromagnetic (EM) spectrum would be attenuated through the lossy medium that is water. For a method such as microwave power transmission, this would severely lower efficiency at distance because water attenuates signals with lower frequency more than signals with high frequency (Pope & Fry, 1997).

Direct methods of energy transfer are very common in commercial, industrial, and personal application worldwide. For the purposes of examining applications in the AUV space, established standards that are applied to electric vehicles (EVs) provide excellent anchor points to compare figures of merit against indirect energy transfer methods. By and large, these standards fall into one of three categories: Level 1, Level 2, or Level 3. Direct transfer, overall, sees much better performance in our figures of merit, but there are two qualitative elements that must be considered – degree of automation and corrosion of contacts. With a fully autonomous system, there will need to be significant engineering effort applied to engineer a system where ports on the AUV and the service platform will be connected. This is a non-insignificant process that merits significant consideration in the scheme of architectural goals. Secondly, whereas an indirect method of energy transfer can be completely isolated from the elements (specifically seawater) direct connections will expose the connectors between the AUV and the service platform. Corrosion of the contacts that facilitate energy transfer will be an issue requiring regular maintenance, which further impacts the viability of a completely autonomous relationship between the service platform and the AUV. This can be mitigated with automated cleaning and maintenance procedures applied to the connectors between the AUV and the service platform, but those processes would require further power demands and design efforts.

For direct connection standards and methods, the EV market has seen massive progress in recent years. Due to the similarity between AUVs and EVs (both are vehicles that travel from one point to another, or from one point returning to the same point), EV infrastructure provides a wealth of information about what modern energy transfer rates can be. Recharging electric vehicles with a Level 1 AC charging station means that household current is used to provide the power delivery. According to the industry standard SAE J1772 (revised October 13, 2017), at 120V, there are ranges of recharging rate currents from 12A to 16A delivering power between 1,400 and 1,900W. Charging efficiencies vary depending on the temperature of the surrounding environment, and how much energy was delivered to the battery overall. For Level 1 AC charging, average efficiency was found to

be 83.8% (J. Sears, 2014). The transmission distance is limited by cable length, but for most practical solutions, less than five meters is ideal.

Level 2 AC charging standards are different than Level 1 standards because of the operational voltage and recharging rate current. SAE J1772 defines the operational voltage for a Level 2 AC charger to be between 208V and 240V with currents ranging between 12A – 80A and typical values of 30A. The power delivery of these systems is considerably greater than Level 1 AC charging stations with 2,500W – 19,200W delivered, and typical values of 7,000W. Efficiencies of Level 2 AC charging stations are also considerably better than those of Level 1 AC charging stations with average values of 89.4% (J. Sears, 2014). Similar to Level 1 AC charging stations, the transmission distance is limited to approximately five meters before further performance degradation is to be expected.

The most powerful charging stations are classified as Level 3. These are far less widespread than the previous two types of charging stations, but their planned deployment has increased in recent years (Li Zhang, 2015). SAE J1772 defines the operational parameters for Level 3 AC charging as: using between 208V and 600V to produce a recharging rate current ranging from 50A to 400A (typically 60A), and a charging power of up to 240,000W with typical values of 50,000W. There are very few estimates available for the efficiency of Level 3 AC chargers, but initial trials demonstrate efficiencies between 84% and 88% (J. Channegowda, 2015).

When weighing the options between direct and indirect methods of energy transfer between an AUV and a power supply, there are several key features that have been demonstrated. First, by and large, indirect energy transfer methods deliver lower recharging rate currents and power delivery. This means that in any comprehensive architectural review, a service platform that functions as a recharging station would take longer to recharge a single AUV using indirect energy transfer methods. To accommodate an operational fleet size equal to one supported by a faster charging solution, the service platform would have to have the ability to recharge more vehicles at any given time, and the total idle fleet size would be greater by comparison. Second, while direct connections can accommodate much faster charging rates, there are issues that would arise in mechanical complexity and product maintenance. Two issues that are not captured by our four primary figures of merit. A summary of these findings is found in Table 2-3.

Method	Recharging Rate Current (A)	Power Delivery (W)	Efficiency (%)	Transmission Distance (m)	Direct or Indirect	Source
Electromagnetic Induction (low-power)	1.67	15	~90	0.1 - 0.5	Indirect	(1)
Electromagnetic Induction (high-power)	4	1,000	~80	0.1 - 0.5	Indirect	(2)
Magnetic Resonance	4 - 40	1,000 - 10,000	40 - 90	0.5 - 2	Indirect	(3, 4, 5)
Electric Field Coupling	7.5	2,000	80	0.15	Indirect	(6, 7)
Radio Reception	1	100	10 - 30	10	Indirect	(8, 9)
Level 1 AC	10 - 16	1,400 - 1,900	83.8	5	Direct	(10, 11)
Level 2 AC	12 - 30	2,500 - 19,200	89.4	5	Direct	(10, 11)
Level 3 AC	50 - 400	20,000 - 240,000	84 - 88	5	Direct	(12, 13)

Table 2-3: Figures of merit compared across energy transfer architectures. NOTE: transmission distance is reported for transmission in water. If transmission occurs in air, the attenuation would affect the system differently and distances would increase for indirect transmission, while stay constant for direct transmission. Sources: 1 - (Wireless Power Consortium, 2017), 2 - (A. Berger, 2016), 3 – (Aristeidis Karalis, 2007), 4 - (Takehiro Imura, 2009), 5 - (Taylor M. Fisher, 2014), 6 - (Bien, 2013), 7 - (H. Zhang, 2016), 8 - (Matsumoto, 2002), 9 - (Brown, 1984), 10 – (SAE Standard J1772), 11 - (J. Sears, 2014), 12 - (Li Zhang, 2015), 13 - (J. Channegowda, 2015).

2.2.2.3 Energy Harvesting Method Co-located With the Servicing Platform

Fundamentally, there are two categories that are under consideration for harvesting energy: renewable sources of energy, and non-renewables sources. Potential candidates for renewable sources of energy include solar, wind, and wave power generation. Diesel and gas generators and gas microturbines are likely the most viable options for non-renewable power sources due to their size, advanced capabilities, and power production characteristics. Across the planet, 26,951TWh of electricity was generated in 2019 (IEA, 2020), with approximately 97% of that electricity generated by turbines driven by combusted gases, steam, wind, or water. When considering a system to harvest energy from the operating environment of the AUV, this fact should remain at the forefront of the system: turbines are highly mature, reliable, and robust architectures that are generally not prone to failure or excessive maintenance. In order to compare across renewable and non-renewable architectural options, the following figures of merit are considered: electrical power output (Watts) and 10% discounted cash flow over ten years per electrical power output (dollars/Watt). For the purposes of this work, size restrictions will not be considered, and calculations will assume that any of the architectures could be built in such a way that the service platform and the energy harvesting system could physically operate in the same location.

Solar power is a very promising technology for an integrated AUV and service platform architecture. Solar panels have recently greatly decreased in cost and are much more viable options for energy harvesting than in the past (J. Hernandez-Moro, 2013). There are issues of frequency of power delivery (for instance if the sun does not shine), but most of these concerns can be addressed through increasing power delivery and power storage options, effectively increasing the reserve of power onboard the service platform, and increasing the rate at which that storage could be refilled in times of sunlight. Importantly, solar power systems do not perform identically in different locations. For instance, high latitudes receive less solar radiation per unit space (Coddington, Lean, Pilewskie, Snow, & Lindholm, 2016), and thus solar panels are less productive in such environments.

To create a solar array on the service platform, a collection of commercially available solar panels would be integrated into a larger system. The standard size of a single solar panel is approximately 1.65m^2 and the top ten solar panels for 2020 produce between 285 and 360 Watts at standard testing conditions (Zientara, 2020), or between 174 and 220 W/m^2. For standardization purposes in the following calculations, a 32-panel solar array (with each panel measuring a standard 165cm by 100cm) is assumed, creating a solar array with an area of approximately 53m^2. The nameplate power capacity of this system at standard test conditions would be between 9,100W and 10,200W. The average solar radiation that arrives at the top of the earth's atmosphere is 1,361W/m^2 (Coddington, Lean, Pilewskie, Snow, & Lindholm, 2016). As the sun's energy travels through the atmosphere, it is attenuated to approximately 1,120 W/m^2 on a horizontal surface at ground level (Newport Corporation, 2020) which represents a decrease of approximately 18% of all the energy that intersected the upper atmosphere. Furthermore, this represents only the instantaneous peak irradiance that can only be experienced when the sun is at its zenith on a cloudless day. In an effort to average this value over an hour, and evaluate commercial panels at a standard irradiance level, standard testing conditions are set to an irradiance of 1,000W/m^2 which is subsequently referred to as a "peak sun hour." The capacity of a system is thereby governed by the number of peak sun hours that a specific location may experience on average over a given period of time. In other words, in counting the number of peak sun hours at a given location, one can account for seasonal and location specific variability in solar irradiation variation. For instance, across areas near the equator, average annual peak sun hours per day are between four and six hours (Bowden, 2019). Theoretically, the power output is limited not by the solar panel, but rather by the footprint of the array. The space-efficiency of this footprint expansion will be governed by the distance the array is from the equator – the farther

north or south from the equator, the less space-efficient a solar array will be. To account for this variation from standard testing conditions, in this thesis, the total output of the system will be cut by 80% resulting in a capacity factor of 20%. This discounting is verified through publications which examine the performance of offshore solar power plants (C. Diendorfer, 2014) which estimate total solar irradiance in offshore environments from raw high-resolution satellite data (Lamont-Doherty Earth Observatory/Columbia University, 2020).

When examining commercially available solar photovoltaic power solutions, costs per Watt are approximately $3.10 for systems that are approximately 4kW – 6kW in size (Solar Reviews, 2020), which verifies a continued trend of lower costs per Watt over time (J. Hernandez-Moro, 2013). The total system under consideration would have a power output at standard testing conditions between 9,100W and 10,200W, and cost between $28,200 and $31,600. A major advantage to solar arrays powering the support platform and the AUV system is the considerably low requirement for ongoing maintenance costs and operational expenditures (OPEX). The solar power inverter that is present within most systems is replaced on average once every ten years and generally costs approximately 1.5% of the total capital expenditure (CAPEX) (Power from Sunlight, 2017). If the system is located in a very remote location and requires maintenance, then these numbers will increase dramatically. For offshore environments, marine operations costs (including boat rental, fuel, and crew) are usually approximately $0.03/kWh for large systems which have capacities of tens of MW (Vincent S. Neary, 2014). It is assumed here that these estimates for marine operations are quite low for high-end estimates, and as such are taken at full rental and crew costs, rather than normalized. In this case, the rental, operation, and support for a medium vessel with the capacity to service remote offshore environments ranges from $1000/kW to $2500/kW (Vincent S. Neary, 2014). This range is expected to scale up and down depending on what type of vessel is required and how frequently maintenance is required. For the purposes of this study, a static value of $20,000 is assumed for each round trip a service vessel must make. If the AUV and is service platform were located in less remote environments (beyond the scope of this thesis) then it is likely that this annual cost estimate is inaccurate and high. This means that the total 10% discounted cash flow over ten years per electrical power output is between $23/W and $136/W. These values can be linearly scaled up to systems that are upwards of 10,000W of power delivery with larger and larger solar arrays. Finally, it is worth noting that upscaling the size of the solar array would have the added benefit of increasing tolerance when there are

extended periods of time without ideal sun conditions. Larger farms could recharge battery banks quicker making better use of shorter time windows.

Similar to solar panels, wind turbines could be used to create an arrayed power generation site. Wind turbines are well established, but still evolving in the technology space today. The range of products that could be deployed is very broad. The largest turbines have rotor diameters of hundreds of meters and produce over 10MW of power (General Electric, 2020), with small personal turbines with rotor diameters just over one meter and producing power on the same order as a single solar panel (Avant Garde Innovations, 2020). The price of a wind turbine tends to scale directly with the power that is produced. Existing turbines cost approximately $1.1 million/MW (WEPD Staff, 2019).

From the perspective of power output, there are few practical options that provide less than 500W of power delivery. Additionally, for the purposes of this exploration, there is little reason to consider using more than several 10,000W turbines which would require significant engineering to be properly anchored and secured aboard the service platform. For the purposes of modelling in this thesis, a standard operational size of ten wind turbines with 1,000W nameplate capacities, for a total of 10,000W capacity, will be used.

From an operational perspective, both the OPEX and maintenance costs associated with onshore wind scale with installed capacity as well. Average OPEX and maintenance costs are approximately $38/kW (IHS, 2018), which means that a small wind farm with a 10kW capacity would have annual OPEX costs of approximately $380. However, based on the distance from the project to the maintenance facilities and the meteorological ocean climate where the AUV service platform is operating, maintenance costs could scale annually up to $144/kW for relatively nearshore projects (for a total of $1,440 annually), up to annual costs of $20,000 for emergency maintenance (specifically marine operations and several hundred dollars in repair parts) in highly remote areas similar to the emergency repairs required for solar arrays (Tyler Stehly, 2018). Finally, similar to solar arrays, output from wind farms must be discounted against their installed capacity via a capacity factor to account for time that wind is not blowing within ideal speed windows. In 2019, there were 105,583MW of installed wind capacity in the United States (American Wind Energy Association, 2019). This means that if all wind farms in the United States operated at nameplate capacity, there would be 924,907GWh of energy generated in 2019. However, only 300,071GWh were produced. This means that on average, wind farms across the U.S. are only 32% efficient relative to their nameplate capacity. Estimates for offshore windfarms suggest that offshore wind capacity factors could range between 29% and 52%

(International Energy Agency, 2019). For our model, a 32% capacity factor will be applied to our 10x 1,000W type architecture, which brings total power output to 3,200W. The range of discounted cost/power output for wind power generation then, ranges from $5.0/W to $44/W.

A third viable option to harvest energy for the service platform and the associated AUVs would be to utilize the emerging field of wave energy. Wave power captures energy of waves in the ocean and converts that directly to electrical energy using one of several methods – point absorber buoys, surface attenuators, oscillating wave surge converters, oscillating water column devices, overtopping devices, or submerged pressure differential converters (Figure 2-4). A limiting factor that is common among many of the wave energy harvesting architectures is that they rely on being moored or anchored to the ocean floor. It is this mooring or anchoring that provides a static point against which the waves can move and generate forces to either pump hydraulic fluid through turbines or to actuate a piston. If this architectural hurdle could be overcome and a design could be fitted with sea drogues or other forms of position management, then there could potentially be viable options to supply power to the service station. Currently, however, this has not been commercialized. There are active areas of research that are working to resolve this technical limitation. Power output can range between 3,000W and 7,500W depending on the selected architectures at peak performance (Ocean Power Technologies, 2020). Similar to solar and wind power options, this power output should be discounted via a capacity factor to represent the reality that there will not always be ideal circumstances for the wave power generators to operate. Comprehensive studies on the comparisons of levelized cost of energy suggest that depending on the precise form selected, this capacity factor can range from 30% to 70% (D. S. Jenne, 2015). For this study, a value of 50% is assumed. It is also very difficult to find accurate estimates of pricing, but the units themselves are estimated to cost at least $40,000 (Johnson, 2012). For architectures that are commonly associated with wave ocean energy projects such as point absorbers, the capital cost can range between $13,000/kW for large projects of 100 individual units or more, and $61,000/kW for small projects of fewer than ten individual units (Vincent S. Neary, 2014). OPEX and maintenance for these systems is extremely low by design, and can range between $400/kW for large arrays and $4000/kW for small arrays annually (Vincent S. Neary, 2014).

In examining this system, it is far more likely that the total number of units will be between one and 100, and so in calculating the total CAPEX required, the low-power output option of 1,500W is multiplied by the high CAPEX cost per kW, and the high-power output option of 7,500W is

multiplied by the low CAPEX cost per kW. Thus, the total CAPEX for wave power, is estimated to be between $91,000 and $98,000. For calculating long-term costs, OPEX and maintenance are combined to equal the estimates set forward by national reports. Similar to CAPEX, the high OPEX is paired with and multiplied with the low-power output, and the low OPEX is multiplied with the high-power output option. This means that the total 10% discounted cash flow over ten years per electrical power output is between $79/W and $13/W for the 1,500W and 7,500W systems respectively.

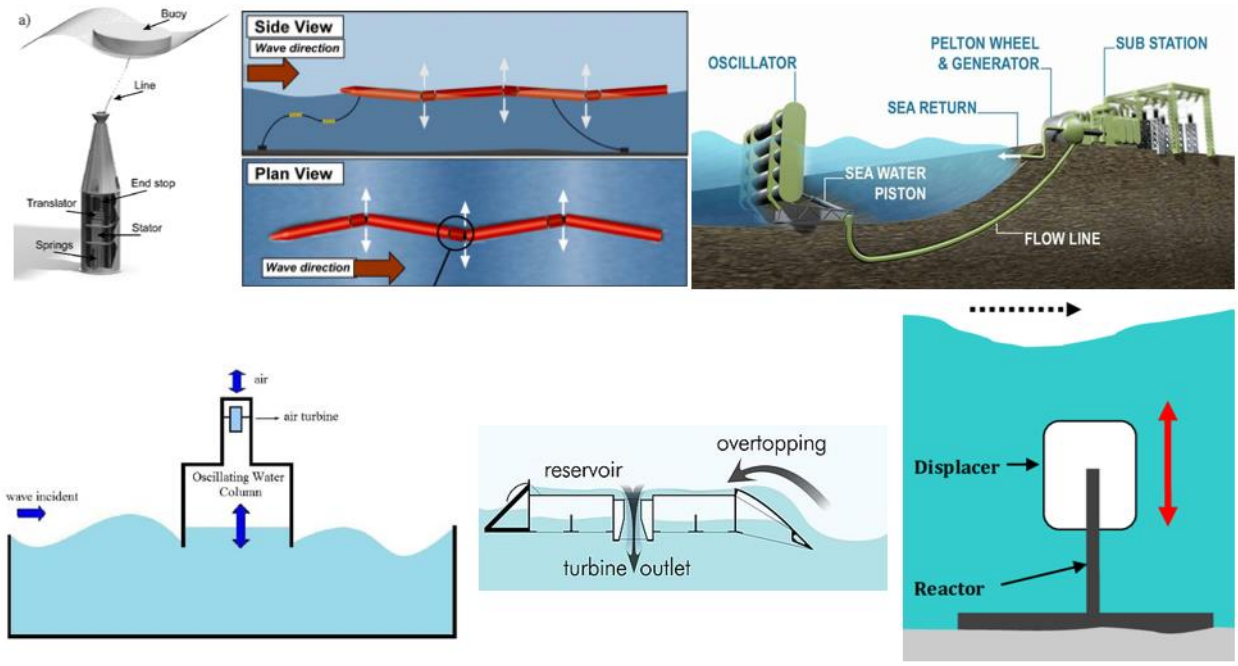

Figure 2-4: Comparison of the six major wave power generation methods. Clockwise from upper-left modified from: (J. Engström, 2013; Robertson, 2010; Ghasemi, 2014; Lorenzini, 2015; B Drew, 2009; Dara O'Sullivan, 2016) point absorber buoys, surface attenuators, oscillating wave surge converters, oscillating water column devices, overtopping devices, and submerged pressure differential converters.

Generators are a reliable technology that are deployed worldwide to produce energy from various hydrocarbon sources. These fuels can either be diesel, gas, methane, or propane. These generators represent the simplest form of creating electricity on the service platform to recharge AUVs. However, there are significant logistical hurdles that would need to be overcome. Using OPEX and maintenance estimates from offshore platforms as analogues, logistics and administration (e.g.,

costs associated with maintenance) are approximately one half of OPEX field facilities costs (Oil and Gas Authority, 2018). However, the maintenance costs that are assumed in our model will use the same $20,000 per service visit that is used to estimate the cost of a single visit to the remote platform for the renewable power options. This means that OPEX costs are dominated by the cost of visiting the service platform. OPEX costs that are commonly associated with small (less than 10kW capacity generators) are approximately $50 annually, and larger models can increase to $2,000 annually (Home Advisor, 2020; Benjamin O. Agajelu, 2013) less fuel costs. Generators that operate under 20kW capacities consume approximately 1.5 gallons of fuel per hour, whereas 25kW systems consume approximately 2.5 gallons of fuel per hour at full load (Diesel Service and Supply, 2020). Average retail fuel costs in early 2020 are approximately $3 per gallon (U.S. Department of Energy, 2020) which means that if these generators are run at full load for 24 hours a week, the fuel costs would be between $39,420, and $65,700 annually. Assuming that generators' fuel tanks would have to be refueled twice monthly, maintenance costs would balloon to $480,000. If a much larger fuel tank is utilized, and refueling can be achieved only six times annually, then the maintenance costs will be reduced to $120,000. This would clearly reduce autonomous functionality of the service platform, as the service platform is now required to receive fuel at regular intervals. However, there are generators that could provide very wide ranges of power delivery which could be scaled to the size of the system – power output can range from 1,000W to upwards of 25,000W. Additionally, given how advanced generator technology is, and how saturated the market is, there will rarely be any problems securing replacing equipment as needed. Considering fuel consumption and maintenance costs, and discounting them over a 10-year operational lifespan, the cost/power ratio of most generators is between $1,097/W and $149/W for 1kW and 25kW systems respectively.

Another option to generate power with non-renewable fuel is to use microturbines. Microturbines are effectively very small-scale powerplants that evolved from auxiliary power units. They are comprised of relatively few moving parts, they are compact in size, scalable in series (i.e., multiple units can be connected in series to increase power production linearly) and are generally quite efficient (Capehart, 2016). Most microturbines are run on an external fuel source – either propane or natural gas. Microturbines have CAPEX costs that range from $2.5/W to $3.2/W and for systems with capacities up to 1,000kW, OPEX costs which are between $50 and $1,000 annually (U.S. Department of Energy, 2016). From a CAPEX perspective, this means that 10kW systems would cost $25,000 to $32,000, and 200kW systems could cost between $500,000 and $640,000. Depending on

system size, fuel consumption rates range from 0.38MCF to 4.05MCF of natural gas per hour (U.S. Department of Energy, 2016), and assuming natural gas prices of an average of 2019 prices which equals $3.85/MCF (U.S. Energy Information Administration, 2020) this would mean that fuel costs for microturbines could range from $12,700 to $136,000 annually However, a 200kW system only consumes approximately 2.2MCF of natural gas per hour, which suggests that a more reasonable high-end estimate for the system under consideration would be $94,400 annually. Similar transport assumptions must be made to those of diesel generators, where the maintenance costs are largely related to the costs of shipping the fuel to the platform. Combining these variables together, the average cost per Watt of power output over a discounted 10-year timespan could range from $92 to $23 for a 10,000W system or 200,000W system respectively. Table 2-4 summarizes the findings of this architectural analysis.

Method	Nameplate Capacity (W)	Power Output (W)	Cost/Power Output ($/W)	CAPEX ($)	OPEX ($)	Maintenance Cost ($)	Source
Solar	9,100 - 10,200	1,820 - 2,040	18 - 83	28,200 - 31,600	130 - 500	500 - 20,000	(1, 2, 3, 4)
Wind	10,000	3,200	5.0 - 44	4,000	380	1,440 - 20,000	(5, 6, 7)
Wave	3,000 - 15,000	1,500 - 7,500	79 - 13	91,000 - 98,000	200 - 3600	200 - 400	(4, 8, 9, 10)
Generator	1,000 - 25,000	1,000 - 25,000	1,097 - 149	200 - 20,000	39,470 - 67,700	120,000 - 480,000	(11, 12, 13, 14)
Mircoturbine	10,000-200,000	10,000-200,000	92 - 23	25,000 - 640,000	12,750 - 95,400	120,000 - 480,000	(15, 16)

Table 2-4: Comparison of formal elements to harvest energy for AUV platforms. Sources: 1 - (C. Diendorfer, 2014), 2 - (Lamont-Doherty Earth Observatory/Columbia University, 2020), 3 - (Solar Reviews, 2020), 4 - (Vincent S. Neary, 2014), 5 - (WEPD Staff, 2019), 6 - (Tyler Stehly, 2018), 7 - (International Energy Agency, 2019), 8 - (Ocean Power Technologies, 2020), 9 – (D. S. Jenne, 2015), 10 - (Johnson, 2012), 11 - (Oil and Gas Authority, 2018), 12 - (Benjamin O. Agajelu, 2013), 13 – (Diesel Service and Supply, 2020), 14 - (U.S. Department of Energy, 2020), 15 - (U.S. Department of Energy, 2016), 16 - (U.S. Energy Information Administration, 2020).

2.2.3 Propelling and orienting the AUV

The combinations of the propelling and orienting functions of the AUV are implicitly interlinked. The combined function of propelling and orienting an AUV in an underwater environment are considered under an umbrella emergent function referred to henceforth as "controlling." The reason to collapse these functions into a single higher-order function is because of a very small number of architectures that can accomplish the tasks of propelling and orienting, and they are mutually exclusive of one another. There are two architectures to propel an AUV – propellers and impellers – and there are two architectures under considerations to orient and AUV – rudders

and thrusters. Fundamentally, in order to accomplish controlling, the acts of propelling and orienting must be accomplished (to some degree) simultaneously. By forcing water to flow over control surfaces, the orientation of the craft can be changed. If the control surfaces are completely independent of the propulsion architecture, then in the case where there is no propulsion, the orientation of the AUV cannot change. Similarly, if the control surfaces are the same surfaces as the propulsion architecture, then without propulsion, there can be no orientation change. The figures of merit to consider are largely qualitative or binary for the combinatorial function of controlling the AUV. There are six total architectures that will be evaluated across the figures of merit: power consumption (low/medium/high) high velocity maneuvering capability (very poor/poor/medium/good/very good/exceptional), low velocity maneuvering capability (medium/good/very good), zero velocity maneuvering capability (very poor/poor/medium/good/very good/exceptional), and overall complexity.

The function of propelling an AUV is accomplished by converting slow moving or static water and speeding it up to faster moving water by a mechanism mechanically attached to the AUV. This conversion applies an equal force to the AUV and creates motion in the opposite direction of the force applied to the water. The oldest architecture to accomplish this function was a standard propeller (United States Naval Undersea Museum, 1980), which converted power into thrust by accelerating the water and creating a pressure differential behind the propeller. Modern propellers function in precisely the same way. There are many advantages of propellers as a method of propelling a system: it is a tried and true and very robust architecture. The main drawbacks exist in operation environments when there is a high possibility of debris getting tangled around the propeller. However, shrouds and grates can prevent this from happening and in some cases also improve the efficiency of the drive system. As a principle, propeller efficiency increases at lower speeds and denser fluids (Rawson, 2001).

Another modern method of propelling vessels through the water is by the use of impellers. Impellers spin and create a low pressure at the center of an impeller and shoots water out of the impeller radially in channels because of the associated centripetal force generated at the center of the impeller blades. As water exits the impeller, its pressure increases and exits the system at high pressure and eventually high velocity. By pushing the low or zero velocity water through the impeller system, the and equal and opposite force is imparted on the vehicle. One inherent disadvantage to impellers is the requirement for the water intake to constantly be clear. If any debris is caught in the input, then there will be decreased performance to the point where it could stop performing its primary function.

In contrast to propellers, different designs of impellers have efficiency curves that generally increase with greater capacity and specific speeds (Evans, 2012)

The oldest method of orienting an AUV was to include control surfaces that were rudders oriented about normal axes to one another (United States Naval Undersea Museum, 1980). These rudders were oriented at the aft section of the AUV and would be able to control pitch and yaw of the craft when it was in motion by flexing either up, down, left, or right. Early AUVs were not capable of controlling roll because the vertical and horizontal rudders were interconnected. Modern architectures exist that can control roll with the same four rudders that are independently controlled (Yinghao Zhang, 2017). These advanced rudder systems still require water to flow over the control surfaces to orient the craft – thus inexorably pairing propelling and orienting.

A second method of orienting an AUV is to use devices called thrusters along all three axes of orientation (Xianbo Xiang, 2020). Thrusters generate thrust in any of these directions using either of the methods outlined in the propelling function. Thrusters are generally equally effective at orienting an AUV at any velocity, as they contribute new force vectors that act upon the vessel, rather than alter existing ones. One downside to thrusters is their placement often must be precisely located at equal distances away from or exactly at the center of mass of the vehicle. This can lead to shapes that are far less hydrodynamic which can reduce the operational capacities of a vehicle, although through-body thruster designs have begun to improve this aspect of thrusters (Xianbo Xiang, 2020).

One other method of orienting an AUV is through the use of thrust vectoring and the novel control algorithms that are associated with it (Tao Liu, 2019). This method allows whichever method of propulsion is under consideration to gimble about two axes. If the main forward propelling method is gimbled, then the vectoring allows for control of pitch and yaw.

There are six distinct architectural combinations to take into consideration when examining the function of controlling an AUV. They are compared across qualitative figures of merit – as quantitative figures of merit require specific operational parameters and lower decisions in place. The figures of merit to evaluate controlling an AUV are power consumption, high-, low-, and zero-velocity maneuvering capability. These findings are summarized in Table 2-5. These architectural combinations represent real decisions required to successfully create an AUV that can autonomously operate. There is no dominant combination of figures of merit – however all solutions that use propellers instead of impellers will likely have lower power consumption than their impeller counterparts because of their

aforementioned efficiency differences. For that reason, it is likely that there will be very few cases where impellers would be the ideal architectural selection, and architectures with propellers would be able to achieve the same performance with lower power consumption. Effectively, depending on the specific mission parameters or operating environment, the controlling system will likely be different. For instance: if very large swaths of ocean floor are to be examined by acoustic imaging, then speed is of critical importance, and orientation via vectoring would likely be the best solution, but if very precise control near reefs or sensitive equipment is required, then thrusters would be ideal.

Architecture ID	Propelling	Orienting	Power Consumption	High-Velocity Manuvering	Low-Velocity Manuvering	Zero-Velocity Manuvering	Sources
1	Propeller	Rudder	Low	Good	Medium	Poor	(1, 2, 3)
2	Propeller	Thruster	High	Medium	Good	Exceptional	(1, 4)
3	Propeller	Vectoring	Medium	Very Good	Medium	Very Poor	(1, 5)
4	Impeller	Rudder	Medium	Good	Medium	Poor	(2, 3, 6)
5	Impeller	Thruster	Very High	Medium	Good	Exceptional	(4, 6)
6	Impeller	Vectoring	High	Very Good	Medium	Very Poor	(5, 6)

Table 2-5: Comparison of all possible architectures that could be evaluated for controlling an AUV. Sources: 1 - (Rawson, 2001), 2 - (United States Naval Undersea Museum, 1980), 3 - (Yinghao Zhang, 2017), 4 - (Xianbo Xiang, 2020), 5 - (Tao Liu, 2019), 6 - (Evans, 2012).

2.2.4 Sensing the surrounding environment

While there may be hardware that is specific to a certain mission or operational environment, all AUVs, by definition, need the capacity to sense and negotiate the surrounding environment. In effect, there must be some method of identifying where the AUV is relative to where it should be and making an autonomous decision about how to reach the desired location. Methods to sense and negotiate the environment include dead reckoning methods and paired acoustic sensors (or laser range finders) with decision making software to avoid collisions, and finally more advanced software which utilizes acoustic data to create on-board geometric models of locations visited.

Dead reckoning as a location and navigation tool has long existed in the nautical realm. Dead reckoning utilizes velocity, depth, and directional data to calculate deviation away from a known fixed starting location (Zheping Yan, 2010). Dead reckoning requires very few instruments to run in order to function, and as such is a very low power option to achieve the function of sensing and negotiating

along a path. However, a critical drawback to this method is that the area under consideration for investigation must already be known – a plan must already be in place for the AUV to execute. There is implicit error associated with all dead reckoning, and this error propagates as time goes on. The result being an increased error through longer and longer operations of an AUV that relies exclusively on dead reckoning, although modern processing techniques utilizing onboard navigation software have reduced these propagation rates significantly (M. T. Sabet, 2018). Additionally, given that there are no sensors to detect and avoid collisions, there must be reasonable confidence that there will not be any such surprises. This also excludes this architecture from any system that would perform detailed, close-range investigations of any features of the ocean floor.

Collision avoidance systems are a second architecture that assist in sensing the surrounding environment. It is a major field of study in the AUV sector, as any work that requires close examination of material in the ocean requires such a system to assure no damage comes to the vehicle. A common method to detect possible collisions utilizes a sonar beam which provides return times to the AUV which are then converted to a distance to possible objects. Rapid scanning rates provide a grid of data that the AUV can find an obstacle free path to navigate (Schjølberg, 2018). These collision avoidance systems have become more nuanced over time, and are quite advanced at this point with early detection allowing for highly efficient route planning (Alexander Inzartsev, 2010). A drawback of using exclusively collision avoidance systems is that they can only be used for upcoming obstacles. Effectively, there is no way to carry out a specifically located mission because there is no way for the AUV to navigate to or from a known (or nearly-known) location. As such, relying exclusively on this architecture can have significant challenges in remote environments.

Environmental modeling is a method of location and mapping which is the most advanced and power intensive method of those explored. From this technique, forward facing sonar data are obtained and utilized to develop an environmental model of the surroundings. As the AUV travels through the ocean, the environmental model of the surrounding area is updated and referenced back against earlier iterations to locate the current position of the AUV by matching features (Tiedong Zhang, 2008) . This emerging technique requires a much higher power requirement from the AUV as the computations that are undertaken are substantial, but unlock new pathing methods in an operational environment (C. Denniston, 2018) in which efficient route planning with specific mission objectives can be achieved, as opposed to less-efficient pathing. Thus, it is not entirely known if this method would necessarily lead to higher power consumption over many missions. Similar to collision

avoidance systems, this system operating on its own has problems navigating over long distances as there is no way to reach a certain target that is outside of the range of its sonar.

In reality, with higher capability computers which utilize less power, and increased capability required from AUVs in recent years, collision avoidance systems have been more or less replaced (or are in the process of getting replaced by) environmental modelling methods to generate paths in operational environments that require medium- and close-range encounters. Both of these methods must be paired with dead reckoning in order to achieve full autonomy and both start and return to a known location. The result is that a common practice is to pair these two methods to allow for significant improvements to performance and capability for a very low material, power, and computational cost. For that reason, the function of sensing the surrounding environment and negotiating obstacles is effectively a dominated tradespace with only one high-level architectural solution. Recent research has also been delivering promising results in using leader-follower architecture to help enable sense ranges to and from other AUVs in swarm environments (E. M. Fischell, 2020).

2.3 Scaling relationships between architectural decisions

Most of the architectural decisions that have been outlined above have complex, systemic interactions as they scale in size. For instance, while it is possible to add more and more battery capacity to a single AUV, the marginal utility of the energy supplied through that addition may not be consistent – likely, the marginal utility would increase to some point, and then decrease. To this particular example, there has been substantial work to constrain and optimize AUV operations from a generalized perspective where any particular scalar field's error is minimized by tuning the parameters governing the AUV's operation. Specifically, two common trade-offs during surveys are AUV speed in tension with survey resolution, assuming a consistent survey area. In several studies, it was found that decreasing the electrical load of all sub-systems active in a specific AUV would result in no improvement in minimum error collected by the vehicle (Bellingham J. S. and Willcox, 1996; Willcox, 2001). Using a faster vehicle (which would effectively lower the resolution of a given survey) would result in minor improvements in error, while in total energy capacity (e.g., quadrupling battery capacity) would result in minimum error improvements on the order of 8% (Bellingham J. S. and Willcox, 1996; Willcox, 2001). However, the largest improvement that can be made is by increasing the number of

AUVs operating. Two AUVs performing the same task as a single AUV could result in a twofold improvement of using a faster AUV (Willcox, 2001), and using four AUVs instead of one would result in a minimum error reduction of 19% (Bellingham J. S. and Willcox, 1996). Thus, the complex systemic interaction of scaling AUV systems can be summarized in one simple conclusion – if the objective of an AUV is to collect data with minimum error, then the best way to achieve that goal is to increase the number of AUVs rather than attempt to dramatically increase the performance of a single AUV.

Given this substantial increase in performance – that one can improve by scaling the number of AUVs in operation, rather than the individual components of the AUVs – what have the limiting factors been on preventing AUV swarm operations to date? For this research, swarm operations is a term which refers to operational parameters in which two or more AUVs are working together to achieve the same mission. As outlined in the previous sections, there are highly specific decisions that can be made within the design space of AUVs that can inherently prevent swarm operations. One of the most critical factors that has faced the industry is the ability for multiple craft to communicate with each other during mission operations (Zimmer, 2007). In order for craft to communicate with each other, there must be specific intent at the early design phase to create a craft which is capable of sending and receiving communications, as well as making decisions based on the communications it has received from other AUVs during operation. While there have been significant gains in modelling the decision capabilities of AUVs (C. Cai, 2019) fundamental physical constraints exist with the communication mechanisms. Depending on which form is selected for communication between AUVs (Table 2-1) there will be limitations on which tasks can be accomplished with some number of AUVs. Put another way, if an AUV can only communicate with another AUV within 1m, then they can only ever take the data gathered from the other AUV into account when they are very close to each other. In order to achieve "swarm behavior" (where decisions are made with constant input from all swarm members), neither AUV could ever be more than 1m away from another. This would seem at first glance to be an extraordinarily inefficient use of resources. Emerging research has shown that by exploiting doppler effect changes in known frequencies from a leader AUV, coupled with changes in the magnitude of these known frequencies, swarm communication could be enabled via acoustic methods (E. M. Fischell, 2020). From a practical standpoint, this means that AUVs in this system could operate with greater autonomy, and potentially network tasks. Communication could be more

frequent as well, which would allow for changing mission parameters based on the conditions encountered during operations.

However, the truth is that depending on which figures of merit are of most importance to the user, and depending on the specific operational environment of the system, there could, in fact, be cases where such an architecture would be a viable option. Granted, that for the sake of argument, these use cases would be the extreme minority – there are rarely circumstances where having multiple AUVs within 1m of each other would make any sense – as soon as the range expands, the possibilities grow. Simultaneously, if there is no need for complete uptime of swarm behavior, and instead it is appropriate for the AUVs to operate in a solo configuration for some period of time, then converge with other AUVs to decide collectively what the next step in operation would be, then the possibilities once again expand.

2.4 Summary and Conclusion

In this Chapter, usable definitions of systems, and their component entities were established. The component entities of a level of a system are comprised of both functional and formal elements. The decomposition exercise is undertaken as a functional decomposition. Each functional element is broken down into different forms which can accomplish that function. Following a functional decomposition, formal elements were proposed which can perform each constituent function.

Throughout this exploration of the functional and formal elements that comprise AUVs the specific architectural components have been identified and examined. The functions that have been analyzed include communicating between elements of the system, energizing the system, propelling and orienting the system (collectively forming a functional module which achieves controlling the system), and sensing the surrounding environment. There are multiple viable forms (Table 2-6) that can accomplish these specific functions. Tensions exist between different figures of merit that are used to govern the efficacy and performance of each functional element. For instance, in the case of data communication, there is a tension that is exposed between data transfer rate and data transfer distance. It is the combination of all of these tensions that will yield differential architectures through an exhaustive evaluation of all possible concepts using each viable formal solution to functional requirements.

	AD1 - Communication method	AD2 - Battery	AD3 - Energy Transfer	AD4 - Power generation	AD5 - Propulsion and Orientation
Option 1	Ethernet	Lithium Polymer	Electromagnetic Induction (low-power)	Solar	Propeller and Rudder
Option 2	WiFi	Lithium Ion	Electromagnetic Induction (high-power)	Wind	Propeller and Thruster
Option 3	Radio Waves	Lead Acid	Magnetic Resonance	Wave	Vectored Propeller
Option 4	Lasercom	Nickel Metal Hydride	Electric Field Coupling	Diesel Generator	
Option 5	Acoustic		Radio Reception	Natural Gas Microturbine	
Option 6			Level 1 AC		
Option 7			Level 2 AC		
Option 8			Level 3 AC		

Table 2-6: Summary of all architectural options and decisions summarized above.

3 AUV and Service Platform Architectural Evaluation

In this chapter, a deterministic evaluation of a proposed AUV system is proposed. In order to ground-truth the model, a case study of historical AUV operations is used as an anchor. To generate this evaluation, seven performance metrics are proposed. Of these seven performance metrics, three are directly calculated from figures of merit – properties implicit to the architectural option selected for a single architectural decision. A detailed exploration of some architectural decisions and their formal options is undertaken. Finally, the deterministic evaluation examines which performance metrics are in tension, which architectural decisions have the largest impact on the results, and which architectures dominate which tradespace.

3.1 Defining Operational Environments – Introduction

For the purposes of these analyses, the whole system includes AUVs and a service platform. In order to adequately examine the entire system for the AUV, specific operational environments must be taken into consideration. These restrictions will place several needed constraints in tradespace evaluation and in the architectural review. In constraining the system, selected architectures will be subject to review from a less neutral ground. However, the tensions that will emerge between figures of merit will have far more bearing than if speaking in purely abstract or hypothetical terms. The guiding questions that we aim to answer in this section are: what are the specific architectural choices that can lead to improved functional performance in an AUV's operating environment? And what functionality is improved through the use of simultaneous operation of AUVs as opposed to individual AUVs?

Additionally, in defining specific use cases, it is important to note that the figures of merit to be analyzed will change significantly from one case to another. This is because each operational environment and use case will have different mission critical objectives. If those objectives are not met, then other figures of merit are effectively meaningless.

3.2 Operational environment: Deep-Water Search and Rescue

The first operational environment that will be examined is one where AUVs have successfully seen deployment in the past. Some search and rescue operations have historically used AUVs. One such example that is often highlighted is the search for the wreckage of flight Malaysia Airlines flight

370 (MH370). MH370 was a commercial passenger flight in which a Boeing 777 disappeared en route from Kuala Lumpur International Airport to Beijing on March 8th, 2014. All 239 people on board at the time perished. The final sighting of the airline was from a military radar where its location was above the Andaman Sea, north of Indonesia and east of the Indian Ocean. The search for MH370 was the costliest in aviation history (Australian Transport Safety Bureau, 2017).

In the search of MH370, AUVs were used to conduct detailed surveys. AUVs were run in series operations over the course of three phases of investigation – which combined accounted for approximately 285 days of AUV operation, 17,156 line km flown, and 34,312km^2 mapped (Australian Transport Safety Bureau, 2017; Gartland, 2018). The operating conditions for this particular environment were particularly challenging – specifically the water depth of up to six km at which the investigation took place was much deeper than the initially anticipated four km water depth (Trauthwein, 2014; Australian Transport Safety Bureau, 2017).

The reference architecture that will be used as an anchor point in this analysis is a Bluefin-21 AUV (Figure 3-1) from Bluefin Robotics – now General Dynamics (Orr, 2014). The Bluefin-21 is described as "highly modular autonomous unmanned underwater vehicle able to carry multiple sensors and payloads at once" (General Dynamics, 2020). It is 4.9 meters in length, and can cruise up to 4.5 knots. It communicates with computers after missions via ethernet interfaces. There are 13.5kWh of every stored aboard nine 1.5kWh lithium-polymer batteries. It navigates the subsea environment with a gimbaled thrust vector. Additionally, it is equipped with standard payloads including side scan sonar packages, sub-bottom profilers, and multibeam echo sounders (General Dynamics, 2020). This AUV was used during the search for MH370, and so it is an excellent benchmark against which our system can be evaluated. This AUV can operate for up to 24 hours in a single mission with its standard payload operating on its 13.5kWh of internal energy (Bluefin Robotics, 2010). The time that this AUV takes to dive to the operational depths or resurface from those depths is approximately 2.5 hours (MIT Spectrum, 2014) and it operates moving at approximately three knots throughout its mission.

Figure 3-1: Bluefin-21 AUV from general dynamics.

The first figure of merit that any new system attempting to operate in this environment must tackle is the speed at which it can search a square kilometer of ocean floor. Each reference AUV was capable of collecting side scan sonar data at a width of 1,000m on either side of the AUV at an altitude of 45m from the sea floor moving at 5.5km/h. Knowing that the AUVs operated lines summing to 17,156km during the most intensive parts of the investigation, we can surmise that a total of 34,312km^2 were mapped (Australian Transport Safety Bureau, 2017). An average single mission collected side-scan sonar data that covered an area of approximately 205km^2 having traversed tracklines of approximately 102.7km. Side-scan sonar data are collected by a vehicle by using sonar emitted normal to the pathway of the vehicle creating a large swath (or plane) of measurements at high collection rates. It is worth noting that the AUVs that were used in this investigation (the reference architecture) never fully searched the initially defined 60,000km^2 area, nor the 120,000km^2 expanded search area. Figure 3-2 shows the initial 60,000km^2 area, and the 120,000km^2 expanded search area in context with the Indian Ocean. Figure 3-3 shows traces of the tracklines of each of the three operating AUVs during the search for MH370 against the expanded search area.

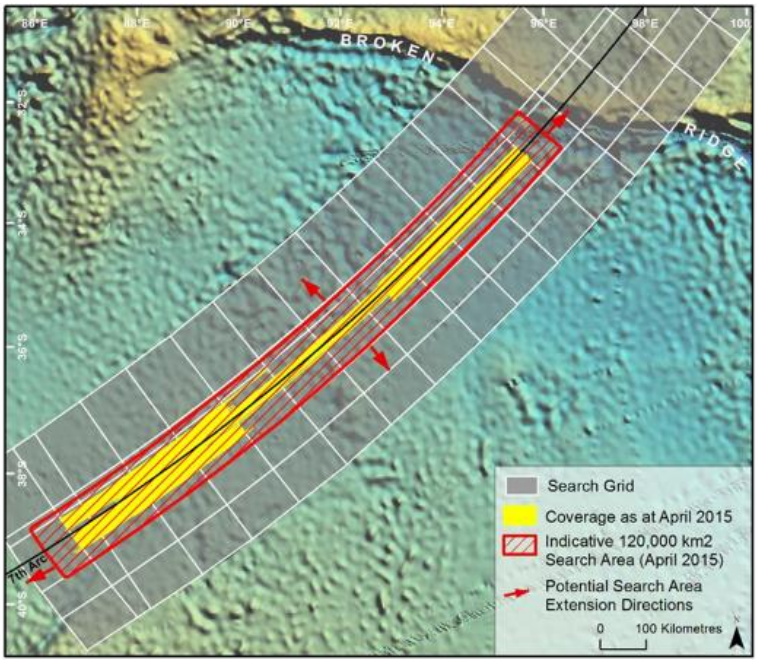

Figure 3-2: Initial area designated for search for MH370 (Yellow), and the expanded search area (red outline). Figure 51, (Australian Transport Safety Bureau, 2017)

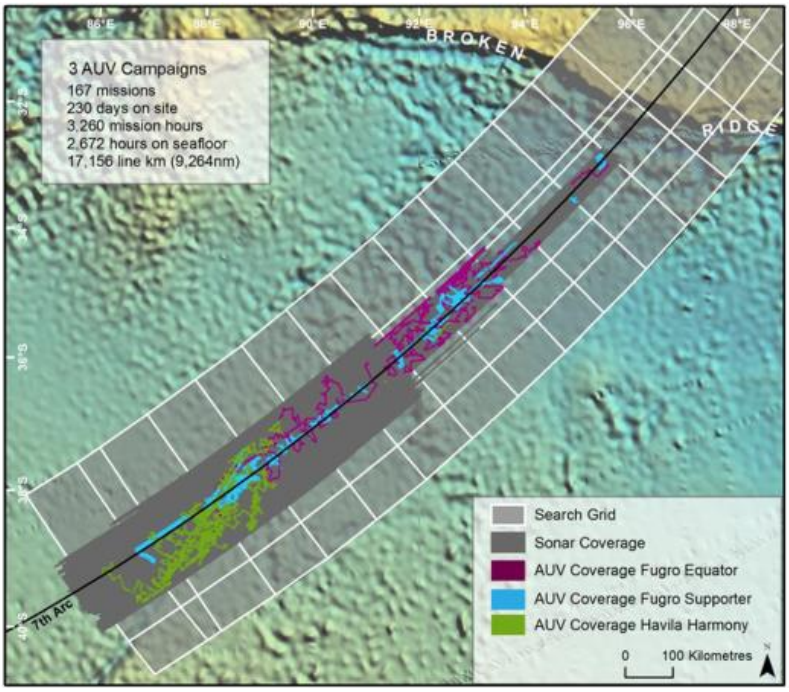

Figure 3-3: Trace of tracklines which AUVs followed during the search for MH370. Figure 65, (Australian Transport Safety Bureau, 2017). In this image, the 230 days refers to the number of days which constituted days in which AUVs were operating. The figure of 285 days represents the total number of days during which the system which supports the AUVs was active (i.e., travel time, refueling, and so forth.)

There are two key differentiators in our architectural concepts that deviate from this historical example: first, the AUVs will be completely autonomous, rendering the costs of maintaining and fielding large support craft moot, and second the AUVs will operate in this system as elements in a swarm (E. M. Fischell, 2020). The lack of autonomy in the search is due to a system boundary that has changed. The individual AUV could carry out its mission autonomously, but it had to be launched, programmed, caught, have its batteries changed, and download data all non-autonomously (Figure 1-5). Additionally, during the search and rescue mission, there was only one AUV which was ever operating at any given time. For the purposes of this thesis, in order to achieve complete autonomy, a given AUV or set of AUVs will need to perform all functions – except for emergency operations – without direct input from human operators.

As previously discussed, adding AUVs to the system is a very efficient way to improve system-wide performance relative to individual component changes (e.g., speeding a reference architecture up, or increasing battery life by adding more batteries) because the area that any single AUV needs to

evaluate is equal to $\frac{1}{n}$ where n is equal to the number of AUVs present in the system (Bellingham J. S. and Willcox, 1996). Based on this, the answer would seemingly be to add an ever-increasing number of AUVs to the system to instantaneously examine the entire 34,312km^2 area. However, there is a limit on how quickly a swarm could accomplish the same task as a single AUV. The time to reach the start of the survey point is effectively constant (~2.5 hours) in the case of the single launched AUV. For a swarm, however, the more agents added, the longer it will take for an individual AUV to reach the starting point for their survey. For the purposes of this thesis, an arbitrary mission profile of 2.2 million m^2 per mission will be considered (Figure 3-4). This profile can change depending on mission parameters or program goals. The governing principle that will determine the degree to which the operational time will shrink is that the platform will remain stationary during remote operations. Thus, each AUV will launch from a single location and steer itself to the predetermined starting location at the seafloor. If there are up to four AUVs working a single mission, then the time to the seafloor remains unchanged, but the addition of a fifth AUV would result in horizontal distance as well as vertical distance to reach the mission start location (Figure 3-4). This scaling in non-linear. There will variations in the increases in time as more vehicles are added because of the geometry of the square search grids (Figure 3-5).

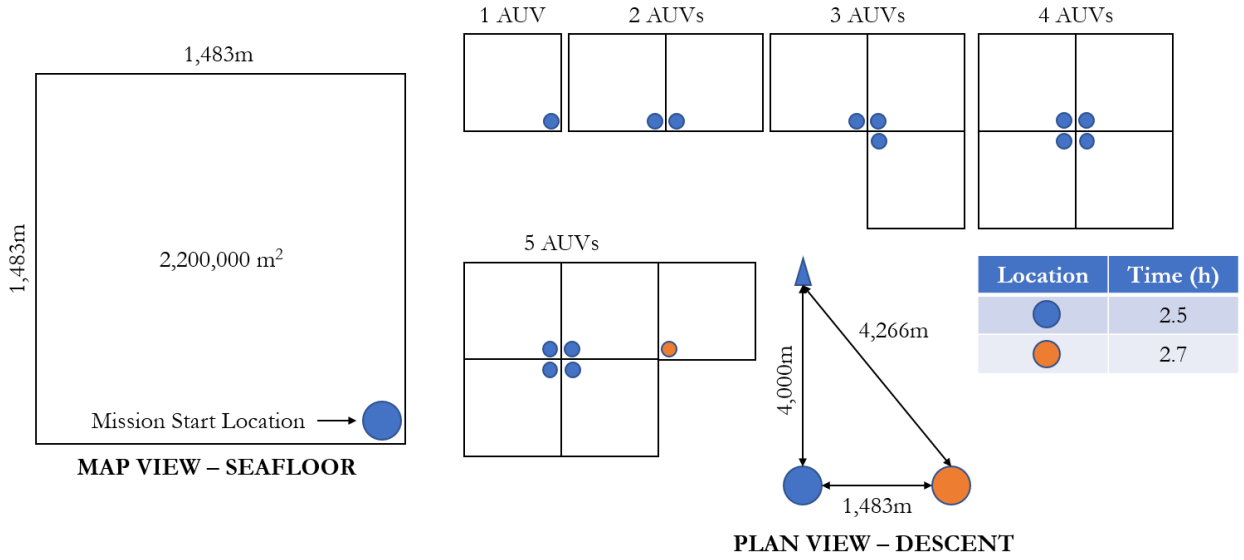

Figure 3-4: Schematic example of descent time increasing as AUVs are added to the system. Leftmost box represents the area that a single AUV can survey in a single given mission.

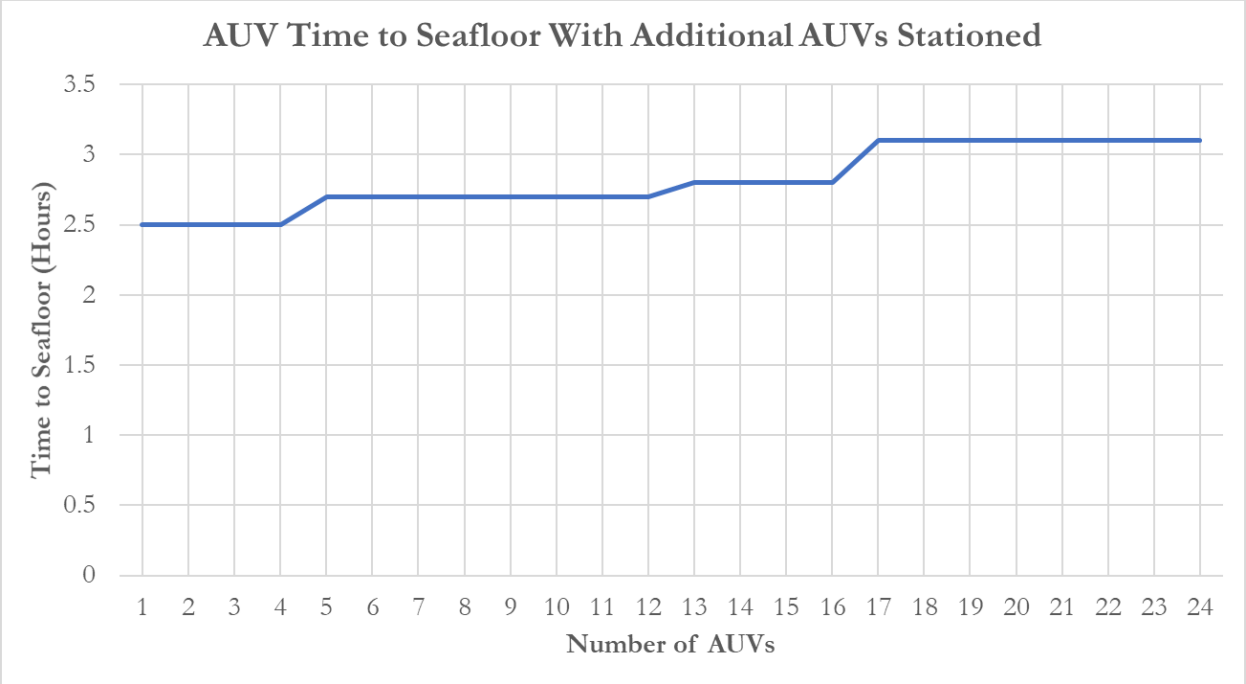

Figure 3-5: Time to seafloor scales non-linearly with the addition of more AUVs to the system.

Because of this factor, the operational time scales negatively and non-linearly with the distance away from the service platform with the addition of additional AUVs to the system. In other words, daily operational time (which is related to scannable area in a single dive mission) decreases as the scale of the swarm increases. For the purposes of this examination, average operational depth will be 4km (MIT Spectrum, 2014). With this information, it is clear that a figure of merit that would adequately quantify the performance of an AUV in this deep-water search and rescue environment is calendar time to complete a sea-floor survey of 34,312 continuous km^2 measured in days. This time is formally split into two distinct metrics: operational days for mission completion time (i.e., how many days involved active AUV survey missions) and mission completion time (i.e., total duration of subsea operations, including port days and non-operation days). In the case of the reference architecture, 285 days of operation were required for mission completion (230 of which were occupied performing maritime operations), but those days were spread in a total mission completion time of 730 days (Australian Transport Safety Bureau, 2017).

This primary figure of merit (days to complete total survey) will be the product of average daily operational time in hours of a single AUV and the average area in km^2/hour that any given AUV would survey in that same day. These two separate variables are the values that will change as the

architectural decisions shift. The architectural decisions will drive average operational time or average survey area per hour up or down. As the morphological matrix evolves it is here where many system-wide tradeoffs will be made.

A second set of highly important figures of merit to enter into the evaluation of this architecture concern costs. The reference architecture for this operational environment costs approximately $5 million (Parker, 2014). While the total cost for a single AUV is important to consider, this study assumes that any AUV architecture that is produced will have comparable costs in initial production for the AUV. Each AUV was also paired with a multi-purpose survey vessel to act as support. Each vessel (the Fugro Equator, the Fugro Supporter, and the Havila Harmony (Australian Transport Safety Bureau, 2017)) carried approximately 50 support personnel during the operation (Fugro, 2017; Fugro, 2014; Havila, 2020). According to the Australian Transportation Safety Board, A$170 million were spent on the underwater search. 1,904 days were spent during the underwater search operations, and 285 of those days were dates when the Equator, the Supporter, and the Harmony were engaged in AUV operation (Australian Transport Safety Bureau, 2017). Three AUVs were used in this search, and so the total mission costs are estimated to be $17,812,500 (conversion from AUD to USD = 0.7). Since three AUVs were used in the search, $15,000,000 is added to this sum to bring the total estimated costs to $32,812,500. For the purposes of this analysis, the capital costs of all AUVs – for both the existing architectures and the proposed architectures – are assumed to be distributed to a single mission. In reality, these AUVs would all likely be deployed to other mission profiles throughout their operational lifetimes. On an operational basis, this means that each operational day costs $115,000 or $6,100 per operational hour. The entire AUV operation, however, required an additional 450 days to complete, which means that on a per day basis for the total mission, costs were $45,000. Since the remote autonomous system seeks to improve system-wide performance, it is possible that the total cost of the mission and the total mission daily costs will decrease, even if the operational hour costs increase. For the purpose of this study, the remote autonomous service platform's initial capital cost is estimated to be equal to two times the cost of the number of individual AUVs that are using it as a base of operations, or $10 million. As the architecture expands, and AUVs are added to the system, the initial costs for the autonomous service platform are assumed to increase by $2 million. This uncertainty will be modeled probabilistically in Chapter 4.

Table 3-1 summarizes the project metrics and the goals of an autonomous system. These goals are set in context to the reference architecture that was employed during the search and rescue operations for MH370.

No.	Name	Description	Units	Reference Architecture Metric	Qualitative Goal	Quantitative Goal
PM1	Daily Operational Time	The average number of hours in a day a single AUV can survey the seafloor	hours	19	Sufficient to complete the mission within an acceptable budget	18
PM2	Average Survey Area Rate	The average rate at which a single AUV can survey the seafloor	km2/hour	11	Equal to or better than the reference architecture	11
PM3	Operational Days for Mission Completion	Days in which AUVs were actively surveying the seafloor	days	226	Equal to or better than half of the reference architecture	143
PM4	Mission Completion Time	Total time required to search the designated area	days	730	No more than 125% of the operational days	179
PM5	Cost	Estimated cost of the full mission	dollars	32,812,500	No more than 125% the total cost of the reference architecture	41,000,000
PM6	Operational hour cost	Estimated cost for a single hour of operation of a single AUV	dollars/hour	6,100	No more than 115% of the reference architecture	7,000
PM7	Total mission daily cost	Estimated cost for a single day of seach and rescue operations	dollars/day	45,000	No more than 80% of the reference architecture	36,000

Table 3-1: Summary of the seven metrics by which the AUV system will be evaluated.

Finally, there is one additional architectural decision to add to the evaluation procedure, and that is the number of AUVs that will be present in the system. Assuming that a single AUV capable of operating in this environment costs approximately $5 million, then it is highly unlikely that there will ever be a practical use case where more than a handful of AUVs would be cost effective. In order to fully evaluate the tradespace, options for the number of AUVs will be in increments of four – consistent with the increasing time to starting location outlined above – and have a maximum of 20 and include one. This way, a broad range of possible outcomes can be explored.

	AD1 - Communication Method	AD2 - Battery	AD3 - Energy Transfer	AD4 - Power Generation	AD5 - Propulsion and Orientation	AD6 - Number of AUVs
Option 1	Ethernet	Lithium Polymer	Electromagnetic Induction (low-power)	Solar	Propeller and Rudder	1
Option 2	WiFi	Lithium Ion	Electromagnetic Induction (high-power)	Wind	Propeller and Thruster	4
Option 3	Radio Waves	Lead Acid	Magnetic Resonance	Wave	Vectored Propeller	8
Option 4	Lasercom	Nickel Metal Hydride	Electric Field Coupling	Diesel Generator		12
Option 5	Acoustic		Radio Reception	Natural Gas Microturbine		16
Option 6			Level 1 AC			20
Option 7			Level 2 AC			
Option 8			Level 3 AC			

Table 3-2: Summary of all considered options for architectural decisions.

Specific architectural decisions that have been previously outlined will impact the system in different ways:

- The communications option will govern how quickly a set of sea-floor scanning data will be transmitted to the service platform. This could govern the time that a single AUV can operate in a single day if the data rate is too slow. Some processed files have file sizes for side scanning raw sonar data on the order of 1.7KB/km of trackline (Nancy T. DeWitt, 2010). This means that on average, during a single reference 19-hour mission an AUV would collect approximately 178KB of data. However, these processed output files are likely greatly eclipsed by the actual size of files acquired in the acquisition process which scale on the precise sounding parameters (Poole, 2020). In order to accurately model these raw files, a static size of 10GB is assumed. The reference architecture transmits data once it is collected by a ship via gigabit ethernet cable, which results in transmission of the data in under a minute.
- The selection of a battery will impact cost of the overall system. The number of AUVs that will operate will drive the amount of energy that must be stored on the service platform, and the costs to house that energy will be based on which battery is selected. The reference architecture uses a lithium-polymer battery which delivers its energy at 30V (Bluefin Robotics, 2010). Based on the architectural decomposition results detailed in Chapter 2, this is estimated to cost approximately $3,000 total.
- would be recharged in just over 9.5 hours. At a high-power delivery of 1,900W, those same batteries would be recharged in approximately seven hours. Since the reference architecture has people on board the craft who swap out the batteries instead of waiting for the AUV to recharge, the 19 hour daily operational time can be fully utilized, and the 7 to 9.5-hour charge time is not used as a penalty against the reference architecture. The costs associated with having maintenance crews on site to perform this work are reflected in the total operational costs of AUV operations in search and rescue missions.
- Power generation method will have a large impact on cost. The reference architecture that is examined recharges their batteries through AC power generated by the diesel generators on-board the support vessels. The fuel cost that would impact the overall cost of operations in the reference case, however, are already accounted for in the marine operations summaries (Australian Transport Safety Bureau, 2017). Thus, no additional costs will be applied to the reference case to account for fuel or maintenance. In evaluating the system, power generation

method will also influence the number of batteries used to support the system. To account for the variability implicit in renewable sources of electricity, there will be a reverse capacity factor applied. This factor is different for all three renewable sources. The factor will be equal to the inverse of the capacity factor. The purpose of this reverse capacity factor will be to estimate the amount of storage required at the service platform to account for periods of prolonged conditions of non-ideal power generation. This means that the total battery capacity of the service platform will need to be increased by a factor of 5 for solar, 3.125 for wind, and 2 for wave sources of electricity. Power output for generators and microturbines meet their nameplate capacity and refueling costs are structured into maintenance approximately $3,000 total. Because costs are directly related to energy storage, and can be inversely related to voltage (United States Department of Energy, July 2019) the estimates for 9V examples are acceptable for deterministic modelling purposes.

- Additionally, the size of the energy storage available on the platform will scale with the selected power option – e.g., if solar power is used a larger platform battery bank would be prudent in case of inclement weather.
- As a deliberate decision, all AUVs will be assumed to have the same 13.5kWh energy supply that the reference architecture has (Bluefin Robotics, 2010). This choice is made in order to stabilize the initial operational time that any given AUV can utilize. In order to equal the required energy, battery chemistry architectures could lead to differences in either the size or the weight of the AUV, both of which would lead to worse hydrodynamic performance, which would manifest as lower average hourly survey rate. If weight is conserved or if a slightly smaller battery pack is used, then there would be a positive impact on the average survey rate.
- Operational time in a single day will be impacted by power transfer method. The longer a single AUV takes to recharge, the longer it will take to start its subsequent mission. The reference architecture uses what is effectively a Level 1 AC direct connection to charge its batteries. At a low-power delivery of 1,400W, the 13.5kWh batteries and OPEX costs, and so no additional factors should be applied to the number of batteries onboard the service platform for these methods of power generation.
- While the AUV's control systems are critically important for the AUV architecture, they will not have an impact on the figures of merit under consideration for this operational context,

as all architectures are sufficient to maneuver at high speeds. The reference architecture uses vectored propellers to control orientation and speed (Bluefin Robotics, 2010).

3.2.1 Decision and Metric Sensitivity Analysis

Seven key metrics have been selected for this operating environment: daily operational time, average survey coverage per hour, operational days for mission completion, calendar days to mission completion, total mission cost, cost per operational hour, and total mission daily cost. Between these seven metrics, the reference system can be evaluated. The performance metrics include daily operational time (PM1 – hours), average survey area rate (PM2 – km^2/hour), operational days for mission completion (PM3 – days), mission completion time (PM4 – days), cost (PM5 – $), operational hour cost (PM6 –$/hour), and total mission daily cost (PM7 – $/day). These metrics are all effected in some degree by the architectural decisions that have been selected for analysis. The linkage between an architectural decision and a performance metric are described qualitatively as sensitivity. Qualitative sensitivity of an architecture decision is at its highest when a single decision has a high impact across multiple metrics. In this regard, changing a single sensitive architectural decision will impact many performance metrics. Contrarily, a sensitive performance metric is one that is linked across multiple architectural decisions. If a sensitive metric is examined closely, there could be multiple ways in which that metric could be influenced. The qualitative sensitivities that exist between the architectures and performance metrics of this system are summarized in Table 3-3.

No.	Metric	PM1 (Hours)	PM2 (km^2/hour)	PM3 (Days)	PM4 (Days)	PM5 ($)	PM6 ($/hour)	PM7($/day)	Decision Sensitivity
	Decision	Daily Operational Time	Average Survey Area Rate	Operational Days for Mission Completion	Mission Completion Time	Cost	Operational Hour Cost	Total Mission Daily Cost	
AD1	Communication Method	Medium (2)	None (0)	Medium (2)	Medium (2)	Low (1)	Low (1)	Low (1)	9
AD2	Battery Chemistry	None (0)	Low (1)	Low (1)	Low (1)	Medium (2)	Medium (2)	Medium (2)	10
AD3	Energy Transfer	High (1)	None (0)	None (0)	High (3)	Medium (2)	Low (2)	Low (2)	10
AD4	Power Generation	None (0)	None (0)	None (0)	None (0)	Very High (4)	Very High (4)	Very High (4)	12
AD5	AUV Control	None (0)	Low (1)	Low (1)	Low (1)	None (0)	None (0)	None (0)	3
AD6	Number of AUVs	Low (1)	Low (1)	Low (1)	High (3)	High (3)	High (3)	High (3)	15
Metric Sensitivity		4	3	5	10	12	12	12	

Table 3-3: Sensitivity table displaying the most sensitive performance metrics (PM) and architectural decisions (AD) (green) and the least sensitive performance metrics and architectural decisions (red).

It is unsurprising that even from a qualitative standpoint, the least sensitive architectural decision is the AUV control decision. In fact, because of how insensitive it is it will not be included in the morphological matrix analysis as a decision in subsequent analyses. Rather, it will be represented as a single selected option – vectored propeller. The most sensitive decision outlined in Table 3-3 is the number of AUVs present in the system. This means that changing the number of AUVs will have a large qualitative impact across multiple metrics. Similarly, the power generation method will have very high impacts concerning cost related metrics. Operational time, survey rate, and operational days are the least sensitive metrics relative to the architectural decisions considered. This is by and large due to the fact that the purpose of this analysis is not to optimize a single AUV and squeeze marginal performance gains from a single mission. Instead, operational time as a percentage of a single day is largely already optimized, and architectural decisions can only detract from the existing architecture. In as much as they can, the operational time is impacted most by the energy transfer method selected.

3.3 Morphological Matrix and Concept Selection

Table 3-4 summarizes the updated list of all architectural decisions under consideration for concept selection and morphological matrix evaluation. Table 3-5 shows how this table can be used to select individual architectural decisions and create a single concept. The highlighted concept is the reference architecture for the Bluefin-21 AUV against which our system will be judged. There are several minor exceptions to these architectural decisions discussed above, but none that aren't accounted for in the metrics against which the new system and concepts will be evaluated. Within this set of architectural decisions, there are no choices which are mutually exclusive. As such, the full 4800 entry morphological matrix can be explored. In creating this morphological matrix, all decisions are initially based on deterministic input parameters. It is likely that each metric is a function of probabilistic input parameters which will be discussed in detail during probabilistic analysis in Chapter 4.

No.	Decision	Option 1	Option 2	Option 3	Option 4	Option 5	Option 6	Option 7	Option 8
AD1	Communication Method	Ethernet	WiFi	Radio Waves	Lasercom	Acoustic			
AD2	Battery Chemistry	Lithium Polymer	Lithium Ion	Lead Acid	Nickel Metal Hydride				
AD3	Energy Transfer	EM Induction (low-power)	EM Induction (high-power)	Magnetic Resonance	Electric Field Coupling	Radio Reception	Level 1 AC	Level 2 AC	Level 3 AC
AD4	Power Generation	Solar	Wind	Wave	Diesel Generator	Natural Gas Microturbine			
AD5	AUV Control	~~Propeller and Rudder~~	~~Propeller and Thruster~~	Vectored Propeller					
AD6	Number of AUVs	1	4	8	12	16	20		

Table 3-4: Summary of all architectural decisions under consideration for concept selection and morphological matrix evaluation.

No.	Decision	Option 1	Option 2	Option 3	Option 4	Option 5	Option 6	Option 7	Option 8
AD1	Communication Method	Ethernet	WiFi	Radio Waves	Lasercom	Acoustic			
AD2	Battery Chemistry	Lithium Polymer	Lithium Ion	Lead Acid	Nickel Metal Hydride				
AD3	Energy Transfer	EM Induction (low-power)	EM Induction (high-power)	Magnetic Resonance	Electric Field Coupling	Radio Reception	Level 1 AC	Level 2 AC	Level 3 AC
AD4	Power Generation	Solar	Wind	Wave	Diesel Generator	Natural Gas Microturbine			
AD5	AUV Control	~~Propeller and Rudder~~	~~Propeller and Thruster~~	Vectored Propeller					
AD6	Number of AUVs	1	4	8	12	16	20		

Table 3-5: Reference architecture concept mapping.

The first step in creating a comprehensive morphological matrix comprised of all possible architectures that could result from all possible permutations of every architectural decision is to calculate the impact that each decision has on each performance metric. The impact that each architectural decision has is based on their own figures of merit that were uncovered in the architectural decomposition of each functional element.

3.3.1 PM1: Daily Operating Time (DOT)

Daily operational time in hours is a metric which expresses how many hours of active scanning the AUV can perform at the seafloor in a single charge. Table 3-3 shows that this metric is sensitive to communication method, energy transfer method, and the number of AUVs which are operating simultaneously. The reference architecture has a daily operating time of 19 hours (Table 3-1) which is achieved by using ethernet connections for data transfer, and one AUV. The energy transfer method that is used in the reference architecture is not a valid option for exploration in this tradespace, as it requires human intervention. In the reference architecture, when an AUV is retrieved for servicing people swap out the vehicle's depleted batteries with full batteries in order to maximize operational time. As such, the energy transfer time is very close to zero. The impact of this servicing method is that since the reference architecture requires 0 hours to transfer energy to the AUV, no matter which architectural decision is selected for the autonomous platform/AUV system, the output of PM1 within this morphological matrix will be less than 19 hours.

To calculate the impact on PM1 due to the communication method selected for a given architecture, an assumed file size of 10GB is converted to bits, then divided by the data rate and converted to hours. This calculated amount is then subtracted from the daily operating time. The following equation governs the influence of communication method on PM1.

$$\Delta PM1_{Communication\ Method} = -\left(\frac{FileSize * 8}{3600 * DataRate_{AD1_{Option}}}\right)$$

Additionally, the selected method of power transfer will impact PM1. There are eight options for this architectural decision. Each option has a different amount of power that they can deliver to the AUV during a recharge cycle. While it is possible that there will be variation in the actual power delivery of each method, the values outlined in the architectural decomposition are representative averages that each option could reach. The reference battery size which is assumed as a constant across all architectures contains 13,500Wh of energy. This energy value is divided by the Power delivery in Watts to determine the time in hours required to recharge a battery. The following equation governs the influence of power transfer method on PM1.

$$\Delta PM1_{Power\ Transfer} = -\left(\frac{ReferenceBatterySize}{PowerDelivery_{AD3_{Option}}}\right)$$

As previously outlined, as the number of AUVs increase, the distance to the starting location for an individual AUVs survey increases (Figure 3-5). There are six options for the number of AUVs, and in each of the options the single unit travel time is calculated. The average amount of time that it takes for each unit to reach the sea floor is then calculated for each architectural decision. This value is then doubled, as it is assumed that each AUV will take an equal amount of time submerging as surfacing. In actuality, it is likely that AUVs will take different amounts of time surfacing than submerging because AUVs are usually positively buoyant, and they will likely be in a different location at the end of a survey then they were when they started the survey. Such differences are not accounted for in this analysis. The following equation governs the influence of the number of AUVs on PM1.

$$\Delta PM1_{Number\ of\ AUVs} = -\left(2 * TimeToSeafloor_{AD6_{Option}}\right)$$

Each of these architectural decisions output a value in hours. These outputs are deviations away from the 24-hour possible daily operational time. These deviations are summarized in Table 3-6. The governing equation for PM1 is:

$$PM1_{Architecture} = PM1_{Reference} + \Delta PM1_{AD1_{Option}} + \Delta PM1_{AD3_{Option}} + \Delta PM1_{AD6_{Option}}$$

AD1	Communication Method	Data Rate (bps)	Transfer time (hours)
Op1	Ethernet	10,000,000,000	0.002
Op2	WiFi	300,000,000	0.074
Op3	Radio Waves	20,000	1111
Op4	Lasercom	1,000,000,000	0.022
Op5	Acoustic	80	277778
AD3	**Power Transfer**	**Power Delivery (W)**	**Recharge Time (hours)**
Op1	EM Induction LP	15	900
Op2	EM Induction HP	1,000	14
Op3	Magnetic Resonance	3,000	4.5
Op4	Electric Field Coupling	2,000	6.8
Op5	Radio Reception	100	135
Op6	Level 1 AC	1,500	9.0
Op7	Level 2 AC	5,000	2.7
Op8	Level 3 AC	30,000	0.45
AD6	**Number of AUVs**	**Average Time to Seafloor (hours)**	**Travel Time Impact (hours)**
Op1	1	2.5	5
Op2	4	2.5	5
Op3	8	2.6	5.2
Op4	12	2.6	5.2
Op5	16	2.7	5.4
Op6	20	2.8	5.6

Table 3-6: Summary of PM1 impacts from each pertinent architectural decision option.

There are several options which were eliminated from subsequent morphological matrix work based on these calculations. If the time required for any of these methods was over 24 hours, then it was eliminated as a viable design. In the case of communication methods, this mean that using radio waves and acoustic options as a way of communicating data was considered non-viable, as it would take over 1,000 hours for radio waves and over 250,000 hours for acoustic communications to transfer 10GB of data to the service platform. In the case of power transfer methods, low power electromagnetic induction and radio reception were similarly eliminated as non-viable design options. For low power electromagnetic induction, it would take 900 hours to charge a vehicle, and for radio transmission, it would take 135 hours. It is worth noting that these are not inherently non-viable designs, but their slow transfer and charge times were deemed too slow for the purposes of this exercise, and as such eliminated from subsequent analyses.

3.3.2 PM2: Search Area Rate (SAR)

Search area rate (SAR) in km^2/hour is a metric which expresses how quickly an area can be scanned using sonar. Table 3-3 shows that this metric is sensitive to battery chemistry, method of AUV control, and the number of AUVs which are operating simultaneously. The reference architecture has a search area rate of 11 km^2/hour (Table 3-1) which is achieved by travelling at 5.5 km/hour and having a sonar beam width of 1km on either side of the AUV. In the case of the search of MH370, the nadir (a narrow strip of seafloor which can't be imaged by a side scanning sonar) underneath the AUV was covered by multibeam echo sounders which left a continuous swath of 2km at an elevation of 45m above the seafloor (Australian Transport Safety Bureau, 2017). In this architectural exploration, the precise acquisition parameters are left unchanged. Thus, the only way to alter the search area rate metric is to change the efficiency at which an AUV operates. An estimate for this efficiency is derived from mass. A more massive AUV will expend more energy to travel at the same speed, and any increase in craft size will potentially increase drag.

Battery chemistry impacts the search area rate by changing the hydrodynamic properties of an AUV. These properties are generally made worse by increasing the weight of the craft, as more energy would be required to move the craft the same speed. Additionally, if there is any movement in the ocean which is not parallel to all currents, then the reference area of the craft will increase if there is an increase in craft length. This increase in reference area would mean that there would be an increase in the drag that an AUV experiences, further decreasing energy efficiency. To calculate the search area rate impact that the battery chemistry would have, the power density of each option was considered. The reference value was divided by the option value. Lower power densities would then have multipliers above 1, and higher power densities would have multipliers of less than 1. These factors were then multiplied by the reference search area rate to create a value expressed in km^2/hour. The following equation governs the influence of battery chemistry on PM2.

$$\Delta PM2_{Battery\ Chemistry} = SAR_{Reference} - \left(\frac{PowerDensity_{Reference}}{PowerDensity_{AD2_{Option}}} * SAR_{Reference}\right)$$

AUV control methods would also impact the search area rate. For this morphological matrix, only option three was considered for this architectural decision. The reason for keeping this option constant is that vectored propeller designs in this operational space are dominant architectures (as previously explored). Regardless, if operational speeds were lowered because of options selected in

this architectural decision space, then there would be a speed factor applied be dividing the reference architecture operational speed by the option architectural decision speed. This factor would then be multiplied by the reference search area rate to create a value expressed in km^2/hour. This value is held constant throughout all deterministic modeling.

Finally, increasing the number of AUVs will have a positive impact on the search area rate. With an increased number of AUVs simultaneously operating and coordinating with each other, there will be greater edge space covered in each individual mission. Additionally, assuming swarm coordination can be achieved (E. M. Fischell, 2020), with the additional coordination of AUVs, the precise location of each AUV will improve resulting in more usable swaths. This coordination factor scales with the number of AUVs present in the system, and an arbitrary value of 5% is assumed to be a constant with the addition of four AUVs to the system. These factors are then multiplied by the reference search area rate to create a value expressed in km^2/hour. The following equation governs the influence of the number of AUVs on PM2.

$$\Delta PM2_{Number\ of\ AUVs} = SAR_{Reference} - \left[\left(1 + CoordinationFactor_{AD6_{Option}}\right) * SAR_{Reference}\right]$$

The impact of each of these architectural decisions creates an output which is expressed in km^2/hour. From these values, a new search area rate is calculated from the reference architecture. These derived values are summarized in Table 3-7. The calculation of PM2 is summarized by the equation:

$$PM2_{Architecture} = PM2_{Reference} + \Delta PM2_{AD2_{Option}} + \Delta PM2_{AD5_{Option}} + \Delta PM2_{AD6_{Option}}$$

AD2	Battery Chemistry	Power Density (W/kg)	Operational Efficiency Factor	SAR Delta
Op1	Lithium Polymer	250	1	0
Op2	Lithium Ion	300	83%	1.83
Op3	Lead Acid	180	139%	-4.28
Op4	Nickel Metal Hydride	200	125%	-2.75
AD5	**AUV Control**	**Operational Speed (km/hour)**	**Decreased Operational Speed**	**SAR Delta**
Op1	Propeller and Rudder	4	138%	-4.13
Op2	Propeller and Thruster	3.5	157%	-6.29
Op3	Vectored Proeller	5.5	100%	0.00
AD6	**Number of AUVs**	**Coordination Factor**	**Increased Scannable Area**	**SAR Delta**
Op1	1	0	100%	0.00
Op2	4	0.05	105%	0.55
Op3	8	0.1	110%	1.10
Op4	12	0.15	115%	1.65
Op5	16	0.2	120%	2.20
Op6	20	0.25	125%	2.75

Table 3-7: Summary of PM2 impacts from each pertinent architectural decision option.

3.3.3 PM3: Operational Time

Operational time is a metric which measures the amount of time in days that are spent by all AUVs performing operations. It is calculated from the operational hours and the total calendar mission completion time in the model. However, in the case of the reference architecture, this value is calculated slightly differently. In the reference case, the total operation took 730 days, but of those 730 days, only 285 were active mission days (Australian Transport Safety Bureau, 2017). The rest were spent en route to sites, in port, or other marine operations to facilitate the search. To calculate this value for the reference case in Table 3-1 the value of 285 days is multiplied by the quotient of operational hours per day by 24 hours per day. The result of this calculation is 285 days * (19 DOT/24 hours) = 226 days of operation. At its core, this represents the total time when AUVs were actively performing operations. In the subsequent model, this value is much more consistent across architectures with similar search area rates and operational hours per day even with multiple AUVs compared against single AUVs. This metric removes the bias that multiple AUVs could impart on an evaluation. To calculate PM3, the following equation is utilized:

$$PM3_{Architecture} = PM4_{Architecture} * \left(\frac{PM1_{Architecture}}{24 \text{ hours}}\right) * AD6_{Option}$$

3.3.4 PM4: Calendar Mission Completion Time

The time that it will take the system to achieve mission completion is a function of the daily operational time, survey area rate, and the number of AUVs performing the task of scanning the floor. This metric is therefore influenced by all of the architectural decisions that are inputs to these metrics. In other words, communication method, battery chemistry, power transfer method, AUV control method, and the number of AUVs in a specific architecture are all important architectural decisions in this context. The equation to calculate mission completion time takes the mission area of 60,000km^2 and divides it by the product of the daily operating time and the search area rate. This value is subsequently divided by the number of AUVs in the system which represents dividing the task evenly between the different vehicles. This means that the equation used to calculate PM4 is:

$$PM4_{Architecture} = \frac{60{,}000\ \text{km}^2}{PM1_{Architecture} * PM2_{Architecture} * AD6_{Option}}$$

3.3.5 PM5: Total System Cost

The total system cost is a metric which sums up the costs of all system components. Some of the components are static (e.g., the cost of an AUV is held constant at $5million) and some are dynamic. Static costs include the costs associated with communication methods, battery chemistries, and power transfer methods. Dynamic costs are associated with the installation of power generation and service platform storage capacities.

For each member of the morphological matrix, static costs were assigned. The costs were estimated from previous decomposition cost estimates. For communication methods, a cost/AUV was assigned and subtracted from the reference architecture. This cost difference was then multiplied by the number of AUVs present in the system resulting in a summed cost delta over the individual AUV cost. Similarly, battery chemistry costs were compared to the reference case and multiplied by the number of AUVs in the system as were methods of power transfer. The results of this are summarized in Table 3-8. This governing equation is summarized arithmetically as:

$$\Delta PM5_{Communication\ Method} = AD6_{Option} * \left(CostPerAUV_{AD1_{Option}} - CostPerAUV_{Reference}\right)$$

AD1	Communication Method	Est Cost/AUV	Cost Delta
Op1	Ethernet	50	0
Op2	WiFi	100	50
Op3	Radio Waves	150	100
Op4	Lasercom	1,000	950
Op5	Acoustic	750	700
AD2	**Battery Chemistry**	**Est. Cost/AUV**	**Cost Delta**
Op1	Lithium Polymer	14,000	0
Op2	Lithium Ion	14,000	0
Op3	Lead Acid	3,500	-10500
Op4	Nickel Metal Hydride	7,000	-7000
AD3	**Power Transfer**	**Est. Cost/AUV**	**Cost Delta**
Op1	EM Induction LP	1,000	500
Op2	EM Induction HP	1,500	1,000
Op3	Magnetic Resonance	5,000	4,500
Op4	Electric Field Coupling	5,000	4,500
Op5	Radio Reception	50,000	49,500
Op6	Level 1 AC	500	0
Op7	Level 2 AC	1,000	500
Op8	Level 3 AC	5,000	4,500

Table 3-8: Summary of PM5 static costs assigned on a per AUV basis. Cost delta values are calculated in USD.

Dynamic system costs are tied into the architectural systems that surround power generation and storage. For deterministic modeling, a static value was selected from the functional decomposition survey to estimate the power output capacity of each option for this architectural decision. This power output was then multiplied by the previously discussed cost per Watt to calculate a total cost for a single power plant. This cost per power output was an average that was calculated between the high- and low-end costs that are previously discussed (Table 2-4). This cost was then added to each entry in the morphological matrix along with the other AUV associated costs. However, depending on which system concept was selected, this value could change further – thus these costs are termed dynamic. For instance, if the system concept calls for more than a single power plant to be emplaced on the service vessel, than the single unit cost is not the total cost of power generation. There are substantial changes associated with the impact of power generation options associated with specific operating concepts (Table 3-9). The following equation summarizes the costs that are created with emplacing a single power system selected as an option from AD4:

$$PM5_{Power\ Generation_{Single\ Plant}} = SystemOutput_{AD4_{Option}} * CostPerPowerOutput_{AD4_{Option}}$$

AD4	Power Generation	Power Output (1 system, kW)	Cost/Power Output - Mid ($/W)	Cost Delta
Op1	Solar	2	50.5	101,000
Op2	Wind	3.2	24.5	78,400
Op3	Wave	5	46	230,000
Op4	Diesel Generator	10	623	6,230,000
Op5	Natural Gas Microturbine	50	57.5	2,875,000

Table 3-9: Summary of PM5 dynamic cost basis for power generation selection. Cost delta in this architectural decision refers to the increased cost above the previously discussed capital costs associated with the addition of a power plant to the system of a given type.

3.3.6 PM6 and PM7: Operational Hourly Cost and Total Mission Daily Cost

These metrics serve to normalize the total system cost with both temporal elements present in the operational parameters associated with this specific use case. Operational hourly cost is calculated by taking each total system cost and dividing it by the total number of operational hours required to complete the mission. This metric is expressed in $/hour and represents the operational costs per hour. Ultimately, this would be the cost to acquire one hours' worth of data if a user was interested in employing this system. Similarly, the total mission daily cost is calculated by dividing the total system cost by the total calendar mission completion time. This metric is expressed in $/day and represents the costs that a single day of operations would incur for a potential user. It is critical to note that this is based on a total mission that covers a 60,000km^2 area and if the survey area is different, then this value (and many others) would also change. These two equations are summarized as:

$$PM6_{Architecture} = \frac{PM5_{Architecture}}{PM3_{Architecture}}$$

$$PM7_{Architecture} = \frac{PM5_{Architecture}}{PM4_{Architecture}}$$

3.3.7 Operational Concepts

In order to provide a robust analysis, several overarching design concepts were examined. The three operational concepts under consideration are termed "Tiny Battery," "Big Battery," and "Scaled

Power." Each represents very different configurations of the service vehicle which have major implications on the interaction between the AUVs and the service platform. There are many different ways that these concepts could be tuned further, but these provide end-members for future analyses.

3.3.7.1 Tiny Battery Concept

The tiny battery concept is one where cost is treated as a constraint in the model. There are only enough batteries onboard to back up the AUVs in operation for one charge cycle. For instance, if there is one AUV in the system, then there will only be 13.5kWh of energy stored on the service platform in a battery bank. If four AUVs are in operation for a specific design vector, then there will be 54kWh of energy stored (13.5kWh/AUV * 4AUVs). This concept is named "tiny battery" because there are some batteries that are present on the service platform – as opposed to directly recharging without any energy storage capacity – but those batteries may not be sufficient to provide for the entire system. If the power generation option is incapable of recharging those batteries in one day, then the AUVs will have to wait at the service platform until the AUV batteries can completely recharge. This means that daily operational time is relaxed as a constraint as systems become more and more energy-hungry. Effectively, the longer that an AUV has to wait, the lower the average daily operational time will become.

This change in daily operating time is calculated by examining the following parameters. First, the number of AUVs is examined and multiplied by the number of kWh required in each AUV. This value is compared against the product of the power generation capacity of the selected power system (in Watts) over a full day of energy collection. If the energy generation potential exceeds the energy required for that specific system, then the daily operating time remains unchanged for that design vector. However, if more energy is required than is generated in a 24-hour cycle, then further values are computed. The number of days required to reach the energy requirement is calculated by dividing the required energy by the daily power generation capacity and converted. Finally, a new fractional daily operational time is computed by dividing 24 hours per day by the product of static operational time per day and days required to fully charge the system. This fractional daily operational time is then the updated operational time that is used for future calculations and reporting for all products associated with the tiny battery concept. If there is insufficient power capacity to charge the AUVs in the system in a 24-hour period, then the following equation is used to adjust and replace PM2 for that architecture in the tiny battery system concept:

$$PM2_{Architecture_{Tiny\ Battery}} = \frac{PM1_{Architecture}}{\left(\frac{ReferenceBatterySize * AD6_{Option}}{SystemOutput_{AD4_{Option}} * 24\ \text{hours}}\right)}$$

Two practical examples help further clarify this system concept. The first example is a solar powered system, with one AUV, and a ten hour daily operating time. The AUV will consume 13.5kWh of energy in a single mission. A single solar plant operating at the service platform has a power generation capacity of 2kW, which means that over a 24-hour period, 48kWh of energy are produced. The generation capacity of 2kW has already accounted for diurnal cycles and plant capacity factors as described in Chapter 2. A 48kWh supply of energy is sufficient to recharge the single AUV. This means that the AUV will continue to reach its ten hours of daily operation metric – the AUV is not waiting for any extra processes or functions. However, if we examine this same system, only this time, there are four AUVs operating, then the energy requirements of the system increase from 13.5kWh per day to 54kWh. Despite this increased energy demand, the solar plant can still only produce 48kWh of energy every day. There is no way in this system concept to expedite this energy harvesting exercise, and so the AUVs must wait for the solar plant to charge their batteries for longer than a 24-hour operational cycle. The AUVs will no longer operate for ten hours per day. To generate 54kWh of energy, the solar plant will have to operate for 27 hours. If we use the equation outlined above, then we find that instead of a ten-hour daily operational time, this system would on average only achieve 8.89 hours of daily operation.

The costs associated with the tiny battery concept include the static costs associated with the selected power plant, and also a set of costs associated with the onboard energy storage. Just as the AUVs had four different battery chemistry options, the service platform also has four different battery chemistry options. However, their performance is not considered as a limiting factor. Instead, an additional morphological matrix is created for the tiny battery concept in which each of the valid 2,160 concepts from the previous matrix are given platform battery chemistry options. In so doing, the matrix for the tiny battery concept expands to 8,640 individual design vectors which are visualized in Figure 3-6.

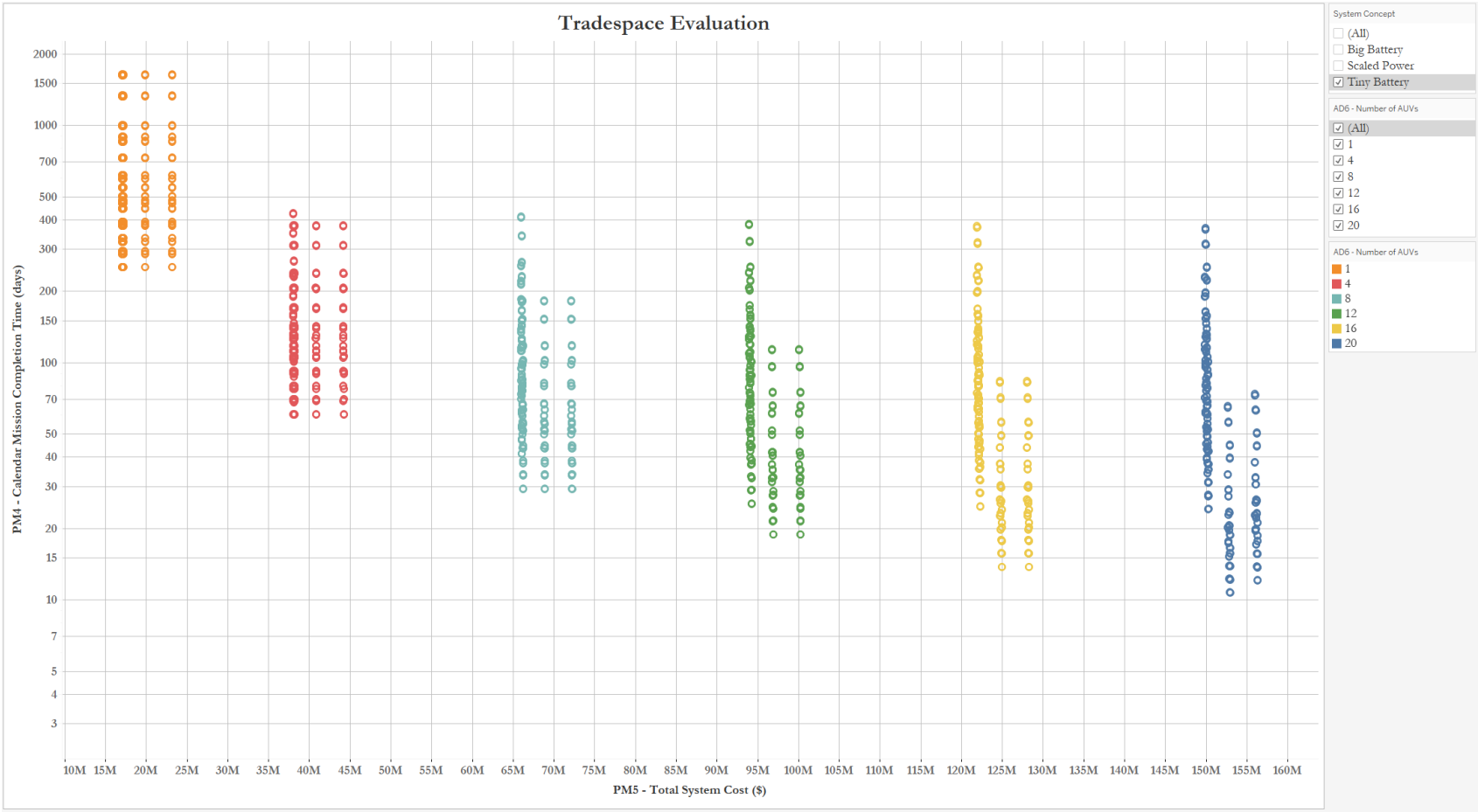

Figure 3-6: Tradespace of the tiny battery concept. 8,640 design vectors are plotted against PM4 and PM5. Points are colored according to the number of AUVs present in the system (AD6).

3.3.7.2 Big Battery Concept

The big battery concept is one where cost is completely relaxed as a constraint, and instead daily operational time is prioritized. In many respects, the big battery concept represents a different end member in solving the energy requirement from the tiny battery concept. The concept assumes that the mission completion time is known *a prioi*. That knowledge is then used to calculate how much energy will be expended by the system throughout the mission, and a battery bank that exactly meets these requirements will be put in place on the service platform such that at the time of mission completion, the battery bank will be completely depleted.

The size of the battery that will be required to accomplish this follows the following reasoning. First, the number of AUVs is examined and multiplied by the number of kWh required in each AUV. This value is compared against the product of the power generation capacity of the selected power system (in Watts) over a full day of energy collection. If the energy generation potential exceeds the energy required for that specific system, then no additional battery banks are required for the specific design vector. However, if there is an energy deficit, then the total daily deficit is multiplied by the calendar time required for mission completion (PM5). This will output a total amount of energy backup required per mission measured in kWh/mission. The following equation summarizes how this energy requirement is calculated:

$$\begin{aligned} &Required\ Energy_{Architecture} \\ &\quad = \left(ReferenceBatterySize * AD6_{Option}\right) \\ &\quad - \left(SystemOutput_{AD4_{Option}} * 24\ \text{hours}\right) * PM4_{Architecture} \end{aligned}$$

The two previous examples used to illustrate the tiny battery concept can again be employed to help understand this concept more fully. Consider again our one AUV system with a solar plant. Every day there is sufficient energy delivered to the AUV to allow for nominal operations. As such, there are no extra batteries that need to be added to the service vehicle. An important effect of this, is that the tiny battery and big battery system concepts are indistinguishable from each other in this case. All metrics will be identical to each other. However, once the single solar plant can no longer deliver sufficient energy to power four AUVs, these concepts will differ. In considering the big battery concept, there will be a daily required energy of 6kWh that will be stored on the service platform (as calculated from the total energy required by four AUVs minus the power harvestable per day by the

platform = 54kWh – 48kWh). These 6kWh of energy will never be replaced or replenished for the mission duration, as the system will operate at an energy deficit for the entire mission. Knowing *a priori* that the mission will take (for example) 70 days to complete with four AUVs, we know then that the total required energy to be stored on the service vessel is 420kWh. By storing this power onboard, there is a considerable cost to consider – but that cost buys the system daily operational time. Since the addition of extra batteries eliminates the daily energy deficit, each AUV will be able to operate at their ten hours of daily operating time.

From the battery chemistry decomposition, an individual battery's cost per kWh can be calculated by dividing the cost of an AUV battery by 13.5kWh – the size of a single AUV battery. This value is then multiplied by the previously calculated energy requirements to be stored on a service platform for any particular mission. This process is repeated across each of the four options for service platform battery chemistry. However, all of these costs represent the additional battery costs, and as such, they are added to the already existed static costs that are assigned to the system. Effectively, these batteries are an add-on to any previously outlined system. The result is the same matrix size as the tiny battery concept of 8,640 unique solutions which are visualized in Figure 3-7.

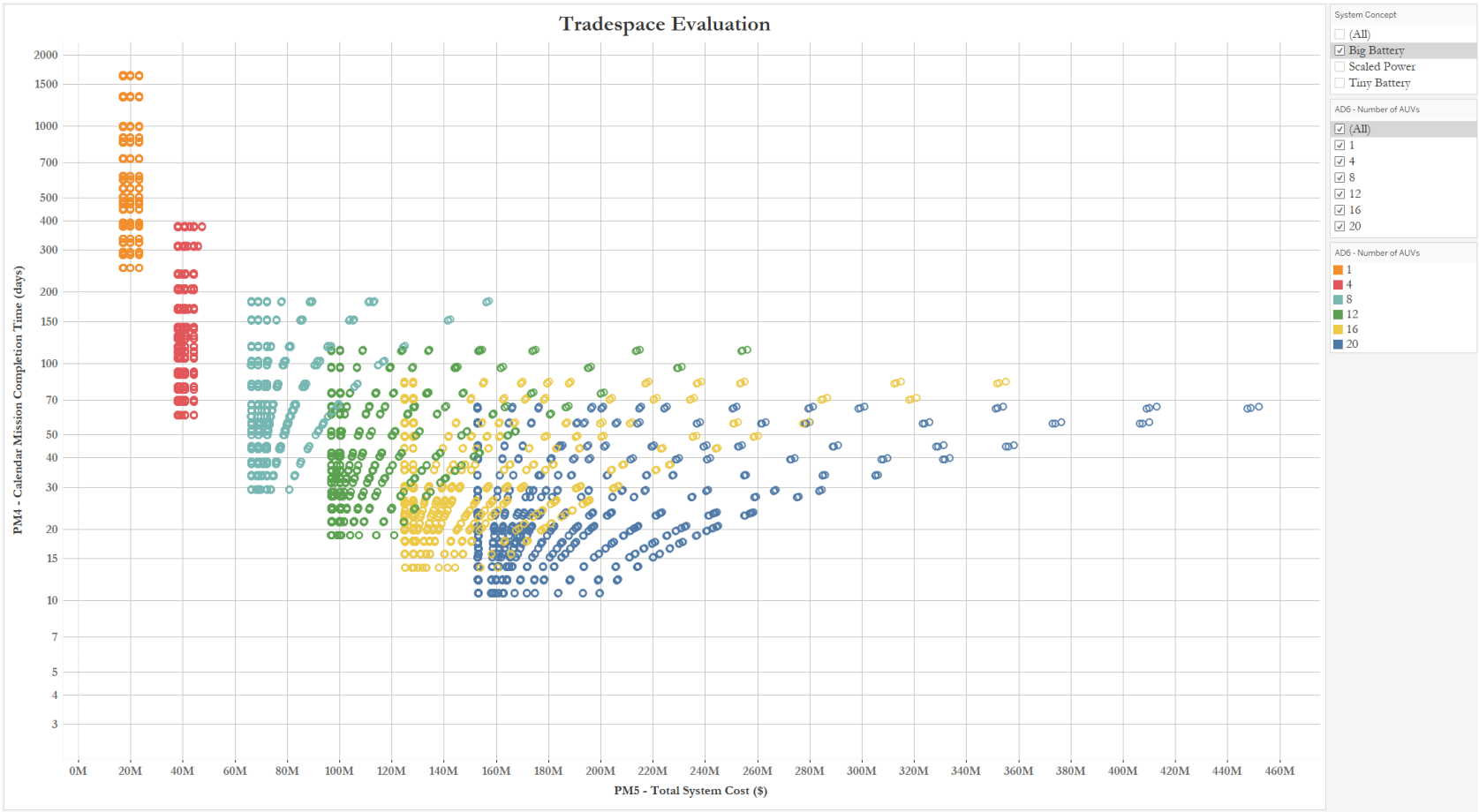

Figure 3-7: Tradespace of the big battery concept. 8,640 design vectors are plotted against PM4 and PM5. Points are colored according to the number of AUVs present in the system (AD6).

3.3.7.3 Scaled Power Concept

If the tiny battery concept constrains cost completely, and the big battery concept constrains daily operational time completely, then the scaled power concept exists in between these two end members. The overarching theme that governs the scaled power concept is that the platform should not operate at a power deficit, but it could be more cost effective to buy additional power plants and place them on the service platform as additional system level costs instead of creating enormous backup battery banks. In so doing, the daily operational time should exactly equal the daily operational times which are achieved in the big battery concepts, but ideally in some cases for a lower total system cost.

To calculate the total cost that each design vector will be assigned, the number of AUVs is examined and multiplied by the number of kWh required in each AUV. This value is compared against the product of the power generation capacity of the selected power system (in Watts) over a full day of energy collection. If the energy generation potential exceeds the energy required for that specific system, then no additional power plants are required for the specific design vector. However, if there is a daily energy deficit, then an additional power plant is added to the system until there is no daily energy deficit. The calculated daily energy deficit is divided by the energy produced by the selected power plant over a 24-hour period. This value is then rounded up to the nearest integer to prevent treating power plants as fractional systems – you either have to purchase a second plant or make due with one for instance. This value represents the additional number of power plants which are required to prevent a daily energy deficit.

$$NumberPowerPlants_{AD4_{Option}} = Roundup\left[\frac{\left(13.5kWh * AD6_{Option}\right)}{PowerOutput_{AD4_{Option}} * 24 \text{ hours}}\right]$$

$$\begin{aligned} Cost_{Architecture} &= \left(AD6_{Option} * Cost_{AUV}\right) \\ &+ \left(NumberPowerPlants_{AD4_{Option}} * CostPowerPlant_{AD4_{Option}}\right) \end{aligned}$$

In considering the same two examples from the previous sections, further insight can be gained concerning the scaled power concept. In the first case, the system has a single solar plant which is sufficient to charge a single AUV every day of the mission. In this case, there will be no difference

between the scaled power option and the other two system options. However, consider the four AUV case. In the tiny battery concept, operational time suffered as the power generation was insufficient. In the big battery concept, the cost suffered as 420kWh of energy had to be stored on the service platform for the case of a 70-day mission. In the scaled power concept, a second solar plant would be purchased explicitly to eliminate the daily energy deficit. Then the total energy harvested daily would be 96kWh (2*2kW*24 hours). In so doing, the four AUVs would have the energy requirements to operate to their prescribed parameters.

To calculate additional costs from this point in the analysis, the specific cost that is associated with that power plant (Table 3-9) is multiplied by the additional plants required to prevent a daily energy deficit and added to the system cost. Each service platform will still need sufficient batteries onboard to store one set of AUVs, so similarly to the tiny battery concept, each of the solutions was compared across each option for service platform battery chemistry. The result is an 8,640-entry morphological matrix which is visualized in Figure 3-8.

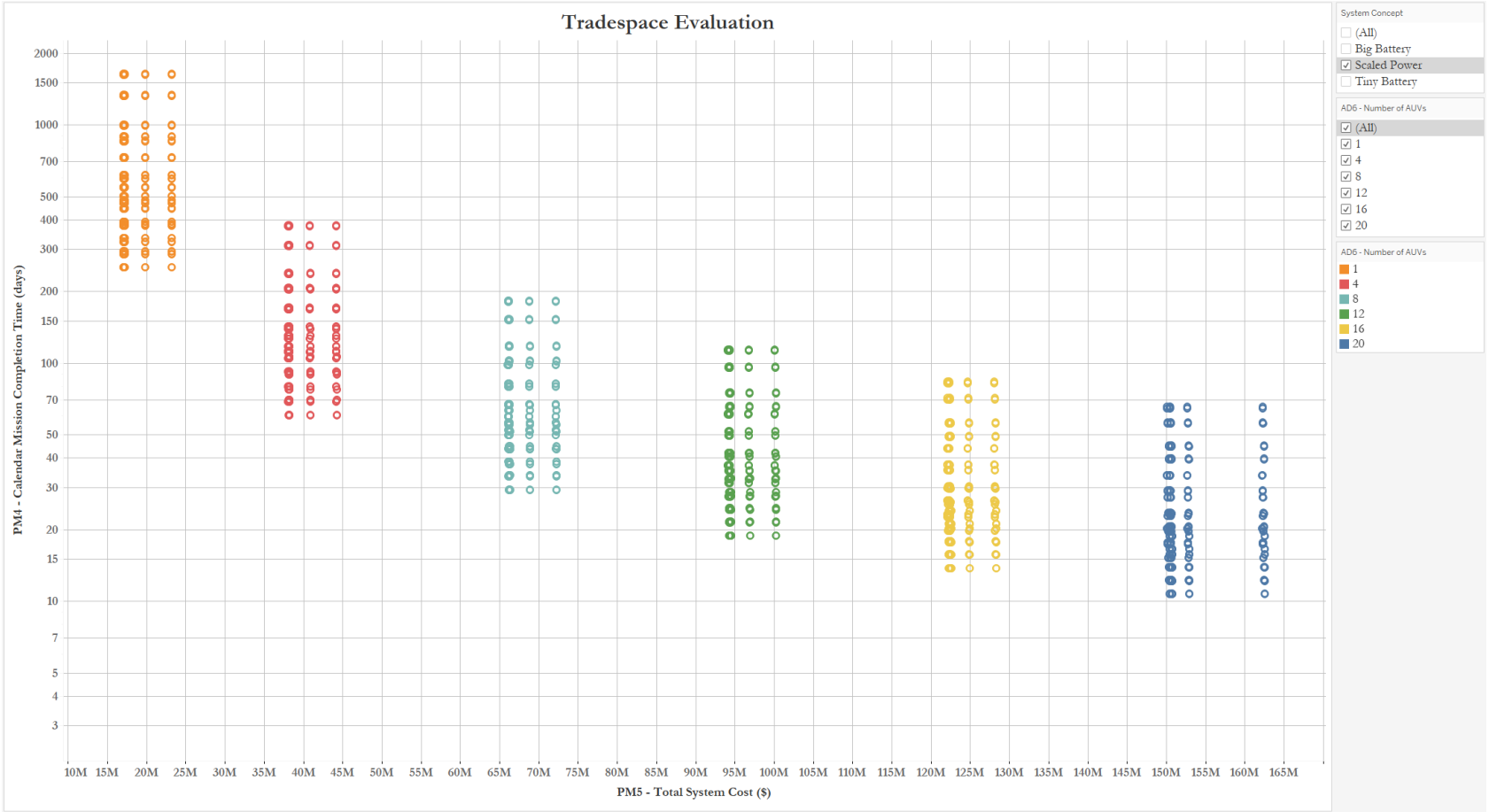

Figure 3-8: Tradespace of the scaled power concept. 8,640 design vectors are plotted against PM4 and PM5. Points are colored according to the number of AUVs present in the system (AD6).

3.4 Deterministic Evaluation

Having created a thorough deterministic model of the paired AUV and service platform, an evaluation of each of the architectural decisions is performed. The order in which the analysis is presented is in the order of impact on two prioritized metrics – PM4 (calendar mission completion time) and PM5 (total system cost). These two metrics are prioritized because they are excellent ways of evaluating the proposed paired system with the existing reference architecture. A utopia point would exist in a tradespace between these two metrics where the mission was accomplished in zero time for zero money. The reference architecture completed the total mission over the course of 730 days and approximately $37 million (Table 3-1). The goal of this evaluation is twofold: first to identify if the reference architecture exists within or without the Pareto frontier established by the constructed morphological matrix, and second to expose the tensions that emerge between the selected metrics and the decisions made within the architecture that lead to such tensions.

3.4.1 Establishing the Pareto Frontier

For the deterministic model, only valid designs were considered across the three previously discussed concepts. The result is a morphological matrix with 25,920 unique design vectors to consider. The full tradespace is shown in Figure 3-9. In this tradespace the x-axis is a measure of total system cost, and the y-axis is a measure of calendar mission completion time (note: the y-axis is on a logarithmic scale), with the existing reference architecture represented as a large red dot. The Pareto frontier that exists within this tradespace is defined by the lines which connect all design vectors wherein no individual metric can be improved without sacrificing another. This Pareto frontier in the PM4-PM5 space is represented as a thick green line. Finally, the utopia point in this space is labelled with a yellow star. From this initial pass, it is clear that the reference architecture does not exist on the Pareto frontier, but is instead well inside the Pareto frontier. In fact, with the deterministic model constructed as described, the reference architecture is worse than every single design vector for at least one of the two metrics shown. The reference architecture only improves calendar time to mission completion compared to 900 design vectors. The reference architecture is a lower cost option than 21,600 design vectors. Finally, there are 3,420 design vectors which are better in both PM4 and PM5 when compared to the reference architecture.

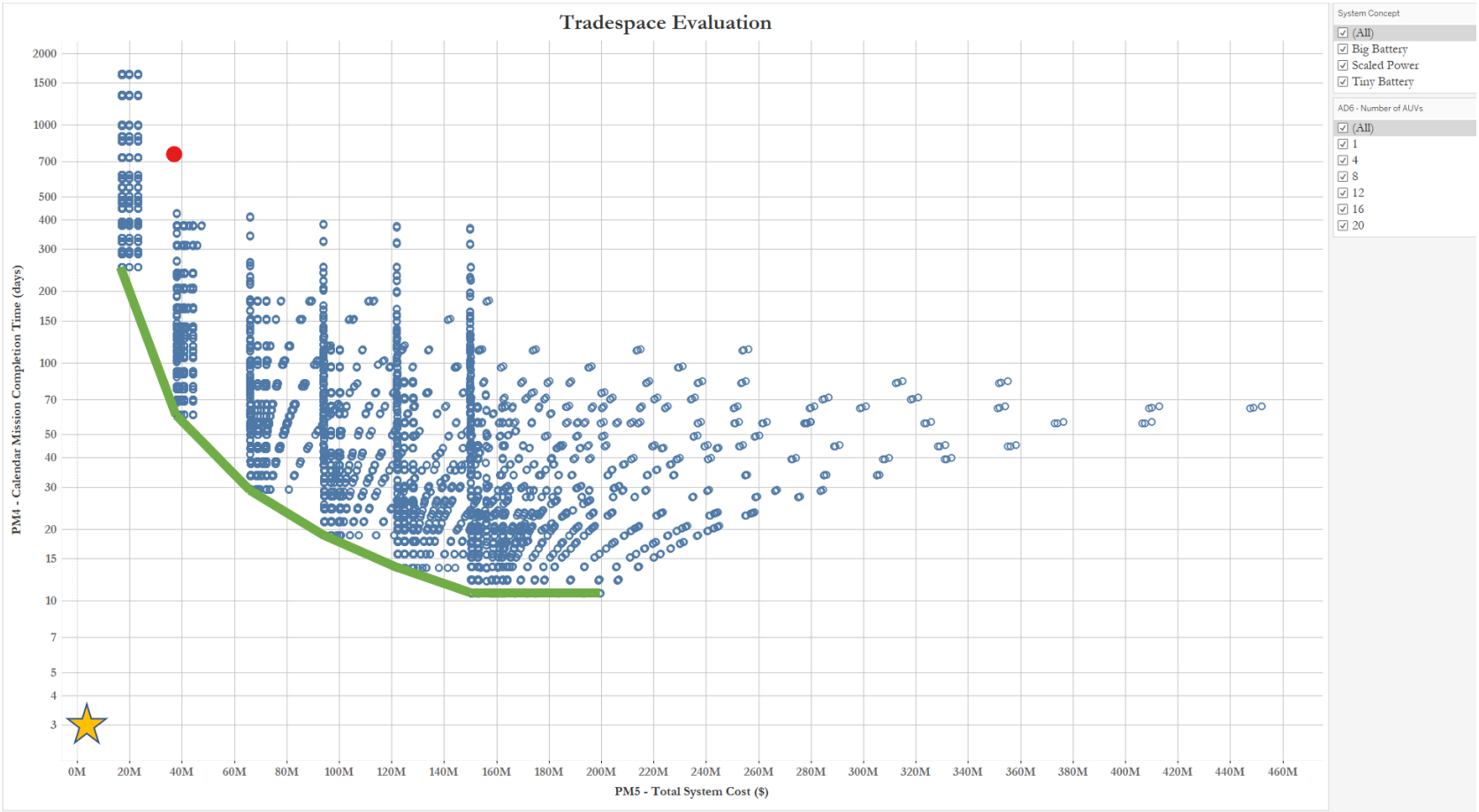

Figure 3-9: Full tradespace for analysis shown comparing PM4 and PM5.

3.4.2 AD6 – Number of AUVs

The number of AUVs that are used has the largest impact on the total cost of the system. This is because the number of AUVs that are selected for a specific design vector is several orders of magnitude greater than any other single individual component that can be selected. In the case of this model, AUV costs are assumed to be static and $5 million with minor changes affecting the component levels which can shift costs slightly above or below this benchmark. These individual changes in architecture are important because they impact other metrics, but concerning cost they simply do not add up to enough to make much of a difference relative to the $5 million price tag of a single AUV. Furthermore, with the addition of more AUVs to the system, the service platform must expand as well. In this model, the platform expansion accounts for less than half the other price expansion due to the number of AUVs, but it still makes a significant impact.

The addition of multiple AUVs is most clearly seen when illustrated first on a single concept. The tiny battery and scaled power system concepts clearly illustrate how the total system cost increases with the changes in AD6 (Figure 3-6 and Figure 3-8). This step-wise increase in cost is also mirrored in the big battery system concept, although the delineation is blurred as battery costs begin to balloon. There is no other architectural decision within this system that has such a dramatic impact on the overall cost of the system.

The number of AUVs that are in the system also carries importance in all metrics concerning daily operational time. The interaction that exists between the number of AUVs and daily operational time is multivariate and will be discussed in greater detail in future sections. However, on first glance, since daily operating time is governed in part by the number of AUVs present in the system, an initial claim is supported that as the number of AUVs increase in the system, the daily operating time decreases because of increased time to the seafloor (Table 3-6). This relationship is shown in the tradespace as well when examining very specific subsets of the data. For instance, Figure 3-10 clearly shows that when the data are filtered to limit the tradespace to a few select architectures, a pattern emerges where higher numbers of AUVs present in the system lead to lower actual daily operational time.

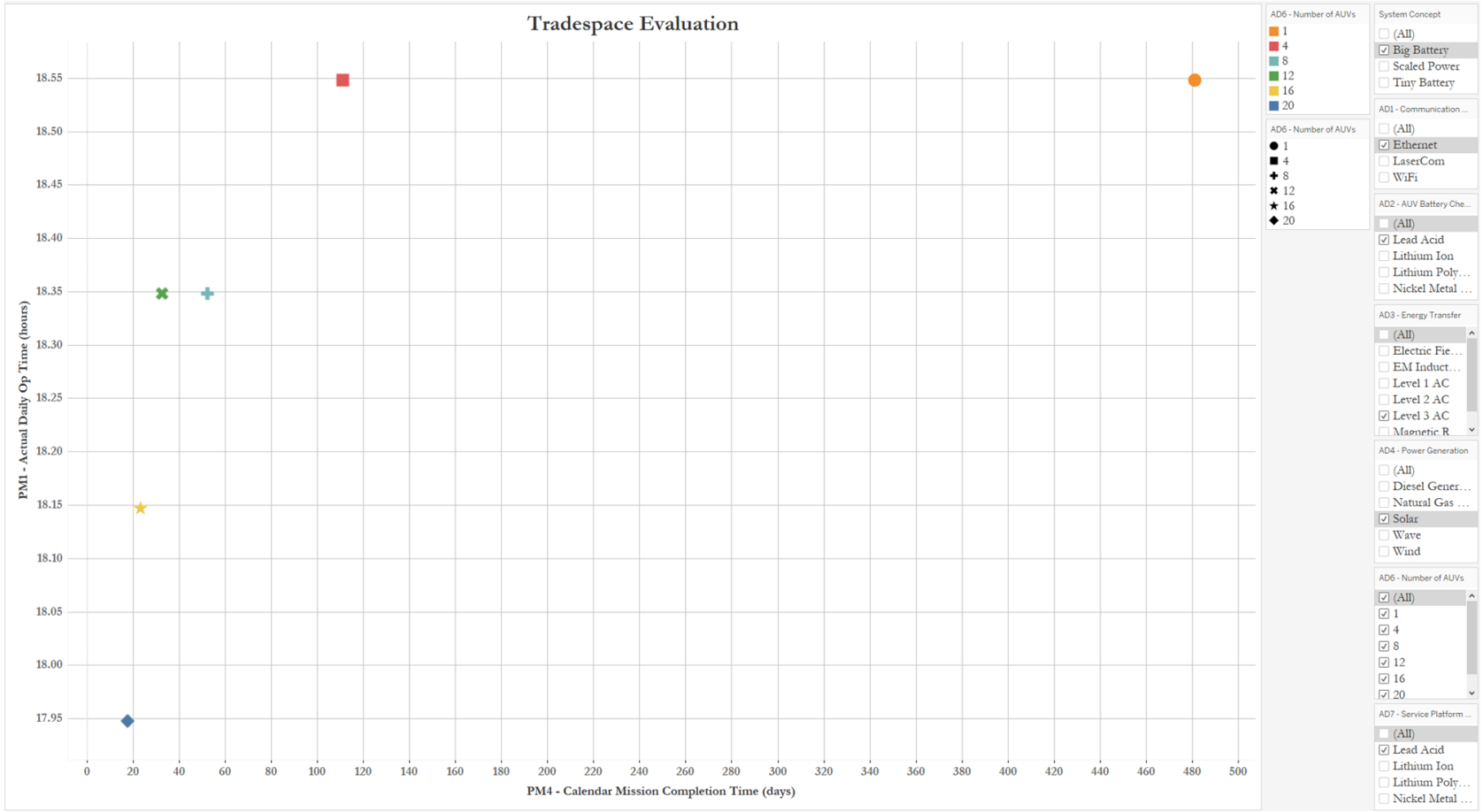

Figure 3-10: Tradespace representing only AD1 = Ethernet, AD2 = Lead-acid, AD3 = Level 3 AC, AD4 = Solar, AD7 = Lead-acid, and Big Battery concept design vectors. The x-axis is total calendar mission completion time (PM4) and the y-axis is actual daily operational hours. The different shapes and colors represent different options for number of AUVs in the system.

3.4.3 AD4 – Power Generation

The method of power generation has the second largest impact on the total cost of the system. Knowing that there are groupings that exist within each set of AD6 options within the PM4 and PM5 tradespace, we can begin to dive into more nuanced changes that influence the metrics. In examining the tiny battery system concept exclusively, in a subset of data which only include one AUV in the system, there is a clear trend which shows that all renewable options are more cost-effective than all non-renewable options (Figure 3-11). Moreover, within the options that are available for renewable sources, it appears that performance in PM4 is equal for each architecture, while wind is the cheapest, and wave power is the most expensive. However, when we examine another case – say with more AUVs present in the system – the pattern is less clear-cut. Figure 3-12 demonstrates that there are differences in cost and PM4 for all of the different possible power generation options within the tiny battery concept and 20 AUVs. The general trend that renewables are cheaper than non-renewables is still present, but in some design vectors, wave power is now less expensive than wind power. Additionally, there is a significant difference in PM4 between otherwise identical architectures – keeping power generation method constant. An otherwise identical design can range in values for calendar days to mission completion from 11 days to 60 days, and cost can range between $150 million to $156 million. Figure 3-13 illustrates this complex relationship emerging in the tiny battery system concept. There are some limitations that begin to impact the system as the number of AUVs scale. As the power plants can no longer supply the number of AUVs with the energy required for daily use, the daily operational time decreases rapidly, and the advantage of increasing the number of AUVs is somewhat eroded. If the value proposition of a paired AUV and service vessel is that the mission completion time will decrease, then this is an integral limitation to explore. Figure 3-14 shows these same points, except compared in PM5 and PM1 (actual daily operating time) space. If the power plants were able to supply all of the required power for this architecture, then the daily operating time should be equal across all design vectors. However, in the case of all renewables, and in the case of a diesel generator in the 20 AUV option, there is a point where daily operating time decreases due to a lack of sufficient power. From this graph, it can be concluded that for this set of architectures, a single solar plant cannot supply sufficient energy to operate four or more AUVs without sacrificing daily operating time. Similarly, for wind power plants, eight AUVs or more require more energy than the power plants are capable of delivering. Wave energy cannot support 12, 16, or 20 AUVs. This trend is alleviated when examining system concepts. If we take only the solar power plant options from this example,

and add the other two concepts in for comparison, then we see that the daily operating time (PM1) stays constant (Figure 3-15).

Figure 3-15 also makes it clear that the costs associated with power generation method vary depending on which concept is selected. When looking at only the architectures described in Figure 3-15, the costs for all three concepts are identical for a single AUV case. However, the differences in cost increase as the number of AUVs increase. By the 20 AUV option for AD6, there is a $12 million cost difference between architectures with the same power generation option for AD4. This relationship where costs are inconsistent across otherwise identical architectures is extant for all power generation methods. Critically, the tension that exists between power generation, energy storage, and cost is at the heart of the AUV and service platform pairing viability question. If the pairing is to be successful, then energy must be generated and stored in such a way that projects are completed with improvement in metrics that are most important for the specific stakeholders.

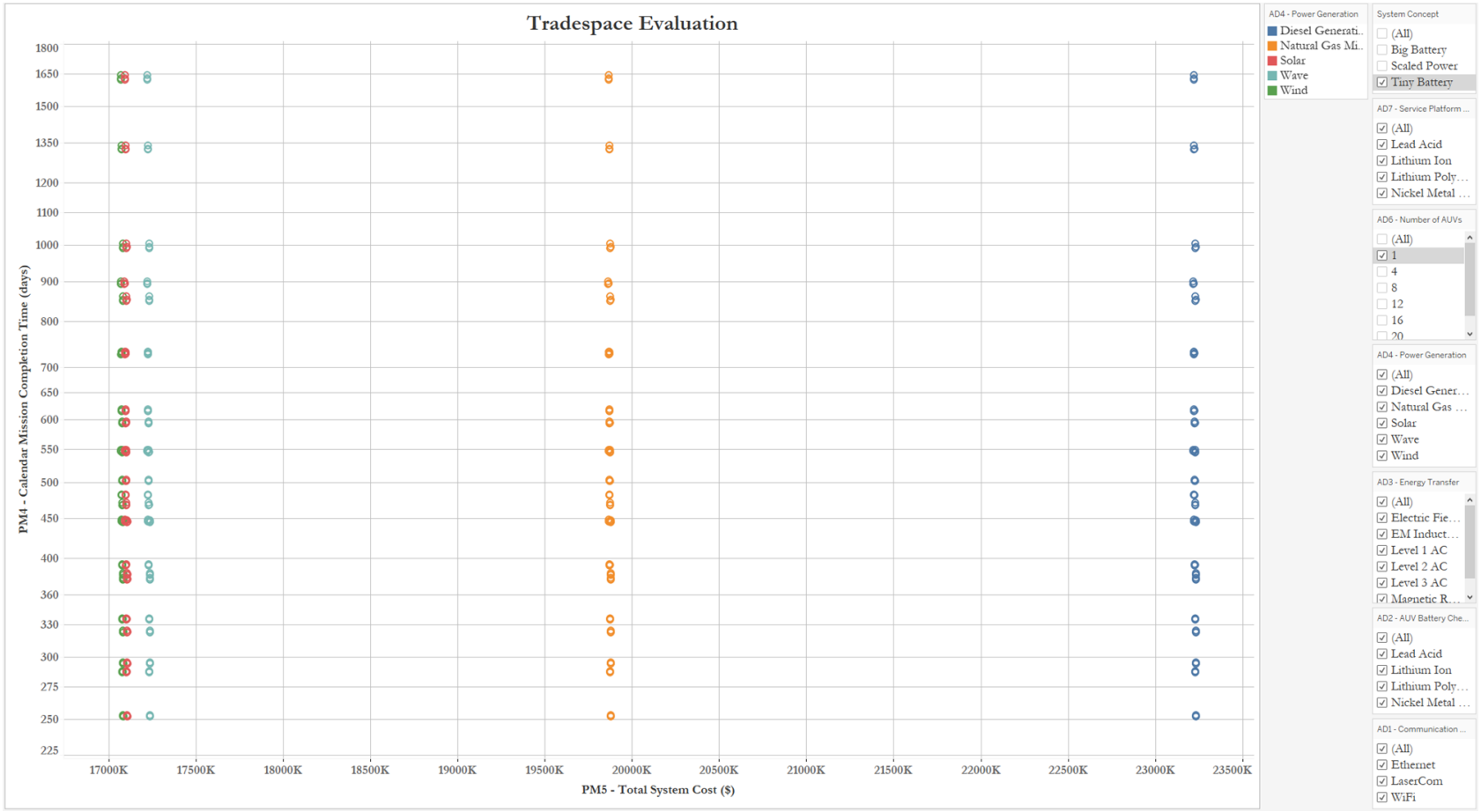

Figure 3-11: Tradespace evaluating a single AUV system with the tiny battery concept. Individual design vectors are colored based on the power generation method selected.

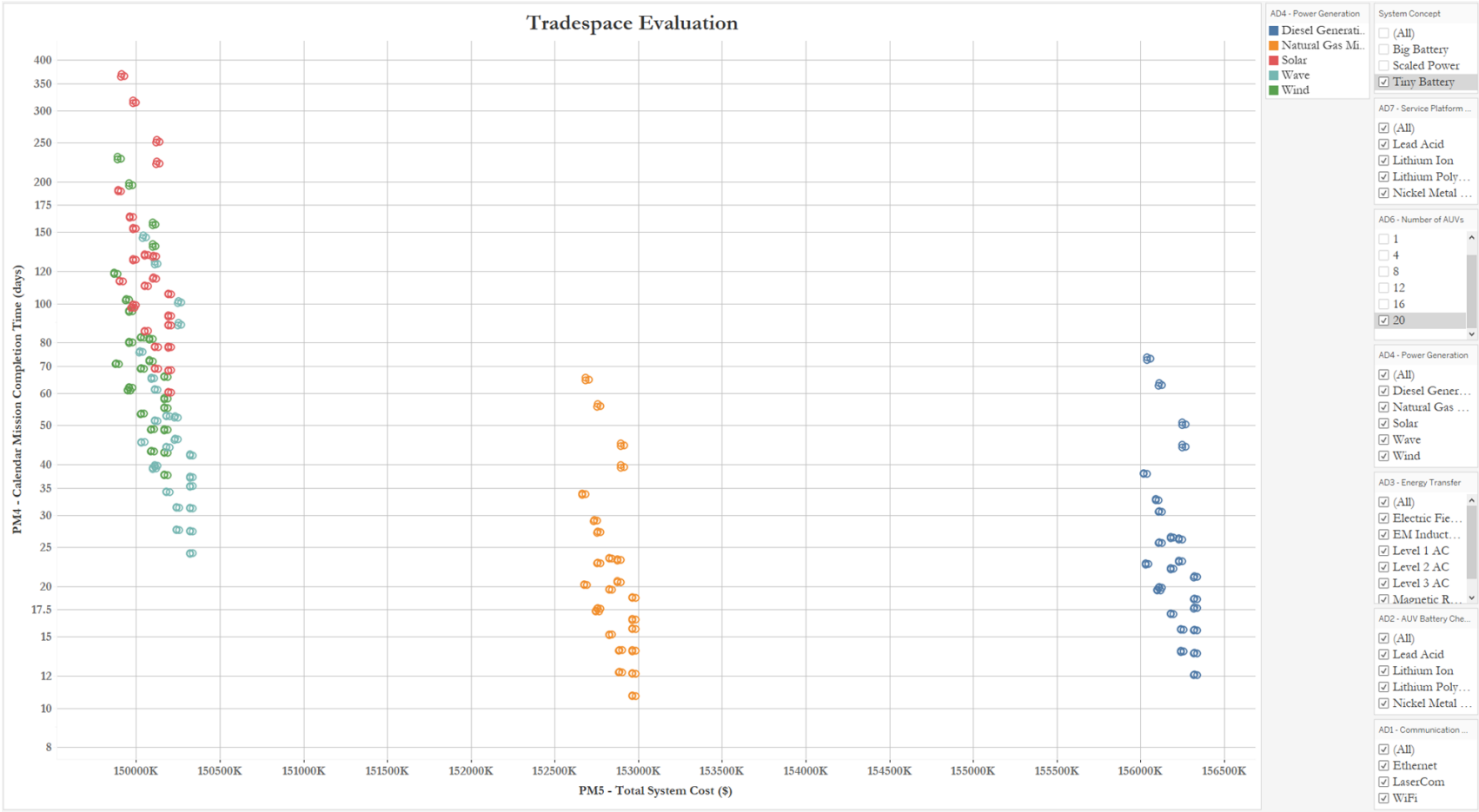

Figure 3-12: Tradespace illustrating a 20 AUV system with the tiny battery concept. Individual design vectors are colored based on the power generation method selected.

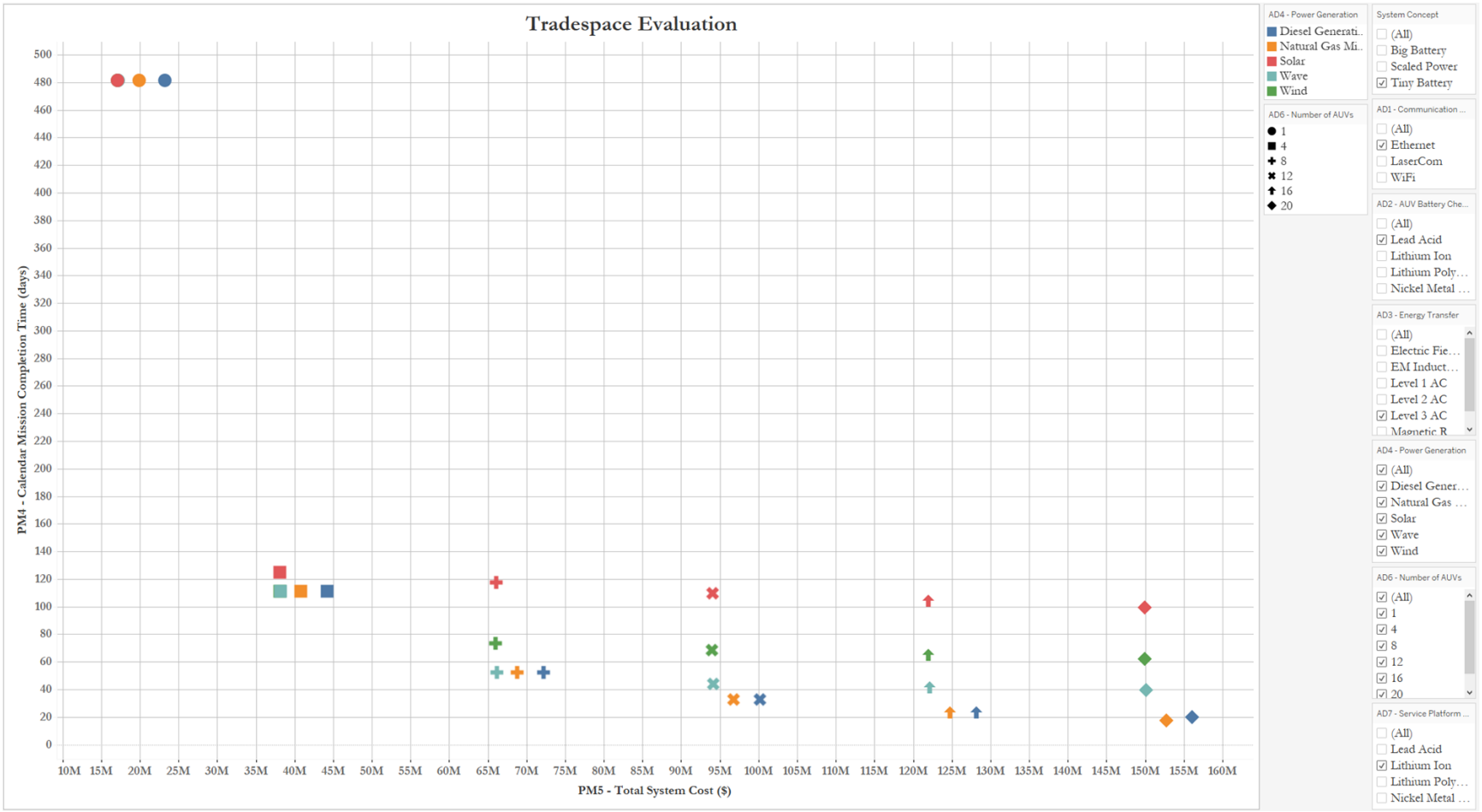

Figure 3-13: Tradespace illustrating all options for AD6 - number of AUVs with all power generation options. Filtered to only include options which only include AD1 = Ethernet, AD2 = Lithium-ion, AD3 = Level 3 AC, AD7 = Lead-acid, and system concept = Tiny Battery.

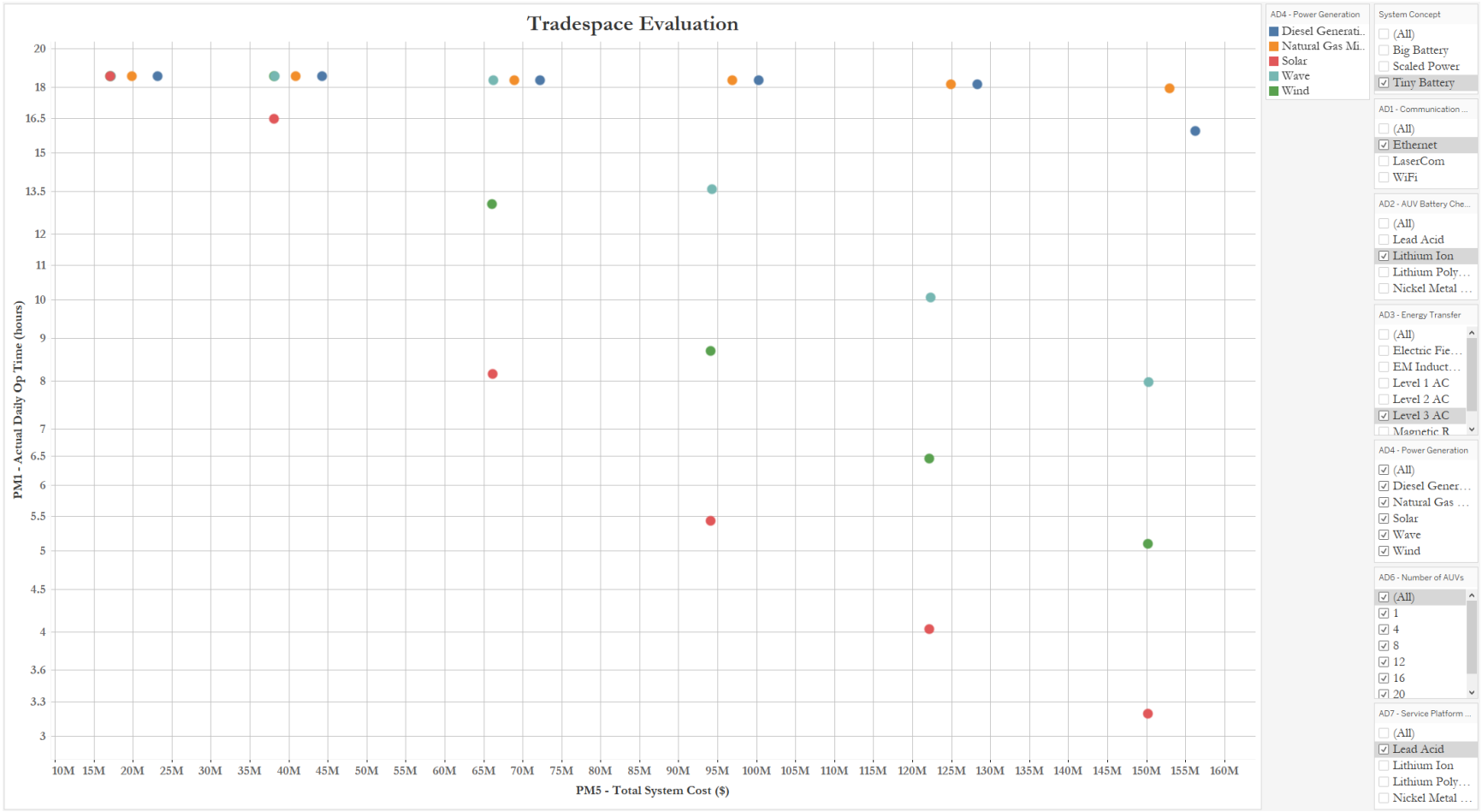

Figure 3-14: Tradespace illustrating otherwise comparable architectures in the tiny battery concepts and the impact that changing the power generation option has on daily operating time. These points are the same as illustrated in Figure 3-13.

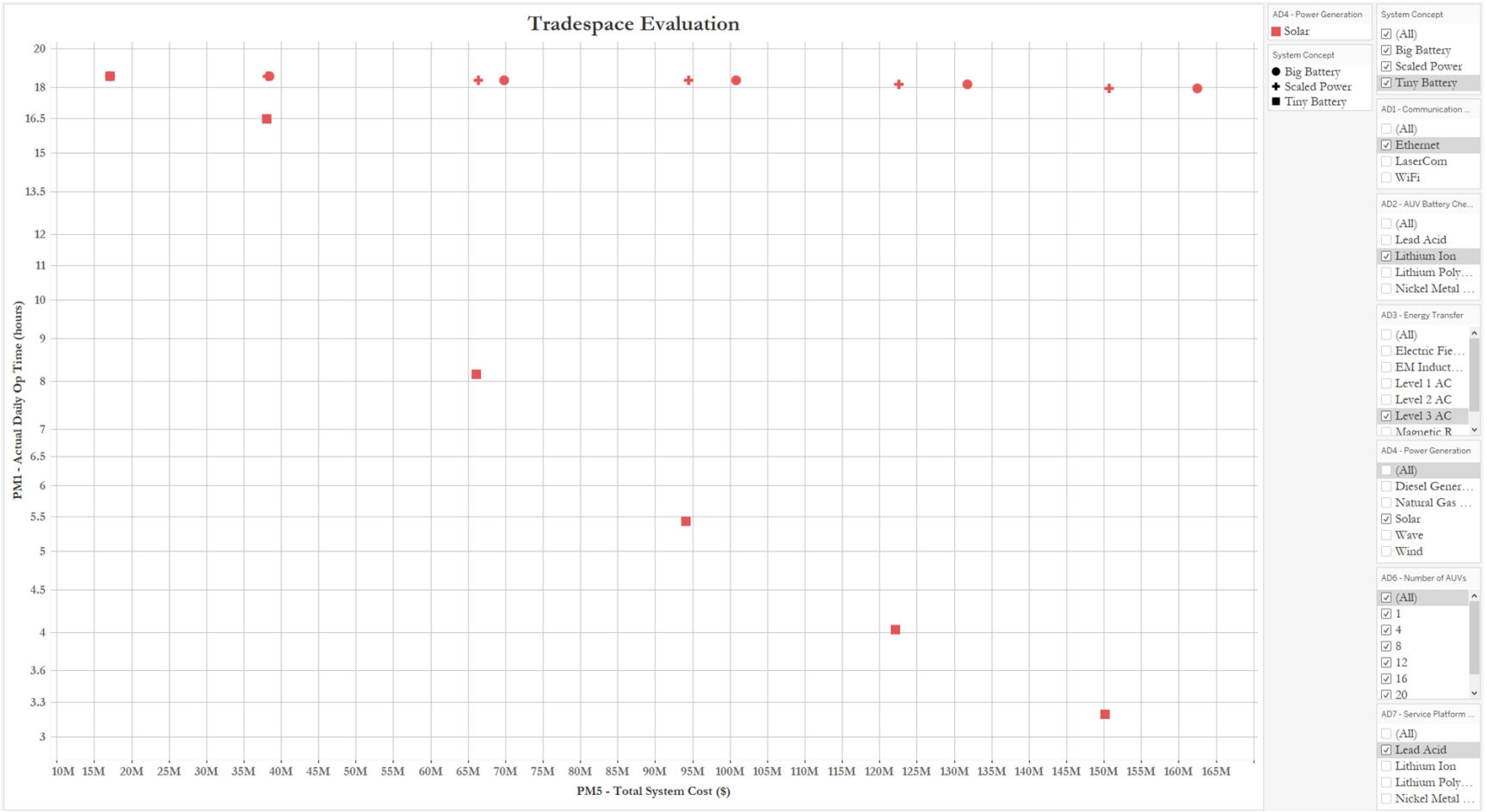

Figure 3-15: Tradespace illustrating the points on Figure 3-14 filtered to show only the solar power plant option across all three design concepts. The daily operating time stays constant across the big battery and the scaled power concepts.

3.4.4 AD3 – Energy Transfer

The primary contributor to increasing or decreasing calendar mission completion time is which energy transfer method is selected. There is a non-linear inverse relationship that exists between actual daily operating time (PM1) and total calendar mission completion time (PM5). This relationship is best explored first through a small subset of the data that simultaneously exposes the impact that energy transfer can have on the system. Figure 3-16 shows this relationship in a very small subset of the data. The data only include architectures with ethernet communication, lithium-ion AUV batteries, solar power generation, one AUV, and a lead-acid battery installed at the service platform. Additionally, these points only include the tiny battery system concept. There are two trends that are revealed in this small subset of data which are consistent across all architectures. First, a higher daily operating time (PM1) will result in a lower calendar mission completion time (PM4). Second, there is a clear pattern that the changes in energy transfer method directly impact the actual daily operational time.

As discussed in Table 3-6, daily operating time is influenced by communication method, energy transfer method, and the number of AUVs. Figure 3-16 shows that there are changes of two operational hours or more as a different option is selected for energy transfer method with otherwise identical architectures. When this restricted selection is expanded to include all design vectors for one AUV systems, it is clear that the trend of decreasing daily operational time is due primarily to energy transfer method (Figure 3-17). This systematic decrease in daily operational time is seen even in more complex interactions. For instance, as AUVs are added to the tiny battery system and the selected power plant is unable to supply the system with sufficient energy for daily operations, the actual daily operational time decreases by definition. The energy transfer method, however still impacts the system across comparable architectures (Figure 3-18). The interaction between number of AUVs and energy transfer is also non-linear depending on which specific design vectors you are comparing. For instance, in Figure 3-18 it is clear that a single architecture with one AUV compared with its identical counterpart with four AUVs loses two hours of operational time per day if the selected option for energy transfer is Level 3 AC. However, this loss is less than one hour if the energy transfer method is EM induction. If there is sufficient energy to transfer (e.g., big battery and scaled power concepts), then the energy transfer method will always show systematic decreases with respect to daily operating time. Figure 3-19 shows this relationship across all architectures that are generated for the big battery concept with ethernet communication methods.

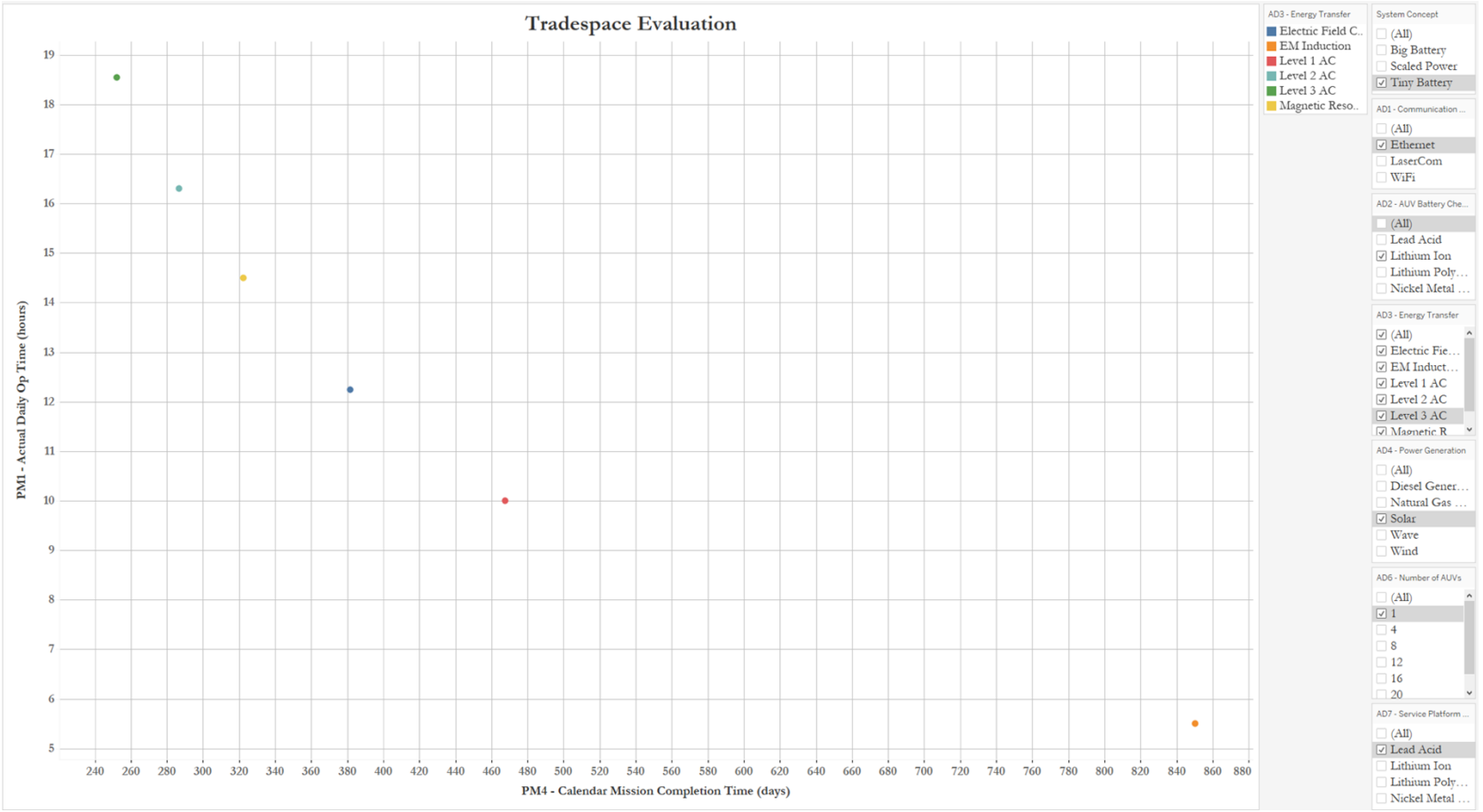

Figure 3-16: Tradespace illustrating the inverse non-linear correlation between actual daily operating time (PM1) and total calendar mission completion time (PM4). Displayed data only show a single set of parameters with variability in the energy transfer method in the tiny battery system concept.

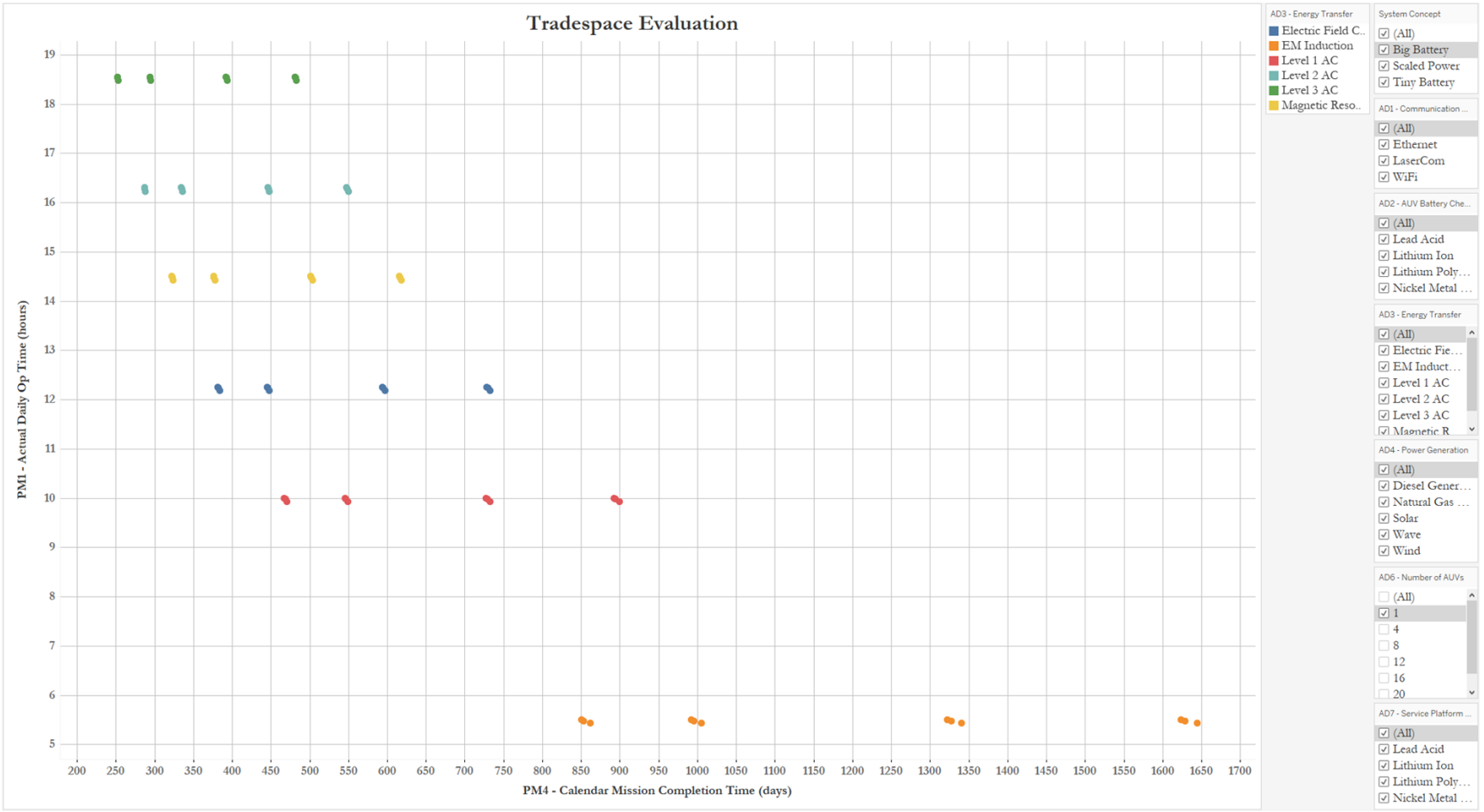

Figure 3-17: Tradespace illustrating an expanded set of design vectors for all options with one AUV. Data are colored by energy transfer method.

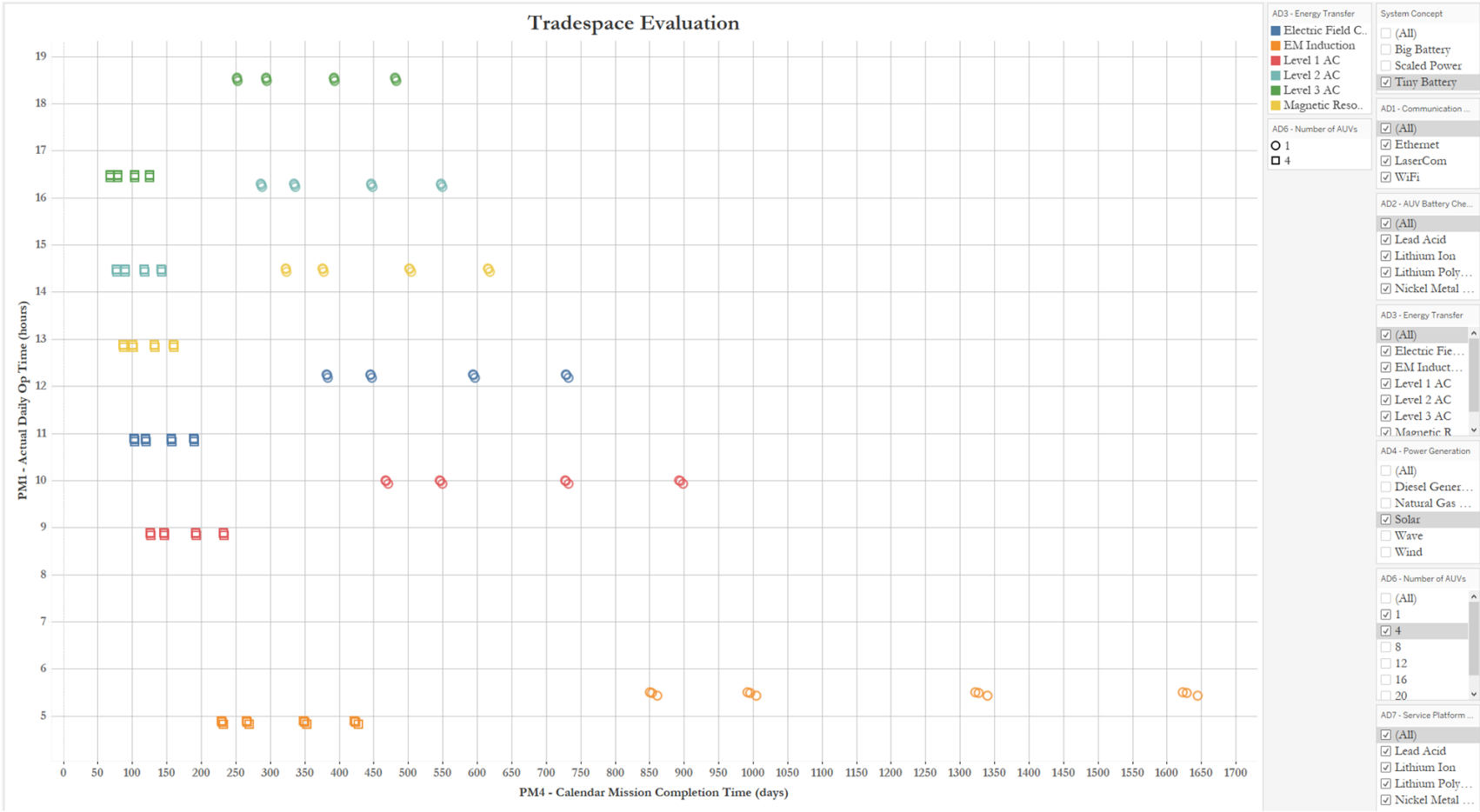

Figure 3-18: Tradespace illustrating the impact of adding additional AUVs to daily operating time in the tiny battery concept. Energy transfer method still accounts for systematic decreases in daily operating time.

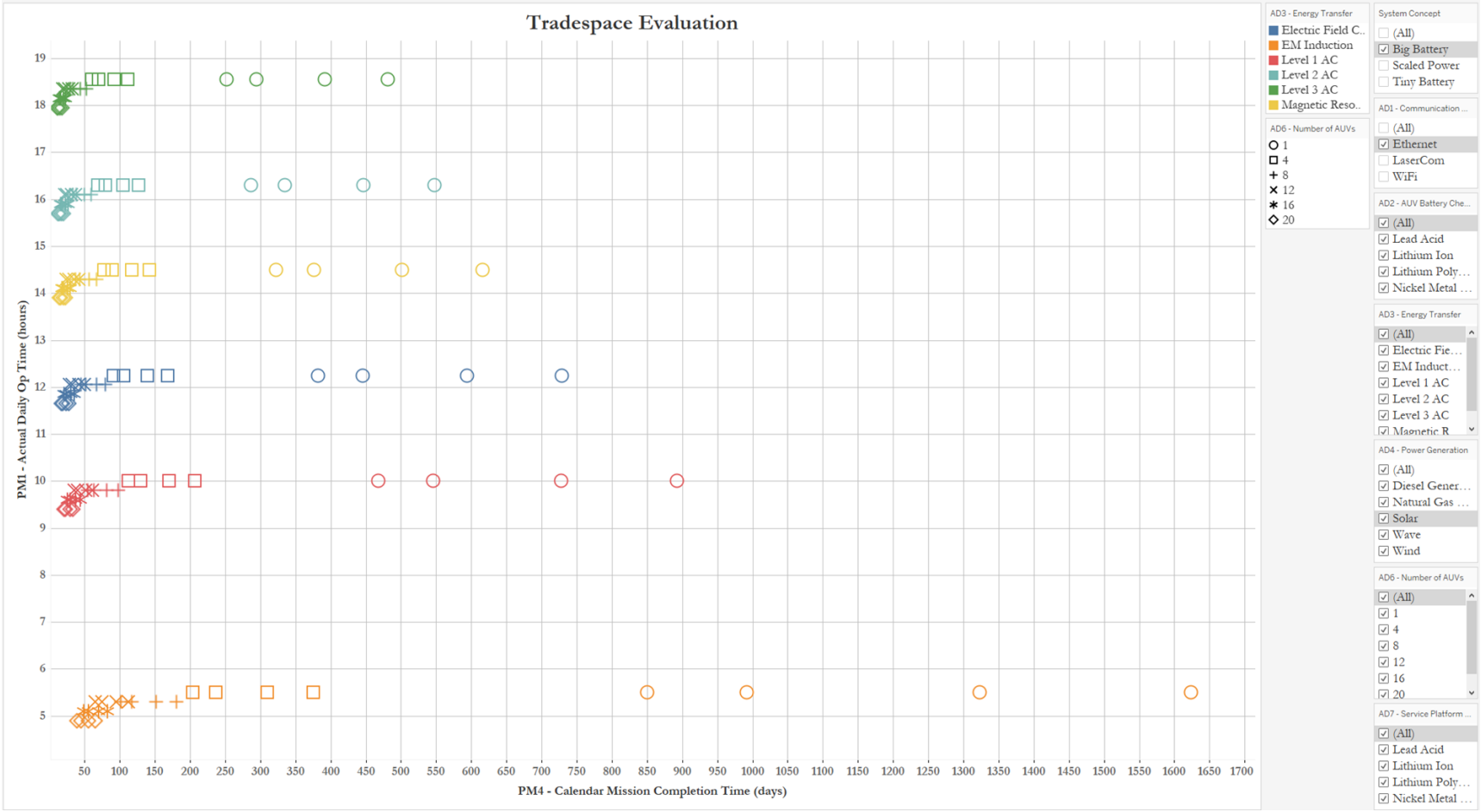

Figure 3-19: Tradespace illustrating all design vectors for the big battery concept with ethernet data transfer methods. The data are colored according to the method of energy transfer and shaped according to the number of AUVs in the system.

3.4.5 AD2 – AUV Battery Chemistry

The next largest contributing factor which impacts calendar mission completion time is which AUV battery chemistry is selected. This architectural decision does not impact the daily operating time of an individual AUV. In Figure 3-20 the different points are plotted with color representing different options for battery chemistry for the big battery concept. Even though mission completion time increases with different architectures, the daily operational time is consistent for the same architectures where the only change is the battery chemistry. Instead, the battery chemistry is an important factor which governs the survey area rate (PM2). Using the same subset of data from the previous figure, Figure 3-21 shows a systematic change in the survey area rate depending on which battery chemistry option is selected. Additionally, given this and previous analyses, it is clear that in these dimensions, a calendar mission completion time is a function of multiple variables. If AUV battery chemistry were the sole governing architectural decision impacting project mission completion time, then there would also be a systematic trend along the x-axis. As previously outlined, total mission completion time is a function of the size of the mission, the daily operational time, and the survey area rate.

AUV battery chemistry plays a minor role in cost as well. The individual batteries which power a single AUV are not identical in cost (Table 3-7), and so as the system increases the number of AUVs, more expensive components will lead to larger cost increases. For a single AUV, these changes are minor. However, when scaled to 20 AUVs, these individual component changes sum to appreciable amounts. While negligible in the sense that they are a minor cost in the system, it is important to note that the costs are not identical (Figure 3-22). In the case of 20 AUVs, the difference in costs due exclusively to different AUV battery chemistries is $140,000. That is approximately $1/10^{th}$ of a percent of the total system cost for a 20 AUV system. Importantly, this would suggest that when considering this architectural decision, the utility gained by selecting a more expensive AUV battery could well be worth it, as the additional cost is so small relative to the entire system.

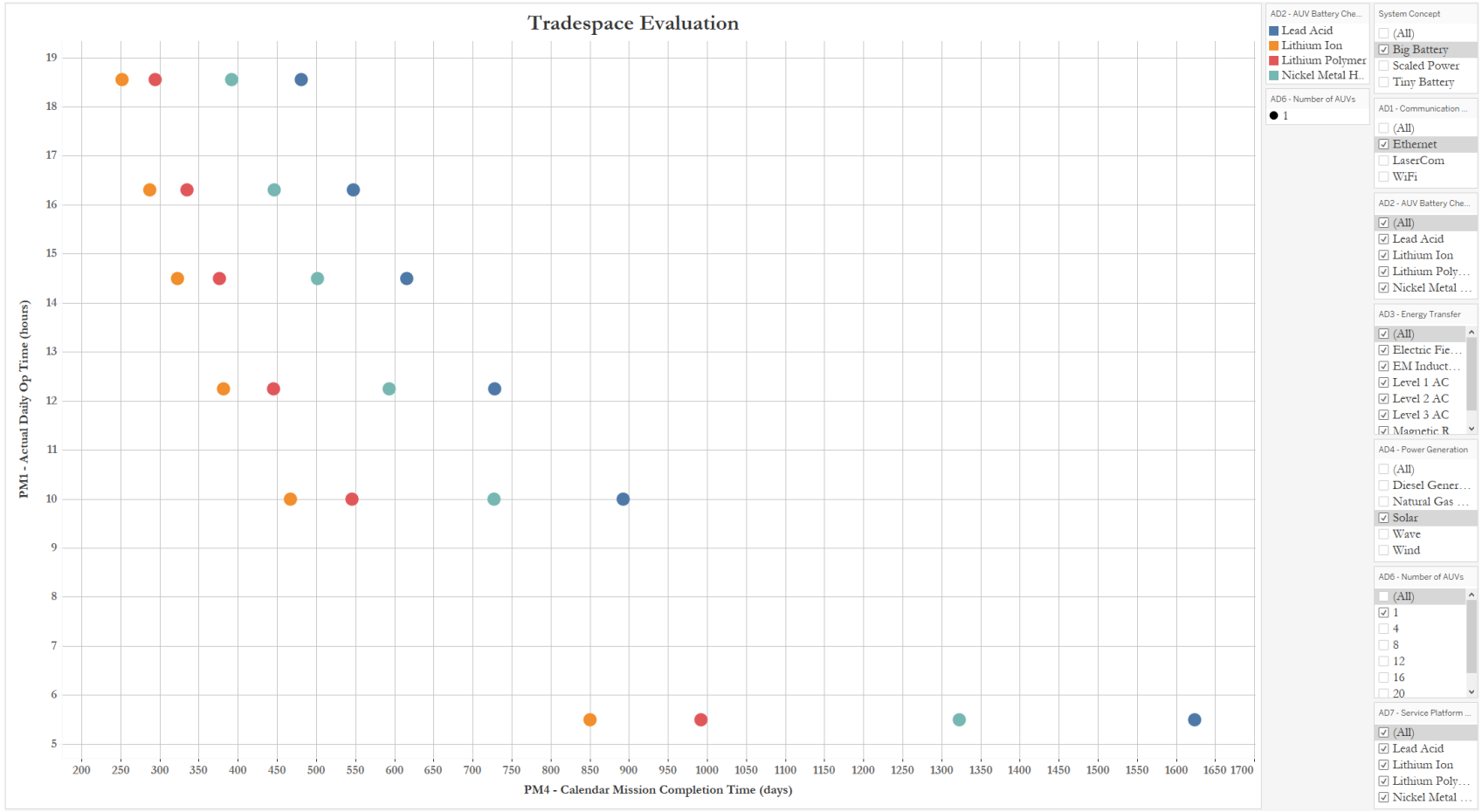

Figure 3-20: Tradespace illustrating how battery chemistries do not influence daily operating time using a subset of data including the big battery concept, ethernet, solar power generation, and one AUV.

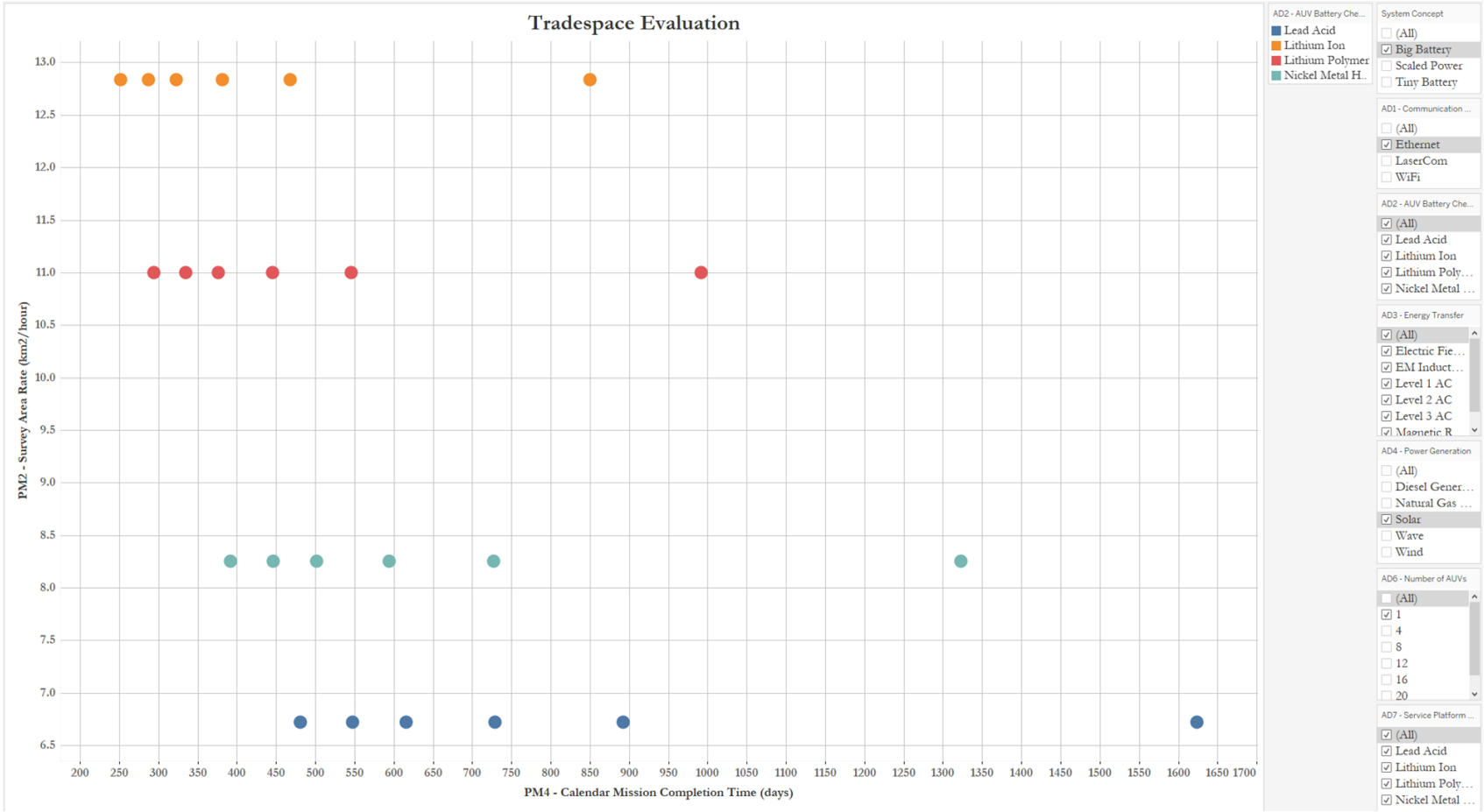

Figure 3-21: Tradespace illustrating how survey area rate is affected by changes in AUV battery chemistry using a subset of data including the big battery concept, ethernet, solar power generation, and one AUV.

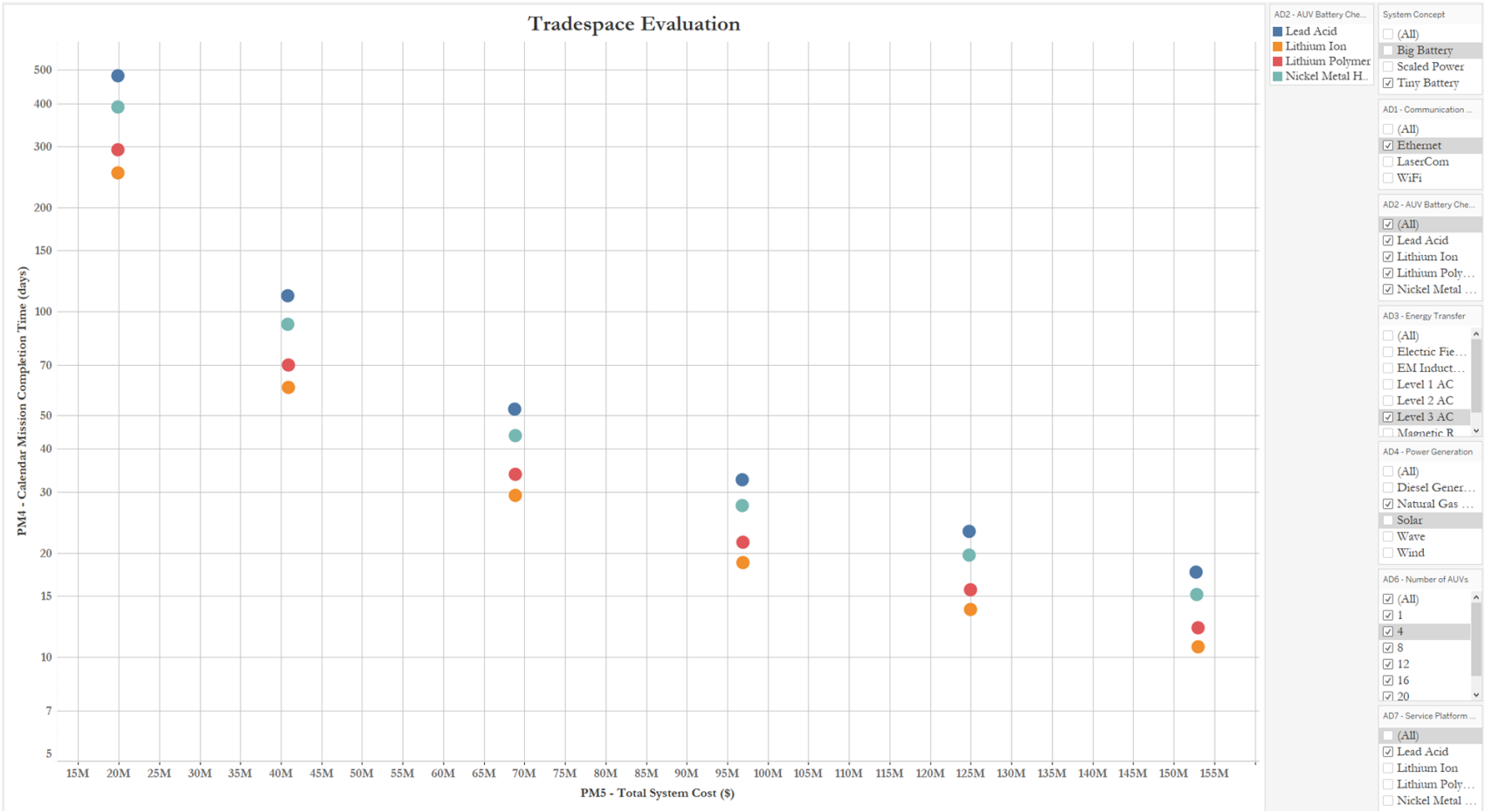

Figure 3-22: Tradespace illustrating the total system cost (PM5) as well as the total calendar mission completion time (log scale). While individual architectures appear to have identical costs comparing different battery chemistries, there are in fact minor differences.

3.4.6 AD1 – Communication Method

Communication method does not impact the calendar mission completion time or the cost in any major fashion. There are minor improvements in completion time, but they are on the order of less than 1% of the total mission completion time or less. With every other design option held constant, the greatest impact that communication method has with respect to mission completion time is one day (Figure 3-23). This impact is seen when the system has the smallest number of AUVs in the system. When there are larger numbers of AUVs this time difference decreases because the number of data transmissions from the AUVs to the platform are handled in parallel rather than in series. Each individual AUV can only transmit its own data at the conclusion of a mission and so simultaneously transmitting more missions results in less calendar time of transmission expiring. On the other hand, from a cost perspective, the cost scales linearly with additional AUVs. The largest cost difference is in the 20 AUV case where a LaserCom option costs $19,000 more than an ethernet connection.

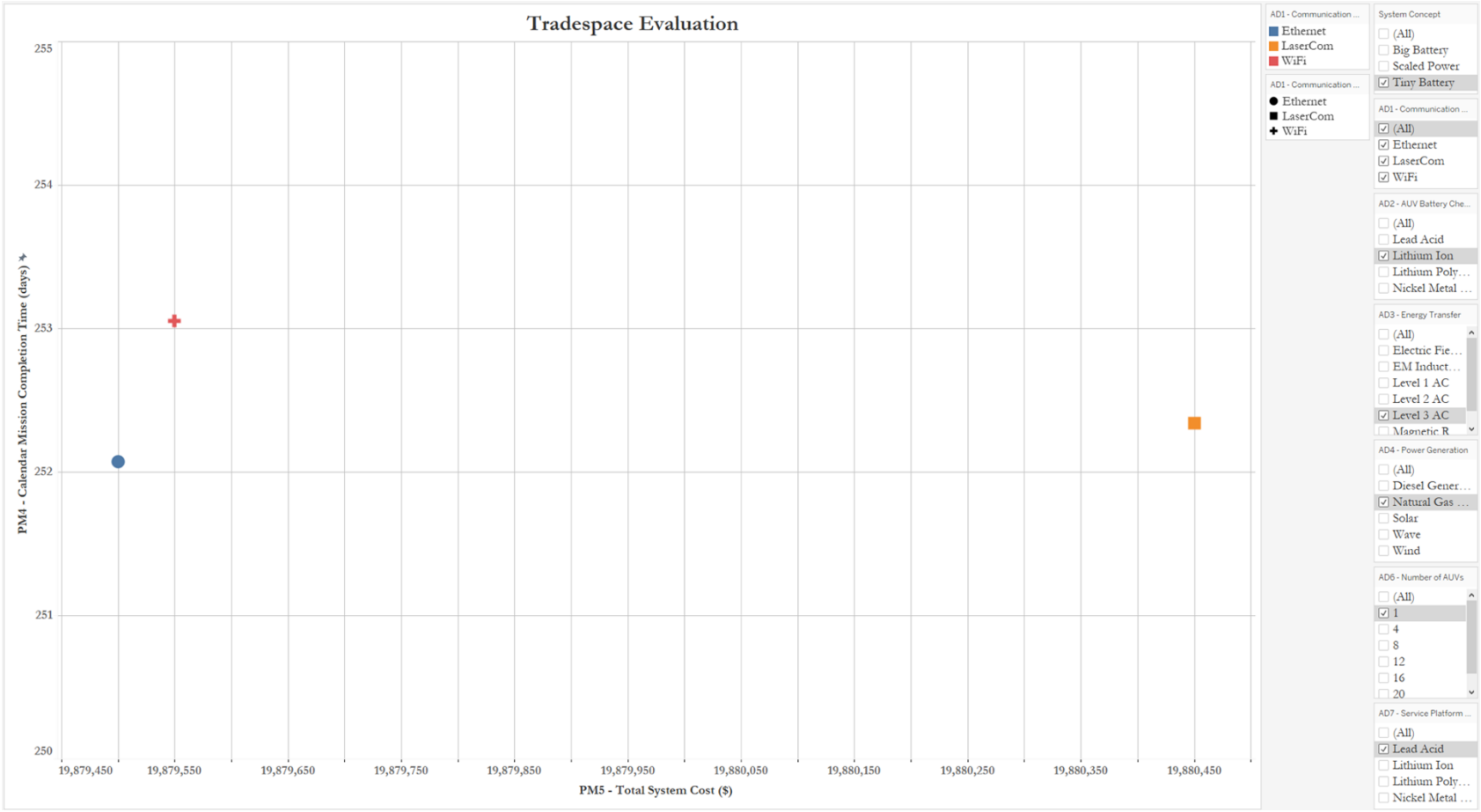

Figure 3-23: Tradespace illustrating the maximum change in mission completion time based on a single set of design vectors changing only communication method.

3.4.7 AD7 – Service Platform Battery

The selection of a specific battery for service platform only holds major impact in the big battery concept. Given how much power is required to be stored, the size of the batteries can in places account for more than the cost of the entire remainder of the system. For the tiny battery and the scaled power concepts, however, there is little impact on cost due to the very small number of batteries required on the service platform. In the big battery concept, there is a complex, non-linear interaction that exists between total system cost, power generation method, and service platform battery chemistry option. Figure 3-24 illustrates this scaling relationship with a subset of data which include only the renewable options for power generation and options for four, eight, and 20 AUVs selected for ease of visualizing. There are several key messages to note from this figure which are consistent across the big battery platform. The first is that the big battery concept balloons in cost in magnitudes that are not seen in other architectures based on service platform battery selection. The reason that this happens is because of the magnitude of batteries that must be stored onboard in order to provide sufficient power to the system for the duration of the mission. Nearly $240 million is added to the project if lithium-ion batteries are selected instead of lead-acid batteries in the case of 20 AUVs with solar power generation options. Considering that the most expensive option of any scaled power or tiny battery concept is less than this difference, this is not to be overlooked.

Second, while there are differences in total system cost (PM5) depending on how many AUVs are selected, there is overlap in the PM5 dimension across the number of AUVs selected. In other words, in some cases, service platform battery chemistry selection can be a more impactful cost driver than the number of AUVs – which was not the case in the tiny battery or the scaled power system concepts. This overlap is pronounced in the case of renewables. However, in the case of non-renewables, there is no such overlap. This is because both the diesel generator and the natural gas microturbine options for power generation are able to provide ample energy to the system on a daily basis lowering or eliminating the requirement for massive onboard energy storage. This phenomenon is captured in Figure 3-25 which uses the same data filters as Figure 3-24 only with non-renewable power generation options selected.

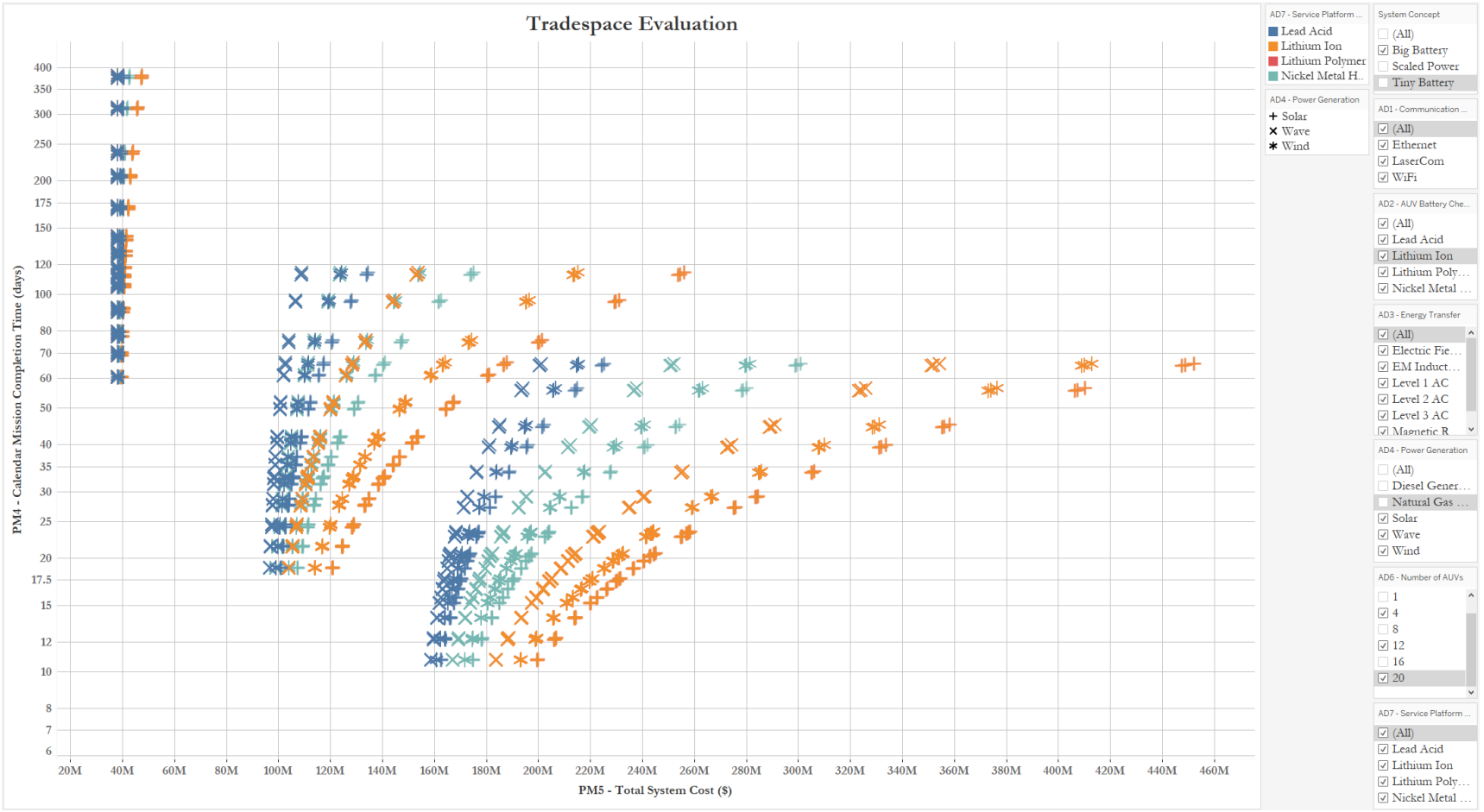

Figure 3-24: Tradespace showing the big battery concept with 4, 12, and 20 options selected for number of AUVs. The only power generation options selected are renewables.

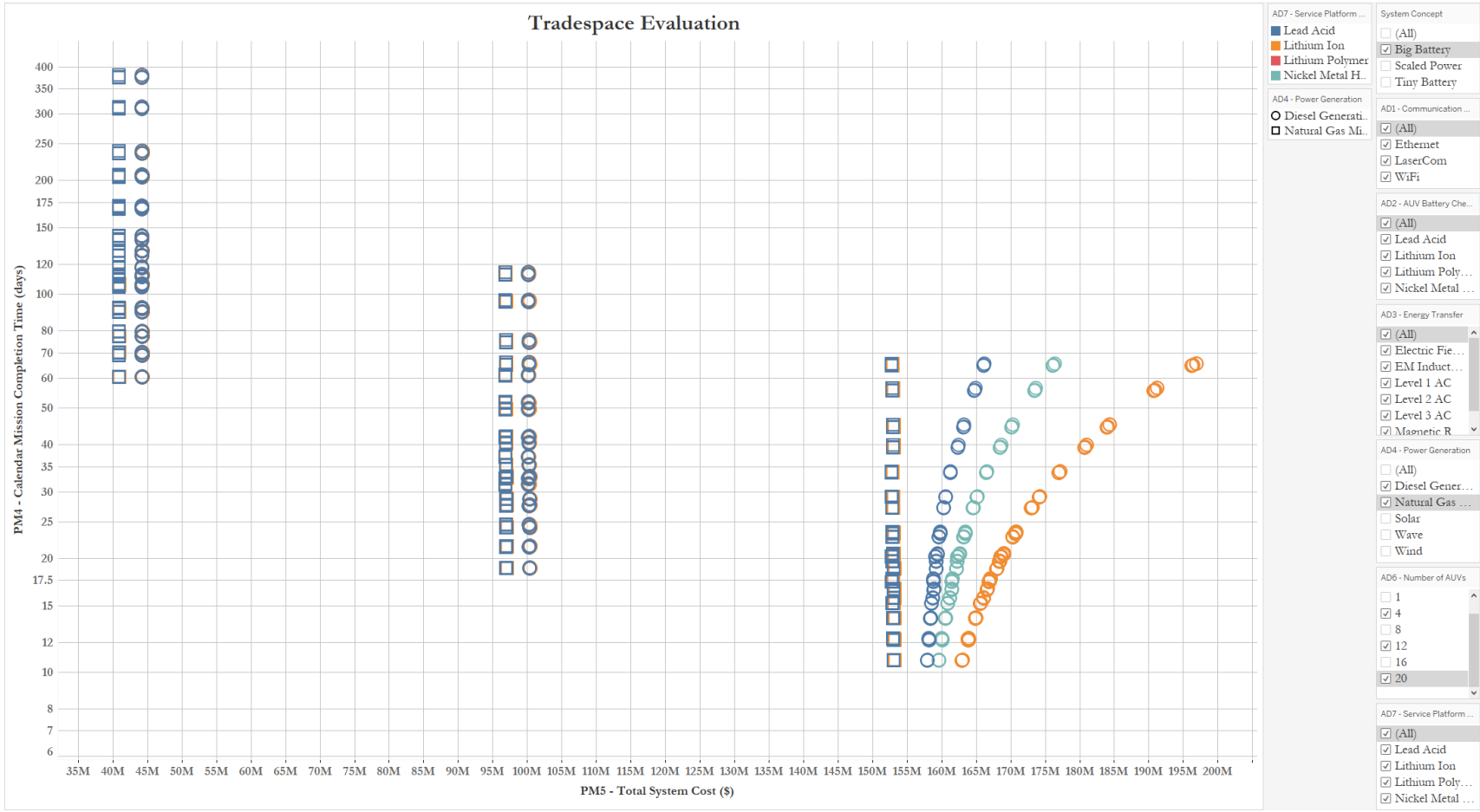

Figure 3-25: Tradespace illustrating the big battery concept with 4, 12, and 20 options selected for number of AUVs. The only power generation options selected are non-renewables.

3.5 Summary and Conclusions

The guiding questions that were posed starting this chapter were: what are the specific architectural choices that can lead to improved functional performance in an AUV's operating environment? And what functionality is improved through the use of simultaneous operation of AUVs as opposed to individual AUVs?

In order to determine the answers to these questions, seven performance metrics were established. Three of the seven performance metrics (daily operating time – PM1, search area rate – PM2, and total system cost – PM5) are derived directly from figures of merit associated with individual architectural decision options. The remaining performance metrics are algebraic transformations performed upon these three foundational performance metrics to examine the system from various normalized perspectives.

The second step to evaluating the system was to create a morphological matrix where every possible design vector was examined and evaluated based on the performance metrics set forth. This morphological matrix was generated by creating a list of unique architectural design vectors. Every permutation of every architectural decision and system concept were evaluated.

Additionally, a deterministic model was employed wherein every design vector from the morphological matrix had every performance metric calculated. A Pareto frontier was established in PM4 and PM5 space where designs from each of the options for number of AUVs was represented. Some architectural decisions were dominant in the tradespace (e.g., communication method was dominated by the ethernet option). Some architectural decisions weakly dominated others (e.g., Level 1 AC charging options outperformed Level 3 AC charging options on price, but not on total mission completion time). Depending on the operational prioritization, different architectural decisions can be made along the Pareto frontier – specifically how many AUVs should be present in the system. Finally, in all deterministic cases, wind power generation options were the most cost effective, followed by solar, then wave power generation. This was true regardless of how many AUVs were present in the system. Importantly, when compared to the tradespace, the existing Bluefin-21 architecture is dominated across multiple dimensions. There is no position in the tradespace where the existing architecture is on the Pareto frontier or outperforming the modeled architectures (Figure 3-9).

The overall system autonomy is improved as well in these architectural frameworks. As previously discussed in Chapter 2, autonomy itself is a property of a system. The measure of autonomy is rather the degree of complexity in the tasks that the system can perform without human

intervention, the number of tasks a system can perform without human intervention, or the longer a system can operate without human intervention. The degree of complexity that the AUV would perform would remain unchanged in this system. However, there are many tasks which would be added to the system by pairing an AUV (or several) with a servicing station. Furthermore, the previous method of operating the reference architecture would only produce a 24-hour mission before human interaction was required. This system is designed intentionally to operate autonomously for much longer intervals of time – on the order of years. Therefore, by two out of the three possible measures for increased levels of autonomy, this system has improved.

One final observation is that the scaled power system concept improves upon multiple performance metrics when compared with the big battery and tiny battery concepts. In many ways, the scaled power concept is the best of both worlds. While not as affordable as the tiny battery concept, the time to mission completion is identical to the big battery concept. In many situations, the constraint imposed on cost will not prohibit a system concept change from the tiny battery to the scaled power concept, as the relative difference between the costs is quite small. Thus, a general recommendation from the deterministic analysis would be to build a system which has sufficient generation capacity to fill each of the AUV batteries within a 24-hour window. Besides the improvements in performance metrics, each of the scaled power options will generate an excess of energy per day. This extra energy could be quite beneficial if some extra storage were to be added in subsequent design refinement to allow for tolerances when circumstances were not ideal for power generation.

4 AUV and Service Platform – Probabilistic Analysis

In this chapter, the deterministic model is refined through probabilistic analysis. In order to accomplish this, a subset of design vectors from the deterministic analysis are selected to represent the best performing architectures from the perspective of calendar time for mission completion and total system cost. Each architectural decision option is assigned a distribution of possible values – as opposed to single inputs in the deterministic case – and a Monte Carlo simulation is run. The results from the Monte Carlo simulation are analyzed to determine confidence intervals around specific design vectors and performance metrics. Finally, the tradespaces which were analyzed in the deterministic space are re-evaluated in the probabilistic realm.

4.1 Selecting Design Vectors for Analysis

The purpose of performing a probabilistic analysis in addition to the detailed deterministic model is twofold. First, to address issues of uncertainty that underly key assumptions in the model. The uncertainties that will be probed are the input parameters that output the metrics of concern. However, in creating a probabilistic model, there is little to be gained from modelling each individual design vector. Instead, an important first step is to consider which vectors merit consideration. If all points are modelled probabilistically, then the resulting point cloud is often too busy to draw meaningful conclusions. Instead, a limited number of design vectors are going to be selected based on specific criteria, and evaluated against one another. The outcome of this probabilistic approach is that the different vectors will be more representative of actual outcomes given uncertainties surrounding system inputs. The second purpose of performing a probabilistic analysis is to begin to quantify degrees of confidence in which different scenarios are in fact different from each other in the multi-dimensional performance metric space. Ultimately, this could lead to conclusions about specific architectures that are more likely than others to outperform.

The goal of selecting a subset of points to model is to pick points that represent important places within the tradespace. Specifically, points that represent the best case given a certain set of parameters. If cases that only exist on the Pareto frontier are modelled, then there would only be six points selected for probabilistic analysis. However, as outlined in the deterministic model, there are some decisions that are possibly too constrained and if these constraints are relaxed and a range of possible inputs are allowed, then the shape of the Pareto frontier could shift dramatically. In other words, if some of the estimates surrounding these parameters change only slightly, the tradespace in

general could be altered significantly. One specific example is well illustrated in Figure 3-12. Here, there are two distinct trends captured in the deterministic model: renewable forms of energy harvesting are more cost-effective, and non-renewable forms of energy harvesting result in shorter mission durations. These conclusions are not completely robust, however, because any individual architecture only captures a single set of input parameters. A probabilistic model allows further exploration by varying these input parameters and producing a set of outputs. Fundamentally, a probabilistic model allows conclusions to quantify the degree of difference between different architectures.

By modelling these decisions probabilistically, over-constraint is examined in a more holistic sense. The three main architectural decisions to be explored are the system concept (tiny battery, big battery, and scaled power), number of AUVs present in the system (AD6), and power generation option (AD4). These decisions are selected specifically because they have the largest impact on the two key metrics that have been discussed at length – total calendar mission completion time (PM4) and total system cost (PM5). All of the inputs which contribute to these metrics will be modelled probabilistically with different distribution parameters assigned to each input variable.

A set of design vectors are selected wherein the metrics of total calendar mission completion time (PM4) and total system cost (PM5) are minimized under specific criteria. Architectural decisions for the number of AUVs (AD6) and the power generation method (AD4) are selected individually such that each design option is optimized. In essence, the decision option set is that which minimizes PM4 with AD4 and AD6 sequentially – selecting specific options will then index to a specific platform design ID with complete architectural decisions listed. The end result is that each system concept has 30 platform IDs which are identified as minimizing either PM4 or PM5 for a total set of 60 platform IDs for each concept, and a total subset of the data which is 180 entries.

There are 13 designs which are duplicated in this examination. When an entry is duplicated, it means that a specific entry simultaneously minimizes total calendar mission completion time and total system cost. All in all, this means that the total number of design vectors to analyze from a probabilistic perspective is 167 unique points. These points are illustrated in a tradespace in Figure 4-1.

In an effort to further downselect a smaller portion of the tradespace on which a detailed probabilistic analysis can be performed, only one system concept was selected for further analysis. Starting the probabilistic modeling process with examining an architecture which is thought to be a generally dominant architecture saves computational and analytical time as well. Learnings from initial probabilistic modelling is also useful in selecting subsequent data to model in future iterations. There are significant constraints that are implicit to both the big battery and the tiny battery system concepts.

The scaled power option provides flexibility where both of these system concepts are constrained. Specifically, the tiny battery concept is constrained in cost, and flexible in daily operational time. The big battery concept is inversely constrained by daily operational time, and flexible in overall project costs. However, by allowing for flexibility in the system architecture, the scaled power option provides solutions for each design vector which only require slight project cost increases (in a deterministic sense) and achieve daily operational times that are equivalent to the big battery concept. This is illustrated clearly in Figure 4-2 where orange stars plot closer to utopia (bottom left of the graph) compared to their identical options with different system concepts. The points in red represent the tiny battery concept and are slightly less expensive than the scaled battery options, however, the time to complete a mission is significantly longer. Similarly, examining points which represent big battery options (blue stars in Figure 4-2) it is clear that the scaled power system concept is less expensive, yet makes little to no sacrifice in mission completion time. For this reason, the scaled power option was selected as the primary option to pursue for probabilistic modelling.

In so doing, the final set of points that were modeled probabilistically was limited to 60 platform IDs in the scaled power system concept. The 60 platform IDs represent 60 different scenarios which are modeled. Each scenario is subsequently examined by a Monte Carlo simulation with 1000 unique case runs. Each scenario has a consistent architecture, but the output from the probabilistic model will differ for each case, as each case will a unique set of values which are determined for input parameters.

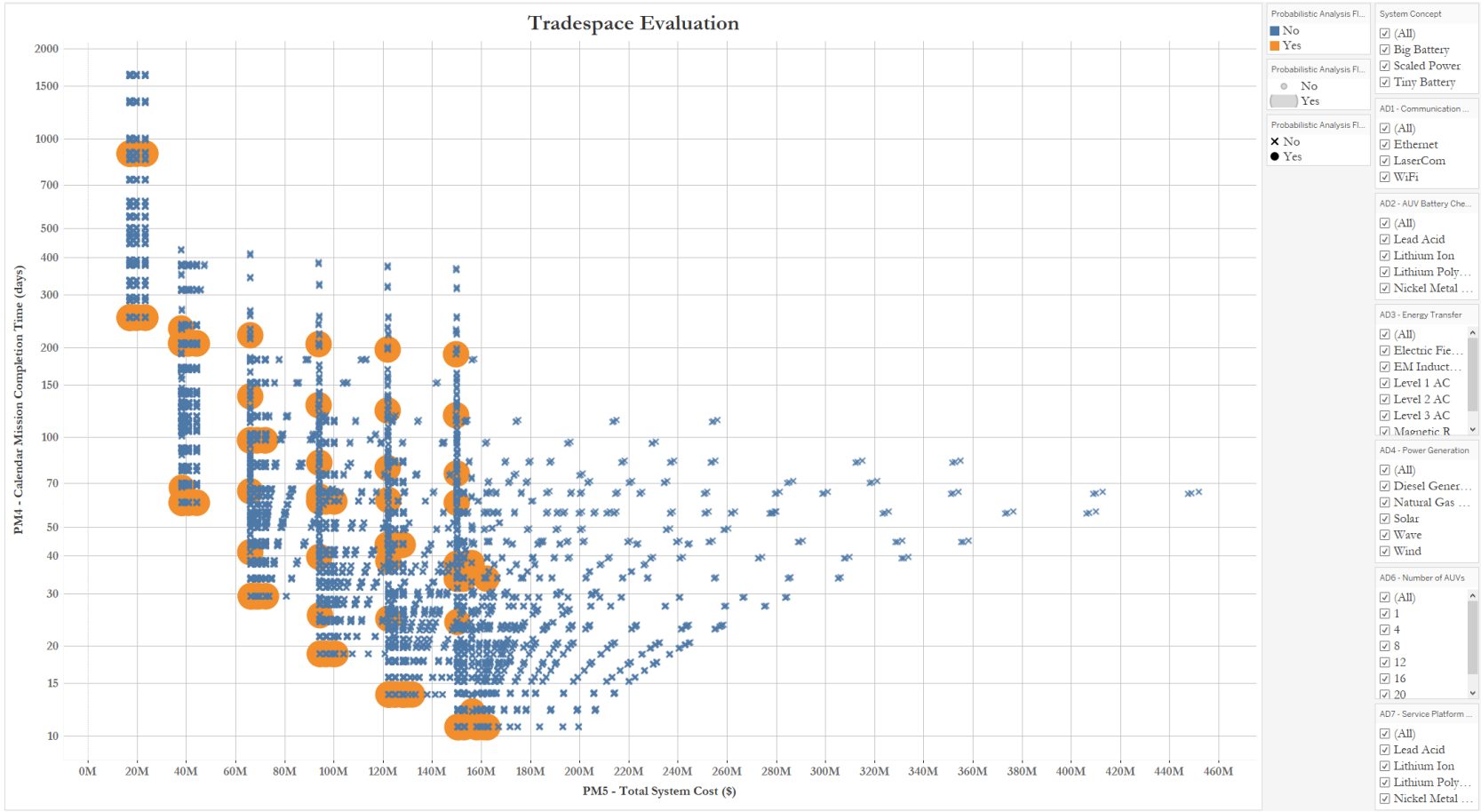

Figure 4-1: Tradespace illustrating the 167 design vectors selected for probabilistic analysis in PM4 and PM5 space. Large orange circles represent the points that will be modeled probabilistically.

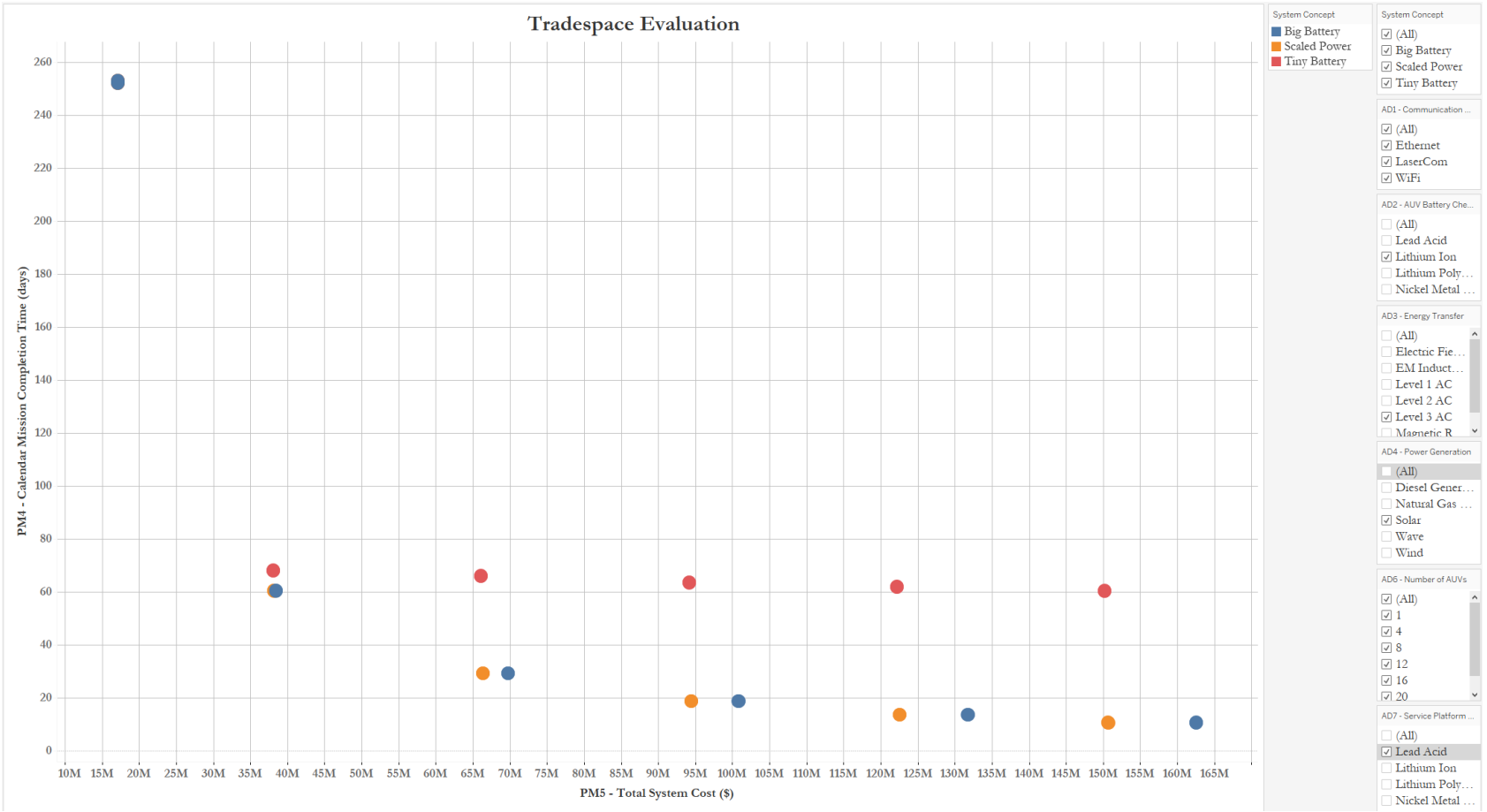

Figure 4-2: Tradespace illustrating how the scaled battery system concept outperforms the big battery and tiny battery system concepts in a deterministic perspective.

4.2 Probabilistic Model: Method and Constraints

In order to create a robust probabilistic model, each governing input from the deterministic model was given a distribution of possible values. These values are summarized in Table 4-1. Each parameter was selected randomly during a Monte Carlo simulation and all performance metrics were calculated from the unique samples. Thus, each case of the 1000 cases that create the tradespace in which a single scenario is likely unique in at least one dimension. Not all architectural decisions contribute to this outcome. AD1 (communication method) and AD5 (AUV control) are both set to constant values in this probabilistic run, and thus, they do not have probabilistic distributions associated with them. Throughout many variables, a technique called the range rule was used to estimate values for a standard deviation about a mean for a given parameter. The range rule claims that $\sigma \sim \frac{X_{max}-X_{min}}{4}$, where σ is the standard deviation, and X_{max} and X_{min} are the maximum and minimum values of the parameter, respectively. This estimate is handy when there are few data points that give an indication for the shape of the curve, but there are well established end-points for the parameter of interest. Wherever the range rule was employed in this analysis, the values for a parameter's minimum and maximum values are catalogued in the architectural decomposition of that specific parameter.

4.2.1 AD2 – Battery Chemistry

Battery chemistry has an impact in calculating search area rate (PM2) and total system cost (PM5). The input parameters that were probabilistically modeled were the power density (W/kg) and the raw cost of a 13.5kWh battery that would charge a single AUV ($). In calculating distributions for power density, the range rule was employed. For calculating ranges of costs for a 13.5kWh battery, standard deviations that were 10% of the mean value were used regardless of the specific chemistry selected. The mean values that were used in modelling were the same values that were used in the deterministic model.

4.2.2 AD3 – Power Delivery

Method of power delivery impacts daily operating time (PM1) and total system cost (PM5). The input parameters that were probabilistically modeled were the power delivery (Watts) and power delivery method cost ($). In selecting the set of design vectors that would be modeled probabilistically,

only two methods of power delivery were viable options: Level 1 AC, and Level 3 AC. Level 1 AC systems were less expensive than Level 3 AV systems, but they all provided lower daily operating time, and thus prolonged mission durations. In this respect then (in deterministic space) there was no single dominant solution for power delivery method. To compute a distribution for both the power delivery and the cost of either option for AD3, the range rule was employed. The mean values for either option was the same as was used for the deterministic case.

4.2.3 AD4 – Energy Harvesting

The method of harvesting energy has a major impact on total cost of the system (PM5). Since the tiny battery system concept was eliminated from probabilistic evaluation, there is no impact that AD4 has with respect to daily operating time (PM1). The input parameters that influence cost of the system include cost per Watt for a single system ($/W) and single system power output (W). There are five different architectural decisions which are iterated through in different scenarios. These five options include three renewable options (solar, wind, and wave power) as well as two non-renewable options (diesel generators, and natural gas microturbines). All standard deviations away from mean values are computed using the range rule. Mean values are all equal to values used in the deterministic model.

4.2.4 AD6 – Number of AUVs

The number of AUVs that are present in the system influences daily operational time (PM1), search area rate (PM2), and total system cost (PM5). The input parameters for AD6 include the time to travel to the seafloor (hours), coordination factor (unitless), AUV cost ($), and number of AUVs. A constant standard deviation of 10% of the mean is applied to the time to travel to the seafloor. For coordination factor and unit cost, the standard deviation of input parameters increases as the total number of AUVs increases. This increase scales non-linearly with the addition of more AUVs to the system. This increase captures uncertainties that surround coordination effects as well as scaling cost

savings and expenses. The actual number of AUVs is a constant with no standard deviation. All mean values for all options in AD6 are the same as values that were used in the deterministic model.

4.2.5 Monte Carlo Simulation

All 60 scenarios were modeled using the same Monte Carlo method relying on repeated random sampling to obtain statistically viable, robust numeric results. The domain of possible inputs within the problem set include all input parameters outlined in Table 4-1. During each case, a single numeric input is randomly selected from the distribution of each defined input function. These input parameters are then treated as a deterministic case with a unique set of input parameters. The subsequent trial run will randomly select a new set of input parameters. Ultimately, there are 1000 cases that are run for each scenario. These 1000 cases are sufficient to define confidence intervals throughout the solution tradespace. The code used to model this are found in Appendix A (modified from (Goolsby, 2020)).

Options	Norm_Mean	Norm_Std	Power Transfer	Notes
AD3_Op6	1500	8%	Level 1 AC	Power Delivery
AD3_Op8	30000	25%	Level 3 AC	Computed using range rule

Options	Norm_Mean	Norm_Std	Number of AUVs	Notes
AD6_Op1	-5	10%	1	Two way travel time
AD6_Op2	-5	10%	4	Constant stdev
AD6_Op3	-5.2	10%	8	
AD6_Op4	-5.2	10%	12	
AD6_Op5	-5.4	10%	16	
AD6_Op6	-5.6	10%	20	

Options	Norm_Mean	Norm_Std	Battery Chemistry	Notes
AD2_Op2	300	8%	Lithium Ion	Power Density
AD2_Op3	180	3%	Lead Acid	Computed using range rule

Options	Norm_Mean	Norm_Std	Number of AUVs	Notes
AD6_Op1	0	3%	1	Coordination factor
AD6_Op2	0.55	5%	4	Uncertainty increases with more AUVs
AD6_Op3	1.1	10%	8	
AD6_Op4	1.65	15%	12	
AD6_Op5	2.2	18%	16	
AD6_Op6	2.75	20%	20	

Options	Norm_Mean	Norm_Std	Battery Chemistry	Notes
AD2_Op2	14000	10%	Lithium Ion	Raw cost
AD2_Op3	3500	10%	Lead Acid	

Options	Norm_Mean	Norm_Std	Power Transfer	Notes
AD3_Op6	500	10%	Level 1 AC	These are 10% of the cost/AUV for power transfer option
AD3_Op8	5000	45%	Level 3 AC	Computed using range rule

Options	Norm_Mean	Norm_Std	Power Generation	Notes
AD4_Op1	51	32%	Solar	calculated using the range rule
AD4_Op2	25	40%	Wind	
AD4_Op3	46	36%	Wave	
AD4_Op4	623	38%	Diesel Generator	
AD4_Op5	58	30%	Natural Gas Microturbine	

Options	Norm_Mean	Norm_Std	Power Generation	Notes
AD4_Op1	2,000	3%	Solar	calculated using the range rule
AD4_Op2	3,000	3%	Wind	
AD4_Op3	5,000	30%	Wave	
AD4_Op4	10,000	1%	Diesel Generator	
AD4_Op5	50,000	1%	Natural Gas Microturbine	

Options	Norm_Mean	Norm_Std	Number of AUVs	Notes
AD6_Op1	5,000,000	3%	1	Constant stdev
AD6_Op2	20,000,000	5%	4	Uncertainty increases with more AUVs
AD6_Op3	40,000,000	10%	8	Same percentage increases as SAR
AD6_Op4	60,000,000	15%	12	
AD6_Op5	80,000,000	18%	16	
AD6_Op6	100,000,000	20%	20	

Options	Norm_Mean	Norm_Std	Number of AUVs	Notes
AD6_Op1	1	0%	1	Constant stdev
AD6_Op2	4	0%	4	Uncertainty increases with more AUVs
AD6_Op3	8	0%	8	Same percentage increases as SAR
AD6_Op4	12	0%	12	
AD6_Op5	16	0%	16	
AD6_Op6	20	0%	20	

Table 4-1: Table summarizing inputs for all parameters for probabilistic modeling.

4.3 Probabilistic Model Outcome and Discussion

The output of the probabilistic model – similar to the deterministic model – includes seven performance metrics. However, of the seven, only three of them are directly computed from the input parameters of the model. The remaining four metrics are simply normalizations applied to these points to compare in more practical terms. The three computed performance metrics are actual daily operational time (hours – PM1), survey area rate (km^2/hour – PM2), and total system cost ($ – PM5). Thus, the entire tradespace as calculated by the probabilistic method outlined above can be illustrated on a single tradespace with three variables displayed (Figure 4-3). In this tradespace, there are two distinct point clusters. These clusters represent the differences between using Level 1 and Level 3 AC charging. Additionally, in selecting the initial 60 scenarios to model, selection was based on minimizing cost and calendar completion time. In minimizing costs, Level 1 AC was always paired with lead-acid battery chemistries. In examining the two distinct clusters of points, charging method governs the position of points on the x-axis (PM1 is a function of AD3) and battery chemistry governs the position of points on the y-axis (PM2 is a function of AD2).

In either of the two clusters of points there is a general trend where more expensive architectures increase the survey area rate. This trend is due to increased costs associated with increased numbers of AUVs. Figure 4-4 illustrates this same tradespace with 90% confidence interval ovals for each scenario. There are only 12 visible ovals in this figure as architectures that differ only in AD4 (energy harvesting, for which there are five options), will have identical plots in PM1(daily operational time) and PM2 (search area rate) space. Thus, each oval is in reality five different ovals. By examining the overlap between these confidence intervals, a complex picture begins to emerge – there is significant overlap between each of the 90% confidence ovals for each scenario. The implication is that there is considerably less distinction between each of the scenarios than initially suggested through the deterministic evaluation.

In order to make more nuanced and specific conclusions, however, we need to further detangle the tradespace. PM1 and PM2 are directly computed from the inputs of the model, however, PM4 (total calendar days to mission completion) combines both of these metrics into a single output. From that, it is possible to better visualize the tradespace between all three dimensions. Figure 4-5 illustrates all of the 60,000 cases for the 60 scenarios in a PM5 (total system cost) vs. PM4 tradespace. Each point is colored and shaped by power harvesting option (AD4). Here, a clear trend is visible where – similar to the deterministic model – with increasing cost, there is an associated decreased calendar mission completion time. Previously, it was noted that with increased daily operating time

and survey area rate, there was an increase in cost. As survey area rate and daily operating time increase, the calendar mission completion time is going to decrease, as the 60,000km^2 search area will be covered in a shorter period of time. Once 90% confidence intervals surrounding each scenario are added to the tradespace examined in Figure 4-5, the ovals unique to each scenario are pulled apart from each other in the cost dimension (Figure 4-6). This demonstrates that the number of AUVs in the system (AD6) impacts both the overall mission time (PM4) and the total system cost (PM5).

There are additional conclusions that can be drawn from the probabilistic model at this point. First, as seen in Figure 4-6, there is no overlap between the 90% confidence intervals in cases with Level 3 AC charging and cases with Level 1 AC charging. This is consistent with findings from the deterministic modelling efforts. The probabilistic model provides robust support that architectures with Level 3 AC charging will complete the mission in fewer days than architectures with Level 1 AC charging. Second, there is no overlap between the 90% confidence intervals for scenarios with Level 3 AC charging when examining architectures across different options for different numbers of AUVs in the system. In other words, within the confidence interval ovals shown in Figure 4-6, there is a 90% chance that the mean values for cost and mission completion time will exist for architectures with any one of the six options for AD6, and with that same confidence, we can conclude that the mean values will not overlap for architectures that have different options for AD6. This does not mean that there are non-exclusive regions in which these architectures exist. Single dimensions of performance can overlap between scenarios (e.g., there is overlap in cost between the 16 and 20 AUV case for L3 charging), but there is not overlap in all dimensions simultaneously. Naturally then, a corollary of this process is that there are specific regions that are defined by each scenario, and once specific architectural decisions have been made – such as the number of AUVs – then there will be strict limitations on the system's performance envelope. This is one of the critical reasons that systems architecture should be performed prior to making architectural decisions. Within this probabilistic exercise, the most critical decisions have been identified, and (given all the mentioned assumptions) performance regions across all metrics have been established. Without changing the assumptions or adding new assumptions, there would be little reason to expect performance outside the realm of these identified regions.

There is a second set of conclusions that are borne from the probabilistic modeling. These conclusions are associated with the lack of confidence in our assertions in differentiating scenarios in the first place. Consider for a moment, the scenarios in which one AUV is modeled probabilistically. There are ten scenarios with different architectural decisions. The deterministic tradespace is shown

in Figure 4-7. It is clear in this figure that all ten scenarios are plotting in unique positions in the tradespace, although the renewable options – solar, wind, and wave options for AD4 – plot very close to one another. When this set of scenarios is modeled probabilistically, the tradespace changes significantly (Figure 4-8). When modelled probabilistically, it is clear that there is at least some degree of overlap between different architectures. The primary question, however, the probabilistic analysis allows us to answer is "with what confidence can it be claimed that the mean value of each design vector will be different that another design vector?" In other words, while it is useful to note some overlap in the cases between different architectures in Figure 4-8, additional information is gleaned where the confidence intervals do and do not overlap.

Figure 4-9 clearly shows where the confidence intervals of individual scenarios overlap. These 90% confidence interval ovals are the same ovals that are seen in the upper left of Figure 4-6. Our previous conclusion – that Level 3 and Level 1 AC charging result in statistically significant differences in performance metrics – are well illustrated. The upper set of confidence intervals never overlaps the lower set of confidence intervals. There are four sets of overlapping confidence intervals in this figure. They correspond to areas associated with specific AD4 options selected.

Figure 4-5 illustrates how the Level 1 and Level 3 AC charging impacts the tradespace in terms of PM4 and PM5. This tradespace is then re-visualized from the perspective of 90% confidence intervals (Figure 4-6). The leftmost sets of ovals which overlap correspond to all architectures with either solar, wind, or wave power options. The right most ovals represent architectures with diesel generators or natural gas turbines (Figure 4-6). The renewable power options all overlap with each other, and the non-renewable options overlap with each other. However, at no point do non-renewable power options and renewable power options overlap with each other. This means that within our 90% confidence ovals, the mean metrics for these specific scenarios is likely to occur, and that mean value will be different between renewably and non-renewably powered options (with a 90% confidence). From a system cost perspective (PM5), this quite simply means that if a one-AUV system is under consideration, then renewably powered systems will cost less than non-renewably powered systems. Moreover, there is currently no definitive method in place to differentiate between the costs associated with any of the renewable methods, which could suggest that the important architectural decision is less "which method of renewable should the system employ?" and more "should the system use renewably sourced energy?"

Figure 4-7 further illustrates that while the deterministic cases may appear to plot in unique positions within the tradespace, it is likely that these design vectors are in actuality not precisely that

different from each other. When these deterministic cases are modeled probabilistically (Figure 4-8) There is still some differentiation between the renewable and the non-renewable power options. By adding 90% confidence intervals to the visualization (Figure 4-9) it is demonstrated that while there is overlap between specific renewable options (solar, wind, and wave power generation) and non-renewable options (diesel generators and microturbines) there is no overlap between the 90% confidence intervals of the renewable and non-renewable sets of options. The implication is that it is reasonable to conclude with 90% confidence that the mean value for cost will be different between the renewable and non-renewable power options. Figure 4-10 then shows these confidence intervals overlain on top of the deterministic outputs to compare the two outputs of the two modelling techniques.

Figure 4-11 illustrates the tradespace for the deterministic model for all architectures selected for probabilistic analysis where there are 20 AUVs present in the system. Similar to the scenario with one AUV present in the system, there are clear differences between where the deterministic points plot. However, when the probabilistic model is run for this set of ten scenarios, the outcome is considerably different than that which is seen in the one AUV scenarios. Even though it represents a deterministic set of cases, Figure 4-12 is equivalent to Figure 4-8 – it shows all modeled cases for the ten scenarios covered by the filtered subset of interest. It is clear even from a cursory inspection that in the scenarios with 20 AUVs modeled probabilistically (Figure 4-8), there is considerably more overlap than what was seen in the one AUV case. Indeed, when the 90% confidence intervals are plotted on top of the cases (Figure 4-13) almost all of the confidence intervals overlap each other. Moreover, Figure 4-14 shows that all five deterministic cases are contained within each of the five 90% confidence intervals for either the Level 3 or Level 1 AC charging cases. Unlike the cases where there is one AUV in the system, this suggests that there is very little difference in the different architectures which can solely be attributed to the number of AUVs given the model's assumptions. As the number of AUVs increase from one to 20, it follows that the influence exerted on metrics by power generation method becomes less and less.

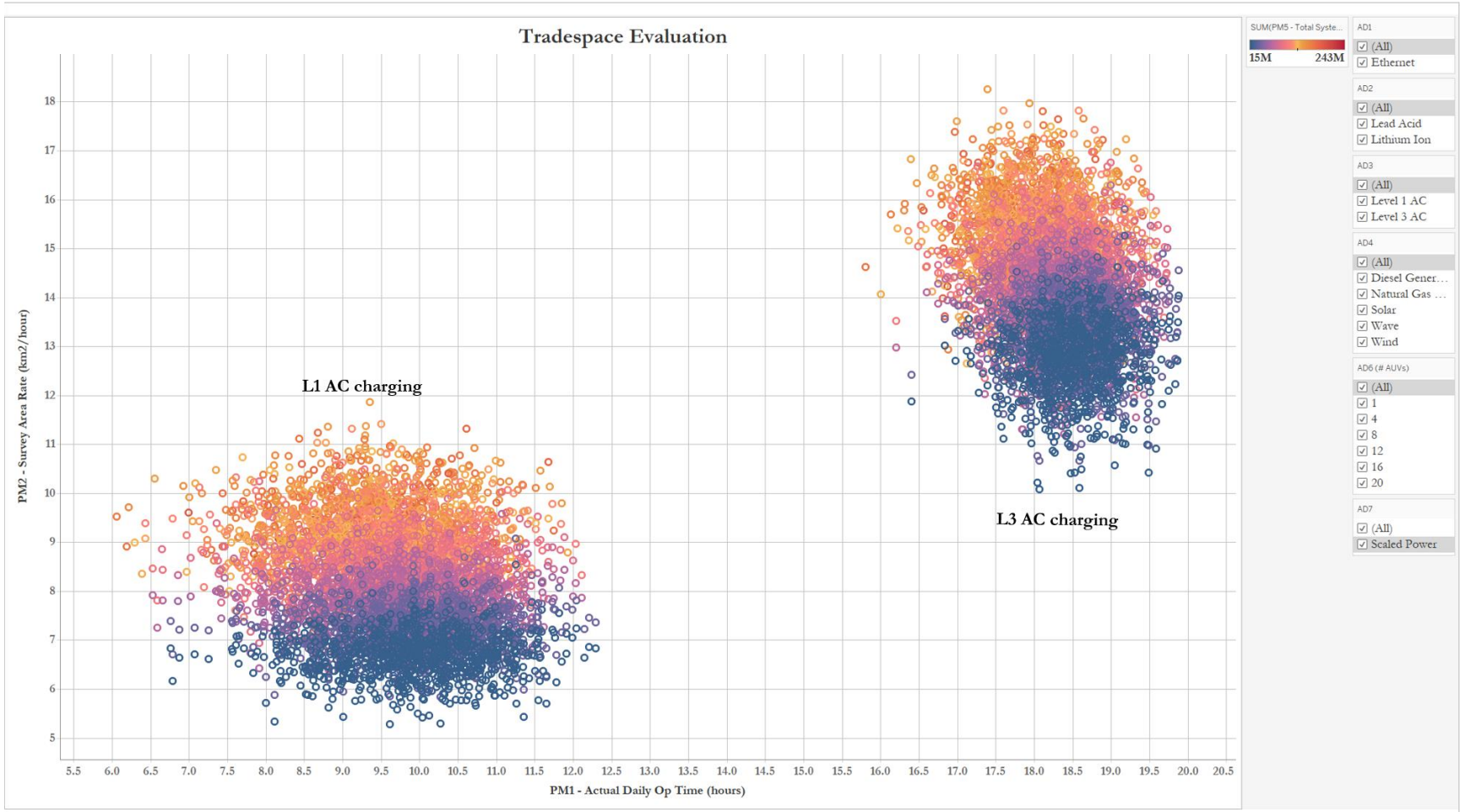

Figure 4-3: Tradespace illustrating the entire probabilistic tradespace. PM1 and PM2 are the axes of the graph, while each point is colored by the value of PM5.

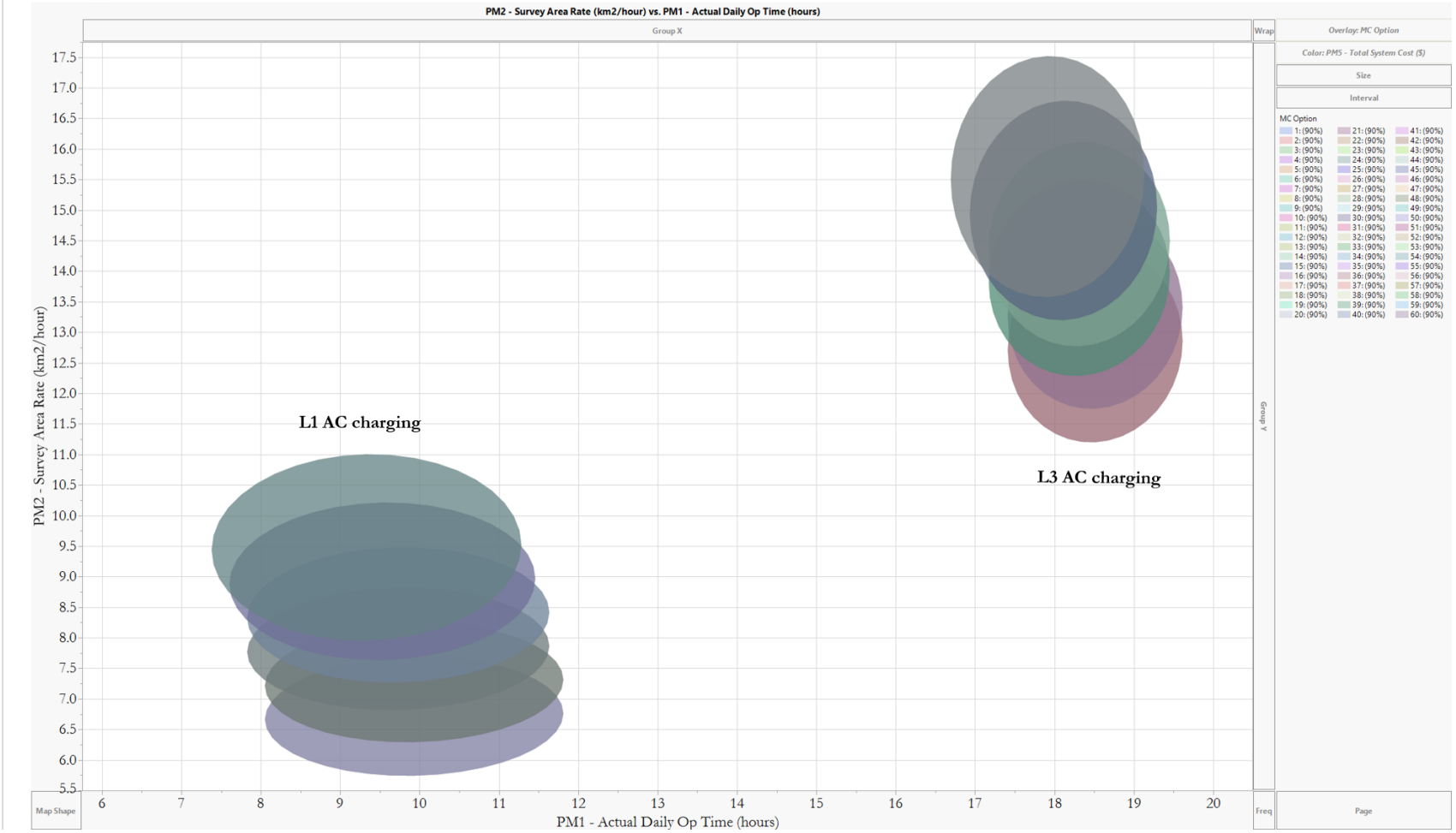

Figure 4-4: 90% confidence intervals surrounding each scenario outlined in the probabilistic model.

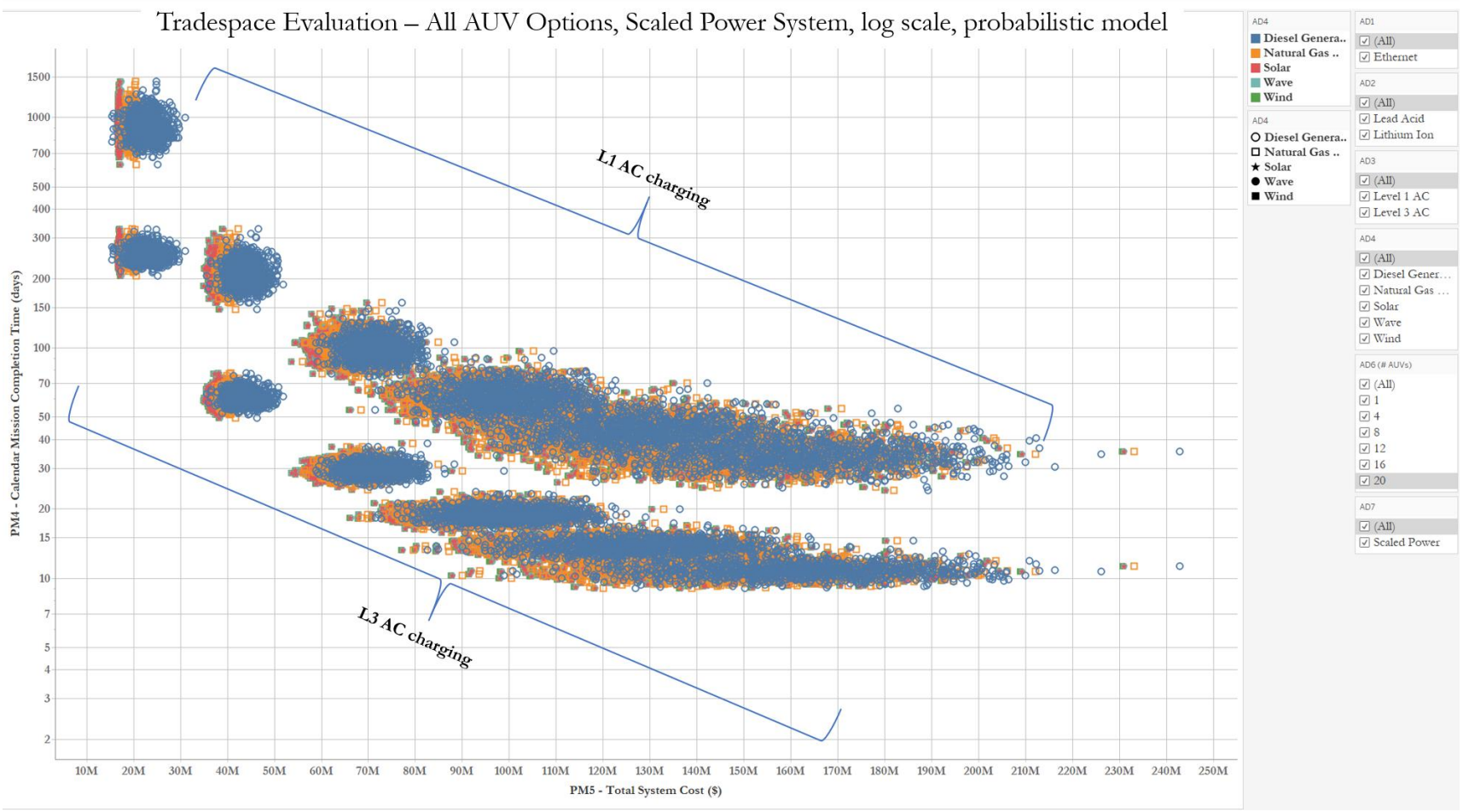

Figure 4-5: Tradespace illustrating the complete probabilistic model in PM5 and PM4 space.

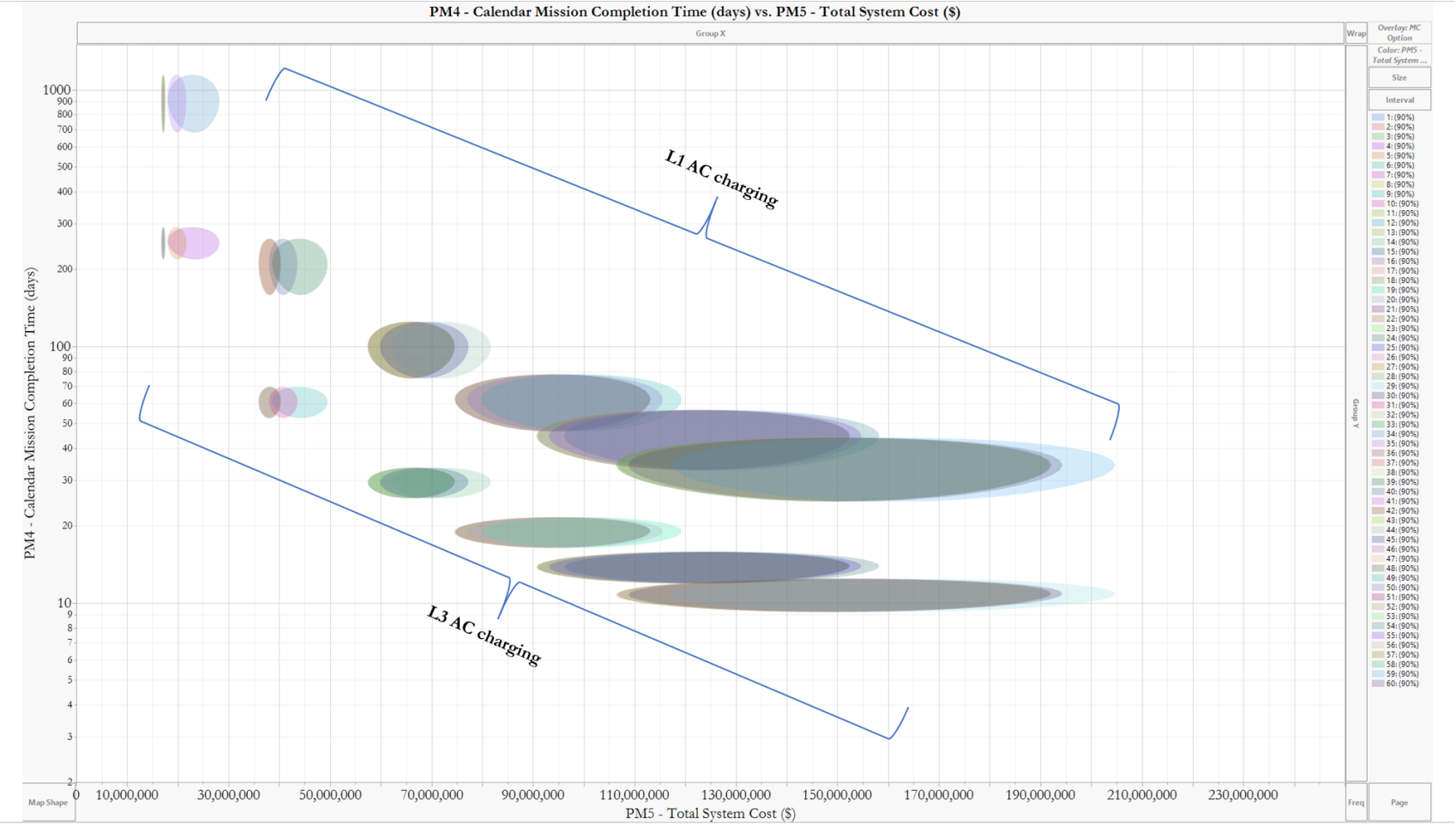

Figure 4-6: 90% confidence intervals surrounding each scenario outlined in the probabilistic model.

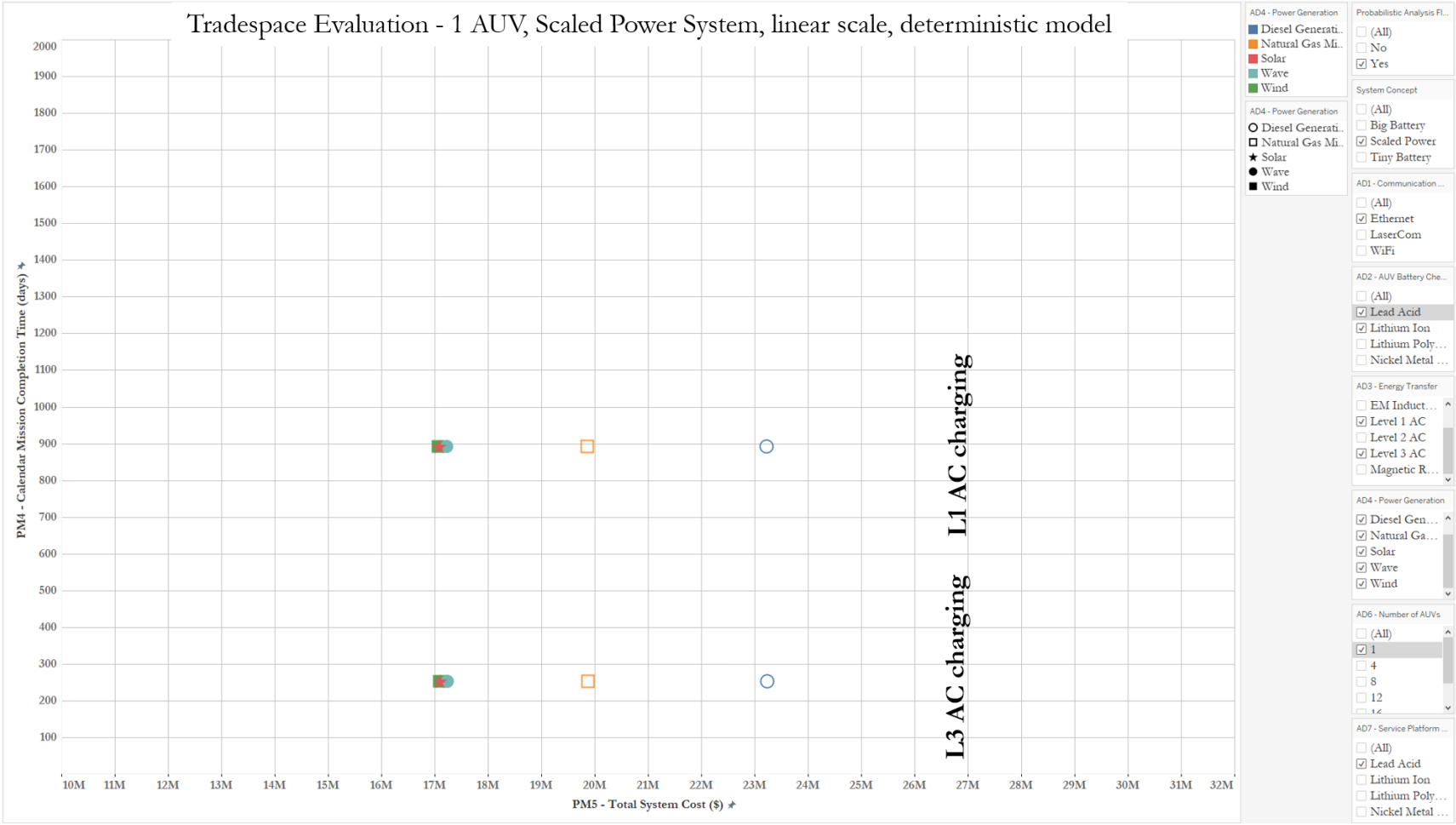

Figure 4-7: Deterministic tradespace with detail of the ten scenarios selected for probabilistic analysis for the 1 AUV case.

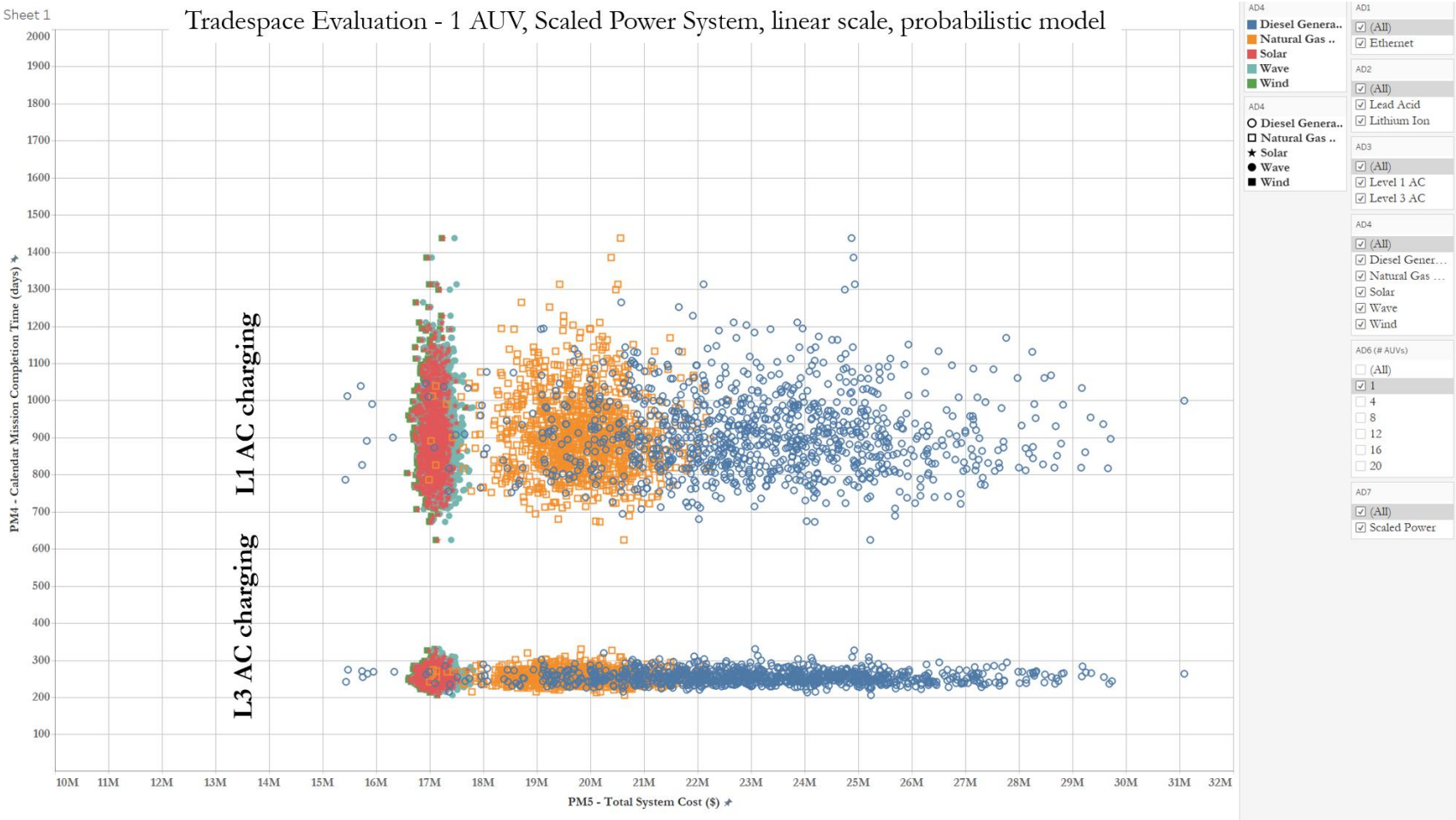

Figure 4-8: Tradespace illustrating the probabilistic model for all architectures with 1 AUV present in the system.

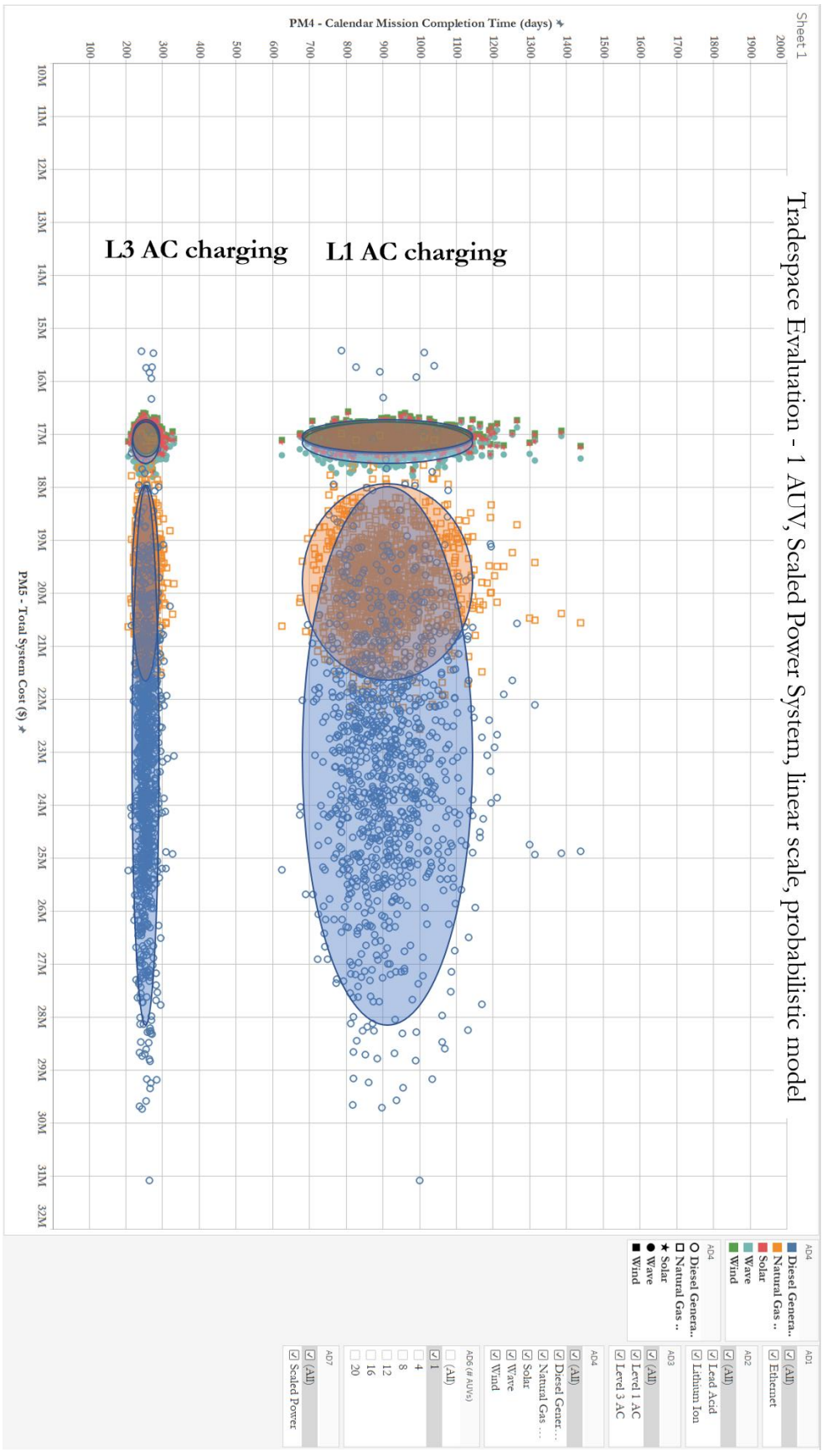

Figure 4-9: Tradespace illustrating the probabilistic model for all scenarios with 1 AUV present in the system with 90% confidence intervals outlined.

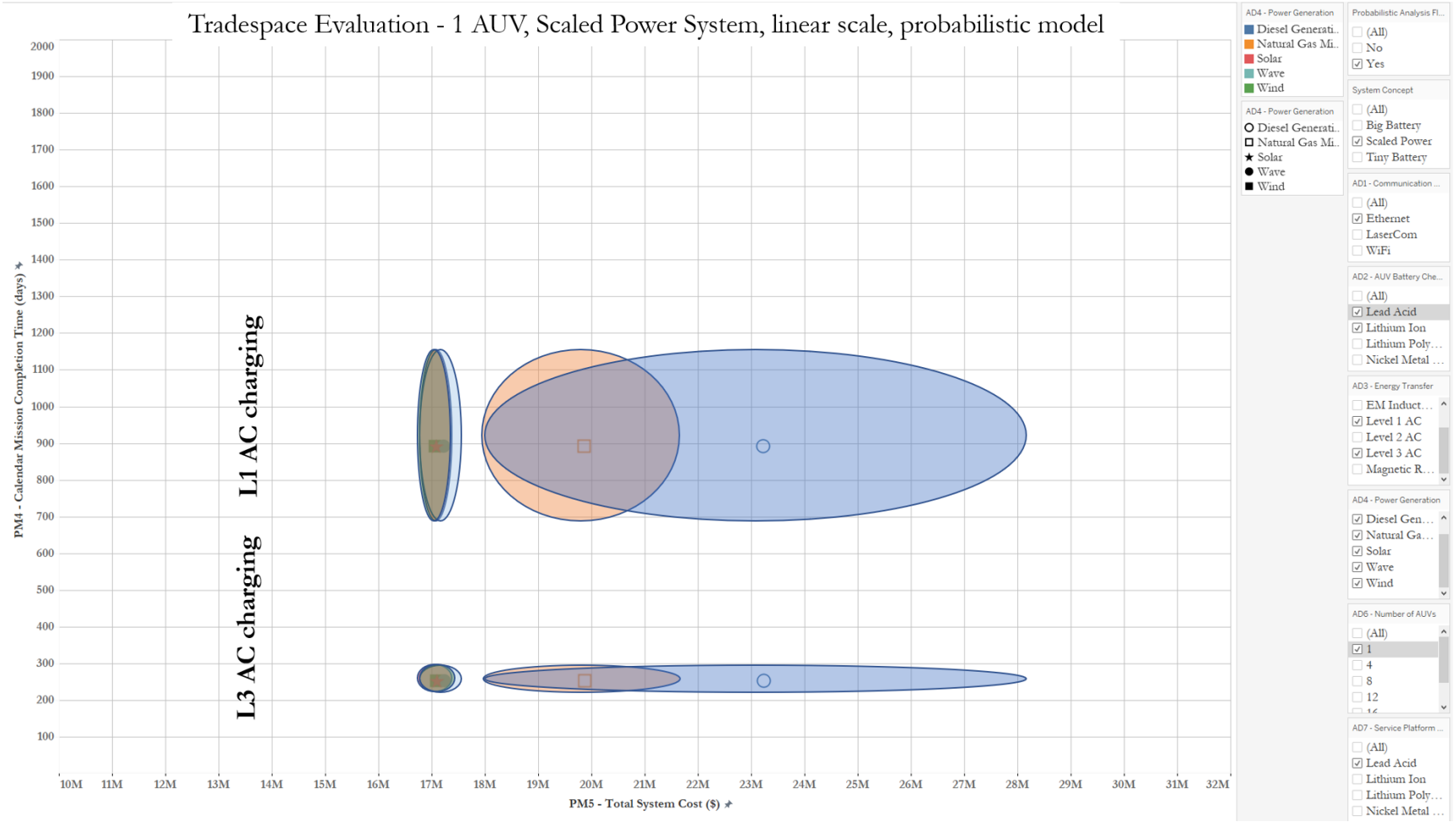

Figure 4-10: Tradespace illustrating the probabilistic and deterministic models for all scenarios with 1 AUV present in the system. 90% confidence intervals are outlined.

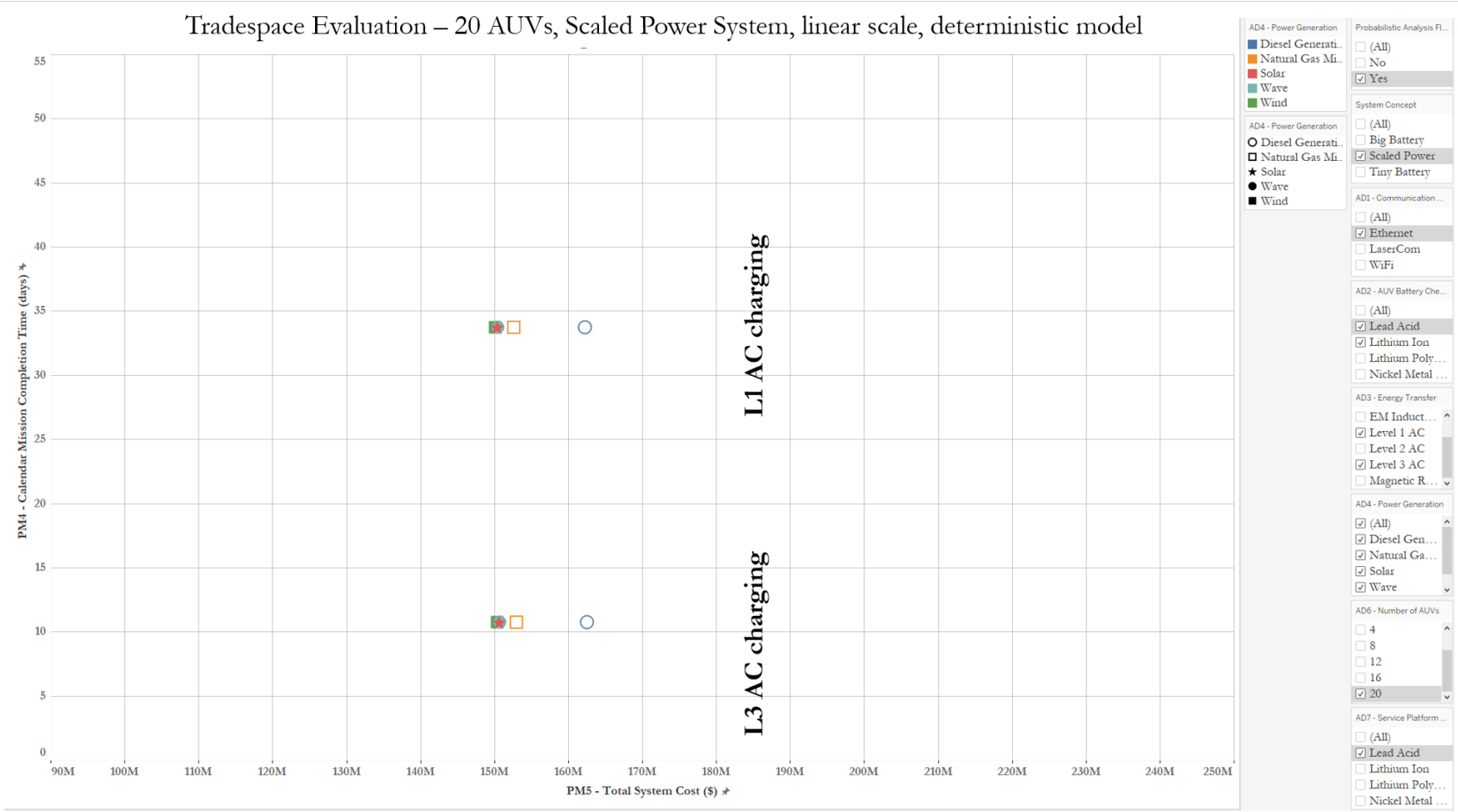

Figure 4-11: Deterministic tradespace with detail of the ten scenarios selected for probabilistic analysis for the 20 AUV case.

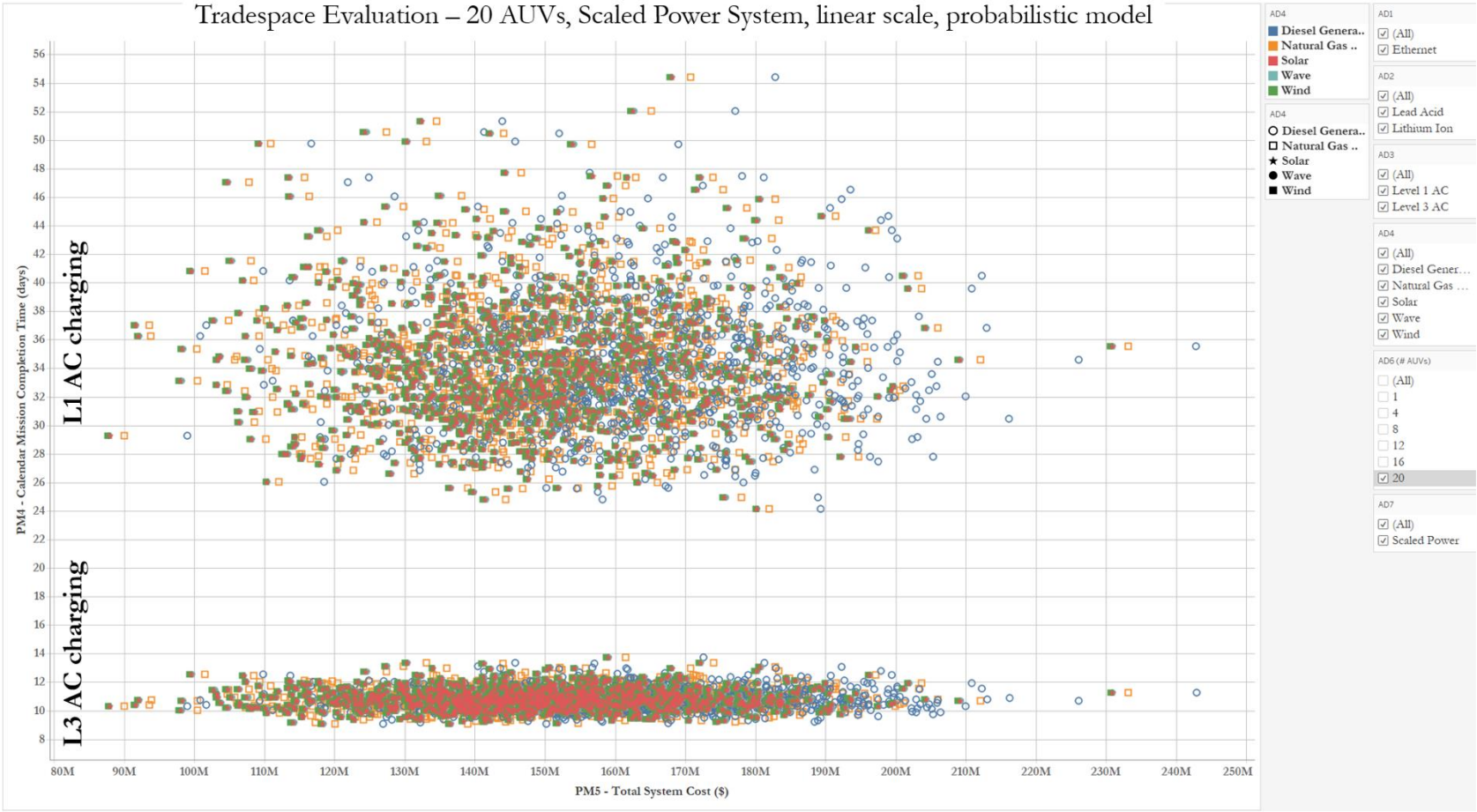

Figure 4-12: Tradespace illustrating the probabilistic model for all architectures with 20 AUVs present in the system.

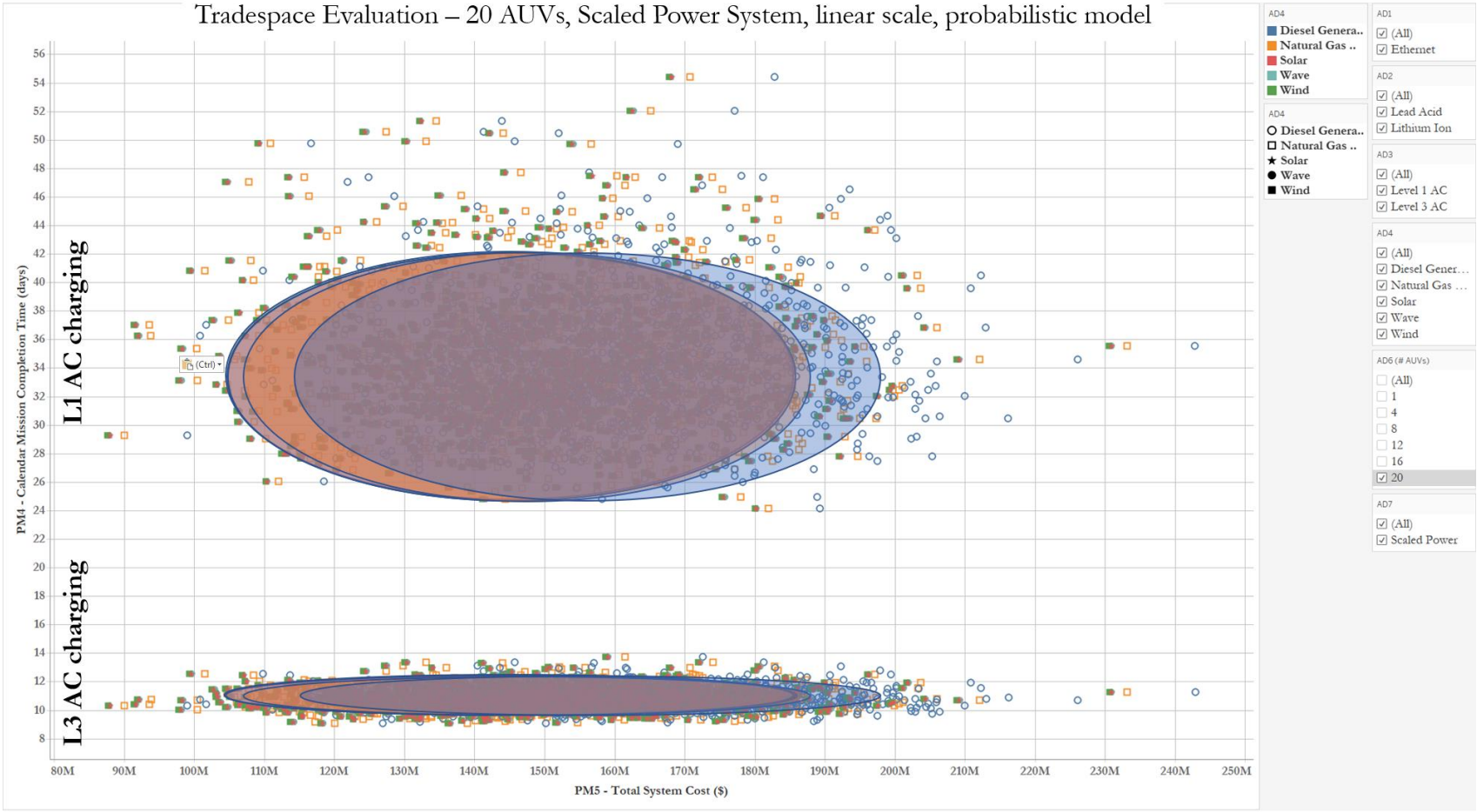

Figure 4-13: Tradespace illustrating the probabilistic model for all scenarios with 20 AUVs present in the system with 90% confidence intervals outlined.

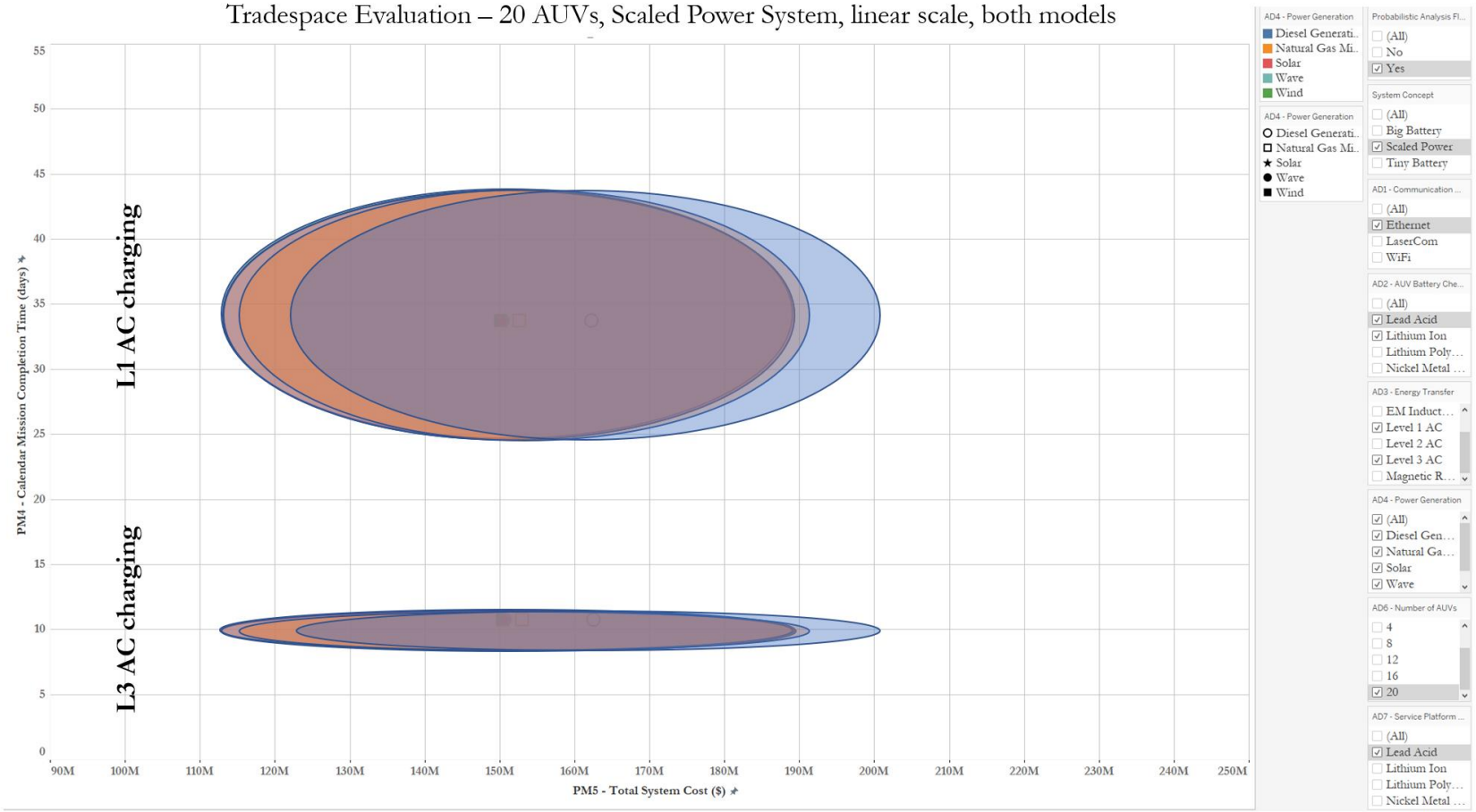

Figure 4-14: Tradespace illustrating the probabilistic and deterministic models for all scenarios with 1 AUV present in the system. 90% confidence intervals are outlined.

4.4 Summary and Conclusions

The probabilistic model was constructed to address specific uncertainties that are present, but not acknowledged in the deterministic model, and to quantify confidence that specific architectural permutations are different from each other. To that end, all input uncertainties were quantified and distributions of those inputs were used in a Monte Carlo simulation, and the outputs of these simulations were captured with 90% confidence intervals. The probabilistic analysis leads us to several key conclusions:

1) With >99% confidence, the mean values for PM4 (total calendar days to mission completion) will be greater for architectures using Level 1 AC charging when compared to Level 3 AC charging. This leads to the conclusion that all else being equal, there are substantial differences between scenarios which use Level 1 AC versus Level 3 AC charging methods. Specifically, there is significant evidence that given this model and the attributes assigned to it, that all scenarios which employ Level 3 AC charging will have improved calendar days to mission completion when compared to their equivalent scenarios which use Level 1 AC charging.
2) For all architectures with Level 3 charging, with 90% confidence, the mean values for PM4 will decrease with increased numbers of AUVs present in the system. This simply means that there is substantial merit to the claim that, given these model parameters, adding AUVs will speed up the mission.
3) For all architectures with Level 3 charging, with 90% confidence, the mean values for both PM4 and PM5 (total system cost) will be different (i.e., non-overlapping) for architectures which use different numbers of AUVs present in the system. This means that the number of AUVs in the system impacts all three primary figures of merit (PM1, PM2, and PM5) which then influences all derived figures of merit (e.g., PM4).
4) For all architectures with one AUV present in the system, with 90% confidence, architectures which employ any of the aforementioned renewable methods of charging service platform batteries will cost less than any architectures which employ either diesel or natural gas microturbines to supply energy to the system. Ultimately, this means that with appropriate caveats surrounding the model itself, renewably powered AUV systems will cost less than non-renewably powered systems when there is one AUV used in the system. There is also no differentiation yet discovered between the methods of renewables.

That is to say that confidence intervals associated with solar, wind, and wave power options all overlap each other.

5) For all architectures with four AUVs present in the system, with 50% confidence, architectures which employ any of the aforementioned renewable methods of charging service platform batteries will cost less than any architectures which employ either diesel or natural gas microturbines to supply energy to the system. The difference that was observed between renewables and non-renewables in the single AUV case is less pronounced in the four AUV case.
6) For all architectures with eight, 12, 16, or 20 AUVs present in the system, the mean values of PM4 and PM5 may be indistinguishable from one another. This means that if 8-20 AUVs are selected for the system, then the method of power generation will likely not be the primary cost driver if the scalable power system concept is utilized.

The probabilistic model has advanced the nuance of understanding in building this AUV and service platform system significantly. By beginning to introduce uncertainty into the analysis and by quantifying degrees of difference between specific architectural design vectors, several explicit design recommendations can be made. In general, there are no circumstances where renewably powered systems are outperformed by non-renewably powered systems. When examining the renewable options in specific detail, there is little differentiation between them. The conclusion to be drawn from this observation is that when evaluating power options, from a system performance standpoint – with all assumptions built in thus far – there will be little advantage to choosing one option over another. For that reason, operational advantages and engineering advantages should be given considerable thought and careful consideration.

This probabilistic model also requires the systems architect to re-consider some options which may have been eliminated early in the architecture process. Knowing now the degree of uncertainty (i.e., the sizes of the confidence intervals) it is possible that some design schemes which were previously deemed "different" in performance metric space, are in fact "very similar" if modelled probabilistically. For future iterations, this should be taken under consideration. Finally, it is worth noting that both the deterministic model and the probabilistic model are operation neutral. They can be adjusted and adapted very easily to fit new mission parameters. For instance, if one shifted to a nearshore shallow operating environment, only constants pertaining to the time to seafloor,

maintenance costs (specifically maritime operations costs), and total search area would need to be altered.

5 Findings, Discussion, and Interpretation

In this chapter, the deterministic and probabilistic models are more thoroughly evaluated and discussed. The explicit goal of this thesis is to zero in on which architectural decisions are most important to consider when designing and AUV system which pairs with a remote service platform. Such conclusions are identified within this chapter. Furthermore, specific recommendations are made for those architectural decisions. These recommendations are made based on the results of a series of Pareto rankings. These rankings examine the Pareto frontier – a set of points which are Pareto efficient – for a multidimensional surface. Design vectors are removed from the dataset as they appear in this Pareto surface, and a new surface is calculated in a second round. This process is repeated, effectively expanding the Pareto frontier with each rank. Architectures which appear more frequently throughout this ranking exercise are the best performing models, and thus the recommended architectures.

During this detailed examination, a fundamental assumption that was implicit to all models was uncovered. In the end of this chapter, the impacts of that error are examined. Beyond categorizing and quantifying the error, actions are recommended for future research which can further expand upon the model. This error revealed elements of complexity in the system that were previously unaccounted for. This complexity should be considered in future architectural modeling efforts. Finally, several methods of re-imagining the underlying assumptions are posited. While none of these reimagined methods are rigorously tested via the same models that are previously established, they lay the foundation for future work in the research pertaining to AUV and service platform pairing.

5.1 Architectural Recommendations

In an effort to reach actionable conclusions, specific recommendations regarding architectural decisions are to be provided. These recommendations are the result of the architectural decomposition in Chapter 2, the deterministic modeling in Chapter 3, and the probabilistic modeling in Chapter 4. These recommendations are all based on the parameters that were used for the models. If parameters change, then the recommendations will possibly also change. However, if the assumptions and parameters are reasonable, then the following methods and recommendations are defensible. The assumptions that are built into the deterministic model in the form of figures of merit, which are variables used to calculate performance metrics, are outlined in detail in Chapter 2. These assumptions are considered to have static values for the deterministic model discussed in Chapter 3 , and normally distributed values in the probabilistic model detailed in Chapter 4. The parameters assigned to specific

assumptions are summarized in Table 4-1. These assumptions are structured around the figures of merit associated with battery chemistry (AD2), power transfer method (AD3), power generation method (AD4), and number of AUVs (AD6). They include battery cost (AD2), energy density (AD2), power transfer method cost (AD3), power transfer rate (AD3), energy cost (AD4), energy generation capacity (AD4), AUV two-way travel time (AD6), AUV coordination factor (AD6), AUV cost (AD6), and number of AUVs (AD6).

5.1.1 Recommendations from Probabilistic Tradespace Analysis

By performing a set of deterministic analyses as was done in Chapter 3, recommendations for architectures can be generated. In fact, the recommendations that would come from that evaluation would be the architectures which define the Pareto frontier. However, if any of the parameters used in calculating performance metrics were inaccurate, then there is a possibility that the recommendation would change. Not only that, but there is an element of implied certainty that surrounds a deterministic model. Since the input parameters are single values, the implication is that those values are accurate and precise. In practice, however, these values – especially at this phase of investigation – are likely inaccurate and imprecise to some degree. This was part of the motivation to perform more thorough evaluation of system performance from a probabilistic perspective.

The probabilistic model, developed in Chapter 4, allowed some of these assumptions to be relaxed. In running a Monte Carlo simulation with 1000 cases for each of the selected scenarios from the deterministic model, a sufficiently large dataset was generated such that conclusions with a firmer basis could be reached and quantified with degrees of confidence. However, when evaluating probabilistic data clouds, it is much less straightforward to recommend specific architectures.

Consider performing the exact same process as the deterministic method employed – identify the Pareto frontier and report the architectures from those points as the system architecture recommendations. This was employed and the results are summarized in Table 5-1. This approach, however, is not ideal. By definition, the cases that are selected for the Pareto frontier are all located outside of the 90% confidence interval of all of the scenarios. The 90% confidence intervals which are discussed at length in the preceding chapters are defined as areas in which 90% of the outcomes of the simulation will fall. The implication is that one can claim with 90% confidence that the mean output of the function will land within that defined space. Since the cases which are selected for the Pareto frontier are the cases which are distant from the centroid of this confidence interval, they

represent the most extreme outputs of an individual scenario. That being said, however, the probability of these extreme cases being the mean performance case for a given scenario are exactly equal to any other case regardless of distance away from a confidence interval centroid.

The strength of the probabilistic evaluation is not that there are single cases which should be anchor points. Rather, the probabilistic model excels at showing a range of outcomes. It follows that the approach to evaluating a probabilistic model should appropriately consider a range of outcomes. Instead of focusing on the first set of cases which define the Pareto frontier, a broader perspective should be adopted.

5.1.1.1 Pareto Ranking Theory

Solving multi-objective optimizations problems (MOOPs) is an area of study which will prove to be useful in teasing recommendations from the probabilistic tradespace. While there are many methods of solving MOOPs, the "onion-peeling", or Pareto ranking, method is one which is particularly applicable to this problem (M. Davoodi Monfareed, 2011). These methods search through a feasible search area (e.g., an n-dimensional tradespace) with the objective to identify a Pareto optimal front. Following that, subsequent frontiers are established after the previous frontiers are eliminated from the feasible search options. The result is a set of points in n-space which are ranked by their occurrence in sequential Pareto frontiers. In other words, if a point is located on the first Pareto frontier, it is ranked as "1" and if a point is located on the third Pareto frontier it is ranked as "3."

This onion peeling concept was applied to systems concepts by K. Rong as they processed data associated with teamwork dynamics and problem spaces. The code developed (Rong, 2019) would ingest tradespace data and output ranked solutions (Figure 5-1, Figure 5-2). This method was limited to deterministic cases however.

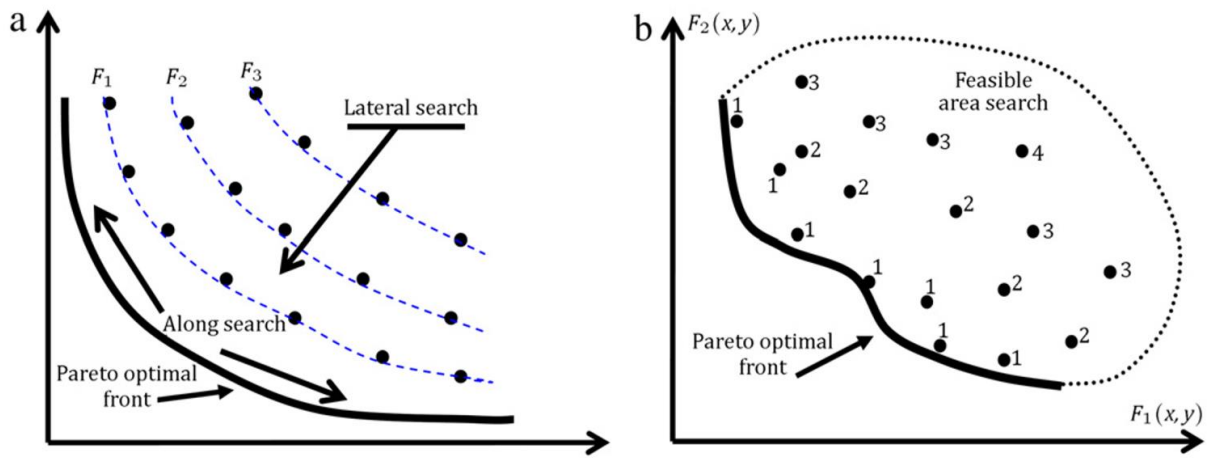

Figure 5-1: Schematic views of the goals of multi-objective evolutionary algorithms. and solutions ranked by non-dominated principles. Figure 4, (M. Davoodi Monfareed, 2011)

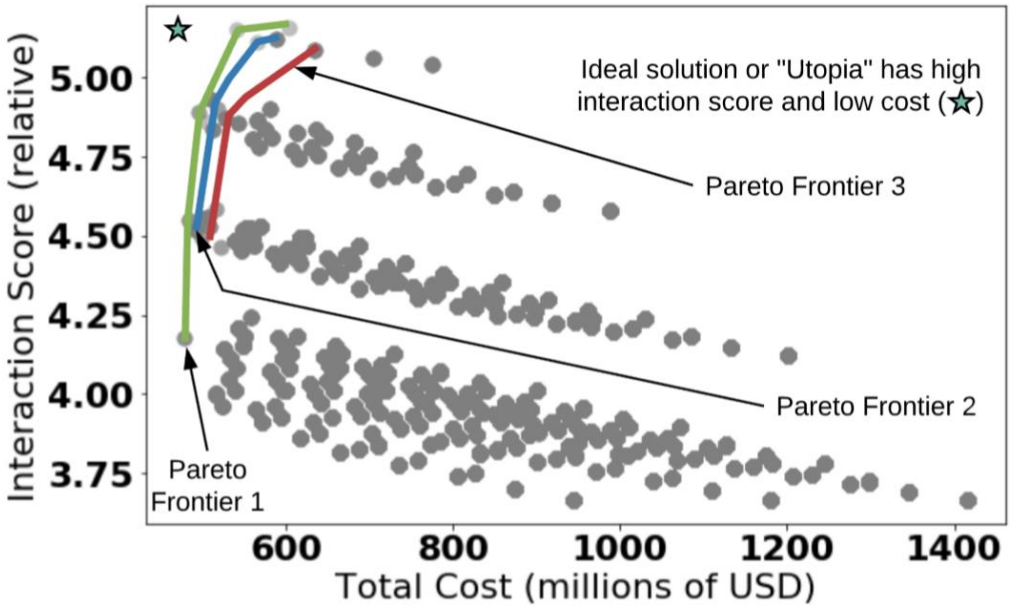

Figure 5-2: Interaction score vs cost showing ranked Pareto frontiers. Utopia is marked in the upper left. Figure 3, (Prakash Manandhar, 2020)

5.1.1.2 Pareto Ranking Execution

The Pareto ranking code (Rong, 2019) was refined (Mandahar, 2020) and generalized to ingest any n-dimensional tradespace and output ranked unique IDs (Appendix B). This code enabled onion-peel style exploration of the probabilistic tradespace in this thesis. In this study, three dimensions were examined to identify a Pareto efficient surface. These dimensions are daily operating time (PM1), search area rate (PM2), and total system cost (PM5). Every probabilistic case was evaluated in every dimension to identify if it was part of the 3-dimensional Pareto surface. Each ranking round completed this process once. After identifying all of the cases which defined the Pareto surface, a list of cases is output, and the cases are removed from the scenario list. A subsequent round then initiates. In these senses, the Pareto ranking process is identical to those outlined above, only applied to a different use case.

It is worth noting that Pareto ranking is not designed to work explicitly on probabilistic tradespaces. It is commonly used in deterministic circumstances and specific architectures are selected based on their pareto rank. With this updated script, each rank round outputs a set of unique identifiers. In this case, the unique identifiers (UIDs) are the unique identifiers associated with every case from the probabilistic tradespace analysis. These UIDs can then be re-associated with their specific scenarios. Thus, the scenarios are tied to their occurrence within specific rank rounds. Table 5-1 shows the scenario associated with each case in column two for ranking round 1 – the first Pareto frontier.

In subsequent rank rounds, the previous cases are dropped from the examined dataset, and a new multi-dimensional tradespace is created. A new Pareto frontier is established, and the second round of ranking is tied to all of the cases which define that subsequent Pareto frontier. In essence, this method is treating a multi-dimensional Pareto frontier not as a single surface, but a set of hierarchically organized surfaces. In considering recommendations, it is this implicit hierarchy that empowers the architect to draw meaningful insight. One way to consider this hierarchical organization of Pareto surfaces is to imagine that as subsequent Pareto surfaces are ranked, the single Pareto frontier thickens and – at least conceptually – the thickened Pareto frontier begins to approach identifying best architectures similarly to the probabilistic method. It relaxes constraints concerning how many cases must be non-dominated in order to define a thicker frontier.

5.1.1.3 Pareto Ranking Results

One limitation in utilizing this method of examining a probabilistic tradespace is that it is inherently computationally intensive. The first run of this script took over two hours, and each subsequent run takes longer than the previous because more points define the Pareto frontier, which means more comparisons must be performed. While optimization would help solve this issue, there are practical computational limitation which exist currently preventing this specific approach from widespread application in very large data sets (i.e., data sets which contain more than 100,000 points). Optimization solutions applied to the method is an area for future work such that these practical limitations can be mitigated.

In this evaluation, 18 consecutive ranking rounds were run over three days of data processing. This equates to the first 18 Pareto frontiers that would be defined in this dataset. It is estimated that approximately 60 Pareto frontiers would be required to fully classify the entire 60,000 case tradespace. Several specific methods of visualizing these data can aid in deriving recommendations for architectures to peruse.

The first method would be to look at which scenarios are most represented in the first Pareto frontier. This is very similar in execution to treating the probabilistic model like a deterministic model and placing importance on the edge cases. There are several pitfalls of this approach outlined above, but if those pitfalls are deemed acceptable, then the ranked list of architecture occurrence in the first round of Pareto ranking would be summarized as Table 5-2. In this summary, there are nine architectures (scenarios) which are represented in the Pareto frontier. Additionally, there are only 72 total cases which are required to define the Pareto frontier (Table 5-1). This Pareto ranking technique allows for an impartial evaluation across multidimensional spaces, and higher ranking architectures are visible.

However, there is still a case to be made that stakeholders needs and preferences could influence architecture selection. If all stakeholder preference was given to the architecture which is most represented in the first Pareto frontier, then the recommended architecture would be scenario 2: an architecture with ethernet data transfer, lithium-ion batteries, Level 3 AC charging, energy captured via wind turbine, a vectored propeller, and 20 AUVs operating in the system occurring 34 times on the Pareto frontier (Table 5-2). There is nothing from a theoretical or practical standpoint which mandates that a stakeholder make this selection however. If there are extenuating reasons for such decisions, a different architecture may be selected by stakeholders even though they are not the highest ranked architectures. What the Pareto ranking method does provide is a neutral,

computationally based analysis of probabilistic models. If a key stakeholder maintains their non-optimal solution preference, then the Pareto ranking method also provides a basis for nuanced discussions and quantitative statements about to what degree a non-optimal solution would impact the system's performance metrics.

In calculating the performance metrics, an average of all calculated performance metrics for cases which have been selected is used (i.e., ignoring metrics which have not landed in the Pareto frontier). For instance, if five cases were selected for the Pareto frontier for a given scenario, the reported performance metrics are an average of those five cases – not the 1000 cases. For subsequent ranks, the performance metrics of all previously selected cases were kept in the dataset to calculate average performance.

In this specific selected architecture (Table 5-2), the total mission completion time would be approximately 233 days, and is predicted to cost approximately $16,848,785. Detailed analysis of the statistical distribution of the performance metrics for ranked scenarios is outside the scope of this examination. To compare these performance metrics back to the human operated designs that were used in the search for MH370, the mission was completed in 285 days (using only days where the survey vessels were actively deploying the AUVs – this number could be as high as 730 days to encompass all days in which the survey vessels were operating) and cost a total of $32,812,500. To put it simply: if all assumptions and estimates are valid up to this point in the analysis, then the expectation would be for this architecture to complete the mission profile faster, and for almost half the cost. This improvement is possible because of several factors. First, the reference architecture uses a lithium-polymer battery, which can have lower energy density than lithium-ion batteries. This results in a new architecture with a higher search area rate. Second, the reference architecture used a battery hot-swap method and this new architecture uses Level 3 AC charging which minimizes time lost at the service platform waiting for batteries. Finally, by using an autonomous service platform, the overhead costs associated with the reference architecture are laid bare, as the new architecture is far more affordable.

More power can be brought to bear from the MOOP method, however. If multiple ranking runs are considered, then a far more detailed picture emerges showing how certain architectures are dominant at different points in the tradespace. When the 18 consecutive ranking runs are visualized there is more information to absorb. For instance, one can examine how the number of cases for each scenario exist on Pareto frontiers for each round (Figure 5-3). From this, it is clear that within the first 18 Pareto frontiers, there are three architectures which tend to be selected more frequently than all other architectures. These architectures are scenarios 1, 2, and 3. These architectures are identical to

each other, save the power generation method (AD4). These three scenarios represent the renewable options for generating power. To examine the cumulative impacts of selecting n-dimensional Pareto surfaces, the number of cases selected for each scenario in each rank round can be summed. The results of this are summarized in Figure 5-4. Scenarios 1, 2, and 3 are clearly selected above other scenarios through the first 18 rank rounds. However, this graph also supplies a new way to select architectures based on when they cross arbitrary thresholds. For instance, scenarios could be prioritized based on when they cross 100 cases selected for Pareto frontiers. This would represent greater than 10% of a scenario's cases selected as an optimal solution to the MOOP. This could be analogous thinking to a specific percentage selected for a confidence interval. As the cutoff percentage increases, the requirement is stricter. For instance, using the 10% cutoff, there are 16 scenarios which meet selection criteria. However, if a stricter cutoff of 20% were used, then only seven scenarios meet the selection criteria. The ranking for 18 cumulative ranking runs is summarized in Table 5-3.

A third method for selection can also be used. For this method, a scenario's rank (i.e., low ranks have the most cases present in a single ranking round) is noted for each iteration. Then that overall rank is tracked for each subsequent round. Initially, this is a somewhat chaotic evolution of cases, however, in subsequent rank rounds, scenarios begin to detangle and fall into constant overall ranks. This is visualized in Figure 5-5. Note how after ranking round 13 there is considerably less shifting in the rankings when compared to ranking round five. Architecture selection using this method focuses on the stability of a given scenario. If a given architecture is broadly distributed in the tradespace then the ranking will likely be much lower than a similar architecture with a narrower distribution.

Using any one of these three outlined methods will result in defensible architectural selections. However, in looking at all three simultaneously, there is a glaring trend that emerges for this particular examination. Regardless of which method is selected, there is a consistent high ranking for architectures which have a single AUV. Table 5-3 shows the cumulative cases for scenarios after 18 ranking rounds, and of the top ten selected scenarios, seven of them are architectures which include one AUV. When looking at when specific cutoffs (as a percentage of the total number of cases) scenarios 1, 2, and 3 greatly outperform other architectures – all of these architectures have over half of their cases selected on Pareto frontiers within the first 17 ranking rounds. Additionally, the only differentiator of these architectures is that they utilize different renewable methods of energy harvesting (AD4). As previously discussed in Chapter 4, it is not demonstrable that the different renewable methods can be distinguished from each other with regards to the performance metrics of

interest. With that in mind, the Pareto ranking method of high-grading specific architectures would suggest that an architecture with one AUV, utilizing ethernet data transfer methods, lithium-ion batteries, Level 3 AC charging, and renewable energy harvesting methods is the best architecture to pursue. Given all the modelling assumptions, such a system would be able to complete the mission in between 243 and 247 days with a cost of approximately $17 million. This is faster than the existing methods (between 285 days and 730 days), and almost half the cost ($32,812,500). The major caveat to these conclusions, however, is that they are only valid for a single, very specific use case where the area of interest is in four km of water, in a highly remote location, and has an area of 60,000km^2. For other scenarios, this advantage may not be as pronounced, or present at all.

Pareto UID	Scenario	AD1	AD2	AD3	AD4	Plant Size (kW)	AD5	AD6 (# AUVs)	System Concept	PM1 - Actual Daily Op Time (hours)	PM2 - Survey Area Rate (km2/hour)	PM5 - Total System Cost ($)
33838	2	Ethernet	Lead Acid	Level 1 AC	Diesel Generator	10	Vectored Proeller	1	Scaled Power	11.2	6.8	15,430,481
26918	2	Ethernet	Lithium Ion	Level 3 AC	Wind	3.2	Vectored Proeller	20	Scaled Power	17.3	16.7	91,402,160
26252	2	Ethernet	Lithium Ion	Level 3 AC	Wind	3.2	Vectored Proeller	20	Scaled Power	17.4	18.3	141,064,976
26605	2	Ethernet	Lithium Ion	Level 3 AC	Wind	3.2	Vectored Proeller	20	Scaled Power	17.6	17.8	120,713,230
1587	2	Ethernet	Lithium Ion	Level 3 AC	Wind	3.2	Vectored Proeller	1	Scaled Power	17.8	14.5	16,813,744
26782	2	Ethernet	Lithium Ion	Level 3 AC	Wind	3.2	Vectored Proeller	20	Scaled Power	17.8	17.1	113,242,400
1918	2	Ethernet	Lithium Ion	Level 3 AC	Wind	3.2	Vectored Proeller	1	Scaled Power	17.9	13.8	16,647,211
26761	2	Ethernet	Lithium Ion	Level 3 AC	Wind	3.2	Vectored Proeller	20	Scaled Power	17.9	18.0	141,909,402
1570	2	Ethernet	Lithium Ion	Level 3 AC	Wind	3.2	Vectored Proeller	1	Scaled Power	18.1	13.0	16,684,526
1350	4	Ethernet	Lithium Ion	Level 3 AC	Wind	3.2	Vectored Proeller	1	Scaled Power	18.2	14.3	16,916,418
1261	7	Ethernet	Lithium Ion	Level 3 AC	Wind	3.2	Vectored Proeller	1	Scaled Power	18.3	13.8	16,736,079
11761	7	Ethernet	Lithium Ion	Level 3 AC	Wind	3.2	Vectored Proeller	8	Scaled Power	18.3	15.8	64,524,543
16761	7	Ethernet	Lithium Ion	Level 3 AC	Wind	3.2	Vectored Proeller	12	Scaled Power	18.3	16.5	90,495,306
1567	7	Ethernet	Lithium Ion	Level 3 AC	Wind	3.2	Vectored Proeller	1	Scaled Power	18.3	14.1	16,815,250
1392	7	Ethernet	Lithium Ion	Level 3 AC	Wind	3.2	Vectored Proeller	1	Scaled Power	18.4	13.3	16,713,776
1782	7	Ethernet	Lithium Ion	Level 3 AC	Wind	3.2	Vectored Proeller	1	Scaled Power	18.4	13.9	16,789,502
1198	7	Ethernet	Lithium Ion	Level 3 AC	Wind	3.2	Vectored Proeller	1	Scaled Power	18.5	14.3	16,972,494
1147	7	Ethernet	Lithium Ion	Level 3 AC	Wind	3.2	Vectored Proeller	1	Scaled Power	18.5	14.0	16,897,530
1761	12	Ethernet	Lithium Ion	Level 3 AC	Wind	3.2	Vectored Proeller	1	Scaled Power	18.5	14.6	17,038,243
26523	12	Ethernet	Lithium Ion	Level 3 AC	Wind	3.2	Vectored Proeller	20	Scaled Power	18.6	17.8	118,069,459
26136	12	Ethernet	Lithium Ion	Level 3 AC	Wind	3.2	Vectored Proeller	20	Scaled Power	18.6	17.6	151,588,628
1248	12	Ethernet	Lithium Ion	Level 3 AC	Wind	3.2	Vectored Proeller	1	Scaled Power	18.7	13.0	16,599,087
1215	12	Ethernet	Lithium Ion	Level 3 AC	Wind	3.2	Vectored Proeller	1	Scaled Power	18.7	13.8	16,788,323
1781	12	Ethernet	Lithium Ion	Level 3 AC	Wind	3.2	Vectored Proeller	1	Scaled Power	18.8	14.2	16,906,907
21523	12	Ethernet	Lithium Ion	Level 3 AC	Wind	3.2	Vectored Proeller	16	Scaled Power	18.8	17.0	99,042,844
26889	17	Ethernet	Lithium Ion	Level 3 AC	Wind	3.2	Vectored Proeller	20	Scaled Power	18.8	17.4	113,729,231
21136	17	Ethernet	Lithium Ion	Level 3 AC	Wind	3.2	Vectored Proeller	16	Scaled Power	18.8	17.2	123,199,509
1174	17	Ethernet	Lithium Ion	Level 3 AC	Wind	3.2	Vectored Proeller	1	Scaled Power	18.9	14.1	16,899,332
11136	17	Ethernet	Lithium Ion	Level 3 AC	Wind	3.2	Vectored Proeller	8	Scaled Power	19.0	16.3	66,547,619
16136	17	Ethernet	Lithium Ion	Level 3 AC	Wind	3.2	Vectored Proeller	12	Scaled Power	19.0	16.8	94,917,007
1100	17	Ethernet	Lithium Ion	Level 3 AC	Wind	3.2	Vectored Proeller	1	Scaled Power	19.0	13.5	16,766,220
1988	17	Ethernet	Lithium Ion	Level 3 AC	Wind	3.2	Vectored Proeller	1	Scaled Power	19.1	13.3	16,720,014
1598	22	Ethernet	Lithium Ion	Level 3 AC	Wind	3.2	Vectored Proeller	1	Scaled Power	19.1	14.6	17,089,758
1523	22	Ethernet	Lithium Ion	Level 3 AC	Wind	3.2	Vectored Proeller	1	Scaled Power	19.1	14.0	16,827,386
16889	27	Ethernet	Lithium Ion	Level 3 AC	Wind	3.2	Vectored Proeller	12	Scaled Power	19.1	16.0	77,738,381
1631	27	Ethernet	Lithium Ion	Level 3 AC	Wind	3.2	Vectored Proeller	1	Scaled Power	19.1	13.3	16,806,023
21734	27	Ethernet	Lithium Ion	Level 3 AC	Wind	3.2	Vectored Proeller	16	Scaled Power	19.1	16.1	107,704,975
3838	27	Ethernet	Lithium Ion	Level 3 AC	Diesel Generator	10	Vectored Proeller	1	Scaled Power	19.1	12.9	15,443,315
1052	27	Ethernet	Lithium Ion	Level 3 AC	Wind	3.2	Vectored Proeller	1	Scaled Power	19.2	11.0	16,741,510
1136	27	Ethernet	Lithium Ion	Level 3 AC	Wind	3.2	Vectored Proeller	1	Scaled Power	19.2	15.3	17,133,814
6136	34	Ethernet	Lithium Ion	Level 3 AC	Wind	3.2	Vectored Proeller	4	Scaled Power	19.2	15.8	38,229,840
26072	37	Ethernet	Lithium Ion	Level 3 AC	Wind	3.2	Vectored Proeller	20	Scaled Power	19.2	17.2	136,217,227
1695	38	Ethernet	Lithium Ion	Level 3 AC	Wind	3.2	Vectored Proeller	1	Scaled Power	19.3	13.1	16,756,346
1889	39	Ethernet	Lithium Ion	Level 3 AC	Wind	3.2	Vectored Proeller	1	Scaled Power	19.3	14.0	16,819,270
6889	40	Ethernet	Lithium Ion	Level 3 AC	Wind	3.2	Vectored Proeller	4	Scaled Power	19.3	14.6	36,187,948
1579	41	Ethernet	Lithium Ion	Level 3 AC	Wind	3.2	Vectored Proeller	1	Scaled Power	19.3	13.0	16,786,151
26193	42	Ethernet	Lithium Ion	Level 3 AC	Wind	3.2	Vectored Proeller	20	Scaled Power	19.3	16.8	141,133,912
11734	43	Ethernet	Lithium Ion	Level 3 AC	Wind	3.2	Vectored Proeller	8	Scaled Power	19.3	15.1	62,123,559
16734	44	Ethernet	Lithium Ion	Level 3 AC	Wind	3.2	Vectored Proeller	12	Scaled Power	19.3	15.6	85,118,583
21072	45	Ethernet	Lithium Ion	Level 3 AC	Wind	3.2	Vectored Proeller	16	Scaled Power	19.4	16.6	112,208,429
1580	46	Ethernet	Lithium Ion	Level 3 AC	Wind	3.2	Vectored Proeller	1	Scaled Power	19.4	13.5	16,863,045
26278	47	Ethernet	Lithium Ion	Level 3 AC	Wind	3.2	Vectored Proeller	20	Scaled Power	19.4	16.3	162,166,366
26448	48	Ethernet	Lithium Ion	Level 3 AC	Wind	3.2	Vectored Proeller	20	Scaled Power	19.4	16.2	139,485,245
1097	49	Ethernet	Lithium Ion	Level 3 AC	Wind	3.2	Vectored Proeller	1	Scaled Power	19.4	13.5	16,933,711
1353	50	Ethernet	Lithium Ion	Level 3 AC	Wind	3.2	Vectored Proeller	1	Scaled Power	19.4	13.5	16,818,035
21193	51	Ethernet	Lithium Ion	Level 3 AC	Wind	3.2	Vectored Proeller	16	Scaled Power	19.5	16.2	115,642,129
1372	52	Ethernet	Lithium Ion	Level 3 AC	Wind	3.2	Vectored Proeller	1	Scaled Power	19.5	12.4	16,856,138
1734	53	Ethernet	Lithium Ion	Level 3 AC	Wind	3.2	Vectored Proeller	1	Scaled Power	19.5	14.0	16,935,580
6734	54	Ethernet	Lithium Ion	Level 3 AC	Wind	3.2	Vectored Proeller	4	Scaled Power	19.5	14.6	37,071,365
1883	55	Ethernet	Lithium Ion	Level 3 AC	Wind	3.2	Vectored Proeller	1	Scaled Power	19.5	12.8	16,865,568
1753	56	Ethernet	Lithium Ion	Level 3 AC	Wind	3.2	Vectored Proeller	1	Scaled Power	19.5	12.3	16,841,020
11072	57	Ethernet	Lithium Ion	Level 3 AC	Wind	3.2	Vectored Proeller	8	Scaled Power	19.5	15.5	63,442,207
16072	58	Ethernet	Lithium Ion	Level 3 AC	Wind	3.2	Vectored Proeller	12	Scaled Power	19.5	16.0	87,971,370
21236	59	Ethernet	Lithium Ion	Level 3 AC	Wind	3.2	Vectored Proeller	16	Scaled Power	19.6	15.8	115,530,524
16193	60	Ethernet	Lithium Ion	Level 3 AC	Wind	3.2	Vectored Proeller	12	Scaled Power	19.6	15.5	90,163,415
1072	61	Ethernet	Lithium Ion	Level 3 AC	Wind	3.2	Vectored Proeller	1	Scaled Power	19.7	14.3	16,996,019
6072	62	Ethernet	Lithium Ion	Level 3 AC	Wind	3.2	Vectored Proeller	4	Scaled Power	19.7	14.9	37,438,377
11236	63	Ethernet	Lithium Ion	Level 3 AC	Wind	3.2	Vectored Proeller	8	Scaled Power	19.7	15.0	64,280,770
16236	64	Ethernet	Lithium Ion	Level 3 AC	Wind	3.2	Vectored Proeller	12	Scaled Power	19.7	15.4	90,041,936
1894	65	Ethernet	Lithium Ion	Level 3 AC	Wind	3.2	Vectored Proeller	1	Scaled Power	19.9	13.5	16,922,862
1236	66	Ethernet	Lithium Ion	Level 3 AC	Wind	3.2	Vectored Proeller	1	Scaled Power	19.9	14.0	17,010,578
6236	67	Ethernet	Lithium Ion	Level 3 AC	Wind	3.2	Vectored Proeller	4	Scaled Power	19.9	14.6	37,586,795

Table 5-1: Table listing the probabilistic cases which generate the Pareto frontier.

Scenario	Rank	AD1	AD2	AD3	AD4	Plant Size (kW)	AD5	AD6 (# AUVs)	System Concept	PM1 - Actual Daily Op Time (hours)	PM2 - Survey Area Rate (km2/hour)	PM4 - Calendar Mission Completion Time (days)	PM5 - Total System Cost ($)
2	35	Ethernet	Lithium Ion	Level 3 AC	Wind	3.2	Vectored Proeller	1	Scaled Power	18.9	13.6	233	16,848,785
27	12	Ethernet	Lithium Ion	Level 3 AC	Wind	3.2	Vectored Proeller	20	Scaled Power	18.4	17.3	9	130,893,520
17	7	Ethernet	Lithium Ion	Level 3 AC	Wind	3.2	Vectored Proeller	12	Scaled Power	19.2	16.0	16	88,063,714
22	6	Ethernet	Lithium Ion	Level 3 AC	Wind	3.2	Vectored Proeller	16	Scaled Power	19.2	16.5	12	112,221,401
7	5	Ethernet	Lithium Ion	Level 3 AC	Wind	3.2	Vectored Proeller	4	Scaled Power	19.5	14.9	52	37,302,865
12	5	Ethernet	Lithium Ion	Level 3 AC	Wind	3.2	Vectored Proeller	8	Scaled Power	19.2	15.5	25	64,183,739
4	1	Ethernet	Lithium Ion	Level 3 AC	Diesel Generator	10	Vectored Proeller	1	Scaled Power	19.1	12.9	242	15,443,315
34	1	Ethernet	Lead Acid	Level 1 AC	Diesel Generator	10	Vectored Proeller	1	Scaled Power	11.2	6.8	786	15,430,481
1	0	Ethernet	Lithium Ion	Level 3 AC	Solar	2	Vectored Proeller	1	Scaled Power	#N/A	#N/A	#N/A	#N/A
3	0	Ethernet	Lithium Ion	Level 3 AC	Wave	5	Vectored Proeller	1	Scaled Power	#N/A	#N/A	#N/A	#N/A
5	0	Ethernet	Lithium Ion	Level 3 AC	Natural Gas Microturbine	50	Vectored Proeller	1	Scaled Power	#N/A	#N/A	#N/A	#N/A
6	0	Ethernet	Lithium Ion	Level 3 AC	Solar	2	Vectored Proeller	4	Scaled Power	#N/A	#N/A	#N/A	#N/A
8	0	Ethernet	Lithium Ion	Level 3 AC	Wave	5	Vectored Proeller	4	Scaled Power	#N/A	#N/A	#N/A	#N/A
9	0	Ethernet	Lithium Ion	Level 3 AC	Diesel Generator	10	Vectored Proeller	4	Scaled Power	#N/A	#N/A	#N/A	#N/A
10	0	Ethernet	Lithium Ion	Level 3 AC	Natural Gas Microturbine	50	Vectored Proeller	4	Scaled Power	#N/A	#N/A	#N/A	#N/A
11	0	Ethernet	Lithium Ion	Level 3 AC	Solar	2	Vectored Proeller	8	Scaled Power	#N/A	#N/A	#N/A	#N/A
13	0	Ethernet	Lithium Ion	Level 3 AC	Wave	5	Vectored Proeller	8	Scaled Power	#N/A	#N/A	#N/A	#N/A
14	0	Ethernet	Lithium Ion	Level 3 AC	Diesel Generator	10	Vectored Proeller	8	Scaled Power	#N/A	#N/A	#N/A	#N/A
15	0	Ethernet	Lithium Ion	Level 3 AC	Natural Gas Microturbine	50	Vectored Proeller	8	Scaled Power	#N/A	#N/A	#N/A	#N/A
16	0	Ethernet	Lithium Ion	Level 3 AC	Solar	2	Vectored Proeller	12	Scaled Power	#N/A	#N/A	#N/A	#N/A
18	0	Ethernet	Lithium Ion	Level 3 AC	Wave	5	Vectored Proeller	12	Scaled Power	#N/A	#N/A	#N/A	#N/A
19	0	Ethernet	Lithium Ion	Level 3 AC	Diesel Generator	10	Vectored Proeller	12	Scaled Power	#N/A	#N/A	#N/A	#N/A
20	0	Ethernet	Lithium Ion	Level 3 AC	Natural Gas Microturbine	50	Vectored Proeller	12	Scaled Power	#N/A	#N/A	#N/A	#N/A
21	0	Ethernet	Lithium Ion	Level 3 AC	Solar	2	Vectored Proeller	16	Scaled Power	#N/A	#N/A	#N/A	#N/A
23	0	Ethernet	Lithium Ion	Level 3 AC	Wave	5	Vectored Proeller	16	Scaled Power	#N/A	#N/A	#N/A	#N/A
24	0	Ethernet	Lithium Ion	Level 3 AC	Diesel Generator	10	Vectored Proeller	16	Scaled Power	#N/A	#N/A	#N/A	#N/A
25	0	Ethernet	Lithium Ion	Level 3 AC	Natural Gas Microturbine	50	Vectored Proeller	16	Scaled Power	#N/A	#N/A	#N/A	#N/A
26	0	Ethernet	Lithium Ion	Level 3 AC	Solar	2	Vectored Proeller	20	Scaled Power	#N/A	#N/A	#N/A	#N/A
28	0	Ethernet	Lithium Ion	Level 3 AC	Wave	5	Vectored Proeller	20	Scaled Power	#N/A	#N/A	#N/A	#N/A
29	0	Ethernet	Lithium Ion	Level 3 AC	Diesel Generator	10	Vectored Proeller	20	Scaled Power	#N/A	#N/A	#N/A	#N/A
30	0	Ethernet	Lithium Ion	Level 3 AC	Natural Gas Microturbine	50	Vectored Proeller	20	Scaled Power	#N/A	#N/A	#N/A	#N/A
31	0	Ethernet	Lead Acid	Level 1 AC	Solar	2	Vectored Proeller	1	Scaled Power	#N/A	#N/A	#N/A	#N/A
32	0	Ethernet	Lead Acid	Level 1 AC	Wind	3.2	Vectored Proeller	1	Scaled Power	#N/A	#N/A	#N/A	#N/A
33	0	Ethernet	Lead Acid	Level 1 AC	Wave	5	Vectored Proeller	1	Scaled Power	#N/A	#N/A	#N/A	#N/A
35	0	Ethernet	Lead Acid	Level 1 AC	Natural Gas Microturbine	50	Vectored Proeller	1	Scaled Power	#N/A	#N/A	#N/A	#N/A
36	0	Ethernet	Lead Acid	Level 1 AC	Solar	2	Vectored Proeller	4	Scaled Power	#N/A	#N/A	#N/A	#N/A
37	0	Ethernet	Lead Acid	Level 1 AC	Wind	3.2	Vectored Proeller	4	Scaled Power	#N/A	#N/A	#N/A	#N/A
38	0	Ethernet	Lead Acid	Level 1 AC	Wave	5	Vectored Proeller	4	Scaled Power	#N/A	#N/A	#N/A	#N/A
39	0	Ethernet	Lead Acid	Level 1 AC	Diesel Generator	10	Vectored Proeller	4	Scaled Power	#N/A	#N/A	#N/A	#N/A
40	0	Ethernet	Lead Acid	Level 1 AC	Natural Gas Microturbine	50	Vectored Proeller	4	Scaled Power	#N/A	#N/A	#N/A	#N/A
41	0	Ethernet	Lead Acid	Level 1 AC	Solar	2	Vectored Proeller	8	Scaled Power	#N/A	#N/A	#N/A	#N/A
42	0	Ethernet	Lead Acid	Level 1 AC	Wind	3.2	Vectored Proeller	8	Scaled Power	#N/A	#N/A	#N/A	#N/A
43	0	Ethernet	Lead Acid	Level 1 AC	Wave	5	Vectored Proeller	8	Scaled Power	#N/A	#N/A	#N/A	#N/A
44	0	Ethernet	Lead Acid	Level 1 AC	Diesel Generator	10	Vectored Proeller	8	Scaled Power	#N/A	#N/A	#N/A	#N/A
45	0	Ethernet	Lead Acid	Level 1 AC	Natural Gas Microturbine	50	Vectored Proeller	8	Scaled Power	#N/A	#N/A	#N/A	#N/A
46	0	Ethernet	Lead Acid	Level 1 AC	Solar	2	Vectored Proeller	12	Scaled Power	#N/A	#N/A	#N/A	#N/A
47	0	Ethernet	Lead Acid	Level 1 AC	Wind	3.2	Vectored Proeller	12	Scaled Power	#N/A	#N/A	#N/A	#N/A
48	0	Ethernet	Lead Acid	Level 1 AC	Wave	5	Vectored Proeller	12	Scaled Power	#N/A	#N/A	#N/A	#N/A
49	0	Ethernet	Lead Acid	Level 1 AC	Diesel Generator	10	Vectored Proeller	12	Scaled Power	#N/A	#N/A	#N/A	#N/A
50	0	Ethernet	Lead Acid	Level 1 AC	Natural Gas Microturbine	50	Vectored Proeller	12	Scaled Power	#N/A	#N/A	#N/A	#N/A
51	0	Ethernet	Lead Acid	Level 1 AC	Solar	2	Vectored Proeller	16	Scaled Power	#N/A	#N/A	#N/A	#N/A
52	0	Ethernet	Lead Acid	Level 1 AC	Wind	3.2	Vectored Proeller	16	Scaled Power	#N/A	#N/A	#N/A	#N/A
53	0	Ethernet	Lead Acid	Level 1 AC	Wave	5	Vectored Proeller	16	Scaled Power	#N/A	#N/A	#N/A	#N/A
54	0	Ethernet	Lead Acid	Level 1 AC	Diesel Generator	10	Vectored Proeller	16	Scaled Power	#N/A	#N/A	#N/A	#N/A
55	0	Ethernet	Lead Acid	Level 1 AC	Natural Gas Microturbine	50	Vectored Proeller	16	Scaled Power	#N/A	#N/A	#N/A	#N/A
56	0	Ethernet	Lead Acid	Level 1 AC	Solar	2	Vectored Proeller	20	Scaled Power	#N/A	#N/A	#N/A	#N/A
57	0	Ethernet	Lead Acid	Level 1 AC	Wind	3.2	Vectored Proeller	20	Scaled Power	#N/A	#N/A	#N/A	#N/A
58	0	Ethernet	Lead Acid	Level 1 AC	Wave	5	Vectored Proeller	20	Scaled Power	#N/A	#N/A	#N/A	#N/A
59	0	Ethernet	Lead Acid	Level 1 AC	Diesel Generator	10	Vectored Proeller	20	Scaled Power	#N/A	#N/A	#N/A	#N/A
60	0	Ethernet	Lead Acid	Level 1 AC	Natural Gas Microturbine	50	Vectored Proeller	20	Scaled Power	#N/A	#N/A	#N/A	#N/A

Table 5-2: Table summarizing the occurrence of each scenario and their architectures in the first round of ranking. Architectures are sorted by the most commonly occurring scenarios.

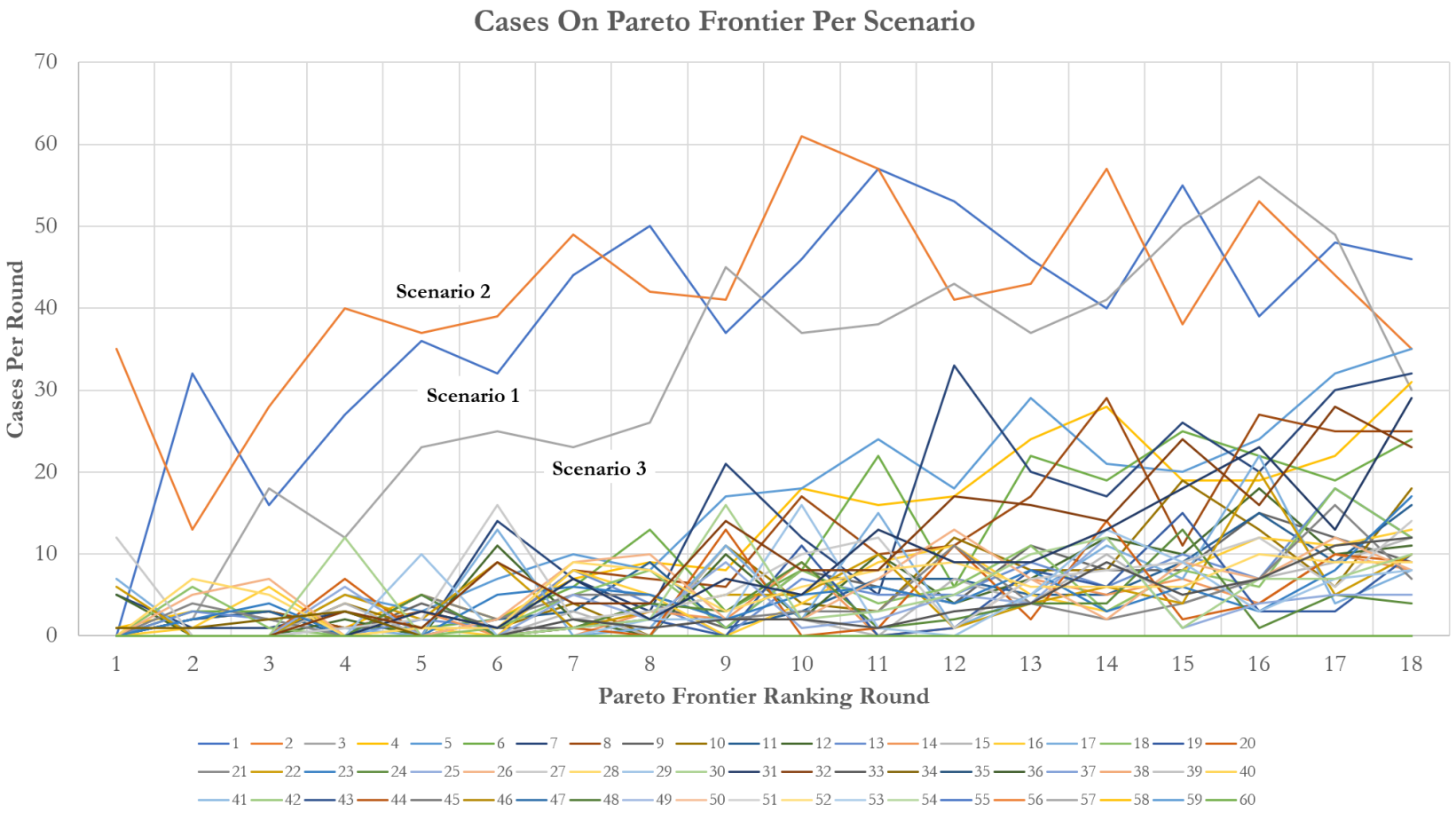

Figure 5-3: Pareto ranking summary. Each line represents a probabilistically modeled scenario, with the number of cases which appear on the Pareto frontier measured on the y-axis. During the first 18 rounds of ranking, Scenarios 2, 1, and 3 have more cases selected per round than other scenarios.

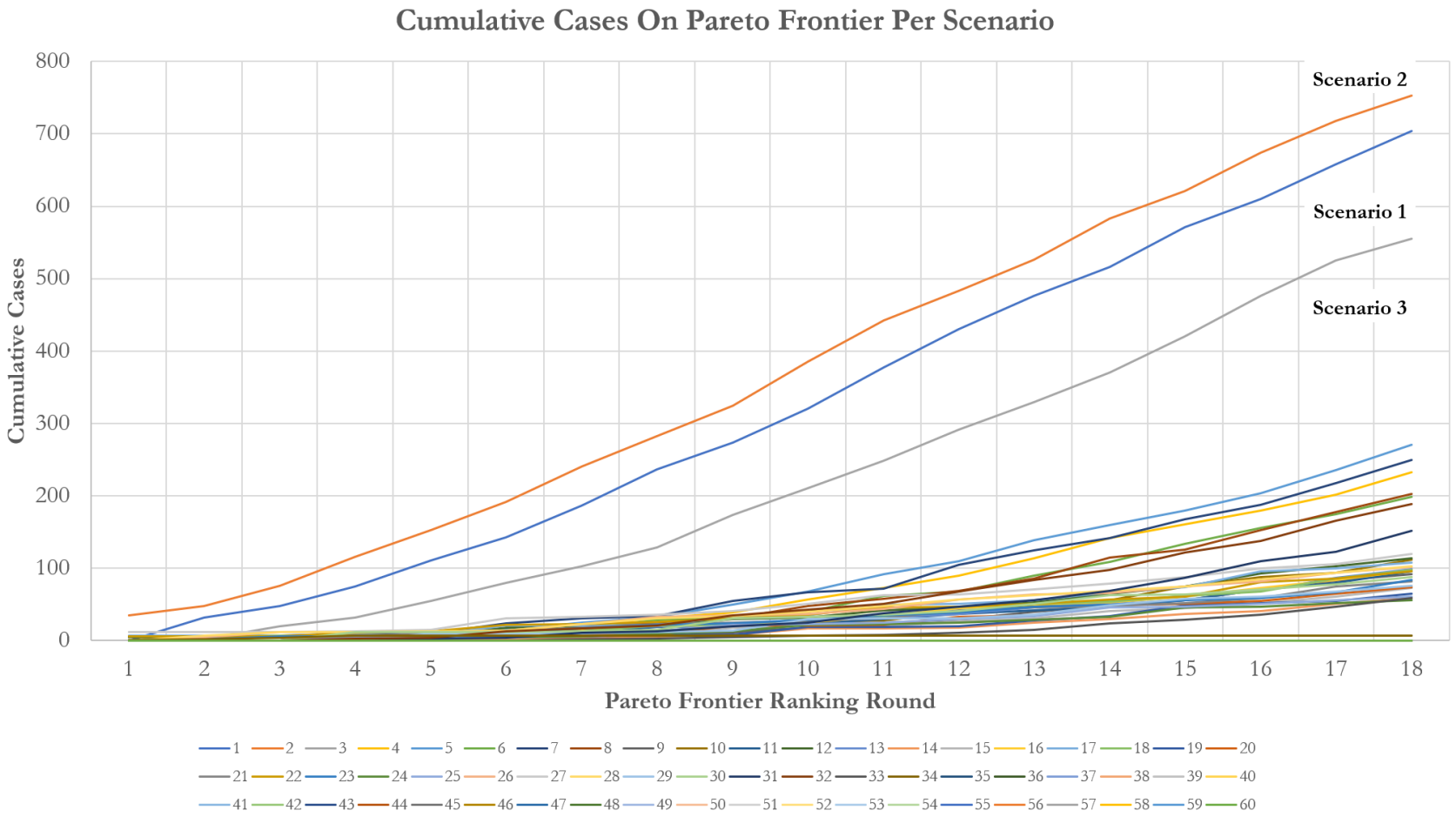

Figure 5-4: Cumulative Pareto ranking summary. Each line represents a probabilistically modeled scenario, wth the number of cumulative cases which appear on the Pareto frontier measured on the y-axis. Cases for Scenarios 2, 1, and 3 are cumulatively selected at a higher rate than other scenarios.

Scenario	Cumulative Cases Present in 18 Rank Rounds	AD1	AD2	AD3	AD4	Plant Size (kW)	AD5	AD6 (# AUVs)	System Concept	PM1 - Actual Daily Op Time (hours)	PM2 - Survey Area Rate (km2/hour)	PM4 - Calendar Mission Completion Time (days)	PM5 - Total System Cost ($)
2	753	Ethernet	Lithium Ion	Level 3 AC	Wind	3.2	Vectored Proeller	1	Scaled Power	18.7	13.0	247	16,987,775
1	704	Ethernet	Lithium Ion	Level 3 AC	Solar	2	Vectored Proeller	1	Scaled Power	18.7	13.0	246	17,009,813
3	555	Ethernet	Lithium Ion	Level 3 AC	Wave	5	Vectored Proeller	1	Scaled Power	18.9	13.2	243	17,112,971
5	271	Ethernet	Lithium Ion	Level 3 AC	Natural Gas Microturbine	50	Vectored Proeller	1	Scaled Power	19.1	13.5	234	19,677,261
7	250	Ethernet	Lithium Ion	Level 3 AC	Wind	3.2	Vectored Proeller	4	Scaled Power	19.0	14.2	56	37,561,844
4	233	Ethernet	Lithium Ion	Level 3 AC	Diesel Generator	10	Vectored Proeller	1	Scaled Power	19.0	13.6	233	22,212,915
8	203	Ethernet	Lithium Ion	Level 3 AC	Wave	5	Vectored Proeller	4	Scaled Power	19.0	14.3	55	37,705,108
6	199	Ethernet	Lithium Ion	Level 3 AC	Solar	2	Vectored Proeller	4	Scaled Power	19.1	14.2	55	37,732,982
32	189	Ethernet	Lead Acid	Level 1 AC	Wind	3.2	Vectored Proeller	1	Scaled Power	10.1	6.8	887	16,775,395
31	152	Ethernet	Lead Acid	Level 1 AC	Solar	2	Vectored Proeller	1	Scaled Power	9.9	6.9	895	16,776,216
27	120	Ethernet	Lithium Ion	Level 3 AC	Wind	3.2	Vectored Proeller	20	Scaled Power	18.4	16.9	10	135,262,588
12	114	Ethernet	Lithium Ion	Level 3 AC	Wind	3.2	Vectored Proeller	8	Scaled Power	19.0	15.0	26	64,273,601
10	112	Ethernet	Lithium Ion	Level 3 AC	Natural Gas Microturbine	50	Vectored Proeller	4	Scaled Power	19.2	14.4	54	40,392,277
17	108	Ethernet	Lithium Ion	Level 3 AC	Wind	3.2	Vectored Proeller	12	Scaled Power	18.9	15.5	17	88,708,915
28	103	Ethernet	Lithium Ion	Level 3 AC	Wave	5	Vectored Proeller	20	Scaled Power	18.4	17.0	10	137,557,408
26	102	Ethernet	Lithium Ion	Level 3 AC	Solar	2	Vectored Proeller	20	Scaled Power	18.4	17.0	10	137,999,833
13	99	Ethernet	Lithium Ion	Level 3 AC	Wave	5	Vectored Proeller	8	Scaled Power	19.0	15.0	26	64,521,990
18	98	Ethernet	Lithium Ion	Level 3 AC	Wave	5	Vectored Proeller	12	Scaled Power	19.0	15.5	17	89,430,360
16	97	Ethernet	Lithium Ion	Level 3 AC	Solar	2	Vectored Proeller	12	Scaled Power	19.0	15.5	17	89,561,645
11	96	Ethernet	Lithium Ion	Level 3 AC	Solar	2	Vectored Proeller	8	Scaled Power	18.9	15.1	26	64,772,591
22	96	Ethernet	Lithium Ion	Level 3 AC	Wind	3.2	Vectored Proeller	16	Scaled Power	18.7	16.3	12	114,552,004
9	92	Ethernet	Lithium Ion	Level 3 AC	Diesel Generator	10	Vectored Proeller	4	Scaled Power	19.2	14.4	54	43,171,285
30	88	Ethernet	Lithium Ion	Level 3 AC	Natural Gas Microturbine	50	Vectored Proeller	20	Scaled Power	18.5	17.0	10	138,924,214
23	84	Ethernet	Lithium Ion	Level 3 AC	Wave	5	Vectored Proeller	16	Scaled Power	18.7	16.3	12	114,034,445
21	82	Ethernet	Lithium Ion	Level 3 AC	Solar	2	Vectored Proeller	16	Scaled Power	18.7	16.3	12	114,323,209
29	76	Ethernet	Lithium Ion	Level 3 AC	Diesel Generator	10	Vectored Proeller	20	Scaled Power	18.6	17.0	9	151,061,771
20	74	Ethernet	Lithium Ion	Level 3 AC	Natural Gas Microturbine	50	Vectored Proeller	12	Scaled Power	19.0	15.6	17	92,146,663
15	73	Ethernet	Lithium Ion	Level 3 AC	Natural Gas Microturbine	50	Vectored Proeller	8	Scaled Power	19.0	15.1	26	67,351,728
19	65	Ethernet	Lithium Ion	Level 3 AC	Diesel Generator	10	Vectored Proeller	12	Scaled Power	19.2	15.6	17	96,304,590
25	61	Ethernet	Lithium Ion	Level 3 AC	Natural Gas Microturbine	50	Vectored Proeller	16	Scaled Power	18.8	16.3	12	115,561,166
14	59	Ethernet	Lithium Ion	Level 3 AC	Diesel Generator	10	Vectored Proeller	8	Scaled Power	19.1	15.1	26	70,426,641
33	59	Ethernet	Lead Acid	Level 1 AC	Wave	5	Vectored Proeller	1	Scaled Power	9.6	6.9	920	16,778,823
24	56	Ethernet	Lithium Ion	Level 3 AC	Diesel Generator	10	Vectored Proeller	16	Scaled Power	18.8	16.3	12	118,168,229
34	7	Ethernet	Lead Acid	Level 1 AC	Diesel Generator	10	Vectored Proeller	1	Scaled Power	10.3	6.4	920	15,771,500
35	0	Ethernet	Lead Acid	Level 1 AC	Natural Gas Microturbine	50	Vectored Proeller	1	Scaled Power	#N/A	#N/A	#N/A	#N/A
36	0	Ethernet	Lead Acid	Level 1 AC	Solar	2	Vectored Proeller	4	Scaled Power	#N/A	#N/A	#N/A	#N/A
37	0	Ethernet	Lead Acid	Level 1 AC	Wind	3.2	Vectored Proeller	4	Scaled Power	#N/A	#N/A	#N/A	#N/A
38	0	Ethernet	Lead Acid	Level 1 AC	Wave	5	Vectored Proeller	4	Scaled Power	#N/A	#N/A	#N/A	#N/A
39	0	Ethernet	Lead Acid	Level 1 AC	Diesel Generator	10	Vectored Proeller	4	Scaled Power	#N/A	#N/A	#N/A	#N/A
40	0	Ethernet	Lead Acid	Level 1 AC	Natural Gas Microturbine	50	Vectored Proeller	4	Scaled Power	#N/A	#N/A	#N/A	#N/A
41	0	Ethernet	Lead Acid	Level 1 AC	Solar	2	Vectored Proeller	8	Scaled Power	#N/A	#N/A	#N/A	#N/A
42	0	Ethernet	Lead Acid	Level 1 AC	Wind	3.2	Vectored Proeller	8	Scaled Power	#N/A	#N/A	#N/A	#N/A
43	0	Ethernet	Lead Acid	Level 1 AC	Wave	5	Vectored Proeller	8	Scaled Power	#N/A	#N/A	#N/A	#N/A
44	0	Ethernet	Lead Acid	Level 1 AC	Diesel Generator	10	Vectored Proeller	8	Scaled Power	#N/A	#N/A	#N/A	#N/A
45	0	Ethernet	Lead Acid	Level 1 AC	Natural Gas Microturbine	50	Vectored Proeller	8	Scaled Power	#N/A	#N/A	#N/A	#N/A
46	0	Ethernet	Lead Acid	Level 1 AC	Solar	2	Vectored Proeller	12	Scaled Power	#N/A	#N/A	#N/A	#N/A
47	0	Ethernet	Lead Acid	Level 1 AC	Wind	3.2	Vectored Proeller	12	Scaled Power	#N/A	#N/A	#N/A	#N/A
48	0	Ethernet	Lead Acid	Level 1 AC	Wave	5	Vectored Proeller	12	Scaled Power	#N/A	#N/A	#N/A	#N/A
49	0	Ethernet	Lead Acid	Level 1 AC	Diesel Generator	10	Vectored Proeller	12	Scaled Power	#N/A	#N/A	#N/A	#N/A
50	0	Ethernet	Lead Acid	Level 1 AC	Natural Gas Microturbine	50	Vectored Proeller	12	Scaled Power	#N/A	#N/A	#N/A	#N/A
51	0	Ethernet	Lead Acid	Level 1 AC	Solar	2	Vectored Proeller	16	Scaled Power	#N/A	#N/A	#N/A	#N/A
52	0	Ethernet	Lead Acid	Level 1 AC	Wind	3.2	Vectored Proeller	16	Scaled Power	#N/A	#N/A	#N/A	#N/A
53	0	Ethernet	Lead Acid	Level 1 AC	Wave	5	Vectored Proeller	16	Scaled Power	#N/A	#N/A	#N/A	#N/A
54	0	Ethernet	Lead Acid	Level 1 AC	Diesel Generator	10	Vectored Proeller	16	Scaled Power	#N/A	#N/A	#N/A	#N/A
55	0	Ethernet	Lead Acid	Level 1 AC	Natural Gas Microturbine	50	Vectored Proeller	16	Scaled Power	#N/A	#N/A	#N/A	#N/A
56	0	Ethernet	Lead Acid	Level 1 AC	Solar	2	Vectored Proeller	20	Scaled Power	#N/A	#N/A	#N/A	#N/A
57	0	Ethernet	Lead Acid	Level 1 AC	Wind	3.2	Vectored Proeller	20	Scaled Power	#N/A	#N/A	#N/A	#N/A
58	0	Ethernet	Lead Acid	Level 1 AC	Wave	5	Vectored Proeller	20	Scaled Power	#N/A	#N/A	#N/A	#N/A
59	0	Ethernet	Lead Acid	Level 1 AC	Diesel Generator	10	Vectored Proeller	20	Scaled Power	#N/A	#N/A	#N/A	#N/A
60	0	Ethernet	Lead Acid	Level 1 AC	Natural Gas Microturbine	50	Vectored Proeller	20	Scaled Power	#N/A	#N/A	#N/A	#N/A

Table 5-3: Scenario summary of the architectures associated with the scenarios through 18 cumulative ranking rounds.

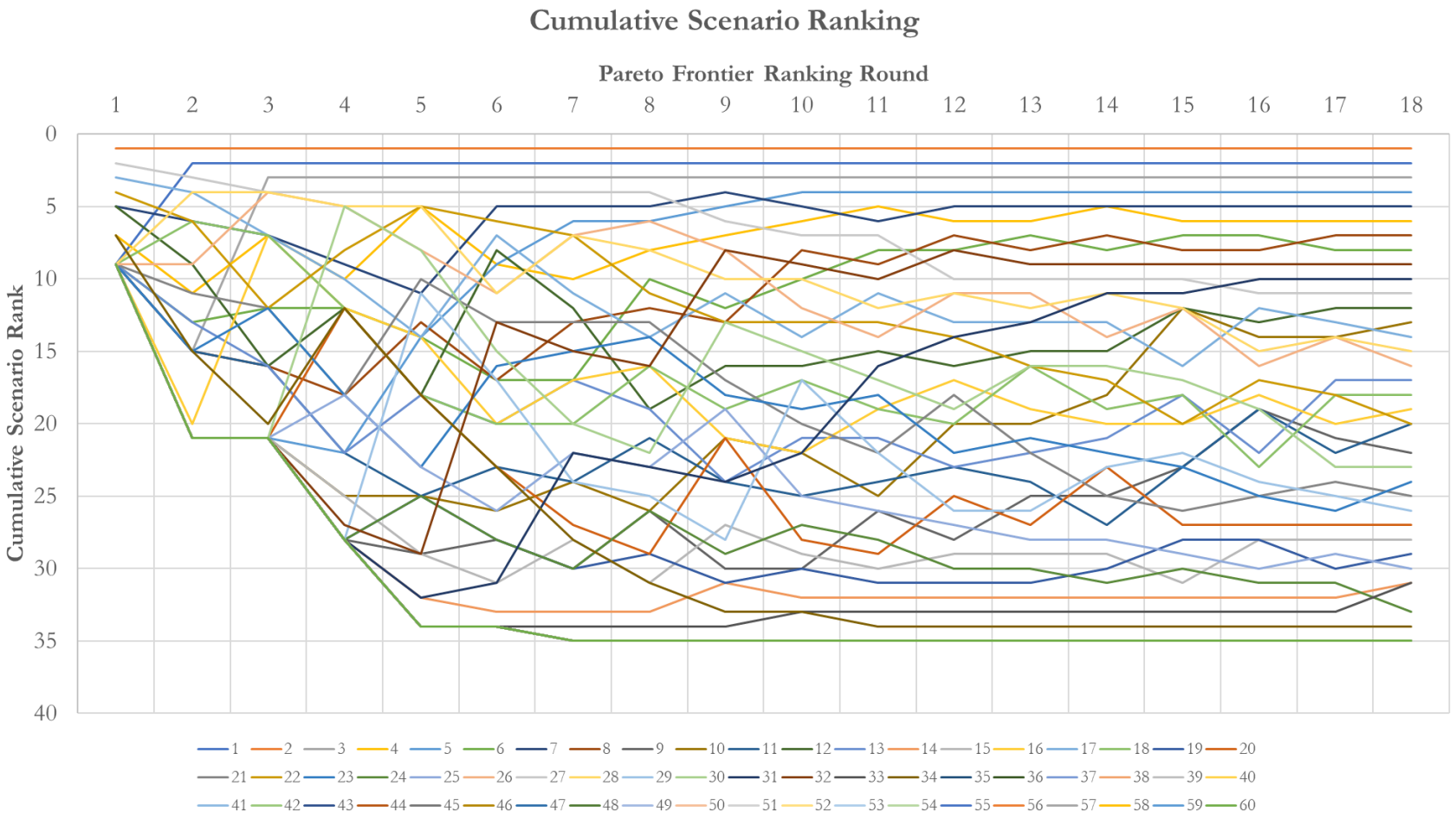

Figure 5-5: Cumulative scenario ranking through 18 ranking rounds. Each line represents a probabilistically modeled architecture, and the y-axis represents their rank within the set of scenarios for any given ranking round. As ranking rounds increase, the cumulative rank of individual scenarios begins to settle and create a flat line. This signifies increased confidence that a specific scenario's mean performance is Pareto efficient as a greater number of cases are selected through each iteration.

5.1.2 Operational Considerations

Several practical and operational considerations have not been included in this thesis and could alter architectural recommendations and performance metrics. These operational considerations have thus far been out of scope of this investigation, but it is certainly worth noting what some of them are in order to qualitatively capture their impact. When examining these operational considerations, they are classified into "-ilities" or broad categories which could have overarching implications across the system. Here, reliability, mobility, durability, flexibility, affordability, and feasibility will be discussed, but there are far more which could have an impact on practical deployment activities. Eventually, these considerations could be integrated into a model if sufficiently impactful.

The first operational consideration to examine is reliability. Reliability in this case refers to elements of the system performing in consistent, repeatable, and predictable ways. Thus far in the analysis, there has been no degree of tolerance that all input parameters were expected to meet or exceed. Reliability has been handled largely by dealing with averages across ranges. However, there are cases where this might not be an appropriate approach. For instance, in the big battery system concept, the precise amount of battery storage required was kept onboard the service platform. However, between battery decay over time, battery exposure to harsh elements, as well as possible battery burn-out over time, there is likely insufficient reliability built into that aspect of the model. One way to refine this aspect would be to perform a comprehensive reliability assessment of the system now that some of the major architectural decisions can be made. Modeling reliability in rapidly evolving systems can be a difficult task, and so by eliminating some variables, such an approach is more realistic. However, this also comes at a cost. During the systems architectural analysis phase, some architectural decisions which may increase reliability were explicitly not considered and thus could be out of scope for systems engineering. For instance, one way to increase energy production reliability could be to have multiple systems present on the service platform for energy generation redundancy – a wind turbine to supply power when the sun does not shine and solar panels to supply power when the wind does not blow.

A second operation consideration that was not included in the existing model is the consideration of mobility – specifically mobility of the service platform. Mobility is defined for the purposes of this discussion as the capability (in terms of speed, range, and agility) of a system and its components to relocate from one position to another. It is not difficult to imagine the problems that would arise in trying to scan a 60,000km^2 area over the course of ten days with 20 AUVs to transport over the course of a few hours before they disembark. This activity would require additional power

(which is not modeled) as well as additional instrumentation for geolocation. Furthermore, if inclement weather was inbound to the service platform, having some degree of capability to move away from a potentially damaging storm could prove to be useful. Since this operational consideration has not been modeled at all, there is no way to know a priori if it would have a significant impact on the performance metrics. It is likely that it is at least partially dependent on the number of AUVs present in the system, as that number will govern the size of the platform which will in turn have implications about how the platform will navigate, and orient. Platform drift must also be considered. It is possible that if little motion on the part of the platform is required, then drift could be utilized in favor of the system by drifting to a new centroid location from which the platform could launch its AUVs. If greater distances were required, than sail plans would have to be planned and executed in a timely manner to ensure acceptable system performance.

Along these lines, there is also a question of durability, which is defined as the propensity of mechanical and electrical components to resist critical failure. Additionally, there are elements of durability system-wide. If redundancies are emplaced, then a single critical component failure may not lead to a system failure. Current models have all AUVs and the service platform performing with zero errors. However, operating in a harsh offshore environment is likely to be fraught with potential dangers for the system. These dangers could be man-made (e.g., a passing ship could run over the service platform, or garbage could get tangled in the docking mechanism for the AUVs), or they could originate from the environment itself (e.g., biofouling and organism growth on the system, or large or small sea creatures investigating the new element to the ocean system). Regardless of the cause, it is important to consider durability from the perspective of the pertinent performance metrics. It is entirely possible that because of issues associated with durability the daily operating time decreases. Additionally, in order to safeguard against possible damage to the service vehicle or the AUVs there could potentially be more robust designs for the exteriors – but this would possibly impact total system price, or daily operating time if the dynamics of the AUV were changed.

Flexibility is possibly the most important operational constraint to consider in future work. Flexibility in this thesis refers to the capacity for an AUV and service platform to operate across a broad set of operational parameters and environments. For the purposes of this examination, a very specific operation was considered. But this limited scope had significant ramifications for some architectural decisions. For instance, in considering the method of energy generation, the largest costs that the non-renewable methods encountered were the costs associated with refueling the generators. If the operating environment itself changed, then it is entirely possible that the performance metrics

associated with these architectural decisions would change. An example of flexibility would be the capacity for the system to operate in remote areas autonomously, but also have the ability to operate close to the shore. The applications for this could be very wide-reaching and the more an architecture can support multiple roles, the more likely it is to solve some of the issues that have plagued widespread adoption of AUVs for so long – specifically high hourly operational costs. However, just because an architecture is well-suited to one operational environment does not mean that it will be successful in another. Capturing some measure of flexibility would be an ideal enhancement to this model.

Affordability, which is to say highly rigid cost constraints – is unique as an operational consideration, as it is explicitly labeled in this model as a performance metric as cost. However, the purpose of calling affordability out as a specific operational consideration is to point out that when examining an architecture for practical deployment, there are almost always going to be real cost limitations that are at play. For instance, if a company developing this technology is unable to fund a $200 million-dollar project, then all architectures above that price point are infeasible regardless of how well they perform in other metrics. That the Pareto ranking method favored low-cost options is very promising for this particular constraint as it would suggest that the Pareto surfaces are not disproportionately dominated by expensive architectures which have comparatively small improvements in some performance metrics.

Feasibility is a wide-ranging subject in the professional AUV realm. Feasibility in this case refers to the technology readiness level (TRL) of the system and its component parts. Currently, the very feasibility of networked AUV swarms is technically not proven. This means that as a practical matter, any architecture with more than one AUV is going to be at some degree of lower technology readiness level . There are other architectural elements which are specifically discussed in this analysis (e.g., Level 3 AC charging) which would be a welcome addition to the tradespace, but frankly, Level three AC charging is not yet widely accepted for standards. This is rapidly changing, however, and it is possible that very soon this particular element be at a much higher TRL.

5.2 Overall Method Strengths and Weaknesses

The method of walking through an architectural decomposition (Chapter 2), then modeling the system deterministically (Chapter 3), and finishing with a probabilistic model (Chapter 4) is entirely viable for performing several evaluations. By breaking down a system into its highest-level

components first, and focusing on functional decompositions, the essence of what a system is designed to accomplish begins to unravel. Through this process, the elements which truly define the system are brought forward and new ideas can be generated for ways to accomplish the function rather than be locked into a form. By creating a deterministic model, macro trends are viewable for any set of architectures. The exercise of walking through a morphological matrix is very useful to define all possible permutations of a system. Some of the permutations may never have been evaluated before and some existing architectures may be used to ground truth your model. Moreover, a probabilistic model allows for quantitative statements to be made about trends between architectures, the likelihood of a single architecture to meet specific performance criteria, and assessing assumptions and acknowledging areas with high uncertainty in the deterministic model. Finally, this process is iterative and can be completed multiple times incorporating the learnings from previous iterations into future iterations. In so doing, the models improve, and the final system that is built will be engineered upon higher confidence principles. The speed with which these iterations can be completed is also a major advantage to this approach.

However, the methods employed in this study are not all encompassing and there are several glaring issues that are not addressed. The first of these issues concerns nominal and contingency operations. There is no operational model associated with the system at this time, and that operational model would help aid in understanding nearly every operational consideration outlined above. Flexibility, mobility, and reliability are operational concerns that are not addressed using the methods outlined in this paper. The decomposition, morphological matrix constriction, and modeling approaches that were followed are simply not the ideal methods to approach such questions in detail. Furthermore, these questions are not easy to approach from a blank slate. By firming up at least some architectural decisions prior to approaching questions about flexibility, mobility, and reliability, the results from operational models can provide much more meaningful conclusions for the architectures under consideration. Just as the systems architecture models are potentially an iterative process, the systems architecture models can be – and should be – revisited following significant systems engineering reviews.

5.3 Critical Model Failure

Following the analysis outlined above, a major fault was identified in the foundations of the models. Figure 3-4 details the method that was used to calculate a figure of merit that was used throughout all of the models called "time to seafloor." This figure of merit is an estimate of the average time it takes the number of AUVs in the system to reach a depth of 4,000m. The amount of time will increase with the number of AUVs as described in Chapter 3. However, upon detailed analysis, the values that were used in order to calculate the spacing were determined to be incorrect. The result of this is a cascading error throughout the model that can potentially invalidate a large portion of the result. In this section this failure is analyzed in detail and its impact quantified. Then, the assumptions which are in place for this are model re-imagined, and recommendations for improvement are made.

5.3.1 Determining Time to Seafloor

In order to calculate the time to seafloor, the distance that the AUV travels must be known as well as the descent rate. For a single AUV, the distance to travel to reach the ocean bottom is equal to the depth of observation. In this model, that distance is 4,000m. Descent rate is determined through analysis of the MH370 case study. A single AUV descends to the seafloor over the course of 2.5 hours (MIT Spectrum, 2014). To calculate descent rate, the following governing equation is used:

$$SingleAUVDescentRate = \frac{DistanceToOceanFloor}{TimeToOceanFloor}$$

or

$$TimeToOceanFloor_{AD6_{Option}} = \frac{DistanceToOceanFloor}{SingleAUVDescentRate}$$

For a single AUV, then, the descent rate is equal to 0.44m/s. This descent rate is assumed to be constant for all AUVs in the system regardless of the number of AUVs present. In the existing model, a grid pattern of AUV deployment is proposed (Figure 3-4, Figure 5-6) with the service platform and started of deployment of all AUVs located at the center. In this grid deployment, the assumption is that each square an AUV would investigate would represent the maximum area that an

individual AUV could cover in a single operational time span. As the number of AUVs increases, the search grid would expand and the distances that an AUV would need to travel from the service platform at the center in order to reach its operational starting location would increase. As soon as more than four AUVs are present in the system, the distance to the ocean floor is no longer 4,000m, but rather a larger value, since the AUVs must transverse across areas that are otherwise scanned by previous AUVs. Figure 5-6 details how sets of AUVs would have the same values for their distance to the ocean floor. A critical error was made at this point in the modelling effort. The transverse distance that was used in the model was assumed to be 1,478m.

This value is too small, as the area scanned within a square of that size would be far less than what a single AUV could scan in a single operation. The correct value to use – assuming a square grid search pattern – would instead be closer to 14,000m – an order of magnitude increase. In order to calculate this number, the original figures of merit from the MH370 report are examined. The total line length that AUVs covered over the course of 167 operations was 17,156km as shown in Figure 3-3 (Australian Transport Safety Bureau, 2017). Each operation was 19 hours in length – the time required to descend 4000m was 2.5 hours (MIT Spectrum, 2014) – and the side scan sonar beam width was 2,000m (Australian Transport Safety Bureau, 2017). By dividing the total mission line length by the number of missions and multiplying by the beam width, the total mission area scanned, and by taking the square root of this number the edge of a square grid search pattern is calculated. This operation is summarized in the following equation:

$$SquareGridEdge = \sqrt{\frac{MissionLineLength}{NumberOfMissions} * BeamWidth}$$

Since we assume that the descent rate remains constant for each AUV, and the performance metric that this figure of merit influences is daily operational time, the value that must be captured by the model is average time to the ocean floor across all AUVs. Thus, the previous equation can be re-written as:

$$AverageTimeToSeafloor_{AD6_{Option}} = \frac{\sum TimeToOceanFloor_{AD6_{Option}}}{AD6_{Option}}$$

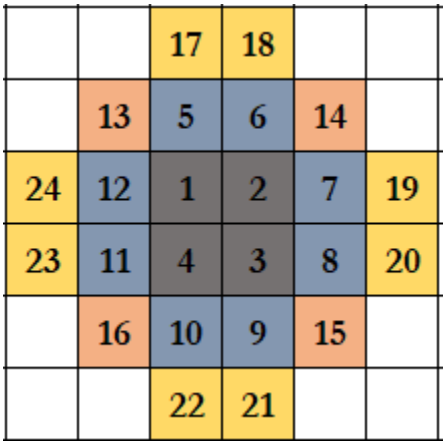

Figure 5-6: Grid pattern of deployment for a System including 20 AUVs. Squares which share the same color have identical distances to ocean floor.

5.3.2 Quantifying Impact to Results

From a practical standpoint this error correction means that for each AD6 option, there will be an increased average time to the seafloor, despite constant times to the seafloor for all AUVs under consideration. This is illustrated in Figure 5-7 where the modelled values are compared against the corrected values. As AUVs are added to the system, the time it takes to reach the seafloor only increases. Table 3-6 details the average times to the seafloor which were used in the model. Table 5-4 details the corrected values, and compares them against the values which were used in the initial design. For cases where there are four or fewer AUVs in the system (AD6 option 1 and option 2) then there is no impact on the output of the model. The reason for this is that the distance to the ocean floor has remained unchanged for those cases. However, as the distance increases and the errors propagate, the disparity between the model which was used in this thesis and the correct version becomes more and more apparent. In the case of 20 AUVs (AD6 option 6) the average time to the seafloor is 23.4 hours (nearly an entire day), but when closely examined, all AUVs 13-20 require more than 24 hours to descent to the seafloor (Table 5-5). Since the batteries onboard the AUVs only carry sufficient energy for 24 hours of operation, this means that if the square grid assumption is to continue to be used in this capacity, there is no reason to pursue any architecture with more than 12 AUVs. The AUVs simply won't have the energy to descend, operate, and ascend barring energy free ascents (e.g., positive buoyancy) which were out of scope for investigation in this thesis.

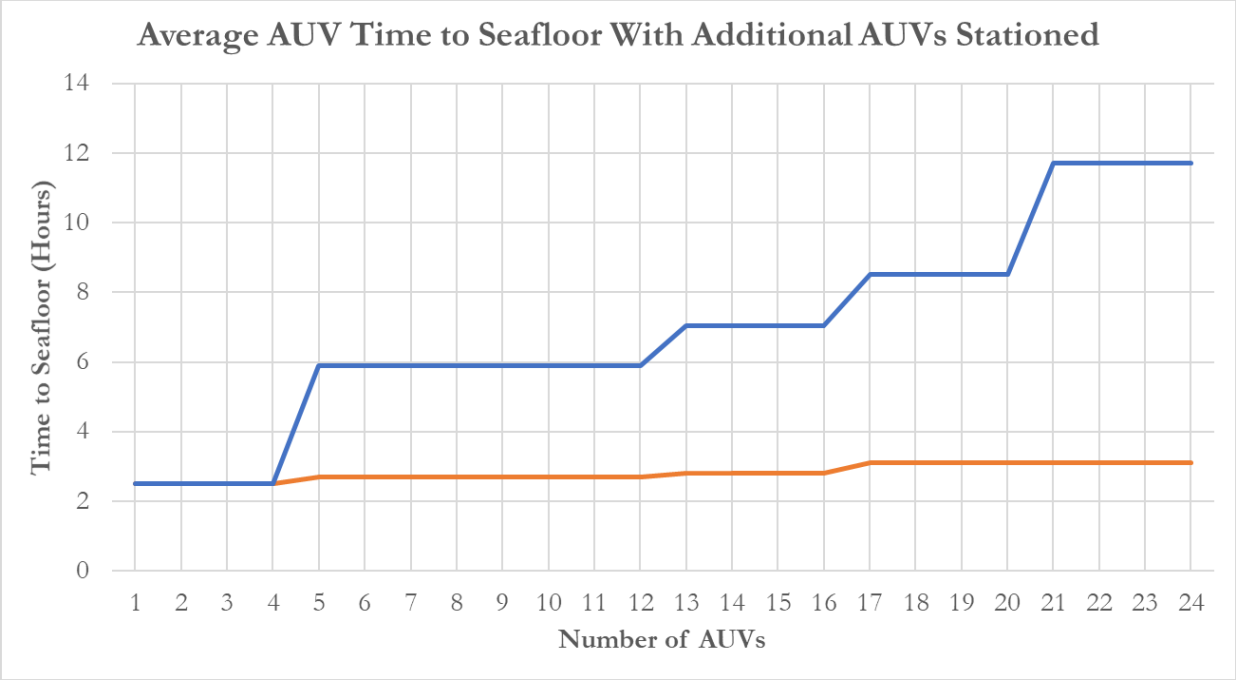

Figure 5-7: Comparison of the average AUV time to seafloor between modelled values (orange) and corrected values (blue). Note that the times are the same for cases where there are 4 or fewer AUVs in the system.

This error sheds insight into several assumptions which were previously unaccounted for. By fixing this error in the underlying model, there would be a substantial bias against architectural solutions which use large numbers of AUVs. The Pareto ranking analysis detailed earlier on the uncorrected model data ran for 18 consecutive Pareto frontiers. Following this ranking exercise, the top ten architectures by Pareto ranking were architectures which only had one or four AUVs present in the system. For those architectures, this correction would have no effect on any of their performance metrics, since their time to reach the ocean floor remained unchanged. Furthermore, after 18 runs of Pareto ranking, 5,530 points were selected along all 18 Pareto frontiers. Over 68% of all points selected were architectures that had either one or four AUVs present in the system. The top ten architectures, therefore, represent over 63% of all selected architectures. These facts all suggest that while there are certainly errors in the initial model, some of the key insights remain unchanged – the recommended architectures including one and four AUVs in the system do not have their underlying figures of merit changed, which means they will continue to be the dominant architectures.

AD6	Number of AUVs	Uncorrected Model Average time to Seafloor (hours)	Corrected Model Average time to Seafloor (hours)	Average Travel Time Impact (hours)	Difference Between Models (hours)
Op1	1	2.5	2.5	5.0	0.0
Op2	4	2.5	2.5	5.0	0.0
Op3	8	2.6	5.9	11.8	6.6
Op4	12	2.6	7.0	14.1	8.9
Op5	16	2.7	8.5	17.0	11.6
Op6	20	2.8	11.7	23.4	17.8

Table 5-4: Summary of system impact of correct values used for time to seafloor. The time to seafloor is unchanged between models for the case of one and four AUVs.

AUV	Time to Starting Location	2-way travel time	Viable?
1	2.5	5.0	Y
2	2.5	5.0	Y
3	2.5	5.0	Y
4	2.5	5.0	Y
5	9.3	18.6	Y
6	9.3	18.6	Y
7	9.3	18.6	Y
8	9.3	18.6	Y
9	9.3	18.6	Y
10	9.3	18.6	Y
11	9.3	18.6	Y
12	9.3	18.6	Y
13	12.9	25.8	N
14	12.9	25.8	N
15	12.9	25.8	N
16	12.9	25.8	N
17	18.1	36.2	N
18	18.1	36.2	N
19	18.1	36.2	N
20	18.1	36.2	N
21	18.1	36.2	N
22	18.1	36.2	N
23	18.1	36.2	N
24	18.1	36.2	N

Table 5-5: Examination of design viability for square grid search patterns where squares have edge lengths of 14,334m. Any design which incorporates more than 12 AUVs is deemed non-viable because it will take greater than 24 hours for the AUV to reach the seafloor.

5.3.3 Reimagining Time to Seafloor Calculations

While it is good to know that some of the key insights are still valid, if this model is to be improved, then there must be a different way to approach the subject of calculating time to seafloor in a way that does not invalidate all architectures which utilize more than 12 AUVs. One major problem in reconsidering the square grid style of deployment is that the distance an AUV must transverse will change as the number of AUVs increases. That is, in order to maintain a truly square grid and ensure total coverage, all squares must be equal in size. In order to accomplish this, the AUV which translates the farthest during descent will be the AUV which determines the search area for all other AUVs as it can spend the least amount of time on the seafloor. Further complicating the square grid search pattern is the fact that the area which can be searched is not only impacted by the time to seafloor, but also by each architectural decision which impacts PM2 (search area rate). For these reasons, the square grid search pattern is likely not an optimal search pattern to develop fully.

There are two methods which can be implemented in order to re-imagine time to seafloor calculations. The first is to re-tool the search pattern away from the square grid. The second is to consider expanding the architectural scope to include methods of improving performance – that is to say ways in which descent time can be improved other than changing search patterns. In considering new patterns for searching the problems that are encountered in the square grid search, pattern must be at the crux of the discussion. There are two implicit constraints which are factors in the square grid: the requirement for all search squares to be the same dimensions, and the requirement for sets of AUVs to begin their search in different locations.

If the constraint for all AUV search paths to be equal is relaxed, then a new possible search pattern emerges, termed the "swim lane" search pattern. In this search pattern, the AUVs travel first to their start location, then out for as long as they can where they then turn around and come back. Much like a swimmer in a lap pool, the AUV will travel in one lane on the outbound trip, and the adjacent lane on the return trip to maximize the total area covered in the scanning operation. Each lane is defined by the side scan sonar beam width. In this case, the lanes are separated by the beam width of 2km, preventing overlap. This concept is schematically represented in Figure 5-8. There are several values to be calculated in order to estimate the impact that this will have on the model: the length of the lane, the width of the lane, and the distance that an AUV must traverse to reach its starting location.

It is known that on average the AUVs operating in the MH370 search and recovery effort scanned 17,156 line km over the course of 167 operations (Australian Transport Safety Bureau, 2017).

This means that on average, the AUVs were collecting 5,406 line meters per hour. Whenever possible, AUV missions were undertaken once every 24-hours (Australian Transport Safety Bureau, 2017) as that was the limitation of the AUVs stored energy reserves. From this a total operational line of 102,731 meters is calculated for a 19-hour operation. The dimensions of the swim lane are therefore defined by the following equations:

$$OperationDuration = 24 \text{ hours} - 2 * (TimeToOceanFloor_{AD6_{Option}})$$

and

$$TotalOperationalLine = OperationDuration * LineMetersPerHour$$

and

$$SwimLaneLength = \frac{TotalOperationalLine - (BeamWidth * 2)}{2}$$

and

$$SwimLaneWidth = BeamWidth$$

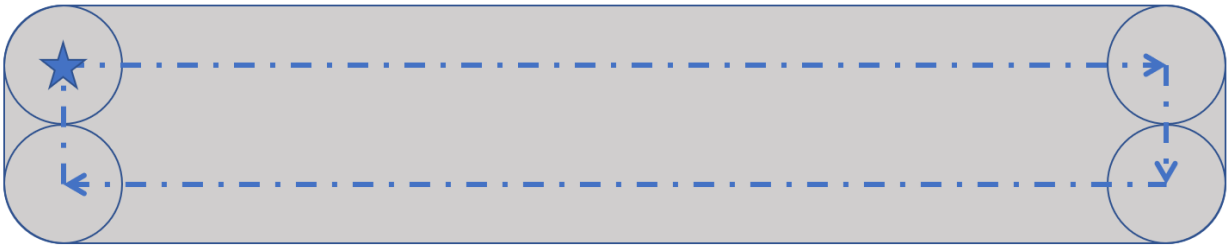

Figure 5-8: Schematic representation (not to scale) of the swim lane search concept. The star represents the start and end location of a single AUV. An individual AUV travels out, turns around, returns, and navigates back to the starting position. This path is represented by a dashed line. The circles represent the beam width of an individual AUV as it turns a corner.

These parameters are sufficient to calculate the area of each AUV as well as the dimensions of all viable designs. The results of these viable designs are summarized in Table 5-6 and the summary compared to the time to seafloor used in the model for this thesis is summarized in (Table 5-7). Similar to the square grid method, there are some designs which are non-viable, but they are only in cases of 20 AUVs or more. When comparing to the values of time to seafloor that were used in the model discussed in this thesis, the values for AD6 option 1 and 2 are identical for the same reason that these

options remained unchanged in the square grid configuration. AD6 option 3 is only slightly larger in the swim lane method, and thus the results are likely going to be similar for many AD6 option 3 outcomes. However, for AD6 option 4, 5, and 6 there are still substantial differences from the model used in the body of the thesis.

AUV	Time to Starting Location	2-way travel time	Viable?
1	2.50	5.00	Y
2	2.50	5.00	Y
3	2.50	5.00	Y
4	2.50	5.00	Y
5	3.54	7.07	Y
6	3.54	7.07	Y
7	3.54	7.07	Y
8	3.54	7.07	Y
9	5.59	11.18	Y
10	5.59	11.18	Y
11	5.59	11.18	Y
12	5.59	11.18	Y
13	7.91	15.81	Y
14	7.91	15.81	Y
15	7.91	15.81	Y
16	7.91	15.81	Y
17	10.31	20.62	Y
18	10.31	20.62	Y
19	10.31	20.62	Y
20	10.31	20.62	Y
21	12.75	25.50	N
22	12.75	25.50	N
23	12.75	25.50	N
24	12.75	25.50	N

Table 5-6: Summary of viable designs for the swim lane method of AUV spacing. Similar to the square grid method, there are designs which become non-viable because of their travel time. Unlike the square grid method, these designs only occur when swarms greater than 20 AUVs are considered.

AD6	Number of AUVs	Uncorrected Model Average time to Seafloor (hours)	Corrected Model Average time to Seafloor (hours)	Average Travel Time Impact (hours)	Difference Between Models (hours)
Op1	1	2.5	2.5	5.0	0.0
Op2	4	2.5	2.5	5.0	0.0
Op3	8	2.6	3.0	6.0	6.6
Op4	12	2.6	3.9	7.8	8.9
Op5	16	2.7	4.9	9.8	11.6
Op6	20	2.8	7.1	14.2	17.8

Table 5-7: Summary of system impact of swim lane values. Reference architecture only used for time to seafloor.

The swim lane method relaxes the constraint of consistent dimensions of the scanned areas, and a cursory examination of the swim lane method shows how significant the scanned areas change. A scale schematic representing 20 AUVs in the system is presented in Figure 5-9. Each lane gets smaller as the transverse distance increases. This representation is to scale only for the reference architecture. Any other architectural decisions which impact the search area rate will have a cascading effect on this scale. Visualizing the scale of the variation in the swim lanes brings up a concern which has to this point gone largely unrecognized in the discussion – how can complete coverage be ensured and how can performance be maximized using a system such as described? If a non-square grid is used, some sort of tessellation will have to be employed to ensure total coverage. This is another set of "-ilities" to be considered in future work. The tradeoffs that exist between the swim lane and the square grid search methods are worth exploring in greater detail. At the surface, there seems to be tension between two new metrics. The swim lane method allows for greater numbers of AUVs to operate – compare Table 5-5 and Table 5-6 – which could lead to performance improvements. However, the imperfect tessellation of a swim lane diamond search pattern may not be worth those improvements, as a square grid can be perfectly tessellated.

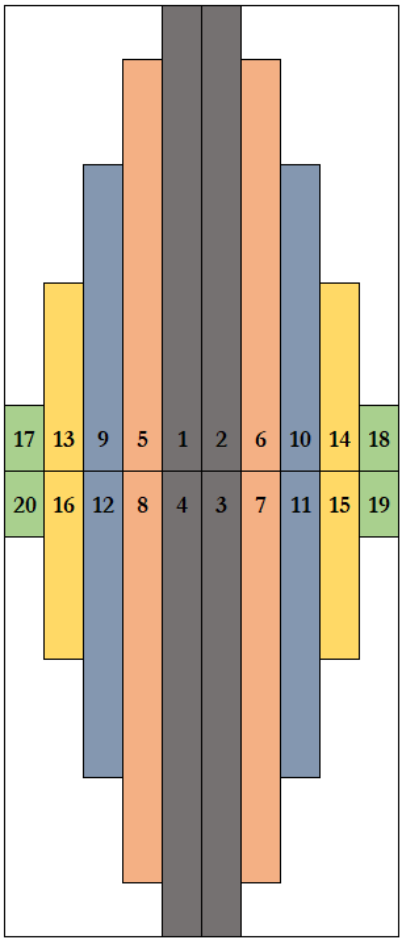

Figure 5-9: Scaled schematic showing how the reference architecture would perform in the swim lane search pattern. Other architectural considerations that impact search area rate are not taken into consideration. This scaling would change with those decisions factored into the examination.

Another option that can be considered as far as re-imagining the square grid search method is termed herein the "flower petal" method. This option keeps the constraint that each AUV scans the same area, but relaxes the constraint that they start their search in different locations as they are all deployed from the same location at the center of the flower. Following a flight path similar to the swim lane method (i.e., out and back) the AUVs would scan in a pattern exhibited in (Figure 5-10). The advantages to such a method would be that each AUV can operate for their full duration scanning a large area. Downsides of this method include overlapping search areas close to the center of the flower and completely unscanned sections at the edges of the circle.

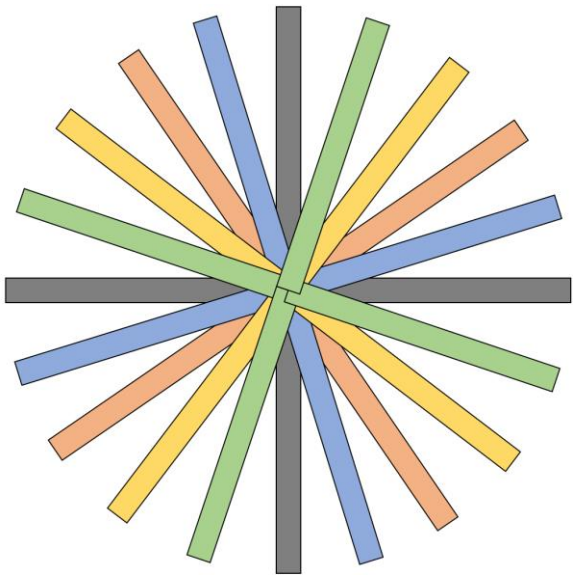

Figure 5-10: Schematic illustration demonstrating the possible lanes for a flower petal search pattern. Note the substantial overlap in the center of the area of investigation and the lack of coverage in the edges of the search area.

A second method altogether that can be employed to address this shortcoming in the model and test for sensitivities is to create a new class of architectural decisions that will directly impact descent functionality. The reference AUV descends through the water column at a rate of 0.44 m/s – a rate that is less than one third the speed at which it can scan the sea floor, and even less than the cruising speed when not collecting data. Thus, increasing the descent speed could considerably improve performance. There are a number of ways that this could be achieved (e.g., detachable dive weights, changing the buoyancy of the AUV itself, etc.) and each one comes with system-wide impacts. Additional architectural decisions could include not launching all AUVs simultaneously and instead moving the service platform to the launch location, eliminating or reducing the transverse distance required to travel for the AUVs, or adding additional service platforms which could in effect act as "catchers" for AUVs after they had completed their operations. With a mobile service platform, the burden of translating to a new seafloor patch to search is shifted from the AUV to the service platform and would have implications for the platform's design and operations.

While the error in discovered in the existing model is important to note, there have been several key conclusions that have come from its identification. First and most importantly, the system is more sensitive to the impact of time to seafloor than was initially thought. Second, despite this sensitivity, the top ten dominant architectures remain unchanged, as they were not influenced by the

change in time to the seafloor value. Third, several options for new ways of imagining the search area grid have been posited to different degrees of depth. Future work should recognize the sensitivity the model has to search patterns and dedicate effort in establishing which search patterns are ideal in which situations, and which architectural decisions – if any – can influence the performance of the system from the perspective of descent time.

6 Recommendations for Future Work

This thesis has focused on evaluating the AUV system from a holistic perspective by broadening the range of what was included inside and outside of the system boundary. While AUV technology has progressed throughout the years (from the Whitehead torpedo to the Bluefin-21), it is challenged in this thesis that a systems-wide view imposed on AUV technology could aid in reaping the benefits that may emerge. This thesis represents a method of evaluating an established technology and within offers real recommendations for practical applications. While the model proved to have a critical fault within its foundational constants, these recommendations remained unaffected, and the design vectors which were affected by the error were impacted negatively. This means that the conclusions reached herein are still supported by the model with all of the built-in assumptions despite the error in construction. Within this chapter, these conclusions are summarized and future areas of research is suggested.

6.1 Research Summary

Chapter 1 was constructed to provide the general context in which this research lies. The motivation for the project was to frame the research as a question – in what ways is the AUV space lagging behind some other similar technologies? In examining the history of AUVs there are several instances where it seemed as though major breakthroughs were just around the corner only to be hampered by technological limitations. The overall structure of research and methods was laid out, and a general structure of the documentation was captured.

Chapter 2 of this thesis was focused on decomposing the AUV system into its component entities. The system boundaries were expanded from conventional thinking to include sub-systems that integrate charging, launching, transferring data, and so forth to and from the AUV. These operational elements are important to understanding the true cost and value that such a technology can bring to bear, yet they can sometimes be left outside of the system boundary for analysis. The component entities which comprised this newly expanded AUV and service platform system were then decomposed into functional elements. The functions that have been analyzed include communicating between elements of the system, energizing the system, propelling and orienting the system (collectively forming a functional module which achieves controlling the system), and sensing the surrounding environment.

Following this decomposition Chapter 3 modelled the system via a deterministic method logy. In order to evaluate a model, seven system performance metrics were established based on the figures of merit identified during decomposition. These seven performance metrics provided a common framework from which different design vectors could be compared. A single design vector is a unique set of options for each identified architectural decision. A morphological matrix containing every permutation of these design vectors was used to compare all possible architectures against each other. This resulted in the deterministic analysis where a Pareto frontier was established in the PM4 and PM5 space. Within this Pareto frontier, there are several key observations. First, there are architectures for each option for number of AUVs in the system. Second, the Scalable Power system concept was favored over other system concepts because it realized improvements cost (PM5) relative to the Big Battery concept without sacrificing calendar mission completion time (PM4) compared to the Tiny Battery concept. The third conclusion that was reached from the deterministic approach was that in renewable power generation options were always more cost effective than non-renewable options.

In Chapter 4, the top performing architectures as well as other design vectors which permutated between several architectural decisions which were inconsistent across the deterministic tradespace were then selected for probabilistic analysis. The purpose of probabilistic analysis was twofold. First, a robust probabilistic analysis allowed for uncertainty (which had been previously been unaddressed) surrounding baseline assumptions to influence the model outcomes. A second objective of the probabilistic analysis was to quantitatively evaluate the similarity (or dissimilarity) between selected architectures. The probabilistic model demonstrated how uncertainty played a larger role in some architectures than others (e.g., there are much wider cost spreads when examining total system cost for 20 AUV systems). Additionally, in some circumstances specific architectural decisions were differentiated with 90% confidence (e.g., renewably charged, single AUV systems are less expensive than non-renewably charged single AUV systems). Some architectures which were clearly distinct in the deterministic model (for instance, all renewable options were more cost effective than their non-renewable counterparts) were no longer differentiated in some circumstances. This effect was especially pronounced in design vectors with large numbers of AUVs selected for analysis.

Chapter 5 saw a detailed analysis of the results of the probabilistic model. A method of Pareto ranking was employed to begin classifying which design vectors occurred most frequently on multi-dimensional Pareto surfaces. In order to perform this, an individual Pareto surface was defined, then the component design vectors were removed from the tradespace, and a second ranking began. This process repeated iteratively over the course of 18 ranks. Architectures with one AUV present which

were powered renewably were the favored architectures, accounting for over half of all selected points. Based on the cumulative modeling efforts, it is herein presented that such an AUV could be able to complete the MH370 mission in between 243 and 247 days with a cost of approximately $17 million. This is faster than the existing methods (between 285 days and 730 days), and almost half the cost ($32,812,500).

In Chapter 5, discussion was also dedicated to an error which was identified in the underlying assumptions built into the models. This error was in the time estimated for AUVs to reach the seafloor. Importantly, not all architectures were impacted by this error to the same degree. Architectures with one or four AUVs were entirely unaffected, as their calculated times to ocean bottom were correct. As the number of AUVs increased in the system, the error propagated to a larger extent. Fundamentally, this error does not change the proposed recommended architecture which consists of one AUV. The discovery of this error also prompted deeper thought surrounding an architectural decision which was not part of the model at all. The search pattern that a set of AUVs utilizes to scan the seafloor may (or may not) have a significant impact on system performance. This and other operational decisions should be an area of focus for future work.

Following the robust deterministic and probabilistic modelling efforts, it is appropriate to return to the initial questions raised about the purpose of these analytical methods. The motivation for this work is ultimately to examine the potential viability of paired AUVs and service vessels. Critical questions surrounding the possible performance envelopes of the entire AUV system were raised. The recommendations that are proposed within this thesis do not represent the final solutions in answering some of the questions about the performance of AUV systems. However, the methods and thought processes which are employed are defensible and present a reasonable framework for future research to stand atop

6.2 Revisiting Key Assumptions and Future Work

The purpose of this thesis was to examine the AUV and the AUV service platform system from a holistic perspective and begin to address some of the implicit and explicit assumptions that have governed the technology since its inception. To that end, some of the large architectural decisions have been laid out, modeled, and evaluated. However, as with any model there are areas in which it could be improved. Future work is herein separated into two different types of possible

improvements: improving the existing models, and expanding the investigation through the introduction of new models.

6.2.1 Improving Existing Models

A key assumption in this thesis is associated with a single mission profile. There is considerable variation that could be further quantified by examining the single mission profiles. Specifically, for this study, a single mission is assumed to cover an arbitrary 2.2 million m^2 per mission. This assumes a square scanning pattern for each AUV. There are system-wide optimization parameters that could and should be further tuned. For instance, if more AUVs are added to the system, then perhaps different mission scanning patterns should be considered, as discussed in Chapter 5. Perhaps there are advantages to "ribbon" scanning (where AUVs scan in a straight line) as opposed to "lawn mower" (where a square area is covered by switching back frequently) which could result in different emergent outcomes of the system. As it stands, there are two emergent outcomes of this initial arbitrary setup. First, since the spacing of AUVs is relatively small, there is an expected overlap of scanning. This means that data will be more robust – readings of one AUV can be duplicated and verified by another AUV. Second, since the AUVs will be operating close to each other emerging technologies which will enable swarm behavior will not be constrained to the most demanding distance requirements between individual AUVs.

Another assumption that is built into these models is that there is a single architecture that is common to the AUV. In Chapter 1 it is noted that, to date, many operating AUVs are highly specialized with their mission profiles in mind. For the purposes of this thesis, a common specialized architecture for all AUVs that were in the system allowed for the assessment of large-scale architectural decisions. As future mission profiles are explored however, this assumption that all AUVs share an architecture should be challenged. It could be possible that there are circumstances where a single architecture is not the optimal solution – in order to optimize multiple mission profiles a set of various AUVs should be maintained, or perhaps single architectures should have their own capacities increased to handle broader sets of missions.

6.2.2 Expanding the Investigation with New Models

Based on the lack of operational focus in this initial exploration, a deep-dive into the operational reality of a system that has been identified from this analysis would be a logical next step (Figure 6-1). There are several methods which could be employed that would capture the behavior of this system, but an agent-based model – defined for the purposes of this discussion as a class of model wherein individual elements of the model behave autonomously and interact with other agents – would appear to be a logical next step. In the framework presented in this thesis, agents may be the AUVs and the service platforms, comprising a "system-of-systems". An agent-based model differs from the deterministic and probabilistic models that are explored in this thesis because it is focused on the execution of a specific mission instead of the end state exclusively. For instance, in this case study an AUV may "choose" to depart a service station at a time before its battery is full in order to make room for the next AUV which is running out of energy. If other service platforms are under consideration, the an AUV could choose to dock at a different service platform than the one that they launched from. There is great promise in developing an agent-based model for this project, especially if other operational environments are under consideration.

A model which focuses on operational elements of the system could answer a great number of questions. From an architectural perspective, there could be substantial refinement surrounding the requirements of visiting the system during regular operations. This includes activities ranging in scope and complexity from refilling fuel tanks to regular required maintenance of individual components. Digging deeper into the architectural influence that such a model could hold, a sufficiently advanced and detailed operational model could examine different missions (specifically those with different water depths and areas of investigation) and classify different architectures vis a vis their appropriateness for individual missions. This could shed light on questions about systems which are tailor made for certain mission profiles versus systems which are built to be more of a jack-of-all-trades style of solution. Following an architectural exploration, an operational model could explore the viability of multiple systems operating in parallel to accomplish single missions. For missions that require rapid flight plan development based on collected data, systems of systems (i.e., multiple service platforms with 1-20 AUVs instead of a single service platform with 1-20 AUVs) could prove to provide a significant opportunity. Beyond the system, such an operational model could begin to examine how the system interacts with its environment. By considering forms and functions that were outside the scope of this thesis (e.g., method of relaying data from the service platform to the data

owners) new performance metrics could be introduced, and existing performance metrics could be refined. Finally, the previously mentioned "-ilities" that have gone largely unexplored could be probed with an operational model. Issues of mobility, reliability, and flexibility could be well constrained, classified, and quantified.

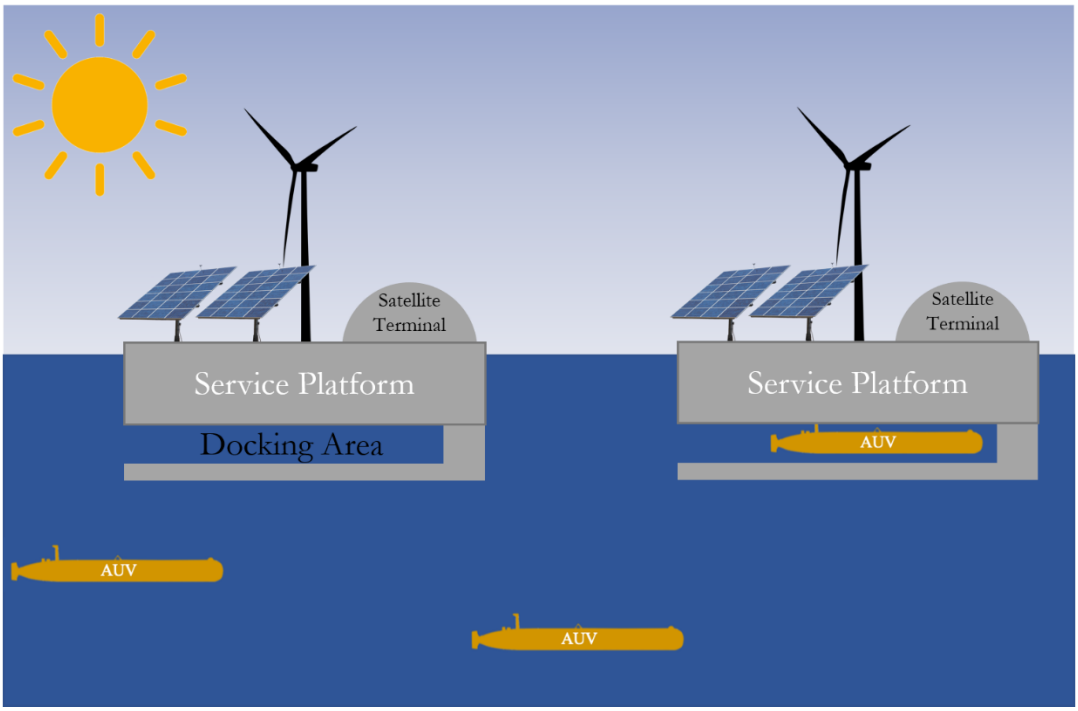

Figure 6-1: Schematic possibility of what a "system-of-systems" of AUVs paired with remote servicing platforms could evolve to. Multiple methods of providing power, shared AUVs between multiple service platforms, and communication outside of the system are all operational considerations not addressed in this thesis. Modified from (M. Haji, 2020).

There are multiple operational environments that should be explored in this operational model in an effort to approach the flexibility questions raised. The first use case that should be examined is the initial search and rescue of MH370. Ideally, this operational model would confirm some of the conclusions that have been witnessed in the modelling to date. Beyond that initial anchoring exercise, there are several other operational environments: surveying the foot of sea ice, monitoring and inspecting sub-sea infrastructure (e.g., oil and gas infrastructure, as well as fiber cable monitoring), and frequent, high-resolution mapping of high-traffic shipping channels. In order to accomplish any of these tasks, a more generalized form of the system will need to be refined. Performance metrics will

need to be either generalized as well, for each individual operating environment and mission will require unique performance metrics.

Both during and following operational modelling, there are several technologies which lag behind in terms of readiness level. The most difficult of these to tackle are the technologies required to have AUVs communicate underwater. Additionally, improving charging methods to approach Level 3 AC charging rates is important. Pushing these technologies to TRLs which are ready to deploy is a critical hurdle for this project to come to fruition. Finally, once the TRLs have advanced, and iterative designs have been refined the next step to follow would be to begin the prototyping process. Even with some technologies which are low TRLs, prototypes could be developed and findings from the prototyping could be integrated into future architectural, operational, and engineering models.

6.3 Concluding Thoughts

The following statements were issued as challenges for this research. Assuming that any specific technological limitations can eventually be overcome – what then would the architectures look like when examining AUV swarms and completely autonomous AUV systems? Is there an architectural concept which has to date remained unexplored through which the system could drastically improve performance? Throughout this research, some answers have been presented. It is herein argued that the architectures that such systems could resemble would have some number of AUVs which paired with at least one service vehicle. This pairing would enable significant development in the nature of AUV autonomy and functionality. This concept to date has not been explored by any large-scale modelling. Assuming the technical challenges that face AUVs can be overcome, there are significant leaps that can be made in many performance metrics. Depending on the user, there may also be a great number of architectures from which to choose.

Bibliography

A. Berger, M. A. (2016). High efficient integrated power receiver for a Qi compliant Wireless Power Transfer system. *EEE Wireless Power Transfer Conference (WPTC)* (pp. 1-4). Aveiro.

Alexander Inzartsev, L. K. (2010). Autonomous Underwater Vehicle Motion Control during Investigation of Bottom Objects and Hard-to-Reach Areas. In F. Casolo, *Motion Control*. Rijeka: InTech.

American Wind Energy Association. (2019). Third quarter 2019. *U.S. Wind Industry Quarterly Market Report*, pp. 1-46.

André Kurs, A. K. (2007). Wireless Power Transfer via Strongly Coupled Magnetic Resonances. *Science*, 83-86.

Anonymous. (2016, July 22). *What is absorption rate of WiFi and Bluetooth RF in water?* Retrieved from Stack Exchange: https://physics.stackexchange.com/questions/269283/what-is-absorption-rate-of-wifi-and-bluetooth-rf-in-water

Aristeidis Karalis, J. M. (2007). Efficient wireless non-radiative mid-range energy transfer. *Annals of Physics*, 34-48.

Australia Department of Infrastructure, Transport, Regional Development, and Communications. (2018, November 14). *Joint Agency Coordination Centre*. Retrieved from Search for MH370: https://www.infrastructure.gov.au/aviation/joint-agency-coordination-centre/

Australian Transport Safety Bureau. (2017). *The Operational Search for MH370*. Canberra: Australian Government.

Avant Garde Innovations. (2020). *1kW Small Wind Turbine + 1.4 kW Aura*. Retrieved from Avant Garde Innovations: https://avantgarde.energy/product/avatar-5kw/1kw-small-wind-turbine-1-4-kw-aura/

B Drew, A. R. (2009). A Review of Wave Energy Converter Technology. *Journal of Power and Energy*, 887-902.

Banggood. (2020, July 30). *RC Quadcopters*. Retrieved from Banggood USA: https://usa.banggood.com/Eachine-E520-WIFI-FPV-With-4K1080P-HD-Wide-Angle-Camera-High-Hold-Mode-Foldable-RC-Drone-Quadcopter-RTF-p-1533310.html?rmmds=search&ID=6266307531930&cur_warehouse=CN

Battery Association of Japan. (2015). *The history of the battery*. Retrieved from Battery Association of Japan: http://www.baj.or.jp/e/knowledge/history04.html

Battery University. (2017, March 21). *What is the Best Battery?* Retrieved from Battery University: https://batteryuniversity.com/learn/archive/whats_the_best_battery

Bekey, G. A. (2005). *Autonomous Robots: From Biological Inspiration to Implementation and Control*. Cambridge: The MIT Press.

Bellingham J. S. and Willcox, J. G. (1996). Optimizing AUV oceanographic surveys. *Proceedings of Symposium on Autonomous Underwater Vehicle Technology* (pp. 391-398). Monterey: IEEE.

Benjamin O. Agajelu, O. G. (2013). Life Cycle Cost Analysis of a Diesel/Photovoltaic Hybrid Power Generating System. *Industrial Engineering Letters*, 19-30.

Berman, A. D. (2016, March 22). *Singularity Hub*. Retrieved from Technology Feels Like It's Accelerating - Because It Actually Is: https://singularityhub.com/2016/03/22/technology-feels-like-its-accelerating-because-it-actually-is/#sm.00Oh4vtmg1

Bien, J. K. (2013). Electric field coupling technique of wireless power transfer for electric vehicles. *Tencon Spring* (pp. 267-271). Sydney: IEEE.

Blidberg, D. (2001). The Development of Autonomous Underwater Vehicles (AUV); A Brief Summary. *Proceedings of the ICRA*. Seol.

Bluefin Robotics. (2010, December 12). *Bluefin-21 Unmanned Underwater Vehicle (UUV)*. Retrieved from Bluefin Robotics Product Sheet: https://gdmissionsystems.com/-/media/General-Dynamics/Maritime-and-Strategic-Systems/Bluefin/PDF/Bluefin-21-BPAUV-Product-Sheet.ashx?la=en&hash=00B8F3DDB86A0421AFD965E085F2409F85FAA9BC

Bluefin Robotics Corporation. (2015). *Standard Payload Interface Specification.* Quincy: Bluefin Robotics Corporation.

Bong-Huan Jun, J.-Y. P.-Y.-M.-M.-K.-H. (2009). Development of the AUV 'ISiMI' and a free running test in an Ocean Engineering Basin. *Ocean Engineering*, 2-14.

Bowden, C. H. (2019). *Average Solar Radiation*. Retrieved from PV Education: https://www.pveducation.org/pvcdrom/properties-of-sunlight/average-solar-radiation

Brown, W. C. (1984). The History of Power Transmission by Radio Waves. *Transactions of Microwave Theory and Techniques*, 1230-1242.

C. Cai, J. C. (2019). A System Modeling Method of AUV Swarms Based on UPDM. *International Conference on Signal Processing, Communications and Computing (ICSPCC)* (pp. 1-4). Dalian: IEEE.

C. Denniston, T. R. (2018). On-line AUV Survey Planning for Finding Safe Vessel Paths through Hazardous Environments. *Autonomous Underwater Vehicle Workshop*, (pp. 1-8). Porto.

C. Diendorfer, M. H. (2014). Performance ANalysis of Offshore Solar Power Plants. *Energey Procedia*, 2462-2471.

Capehart, B. L. (2016, 12 22). *Microtubine Design Recommendations*. Retrieved from Whole Building Design Guide: https://www.wbdg.org/resources/microturbines

Coddington, O., Lean, J. L., Pilewskie, P., Snow, M., & Lindholm, D. (2016). A Solar Irradiance Climate Data Record. *Bulletin of the American Meteorological Society*, 1265-1282.

D. Richard Blidberg, S. C. (2004). Long Endurance Sampling of the Ocean with Solar Powered AUVs. *Symposium on Intelligent Autonomous Vehicles*, (pp. 561-566). Lisbon.

D. S. Jenne, Y.-H. Y. (2015). *Levelized Cost of Energy Analysis of Marine and Hydrokinetic Reference Models.* Washington D.C.: National Renewable Energy Laboratory.

Dà-Jiāng Innovations. (2016, September 27). *DJI Press Release*. Retrieved from My News Desk: http://www.mynewsdesk.com/uk/dji/pressreleases/dji-revolutionises-personal-flight-with-new-mavic-pro-drone-1622367

Dara O'Sullivan, D. M. (2016). *DYNAMIC CHARACTERISTICS OF WAVE AND TIDAL ENERGY CONVERTERS & A RECOMMENDED STRUCTURE FOR DEVELOPMENT OF A GENERIC MODEL FOR GRID CONNECTION.* Cork: International Energy Agency.

DellaMorte, J. (2019, September 4). *PopotoModem announces first, affordable NATO ANEP-87 (JANUS) OEM underwater communications system.* Retrieved from Bloomberg: https://www.bloomberg.com/press-releases/2019-09-04/popotomodem-announces-first-affordable-nato-anep-87-janus-oem-underwater-communications-system

Diesel Service and Supply. (2020). *Approximate Diesel Fuel Consumption Chart*. Retrieved from Diesel Service and Supply: https://www.generatorsource.com/Diesel_Fuel_Consumption.aspx

Divis, D. A. (2019, July 6). *Drone Light Show Planned for Moon Landing Celebration*. Retrieved from Inside Unmanned Systems: https://insideunmannedsystems.com/drone-light-show-planned-for-moon-landing-celebration/

E. M. Fischell, A. R. (2020). Single-Hydrophone Low-Cost Underwater Vehicle Swarming. *Robotics and Automation Letters*, 354-361.

Edward Crawley, B. C. (2016). *System Architecture: Strategy and Product Development for Complex Systems - global edition.* Essex : Pearson.

Evans, J. (2012, 02 22). *Centrifugal Pump Efficiency - Specific Speed.* Retrieved from Pumps and Systems: https://www.pumpsandsystems.com/centrifugal-pump-efficiency-specific-speed

Fugro. (2014). *M.V. Fugro Supporter Equipment Flyer*. Retrieved from Fugro: https://media.fugro.com/media/expertise-docs/fugrosupporter_2014_fcst_lr.pdf?sfvrsn=533051a_14

Fugro. (2017). *M.V. Fugro Equator Equipment Flyer*. Retrieved from Fugro: https://media.fugro.com/media/docs/default-source/about-fugro-doc/vessels/fugro-equator-flyer.pdf?sfvrsn=7e26e419_2

Gartland, A. (2018, June 9). MH370: Ocean Infinity search ends amid calls for new disclosures and further investigation. *Changing Times*.

General Dynamics. (2011, November 9). *General Dynamics Press Release*. Retrieved from General Dynamics: https://gdmissionsystems.com/articles/2011/11/09/press_release_11-9-2011-u-s-navy-awards-general-dynamics-scm-uuv-contract

General Dynamics. (2019). *Knifefish Unmanned Undersea Vehicle Datasheet*. Retrieved from General Dynamics Mission Systems: https://gdmissionsystems.com/-/media/General-Dynamics/Maritime-and-Strategic-Systems/PDF/maritime-knifefish-uuv-datasheet.ashx

General Dynamics. (2020). *Bluefin-21 Unmanned Underwater Vehicle (UUV)*. Retrieved from GD Mission Systems: https://gdmissionsystems.com/products/underwater-vehicles/bluefin-21-autonomous-underwater-vehicle

General Electric. (2020). *Haliade-X 12 MW Offshore Wind Turbine Platform*. Retrieved from GE Renewable Energy: https://www.ge.com/renewableenergy/wind-energy/offshore-wind/haliade-x-offshore-turbine

Ghasemi, A. (2014, September). Computational Simulation of the Interaction Between Moving Rigid Bodies and Two-Fluid Flows. *Masters of Science Thesis in Mechanical Engineering*, 1-13. Massachusetts: University of Massachusetts Dartmouth.

Goolsby, T. F. (2020, February). Monte Carlo Simulation Method. Cambridge, MA, USA.

Griffiths, G. (n.d.). *Technology Needs for Autonomous Underwater Vehicles*. Southampton, UK: Southampton Oceanography Centre.

H. Zhang, F. L. (2016). A Four-Plate Compact Capacitive Coupler Design and LCL-Compensated Topology for Capacitive Power Transfer in Electric Vehicle Charging Application. *Transactions on Power Electronics*, 8541-8551.

Harding Energy. (2020). *Lithium Products*. Retrieved from Harding Energy: https://www.hardingenergy.com/lithium-2/

Havila. (2020). *M.V. Havila Harmony*. Retrieved from Havila: http://reachsubsea.no/content/uploads/2018/08/Havila-Harmony.pdf-1.pdf

Home Advisor. (2020). *Repair a Generator*. Retrieved from Home Advisor: https://www.homeadvisor.com/cost/electrical/repair-a-generator/

Honda. (2017). *Honda Safe Swarm*. Retrieved from Honda Safety: https://www.honda.com/safety/safe-swarm#:~:text=Honda's%20SAFE%20SWARM%E2%84%A2%20concept,to%20change%20lanes%20if%20needed.

IEA. (2020). *Global Energy Review 2019*. Retrieved from https://www.iea.org/reports/global-energy-review-2019

IEEE 802.11 Working Group. (2018). *IEEE 802.11TM WIRELESS LOCAL AREA NETWORKS*. Retrieved from The Working Group for WLAN Standards: http://www.ieee802.org/11/

IEEE 802.3 Ethernet Working Group. (2020, June 10). *IEEE 802.3 Ethernet standards*. Retrieved from IEEE 802: http://www.ieee802.org/3/

IHS. (2018, 10 10). *North American Wind Power O&M Costs to Increase Nearly 40 Percent in Coming Decade*. Retrieved from IHS Markit: https://news.ihsmarkit.com/prviewer/release_only/slug/energy-north-american-wind-power-om-costs-increase-nearly-40-percent-coming-decade-ihs

International Energy Agency. (2019). *Offshore Wind Outlook 2019*. Paris: IEA.

J. Channegowda, V. K. (2015). Comprehensive review and comparison of DC fast charging converter topologies: Improving electric vehicle plug-to-wheels efficiency. *24th International Symposium on Industrial Electronics (ISIE)* (pp. 263-268). Buzios: IEEE.

J. Engström, M. E. (2013). Performance of large arrays of point absorbing direct-driven wave energy converters. *Journal of Applied Physics*.

J. Hernandez-Moro, J. M.-D. (2013). Analytical model for solar PV and CSP electricity costs: Present LCOE values and their future evolution. *Renewable and Sustainable Energy Reviews*, 119-132.

J. Sears, D. R. (2014). A comparison of electric vehicle Level 1 and Level 2 charging efficiency. *Conference on Technologies for Sustainability (SusTech)* (pp. 255-258). Portland: IEEE.

Jeffery Lin, P. S. (2018, January 8). China is making 1,000-UAV drone swarms now. *Popular Science*, pp. https://www.popsci.com/china-drone-swarms/.

Johnson, K. (2012, September 4). Project Aims to Harness the Power of Waves. *The New York Times*, p. 19.

Kinkade, K. (2016, August 5). *What are the transmission speeds for radio waves*. Retrieved from Quora: https://www.quora.com/What-are-the-transmission-speeds-for-radio-

waves#:~:text=small%3A%20twenty%20kilohertz.-,As%20the%20conversion%20from%20bits%20to%20hertz%20is%201%20bit,40%25%20of%20a%20dialup%20modem.

Kurzweil, R. (2006). *The Singularity is Near: When Humans Transcend Biology*. New York: Penguin.

Lamont-Doherty Earth Observatory/Columbia University. (2020, July 15). *High-resolution Surface Solar Irradiance derived from ISCCP DX data. Research Data Archive*. Retrieved from National Center for Atmospheric Research, Computational and Information Systems Laboratory: https://rda.ucar.edu/datasets/ds741.1/

Li Zhang, B. S. (2015). The optimization of DC fast charging deployment in California. *Applied Energy*, 111-122.

Lorenzini, G. &. (2015). Constructal design applied to the study of the geometry and submergence of an Oscillating Water Column. *International Journal of Heat and Technology*.

M. Davoodi Monfareed, A. M. (2011). Convex hull ranking algorithm for multi-objective evolutionary algorithms. *Scientia Iranica*, 1435-1442.

M. Haji, J. N. (2020). A Framework for the Design of Renewably Powered Offshore AUV Servicing Platforms. *Ocean Sciences Meeting 2020*.

M. T. Sabet, H. M. (2018). A Low-Cost Dead Reckoning Navigation System for an AUV Using a Robust AHRS: Design and Experimental Analysis. *Journal of Oceanic Engineering*, 927-939.

Magee, C. B. (2014). Quantitative Empirical Trends in Technical Performance. *Technological Forecasting and Social Change*, 10.

Mandahar, P. (2020, July 26). *Pareto Rank*. Retrieved from GitHub: https://github.com/pmanandhar1452/pareto-rank/blob/master/pareto_rank_algos/ParetoRank.py

Massachusets Institute of Technology - Lincoln Laboratory. (2011). *MIT School of Engineering*. Retrieved from Beaverworks: https://web.archive.org/web/20170112172111/https://beaverworks.ll.mit.edu/CMS/bw/projectperdixcapstone

Matsumoto, H. (2002). Research on solar power satellites and microwave power transmission in Japan. *Microwave Magazine*, 36-45.

MIT Spectrum. (2014, April 14). *A Robot Dives into the Search for MH370*. Retrieved from Spectrum: https://spectrum.mit.edu/continuum/a-robot-dives-into-the-search-for-mh370/

Monterey Bay Aquarium Research Institute. (2014, March 31). *A New Way to Retrieve Data from AUVs*. Retrieved from MBARI: https://www.mbari.org/a-new-way-to-retrieve-data-from-auvs/

Museum, U. S. (1980). Whitehead Torpedo Mk1. *Torpedo Specialty Collection*. Keyport, Washington, USA.

Nancy J Dudney, W. C. (2015). *Handbook of Solid State Batteries*. Singapore: Word Scientific.

Nancy T. DeWitt, J. G. (2010). *Archive of Side Scan Sonar and Multibeam Bathymetry Data Collected during USGS Cruise 10CCT03 Offshore from the Gulf Islands National Seashore, Mississippi, from East Ship Island, Mississippi, to Dauphin Island, Alabama, April 2010*. Denver: USGS.

Newport Corporation. (2020). *Introduction to Solar Radiation*. Retrieved from Newport Photonics: https://www.newport.com/t/introduction-to-solar-radiation

North Atlantic Trade Organization. (2017, April 27). *A new era of digital underwater communcations*. Retrieved from NATO International: https://www.nato.int/cps/bu/natohq/news_143247.htm

Ocean Power Technologies. (2020). *PB3 Power Buoy*. Retrieved from Ocean Power Technologies Products: https://oceanpowertechnologies.com/pb3-powerbuoy/

Oil and Gas Authority. (2018). *UKCS Operating costs in 2017*. London: Oil and Gas Authority.

Orr, A. (2014, April 22). Bluefin-21's search for MH370 nearing completion in the Southern Indian Ocean. *The Sydney Morning Herald*.

Panasonic. (2020). *Panasonic Spec Sheet*. Retrieved from DatasheetsPDF: https://datasheetspdf.com/datasheet/NCR18650GA.html

Parde, N. (2018, August 17). *Advancing undersea optical communications*. Retrieved from MIT News: http://news.mit.edu/2018/advancing-undersea-optical-communications-0817

Parker, L. (2014, April 17). *Can an Unmanned Mini Yellow Submarine Find Missing Flight 370?* Retrieved from National Geographic: https://www.nationalgeographic.com/news/2014/4/140415-flight-370-indian-ocean-submersible-search--sonar-malaysia-airlines/#close

Paul Gerin Fahlstrom, a. T. (2012). *Introduction to UAV Systems, Fourth Edition*. West Sussex: 2012 John Wiley & Sons, Ltd.

Poole, J. (2020, June 30). Personal Communication. USA: Woods Hole Oceanographic Institute.

Pope, R., & Fry, E. (1997). Absorption spectrum (380–700 nm) of pure water. II. Integrating cavity measurements. *Applied Optics*, 8710-8723.

Power from Sunlight. (2017, June 21). *What Are The Operational Costs Of A Solar Panel System?* Retrieved from Powere from Sunlight: https://www.powerfromsunlight.com/operational-costs-solar-panel-system/

PowerTHRU. (2016). *Lead Acid Battery working lifetime study*. Retrieved from Power Thru Technical Papers: http://www.power-thru.com/documents/The%20Truth%20About%20Batteries%20-%20POWERTHRU%20White%20Paper.pdf

Prakash Manandhar, K. R. (2020). *Sensing systemic awareness and performance of teams during model-based site design*. Cambridge, Ma: Massachusetts Institute of Technology.

Randolph, G. (2016, December 9). *Deep Ocean AUV Sensor for Trace Chemical/Biological Material*. Retrieved from Photon Systems: https://photonsystems.com/deep-ocean-auv-sensor/

Rawson, K. (2001). *Basic Ship Theory (Fifth Edition)*. Woburn: Elsevier Science.

Robertson, B. R. (2010). Ocean Wave Energy Generation on the West Coast of Vancouver Island and the Queen Charlotte Islands. *Guelph Engineering Journal*, 9-18.

Rong, K. (2019, December 23). *Post-processing-masie*. Retrieved from GitHub: https://github.mit.edu/MIT-GTL/Post-processing-Masie/edit/master/src/process/methods/MasieTradespace.java

Sabatini, M. (2011, October 18). *Lithium Ion vs. Lithium Polymer – What's the Difference?* Retrieved from Android Authority: https://www.androidauthority.com/lithium-ion-vs-lithium-polymer-whats-the-difference-27608/

Schjølberg, Ø. G. (2018). Navigation and collision avoidance of underwater vehicles using sonar data. *Autonomous Underwater Vehicle Workshop* (pp. 1-6). Porto: OES.

Solar Reviews. (2020). *Solar Panel cost 2020*. Retrieved from Solar Reviews: https://www.solarreviews.com/solar-panels/solar-panel-cost/

Stein, S. K. (2007). *From Torpedoes to Aviation: washington Irving Chamerst and Technological Innovation in the New Navy 1876 to 1913*. Tuscaloosa: Universitty of Alabama Press.

Takehiro Imura, T. U. (2009). Flexibility of Contactless Power Transfer using Magnetic Resonance Coupling to Air Gap and Misalignment for EV. *World Electric Vehicle Journal*, 332 - 341.

Tao Liu, Y. H. (2019). Investigation of the vectored thruster AUVs based on 3SPS-S parallel manipulator. *Applied Ocean Research*, 151-161.

Taylor M. Fisher, K. B. (2014). Electric vehicle wireless charging technology: a state-of-the-art review of magnetic coupling systems. *Wireless Power Transfer*, 87 - 96.

The United States Navy. (2001, June 28). Extremely Low Frequency Transmitter Site Clam Lake, Wisconsin. *The United States Navy Fact File*, p. 4.

Tiedong Zhang, Y. P. (2008). Location and mapping for AUV Using A forward-looking sonar. *7th World Congress on Intelligent Control and Automation* (pp. 9083-9088). Chongqing: IEEE.

Trauthwein, G. (2014, May 29). *Bluefin Robotics on the Hunt for MH370*. Retrieved from Marine Technology News: https://www.marinetechnologynews.com/news/bluefin-robotics-mh370-493120

Tyler Stehly, P. B. (2018, 10). *2017 Cost of Wind Energy Review*. Retrieved from National Renewable Energy Laboratory: https://www.nrel.gov/docs/fy18osti/72167.pdf

U.S. Department of Energy. (2016). *Combined Heat and Power Technology Fact Sheet Series*. Washington D.C.: U.S. Depertment of Energy.

U.S. Department of Energy. (2020, June 16). *Weekly Retail Gasoline and DIesel Prices*. Retrieved from Petroleum and Other Liquids: https://www.eia.gov/dnav/pet/pet_pri_gnd_dcus_nus_m.htm

U.S. Energy Information Administration. (2020, May 29). *United States Natural Gas Industrial Price*. Retrieved from Natural Gas: https://www.eia.gov/dnav/ng/hist/n3035us3m.htm

Umair Mujtaba Qureshi, F. K. (2016). RF Path and Absorption Loss Estimation for Underwater Wireless Sensor Networks in Different Water Environments. *Sensors*, 890.

United States Department of Energy. (July 2019). *Energy Storage Technology and Cost Characterization Report.* PNNL-28866: United States Department of Energy.

United States Naval Undersea Museum. (1980). Whitehead Torpedo Mk1. *Torpedo Specialty Collection*. Keyport, Washington, USA.

Vincent S. Neary, M. P.-H. (2014). *Methodology for design and economic analysis of marine energy conversion (mec) technologies.* Albuquerque: Sandia National Laboratories.

Wang, W. E. (2009). The State-of-Art of Underwater Vehicles - Theories and Applications. *Mobile Robots*, 129 - 152.

WEPD Staff. (2019, October 22). *IntelStor expects wind turbine prices to recover 5% in next two years*. Retrieved from Windpower Engineering and Development: https://www.windpowerengineering.com/intelstor-expects-wind-turbine-prices-to-recover-5-in-next-two-years/

Whited, C. E. (1979, April 1). *Air Force Space Laser Communications*. Retrieved from The Space Congress Proceedings: https://commons.erau.edu/space-congress-proceedings/proceedings-1979-16th/session-2/5

Whitman, E. C. (2002, June). Unmanned Underwater Vehicles: Beneath the Wave. *Undersea Warfare Magazine*, pp. Vol. 4, No. 3. Retrieved from United States Navy.

Wholesale Solar. (2018, October 23). *Lead-Acid vs Lithium Batteries: Which Are Best For Solar?* Retrieved from Wholesale Solar: https://www.wholesalesolar.com/blog/lead-acid-vs-lithium-batteries

Willcox, J. G. (2001). Performance metrics for oceanographic surveys with autonomous underwater vehicles. *Journal of Oceanic Engineering*, 711-725.

Wireless Power Consortium. (2017, February). Introduction to the Power Class 0 Specificiation.

Wireless Power Consortium. (2018). *WPC Knowledge Base*. Retrieved from Wireless Power Consortium: https://www.wirelesspowerconsortium.com/knowledge-base/magnetic-induction-technology/resonance/magnetic-resonance-and-magnetic-induction-making-the-right-choice-for-your-application.html

Xianbo Xiang, C. Y. (2020). Manoeuvring-based actuation evaluation of an AUV with control surfaces and through-body thrusters. *Applied ocean research*.

Yinghao Zhang, Y. L. (2017). Design of X-rudder autonomous underwater vehicle's quadruple-rudder allocation with Lévy flight character. *International Journal of Advanced Robotic Systems*.

Yuh, J. (2000). Design and Control of Autonomous Underwater Robots: A Survey. *Autonomous Robotics*, 7-24.

Zheping Yan, S. P. (2010). Research on an improved dead reckoning for AUV navigation. *Chinese Control and Decision Conference* (pp. 1793-1797). Xuzhou: IEEE.

Zientara, B. (2020, March 2). *How much electricity does a solar panel produce?* Retrieved from Solar Basics: https://www.solarpowerrocks.com/solar-basics/how-much-electricity-does-a-solar-panel-produce/

Zimmer, N. K. (2007). Relative localisation for AUV swarms. *Symposium on Underwater Technology and Workshop on Scientific Use of Submarine Cables and Related Technologies* (pp. 588-593). Tokyo: IEEE.

Appendix A – Monte Carlo Simulation Code

```
from model import Architecture
import tradespaceEvaluator
import monteCarloEvaluator
import constants
import readexcel


''' This File runs all major aspects of model'''
''' This File is modified from monte carlo simulations methods written by T.C. Flemming Goolsby, MIT Systems Design and Management, 2019'''


""" 1)    Test Model"""
AD2 = 'AD2_Op2'
AD3 = 'AD3_Op8'
AD4 = 'AD4_Op1'
PlantSize = 'AD4_Op1'
AD6 = 'AD6_Op4'
NumAUVs = 'AD6_Op4'
Test_Arch = Architecture(AD2,AD3,AD4,PlantSize,AD6,NumAUVs)
print(Test_Arch.DOT)
print(Test_Arch.SAR)
print(Test_Arch.SC)
#
#""" 2)    Tradespace"""
#tradespace = tradespaceEvaluator.runTradeSpace()
#df_X_Pareto_SAR,df_Y_Pareto_SAR=plotter.plotTradespace(tradespace,
NamePrefix="AD2",GroupingFilter=constants.DOT_AD3.index)


"""3)    MonteCarlo"""
```

```
concepts_df = readexcel.createdf('MC_Concepts')
#plotter.plotTradespace(tradespace, NamePrefix="Concepts",GroupingFilter=concepts_df.Name)
concepts = concepts_df.to_dict('records')
monteCarloResults = monteCarloEvaluator.runMonteCarlo(concepts, numberOfSeeds=1000)
#plotter.plotMonteCarlo(monteCarloResults,df_X_Pareto_SAR,df_Y_Pareto_SAR)
#
'''4)    Export to .csv for visualization purposes'''
import pandas as pd

df = pd.DataFrame()
options = list(range(0,2))
#dropcolumns = [0,1,2,3,4,5,6]

for option in options:
    print(option)
    MCR = monteCarloResults[option]
    dftemp= pd.DataFrame(MCR)
    dftemp2 = dftemp#.drop(dftemp.columns[dropcolumns], axis = 1)
    dftemp2['Option'] = option + 1
    df = df.append(dftemp2, ignore_index = True)

df.to_csv('MonteCarloOutput.csv')
```

```
import numpy as np
import pandas as pd
from pandas import ExcelWriter
from pandas import ExcelFile
import readexcel

#create AD option distribtuion inputs
DOT_AD3 = readexcel.createdf('DOT_AD3')
DOT_AD3 = DOT_AD3.set_index('Options')
print("1")

DOT_AD6 = readexcel.createdf('DOT_AD6')
DOT_AD6 = DOT_AD6.set_index('Options')
print("2")

SAR_AD2 = readexcel.createdf('SAR_AD2')
SAR_AD2 = SAR_AD2.set_index('Options')
print("3")

SAR_AD6 = readexcel.createdf('SAR_AD6')
SAR_AD6 = SAR_AD6.set_index('Options')
print("4")

SC_AD2 = readexcel.createdf('SC_AD2')
SC_AD2 = SC_AD2.set_index('Options')
print("5")

SC_AD3 = readexcel.createdf('SC_AD3')
SC_AD3 = SC_AD3.set_index('Options')
print("6")

SC_AD4 = readexcel.createdf('SC_AD4')
```

```
SC_AD4 = SC_AD4.set_index('Options')
print("7")

SC_PlantSize = readexcel.createdf('SC_PlantSize')
SC_PlantSize = SC_PlantSize.set_index('Options')
print("8.5")

SC_AD6 = readexcel.createdf('SC_AD6')
SC_AD6 = SC_AD6.set_index('Options')
print("8")

SC_NumAUVs = readexcel.createdf('SC_NumAUVs')
SC_NumAUVs = SC_NumAUVs.set_index('Options')
print('8.75')

class Constants:
    def __init__(self, AD2, AD3, AD4, PlantSize, AD6, NumAUVs, seed=None):
        self.DOT_AD3 = DOT_AD3.loc[AD3,'Norm_Mean']
        self.DOT_AD6 = DOT_AD6.loc[AD6,'Norm_Mean']
        #print("9")

        self.SAR_AD2 = SAR_AD2.loc[AD2,'Norm_Mean']
        self.SAR_AD6 = SAR_AD6.loc[AD6,'Norm_Mean']
        #print("10")

        self.SC_AD2 = SC_AD2.loc[AD2,'Norm_Mean']
        self.SC_AD3 = SC_AD3.loc[AD3,'Norm_Mean']
        self.SC_AD4 = SC_AD4.loc[AD4,'Norm_Mean']
        self.SC_PlantSize = SC_PlantSize.loc[PlantSize, 'Norm_Mean']
        self.SC_AD6 = SC_AD6.loc[AD6,'Norm_Mean']
        self.SC_NumAUVs = SC_NumAUVs.loc[NumAUVs, 'Norm_Mean']
        #print("11")
```

```
        if seed is not None:
            np.random.seed(int(seed))
            self.DOT_AD3 =
np.random.normal(DOT_AD3.loc[AD3,'Norm_Mean'],DOT_AD3.loc[AD3,'Norm_Mean']*DOT_
AD3.loc[AD3,'Norm_Std'],1)[0]
            self.DOT_AD6 =
np.random.normal(DOT_AD6.loc[AD6,'Norm_Mean'],abs(DOT_AD6.loc[AD6,'Norm_Mean']*D
OT_AD6.loc[AD6,'Norm_Std']),1)[0]
            #print("12")

            self.SAR_AD2 =
np.random.normal(SAR_AD2.loc[AD2,'Norm_Mean'],SAR_AD2.loc[AD2,'Norm_Mean']*SAR_A
D2.loc[AD2,'Norm_Std'],1)[0]
            self.SAR_AD6 =
np.random.normal(SAR_AD6.loc[AD6,'Norm_Mean'],SAR_AD6.loc[AD6,'Norm_Mean']*SAR_A
D6.loc[AD6,'Norm_Std'],1)[0]
           #print("13")

            self.SC_AD2 =
np.random.normal(SC_AD2.loc[AD2,'Norm_Mean'],SC_AD2.loc[AD2,'Norm_Mean']*SC_AD2.lo
c[AD2,'Norm_Std'],1)[0]
            self.SC_AD3 =
np.random.normal(SC_AD3.loc[AD3,'Norm_Mean'],SC_AD3.loc[AD3,'Norm_Mean']*SC_AD3.lo
c[AD3,'Norm_Std'],1)[0]
            self.SC_AD4 =
np.random.normal(SC_AD4.loc[AD4,'Norm_Mean'],SC_AD4.loc[AD4,'Norm_Mean']*SC_AD4.lo
c[AD4,'Norm_Std'],1)[0]
            self.SC_PlantSize =
np.random.normal(SC_PlantSize.loc[PlantSize,'Norm_Mean'],SC_PlantSize.loc[PlantSize,'Norm_Me
an']*SC_PlantSize.loc[PlantSize,'Norm_Std'],1)[0]
```

```
        self.SC_AD6 =
np.random.normal(SC_AD6.loc[AD6,'Norm_Mean'],SC_AD6.loc[AD6,'Norm_Mean']*SC_AD6.lo
c[AD6,'Norm_Std'],1)[0]
        self.SC_NumAUVs = np.random.normal(SC_NumAUVs.loc[NumAUVs, 'Norm_Mean'],
SC_NumAUVs.loc[NumAUVs,'Norm_Mean']*SC_NumAUVs.loc[NumAUVs,'Norm_Std'],1)[0]
        #print("14")
```

```
import constants
import math


class Architecture:
    def __init__(self, AD2, AD3, AD4, PlantSize, AD6, NumAUVs, seed=None):
        "Initialize Variables"
        if seed is not None:
            self.constantValues = constants.Constants(AD2, AD3, AD4, PlantSize, AD6, NumAUVs,
seed)
        else:
            self.constantValues = constants.Constants(AD2, AD3, AD4, PlantSize, AD6, NumAUVs)

        #deterministic tradespace calculations

        self.name = "{}-{}-{}-{}".format(AD2, AD3, AD4, AD6)
        self.DOT = 0
        self.SAR = 0
        self.SC = 0

        self.DOT_AD3=self.constantValues.DOT_AD3
        self.DOT_AD6=self.constantValues.DOT_AD6

        self.SAR_AD2=self.constantValues.SAR_AD2
        self.SAR_AD6=self.constantValues.SAR_AD6

        self.SC_AD2=self.constantValues.SC_AD2
        self.SC_AD3=self.constantValues.SC_AD3
        self.SC_AD4=self.constantValues.SC_AD4
        self.SC_PlantSize=self.constantValues.SC_PlantSize
        self.SC_AD6=self.constantValues.SC_AD6
        self.SC_NumAUVs=self.constantValues.SC_NumAUVs
```

```
        "Run Model"
        # Daily Operating Time
        self.DOT=(24-(13500/self.DOT_AD3))+self.DOT_AD6

        #Search Area Rate
        self.SAR = 11+(11-((250/self.SAR_AD2)*11))+self.SAR_AD6

        #System Cost
        if (self.SC_NumAUVs*13500) < (self.SC_PlantSize*24):
            self.SC = (self.SC_AD2-14000)+(self.SC_AD3-
500)+(self.SC_AD6)+(self.SC_NumAUVs*2000000)+10000000+(self.SC_AD4*self.SC_PlantSize)
        else:
            self.SC = (self.SC_AD2-14000)+(self.SC_AD3-
500)+(self.SC_AD6)+(self.SC_NumAUVs*2000000)+10000000+((self.SC_AD4*self.SC_PlantSize)
*(math.ceil((self.SC_NumAUVs*13500)/(self.SC_PlantSize*24))))+(self.SC_NumAUVs*3500)
```

```
from model import Architecture
import constants


def runTradeSpace():
    architectures, DOT, SAR, SC= [], [], [], []
    for Op_AD2 in constants.SC_AD2.index:
        for Op_AD3 in constants.SC_AD3.index:
            for Op_AD4 in constants.SC_AD4.index:
                for Op_AD6 in constants.SC_AD6.index:
                    ArchitectureInstance = Architecture(Op_AD2,Op_AD3,Op_AD4,Op_AD6)
                    architectures.append(ArchitectureInstance)
                    SC.append(ArchitectureInstance.SC)
                    DOT.append(ArchitectureInstance.DOT)
                    SAR.append(ArchitectureInstance.SAR)

    return {"Architectures": architectures, "SC": SC, "DOT": DOT, "SAR":SAR}

from numpy import linspace
from model import Architecture


def runMonteCarlo(concepts, numberOfSeeds):
    seeds = linspace(1, numberOfSeeds, num=numberOfSeeds)
    for concept in range(len(concepts)):
        architectures,name, DOT, SAR, SC = [], [], [], [], []
        for seed in seeds:
            architectureinstance = Architecture(concepts[concept]['AD2'],
concepts[concept]['AD3'],concepts[concept]['AD4'],concepts[concept]['PlantSize'],
concepts[concept]['AD6'],concepts[concept]['NumAUVs'],seed)
            architectures.append(architectureinstance)
            name.append(architectureinstance.name)
```

```
        DOT.append(architectureinstance.DOT)
        SAR.append(architectureinstance.SAR)
        SC.append(architectureinstance.SC)
    concepts[concept].update({"Name": name,
                              "DOT": DOT,
                              "SAR": SAR,
                              "SC": SC})
return concepts
```

Read Excel

```
import pandas as pd

file = r"C:\...\Probabilistic"

def createdf(sheetname):
    df = pd.read_excel('PythonInput.xlsx', sheet_name=sheetname)
    return df
```

Appendix B – Pareto Ranking Code

```
'''
    MIT License
    Copyright (c) 2020 Prakash Manandhar
    Permission is hereby granted, free of charge, to any person obtaining a copy
    of this software and associated documentation files (the "Software"), to deal
    in the Software without restriction, including without limitation the rights
    to use, copy, modify, merge, publish, distribute, sublicense, and/or sell
    copies of the Software, and to permit persons to whom the Software is
    furnished to do so, subject to the following conditions:
    The above copyright notice and this permission notice shall be included in all
    copies or substantial portions of the Software.
    THE SOFTWARE IS PROVIDED "AS IS", WITHOUT WARRANTY OF ANY KIND, EXPRESS OR
    IMPLIED, INCLUDING BUT NOT LIMITED TO THE WARRANTIES OF MERCHANTABILITY,
    FITNESS FOR A PARTICULAR PURPOSE AND NONINFRINGEMENT. IN NO EVENT SHALL THE
    AUTHORS OR COPYRIGHT HOLDERS BE LIABLE FOR ANY CLAIM, DAMAGES OR OTHER
    LIABILITY, WHETHER IN AN ACTION OF CONTRACT, TORT OR OTHERWISE, ARISING FROM,
    OUT OF OR IN CONNECTION WITH THE SOFTWARE OR THE USE OR OTHER DEALINGS IN THE
    SOFTWARE.
    '''

    import pandas

    class ParetoRank:
        """
```

```
    Performs Pareto based ranking of given tradespace points.
    Args:
        input_file  (str):
            path to file that contains the input data. A CSV
            (comma separated value) file is expected.
        output_file (str): path to file to output data to (existing
             data will be overwritten). The output file is a CSV file with
             columnns: "id" and "rank"

        id_col (str): name of column containing the unqiue identifier. An
            integer valued identifier is expected. Please note that column
            names sometimes need to contain spaces if the names are separated
            by spaces after comma in the CSV file.
        utility_cols (str array): array of column names for the utility
            vector.Please note that column names sometimes need to contain
            spaces if the names are separated by spaces after comma in the
            CSV file.
        utility_minmax (bool array): array of True or False values in the same
            order as utility_cols that indicates whether this utility is to
            be minimized or maximmized.
"""
def __init__(self,
    input_file, output_file, \
    id_col, utility_cols, utility_min):

    self.input_file = input_file
    self.output_file = output_file

    self.id_col = id_col
    self.utility_cols = utility_cols
    self.utility_min = utility_min
```

```
    self.dominates_map = dict()

"""
    returns whether the given id is dominated by the send id
    vector J1 dominates J2 iff
        J1i <= J2i forall i, and
        J1i < J2i for at least 1 i
"""
def dominates(self, id1, id2):
    row1 = self.data[self.data[self.id_col] == id1]
    row2 = self.data[self.data[self.id_col] == id2]
    key = f'{id1}-{id2}'
    if key in self.dominates_map:
         dom = self.dominates_map[key]
    else:
        condition1 = True
        condition2 = False
        for col_i in range(len(self.utility_cols)):
            col_name = self.utility_cols[col_i]
            J1i = row1[col_name].values[0]
            J2i = row2[col_name].values[0]

            if J1i > J2i:
                condition1 = False
                break

            if J1i < J2i:
                condition2 = True

        dom = condition1 and condition2
        self.dominates_map[key] = dom
    return dom
```

```
    """
        checks if a given row index is dominated any other datapoint
    """
    def is_dominated(self, i):
        dom = False
        rowi = self.data[self.data[self.id_col] == i]
        idi = rowi[self.id_col].values[0]
        print(f'is_dominated ({i}) with {len(self.data)} rows')
        for j in self.data[self.id_col].values:
            if i == j:
                continue
            rowj = self.data[self.data[self.id_col] == j]
            idj = rowj[self.id_col].values[0]
            if self.dominates(idj, idi):
                dom = True
                break
        return dom

    def perform_ranking(self):
        # load data
        self.data = pandas.read_csv(
            self.input_file, usecols=[self.id_col] + self.utility_cols)

        # if a given column is not to be minimized, invert the data
        for col_i in range(len(self.utility_cols)):
            if not self.utility_min[col_i]:
                self.data[self.utility_cols[col_i]] = -self.data[self.utility_cols[col_i]]

        self.data = self.data.sort_values(self.utility_cols, ascending=False)
        self.data_orig = self.data.copy()
```

```
ofp = open(self.output_file, 'w')
ofp.write(f'{self.id_col},rank\n')

curr_rank = 1
pareto_front = []
while (len(self.data > 0)):
    print(f'Running pass {curr_rank}...')
    print(pareto_front)
    self.data = self.data_orig.copy()
    self.data = self.data[~self.data[self.id_col].isin(pareto_front)]
    for i in self.data[self.id_col].values:
        #print(f'Checking {self.id_col} == {i}...')
        if not (self.is_dominated(i)):
            rowi = self.data[self.data[self.id_col] == i]
            idi = rowi[self.id_col].values[0]
            ofp.write(f'{idi}, {curr_rank}\n')
            pareto_front.append(i)
        else:
            self.data = self.data.drop(self.data[self.data[self.id_col]==i].index)
    curr_rank += 1
    print('\n')

ofp.close()
```